

Alma Mater Studiorum – Università di Bologna

Dottorato di Ricerca in Chimica Industriale (XX ciclo)

Settore scientifico disciplinare di afferenza: Chim/05

**OPTICALLY ACTIVE PHOTORESPONSIVE
MULTIFUNCTIONAL POLYMERIC MATERIALS**

Presentata da

FRANCESCO MAURIELLO

Coordinatore Dottorato

Chiar.mo Prof. L. ANGIOLINI

Relatore

Chiar.mo Prof. L. ANGIOLINI

Correlatore

Dott. L.GIORGINI

Esame finale anno 2008

*Optically active, photoresponsive
multifunctional polymeric materials*

In the last year [1], Angiolini and co-workers have synthesized and investigated methacrylic polymers bearing in the side chain the chiral cyclic (*S*)-3-hydroxypyrrolidine moiety interposed between the main chain and the *trans*-azoaromatic chromophore, substituted or not in the 4' position by an electron-withdrawing group. In these materials, the presence of a rigid chiral moiety of one prevailing absolute configuration favours the establishment of a chiral conformation of one prevailing helical handedness, at least within chain segments of the macromolecules, which can be observed by circular dichroism (CD).

The simultaneous presence of the azoaromatic and chiral functionalities allows the polymers to display both the properties typical of dissymmetric systems (optical activity, exciton splitting of dichroic absorptions), as well as the features typical of photochromic materials (photorefractivity, photoresponsiveness, NLO properties).

The first part of this research was to synthesize analogue homopolymers and copolymers based on bisazoaromatic moiety and compare their properties to those of the above mentioned analogue derivatives bearing only one azoaromatic chromophore in the side chain. We focused also the attention on the effects induced on the thermal and chiroptical behaviours by the insertion of particular achiral comonomers characterized by different side-chain mobility and steric hindrance (**MMA**, *tert*-**BMA** and **TrMA**).

On the other hand carbazole containing polymers [2] have attracted much attention because of their unique features. The use of these materials in advanced micro- and nanotechnologies spreads in many different applications such as photoconductive and photorefractive polymers, electroluminescent devices, programmable optical interconnections, data storage, chemical photoreceptors, NLO, surface relief gratings, blue emitting materials and holographic memory.

The second part of the work was focused on the synthesis and the characterization polymeric derivatives bearing in the side chain carbazole or phenylcarbazole moieties

linked to the (*S*)-2-hydroxy succinimide or the (*S*)-3-hydroxy pyrrolidiny ring as chiral groups covalently linked to the main chain through ester bonds.

The last objective of this research was to design, synthesize, and characterize multifunctional methacrylic homopolymers and copolymers bearing three distinct functional groups (i.e. azoaromatic, carbazole and chiral group of one single configuration) directly linked in the side chain.

This polymeric derivatives could be of potential interest for several advanced application fields, such as optical storage, waveguides, chiroptical switches, chemical photoreceptors, NLO, surface relief gratings, photoconductive materials, etc.

References

- [1] [1a] L. Angiolini, R. Bozio, A. Daurù, L. Giorgini, D. Pedron, G. Turco, *Chem. Eur. J.* 2002; 8, 4241. [1b] L. Angiolini, T. Benelli, L. Giorgini, A. Painelli, F. Terenziani, *Chem. Eur. J.* 2005, 11, 6053-6353. [1c] L. Angiolini, T. Benelli, R. Bozio, A. Daurù, L. Giorgini, D. Pedron, E. Salatelli, *Eur. Polym. J.* 2005, 41, 2045. [1d] L. Angiolini, T. Benelli, R. Bozio, A. Daurù, L. Giorgini, D. Pedron, E. Salatelli, *Macromolecules* 2006, 39, 489. [1e] L. Angiolini, D. Caretti, L. Giorgini, E. Salatelli, *Macromol. Chem. Phys.* 2000, 201, 533 [1f] L. Angiolini, D. Caretti, L. Giorgini, E. Salatelli, *J. Polymer Sci., Part A Polym. Chem.* 1999, 37, 3257. [1g] L. Angiolini, D. Caretti, L. Giorgini, E. Salatelli, *Polymer* 2001, 42, 4005.
- [2] [2a] J. V. Grazuleviciusa, P. Strohrieglb, J. Pielichowskic, K. Pielichowski, *Prog. Polym. Sci.* 2003, 28, 1297–1353. [2b] W. E. Moerner, A. Grunnet-Jepsen, C. L. Thompson, *Annu. Rev. Mater. Sci.* 1997, 27, 583-623. [2c] K. Meerholz, B. Volodin, B. Sandalphon, N. Kippelen, N. Peyghambarian, *Nature* 1994, 371, 497. [2d] S. Ducharme, J.C. Scott, R.J. Twieg, W.E. Moerner, *Phys. Rev. Lett.* 1991, 66, 1846.

Table of Contents

Chapter 1: Literature survey	1
<i>Azoaromatic Polymers</i>	1
<i>Carbazole containing polymers</i>	14
<i>Photorefractive materials</i>	21
Chapter 2: Optically active bisazoaromatic polymers	41
<i>Optically active methacrylic homopolymers bearing side-chain bisazoaromatic moieties</i>	46
<i>Optically active methacrylic copolymers bearing side-chain bisazoaromatic moieties</i>	57
<i>Optically active methacrylic copolymers bearing side chain bisazoaromatic moieties: modulation of conformational chirality</i>	72
<i>Conclusions</i>	88
Chapter 3: Methacrylic polymers bearing side chain carbazole	103
<i>Methacrylic optically active homopolymers bearing 3 - side chain carbazole moieties</i>	107
<i>Methacrylic optically active homopolymers bearing side-chain 9-phenylcarbazole moieties</i>	122
<i>Conclusions</i>	133
Chapter 4: Methacrylic polymers bearing side chain azocarbazole chromophore	149
<i>Optically active methacrylic polymer containing side-chain azocarbazole chromophore: poly[(S)-MLECA]</i>	152
<i>Methacrylic polymers bearing side-chain 9-phenylazocarbazole moieties</i>	171
<i>Conclusions</i>	183
Chapter 5: Optically active copolymers containing in side chain carbazole and azo chromophores	199
<i>Copolymers containing optically active side chain 3-carbazole and azochromophores</i>	203
<i>Copolymers containing optically active side chain 9-phenylcarbazole and azochromophores</i>	220
<i>Conclusions</i>	230

**Chapter 1: Literature survey on azoaromatic,
carbazole and photorefractive polymers**

Azoaromatic Polymers

Since the discovery of azo dyes in 1863, a wide variety of properties has been discovered. One of the most intriguing properties of azobenzene (and derivatives) is *trans-cis* photoisomerization.

The *trans* form is more stable and the energy difference between the isomers is about 50 kJ/mol. The *trans-cis* interconversion can occur thermally and/or photochemically.

The proposed isomerization mechanism involves two possible pathways [1]: a rotation about the -N=N- bond, with breakage of the double bond, or via nitrogen inversion, with a semi-linear and hybridized transition state (Figure 1). It is generally accepted that the inversion mechanism is involved in the thermal isomerization of azo aromatic group and both mechanisms are possible in the photochemical isomerization process.

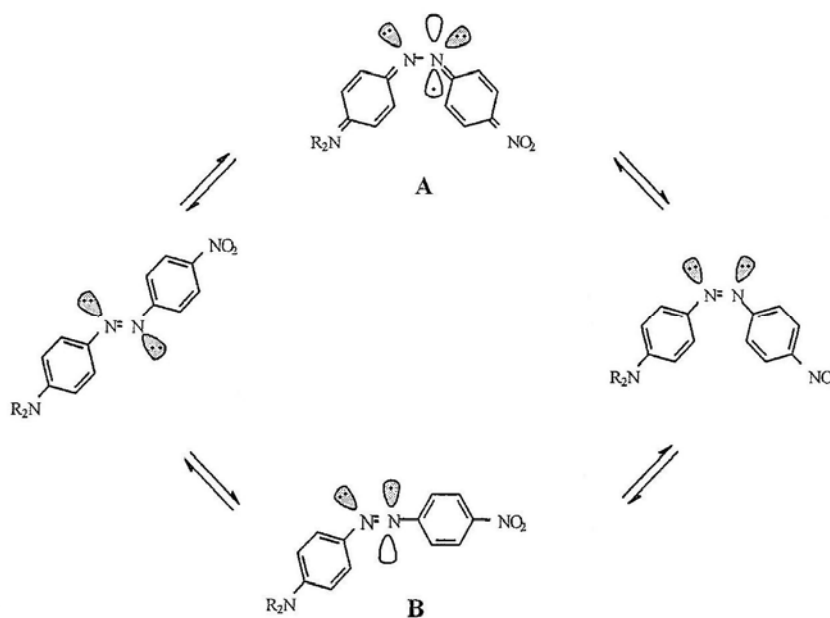


Figure 1. *trans-cis* isomerization of azobenzene: rotation (A) and inversion (B) about the -N=N- bond

Because of the differences in the structure of the isomers, the *trans-cis* photoisomerizations are always accompanied by significant changes of polymer properties, such as the phase, conformation and optical properties.

The influence of the polymer properties on the photochemical and thermal isomerization has been demonstrated by kinetic studies on different azo polymers and the rate of isomerization of azo groups covalently bonded to polymers depends on the structural properties of polymer matrix [1,2].

The conformational changes induced by photochemical *trans-cis* isomerization of the azo groups and their effects on polymer properties or polymer solution properties have been reviewed in 1989 by Kumar and Neckers [3].

Azo polymers can be liquid crystalline, have nonlinear optical properties, and show light-induced dichroism and birefringence.

Liquid-Crystalline Azo Polymers

Liquid crystallinity is a known property of some azo polymers. Liquid crystalline (LC) polymers are an important area of research because of their highly anisotropic optical, electrical, and mechanical properties [4,5].

In order to observe liquid crystallinity, a polymer generally requires the presence of rigid mesogenic groups and sufficient conformational freedom to allow the mesogenic units to form stacks or organized domains. The aromatic azo groups can be used to provide the mesogenic units.

Liquid-crystalline polymers can be divided in two categories: main-chain and side-chain LC azo polymers (Figure 2). Aromatic azo groups can be linked to a polymer chain through flexible connecting groups to give side-chain liquid-crystalline polymers. The polymer backbone can be constituted by simple hydrocarbons, esters, amides, phosphazenes, etc [6].

Another way is to bind aromatic azo groups to the backbone through flexible spacers, interposing several methylene units, for example, between the mesogenic units (main-chain liquid crystalline polymers) [7].

Recently, a variety of LC azo polymers with new architectures has been reviewed [8].

QuickTime™ and a
decompressor
are needed to see this picture.

Figure 2. Main-chain and side-chain LC azo polymer

The LC polymers containing azo aromatic mesogenic groups in the side chain or in the main chain offer the possibility to modify their arrangement by external fields and/or light. Photochemically induced isothermal phase transitions of some side chain liquid crystalline polymers were studied by Ikeda et al. using calorimetry, FT-IR dichroism, polarizing microscopy [6b, 6c].

When a liquid-crystalline azo polymer sample is examined on a polarizing microscope equipped with a hot stage and irradiated with linearly polarized laser beam, the nematic-to-isotropic phase transition can be successfully induced by the photoisomerization of the azogroups in the polymer.

The reverse process, the *cis-trans* isomerization occurs in the dark and restores the polymer to the initial nematic state. The efficiency of the photochemically induced isothermal phase transition was found to be closely related to the initial orientational ordering of the polymer and the photoinduced nematic-to-isotropic isothermal phase transition took place more effectively in a system with a less ordered nematic state. The
Optically active, photoresponsive multifunctional polymeric materials

order depends on the spacer length between the main chain and the mesogenic group and on the molecular weight of the LC polymer.

Nonlinear Optical Properties of azo-polymers

In general, organic molecules bearing electron donor and acceptor groups connected by electronic conjugation show to possess large values of the second order molecular hyperpolarizability. However, efficient nonlinear optical properties can only be achieved in materials having both a large second order hyperpolarizability at the molecular level and a noncentrosymmetric bulk ordering. Azo polymers provide an attractive possibility for NLO properties because of their processability, good optical properties, wide variety and low cost [9].

In order to provide extend conjugation between donor and withdrawing groups, both main chain and side chain azo polymers have been synthesized and their NLO properties tested [10].

In most cases, the electron donor groups are amines (-N-) or oxygen (-O-). The withdrawing groups are cyano (-CN), nitro (-NO₂), or sulfone (-SO₂-).

The optical nonlinearities of the polymers are induced by poling: this process applies an electric field at a temperature above the glass transition of the polymer.

Typically, the sample is sandwiched between two electrodes, heated above T_g in a strong electric field, and then cooled below T_g with the field on. The polar alignment obtained above T_g is supposed to be frozen at room temperature (usually below T_g). This stability turned out to be one of the main drawbacks of this procedure, since dipoles that are parallel to each other will also have a rather strong Coulombic repulsion. Thus, the stability of the poled material is rather poor.

The first report suggesting that photoinduced alignment of azobenzenes can be exploited to enhance electric field poling was published in 1991 [11]. Initially, the electric field is on, creating a parallel alignment of the chromophore dipoles. This alignment saturates relatively soon. When polarized light is used to favor the alignment of the azobenzene groups along the same direction as the electric field, the presence of the electric field makes the dipoles to align preferentially parallel; thus, the NLO coefficient increases by more than 50%. When the optical pump is turned off, there is a

relaxation of the alignment, but the final value is still much higher than the saturated value in the presence of only the electric field. When the field is turned off, the second order nonlinear optical properties of the polymer are achieved. Below the glass transition temperature of the polymer, the segmental motion of the polymer chains is frozen, and thus the orientation of the azo groups can be kept stable for a long period of time.

This procedure is called “photoassisted” alignment and was very popular, because it is a relatively simple and efficient way to improve the electric field poling.

Polar orientation of azo polymers can also be achieved by Langmuir-Blodgett procedures, in which monomolecular layers at the air-water interface are mechanically transferred to a solid substrate [12]. This technique allows the chromophores to align without a poling process.

There is a continuing interest in developing the LB method and exploring its utility to produce materials for nonlinear optics [13].

Optically induced and erased birefringence and linear dichroism.

The possibility of using polymeric systems containing azo molecules as optical recording medium was first suggested in 1983 with azo dyes (methyl red and methyl orange) dispersed into a polymer matrix (polyvinyl alcohol) [14]. When the polymer system is irradiated with a linearly polarized laser beam with a wavelength of 488 nm (close to the maximum absorbance of the azo dye), the optical transmission for light polarized along the polarization direction of the writing light increases and that for light perpendicular to the direction of the writing light decreases. Optical dichroism as well as birefringence is induced. However, the photoinduced optical anisotropy can only be maintained for a short time even when the material is stored in the dark.

In the last decades amorphous azo polymers with high glass transition temperatures have been synthesized and tested for reversible optical storage processes with a significant increase in the stability of the written material [15]. In every case, the writing using linearly polarized (LP) laser light with the same wavelength as the azo group absorbance can be performed at room temperature in the glassy state. The birefringence can be monitored by a light beam whose wavelength is out of the region

of absorbance of the azo polymer. The written information can be erased either by heating the polymer above its glass transition temperature or by irradiating with circularly polarized (CP) light.

Figure 3 shows a typical writing-erasing sequence obtained by measuring the birefringence-induced transmission of a sample placed between crossed polarizers. The time required to reach the saturation depends on a few factors, such as sample thickness and the type of azo groups.

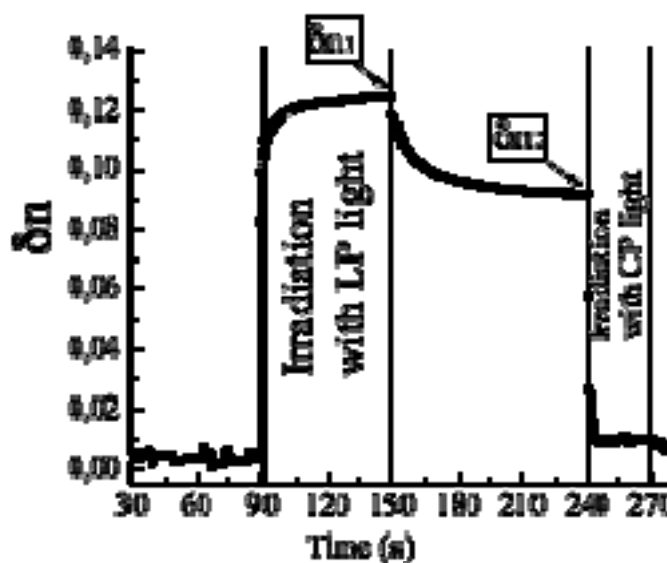


Figure 3. Writing and erasing sequence on an amorphous azo polymer

The laser induced optical birefringence and dichroism is a result of induced molecular reorientation. The mechanism postulated for the laser induced reorientation phenomena is related to the *trans-cis-trans* isomerization processes of the azo groups in the polymers [16].

Subjecting the azo group to light of wavelength close to its own absorbance induces the *trans* to *cis* isomerization of the $-N=N-$ group. The azo group will be inert to photochemical excitation by the laser beam if its orientation is perpendicular to the polarization direction, because the *trans* to *cis* photochemical transition rate can be described by a $I \cos^2 \phi$ term, in which I is proportional to the laser beam intensity and ϕ is the angle between the azobenzene orientation and the laser polarization direction. With a linearly polarized laser beam, the groups parallel to the polarization direction of

the light beam have the highest isomerization probability. The thermally excited *cis* to *trans* isomerization is spontaneous and the resulted *trans* azo group may fall in any direction. However those groups with a component parallel to the polarization direction of the incoming light will be continuously subjected to this *trans-cis-trans* isomerization process while those azo groups which fall perpendicular to the laser polarization direction at the end of one of the *cis-trans* isomerization processes, will remain in this position, because they cannot be reactivated when $\cos(\phi) = 0$. The final state of the material is the state with an excess of azo groups perpendicular to the direction of the laser polarization. Using circularly polarized light, the orientational order is destroyed because of the random *trans-cis-trans* isomerization.

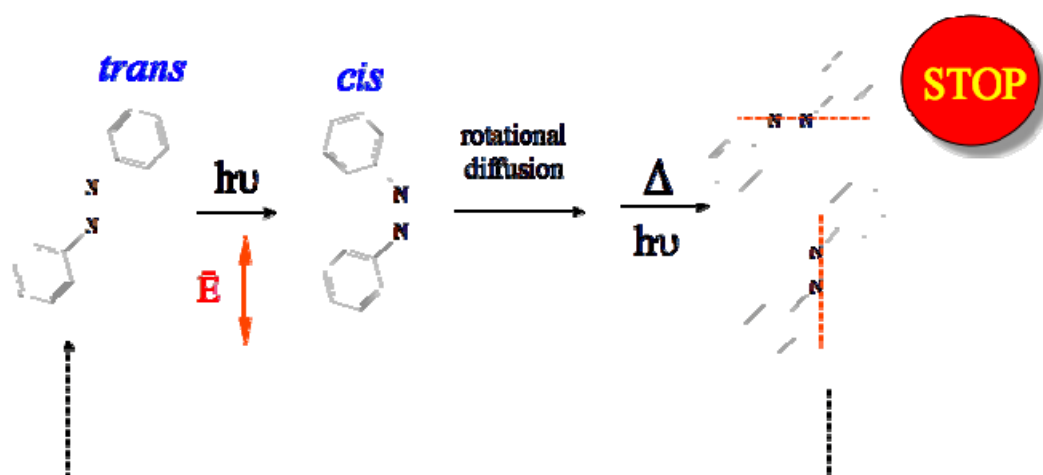


Figure 4. *trans-cis-trans* isomerization processes of the azo groups during a typical experiment of irradiation with LP laser light.

This phenomenon of photoinduced birefringence in azo polymers has been investigated in applications such as polarization holography, birefringence diffraction grating, and electr-optic switching.

The writing-erasing can be performed reversibly for many times without substantial changes. In the case of prolonged writing with a high energy laser beam, bleaching of the sample has been noted. This is possibly the result of an increased number of azo groups being oriented along the propagation direction of the beam (i.e. perpendicular to

the film surface). This bleaching effect can be removed by heating the sample above T_g and restoring the randomness of orientation. Thus this is a reversible fading. Irreversible fading is more complicated and it appears to be dependent on the total energy absorbed at a particular spot. Previous studies revealed that the photofading rate is inversely related to the rate of the thermal cis-trans reaction. The chemistry of photofading reaction of azo dyes in polymers was reviewed by Griffiths [16].

Photoinduced chirality and switching in azo polymers

If the azobenzene group is a part of an helical structure, its photoisomerization may affect the supramolecular helical arrangement in a variety of ways. The first example of a change in the pitch of a cholesteric liquid crystal by photoisomerization of added azobenzene was published in 1971 [18]. Helical polypeptides can contain azobenzene groups in the side chain. The photoinduced isomerization of the azobenzene groups may change the helicity of the main chain. For example, it was noticed that irradiation in solution at 360 nm of a polypeptide having a 60% right-handed helix induces the photoisomerization of the azobenzene groups, thus changing the conformation to a random coil (only 15% helical). The change is reversed by irradiation at 460 nm (*cis-trans* photoisomerization) [19].

Since it is possible to measure the circular dichroism signal at a certain wavelength and switch that signal by illuminating the sample, this procedure has been proposed as a type of chiroptical photorecording as early as 1991 [20].

Of course, helical structures, or otherwise organized supramolecular structures, are not restricted to polypeptides, and azobenzene was incorporated into a variety of other polymers to phototrigger their supramolecular organization. For example, polyisocyanates are known to possess helical structures. If one attaches azobenzene side groups to these helices, the expectation is that the azobenzene photoisomerization may affect the helical structure of the polymer. However, this is not always true [21]; the connection to the main chain has to be tight and the azobenzene group should preferably be chiral itself [22].

Then, the mechanism of photoswitchable helical conformation follows the scheme shown in Figure 5 [22].

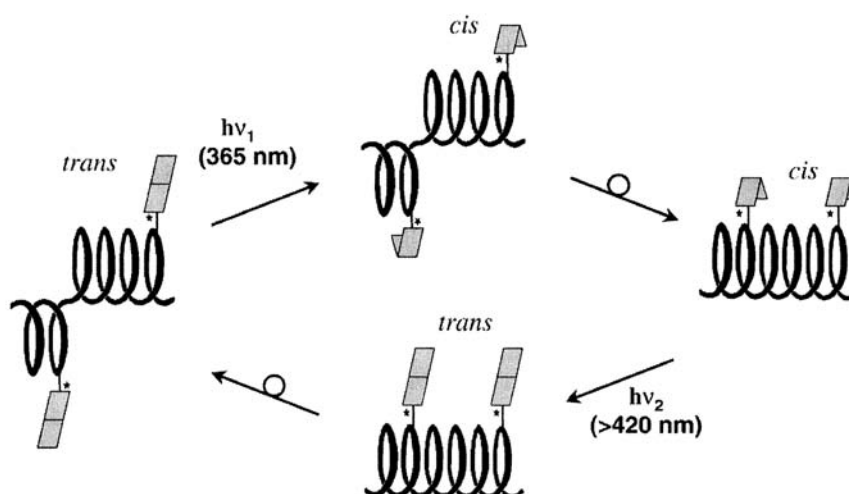


Figure 5. Schematic representation of the shift in the equilibrium between P and M helices of polyisocyanate by the use of chiral photoisomerizable side chains.

A special case of the change in the helical structure of macromolecules when azobenzene photoisomerization is involved, is the case in which no helical structure was initially present. This phenomenon was first reported by Nikolova et al. [23]. A film of azopolymer was subjected to circularly polarized light, and simultaneous measurement at 488 and 633 nm reveals that optical activity (more than 104 deg/cm) is being created in a film that had no initial optical activity, nor had any structural reasons to exhibit this property. These results have then been reproduced on a similar polymer and an amorphous copolymer.

This amorphous copolymer requires preorientation with linearly polarized light for the circular dichroism to be photoinduced. The proposed mechanism in all cases was circular momentum transfer from the circularly polarized light to the azobenzene chromophores. A more in-depth study on the mechanism of this unexpected phenomenon was published by Nikolova and co-workers [24]. The mechanism turns out to be related to the light ellipticity and by the property of the materials (due to its liquid crystalline phase or its preoriented arrangement) to change the ellipticity and the polarization azimuth as light passes through the material. The circular dichroism spectra (Figure 6) give informations about the supramolecular helix conformations of thin film

Optically active, photoresponsive multifunctional polymeric materials

of typical LC azopolymer irradiated in the smectic phase [25].

Probably the most interesting and intriguing finding is that right circularly polarized light induced a right-handed supramolecular helix, and that subsequent irradiation with left circularly polarized light first destroys the supramolecular arrangement, and then creates a left-handed supramolecular helix.

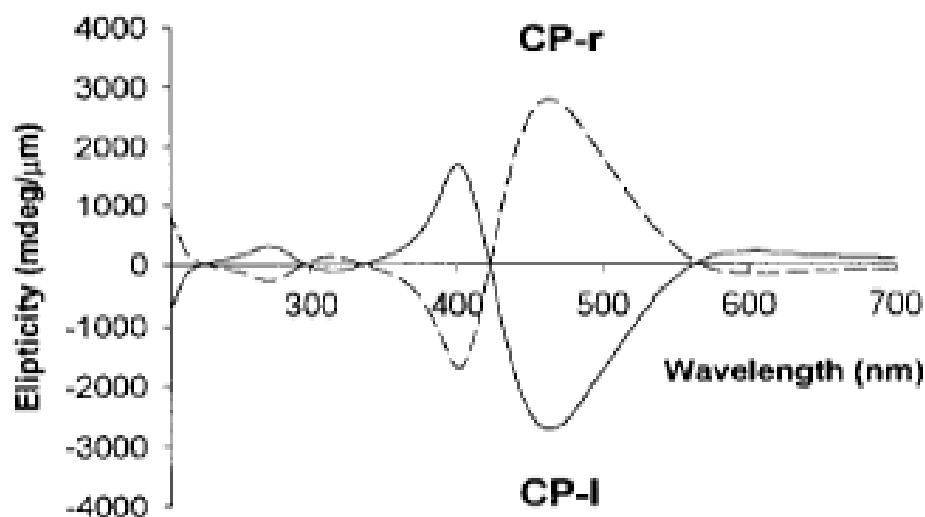


Figure 6. CD spectra of thin film (140 nm) of poly(4MAN) recorded after irradiation with CP light (514 nm, 75 mW/cm²): induced with CP-L (—) and with CP-R (- - -), respectively.

A schematic representation of the possible arrangement of the smectic layers with respect to the film surface after irradiation with elliptically polarized light is shown in Figure 7.

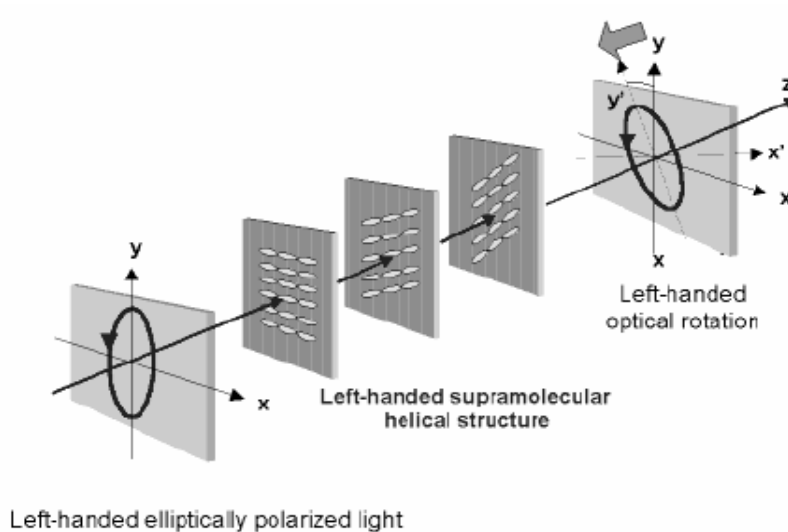


Figure 7. Schematic representation of the helical arrangement of the smectic domains after irradiation with elliptically polarized light.

In the last years Angiolini and co-workers have synthesized and investigated several methacrylic polymers bearing in the side chain a chiral moiety of one prevailing absolute configuration, interposed between the main chain and the trans-azoaromatic chromophore, substituted or not in the 4' position by an electron-withdrawing group [26].

The simultaneous presence of azoaromatic and chiral functionalities allows the polymers to display both the properties typical of dissymmetric systems (optical activity, exciton splitting of dichroic absorptions), as well as the features typical of photochromic materials (photorefractivity, photoresponsiveness, NLO properties).

The CD spectra of the investigated polymers, both in solution and as films, are characterised by two intense dichroic signals of opposite sign and similar intensity. Such behaviour, typical of exciton splitting determined by cooperative interactions between side chain azobenzene chromophores arranged in a mutual chiral geometry of one prevailing handedness, is attributed to the presence of a chiral moiety that favours the adoption of a chiral conformation of one prevailing helical handedness, at least within chain segments of the macromolecules in solution.

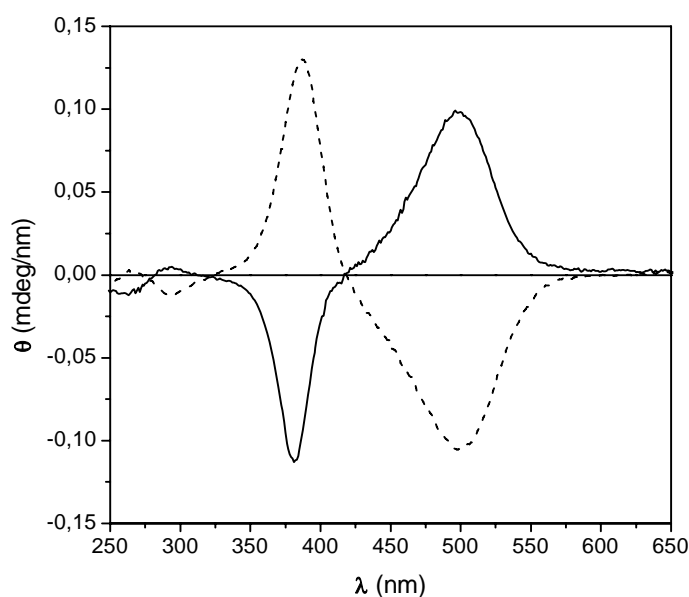


Figure 8. CD spectra of a thin film (340 nm) of poly[(*S*)-**MAP-C**] on fused silica, as prepared (full line) and after a cycle of ordering and erasing (dashed line) with LP and CP-L light at 488 nm ($I=100 \text{ mWcm}^{-2}$).

Monitoring the CD spectra of the films, it was discovered a surprising effect given by irradiation with the left CP (CP-L) pump radiation. As shown in Figure 8, after a cycle of ordering and erasing with LP and CP-L light at 488 nm, respectively, the CD spectrum of a native thin film of poly[(*S*)-**MAP-C**] displays a net inversion of sign, which is particularly evident for the excitonic doublet in the visible region. The two spectra actually appear as mirror images of each other. The observed effect is reversible, and the original shape of the CD spectrum can be substantially restored by pumping with right CP (CP-R) radiation.

Surface grating

Irradiation of the azo polymer films for a longer period of time than that required for photoinduced orientation produces an unexpected modification of the film surface. Gratings with depths of up to one micron could be obtained (Figure 9) and more than one grating can be inscribed consecutively on the same spot on the polymer film.

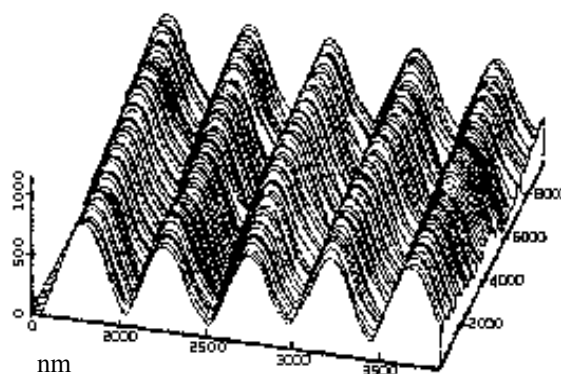


Figure 9. Atomic force microscope surface profile of an optically inscribed surface grating

These surface relief gratings (SRG) could be inscribed on any polymer containing bound azobenzene groups, while no other photosensitive and photochromic groups would be amenable to such inscription.

The depth of the surface profile was shown to depend, at least for some polymer films, on the molecular weight of the polymer [27].

Optical erasure of the SRG was found to depend on the polarization of the erasing beam, and then it is possible to assume that the gratings “memorize” the polarization states of the light that created them. The grating efficiency also depends on the film thickness, which has a lot of (yet not explained) implications on the role of the substrate in the massive motion mechanism [28].

As mentioned above, a variety of materials is amenable to inscription of SRG, as long as they contain some azobenzene groups that isomerize and induce the massive material movement [29].

The orientation of the azobenzene groups in the SRG obtained by massive material motion can be used for many applications in nano-technology [30].

Carbazole containing polymers

Two waves of interest in carbazole-containing polymers can be distinguished. The beginning of the first wave dates back to the sixth decade of the last century. A lot of interest in these polymers was caused by the discovery of photoconductivity in poly (N-vinylcarbazole) (PVK) [31].

Since then numerous carbazole-containing polymers have been described in literature [32].

The ongoing peak of interest in carbazole containing polymers is connected mostly with the discovery of polymeric light emitting diodes and organic photorefractive materials [33, 34]. In the recent investigations of organic electroluminescent devices and photorefractive materials, an important role belongs to the carbazole-containing polymers.

In all these fields of application photoconductive properties of carbazole-containing polymers or their ability to transport positive charges (holes) are exploited.

Carbazole-based compounds are attractive as photoconductors or charge-transporting materials for the following reasons:

- Carbazolyl groups easily form relatively stable radical cations (holes);
- Some carbazole-containing compounds exhibit relatively high charge carrier mobilities;
- Different substituents can be easily introduced into the carbazole ring;
- Carbazole-containing compounds exhibit high thermal and photochemical stability;
- Carbazole is a cheap raw material readily available from coal–tar distillation.

Since carbazole-containing polymers constitute an important group of photoconductive materials much attention is paid to the carbazole-based compounds in studies reviewing photoconductive polymers and organic photoreceptors [35].

During the last decade a new class of amorphous, film-forming photoconductive and charge-transporting materials appeared.

Photoconductivity

The process of photoconductivity involves several steps [35a].

1. Absorption of radiation and formation of excitons

The first step to charge generation is the absorption of radiation. At low light intensities photoconductive materials are truly photoconductive only in the range of the wavelength of absorption. Since carbazole absorbs only in the UV range, PVK and other polymers containing electronically isolated carbazolyl groups are photoconductive only in the UV range. Thus, in order to produce charge carriers by visible light sensitizing dyes or electron acceptors forming coloured charge transfer complexes have to be added.

2. Generation of charge carriers

The active groups are excited by absorption of light and form closely bound electron-hole pairs, i.e. excitons. The excitons are captured and dissociated at the donor/acceptor sites as a result of functional groups that are polarized and appropriately to cause charge separation. The key process that determines the overall photogeneration efficiency is the electric field induced separation of excitons into free charge carriers. Both intrinsic and extrinsic photogeneration of charge carriers in polymers under illumination is discussed in detail in the review of Nespurek et al. [36].

3. Injection of carriers

An injection of carriers occurs only if an extrinsic photogenerator is used together with a charge transporting material. Usually dye particles are dispersed in a polymer matrix or evaporated on top of a conductive substrate and then covered with the charge-transporting polymer. The carriers are generated in the visible light-absorbing material and injected into the polymer. Charge injection, as well as photogeneration and charge transport, is electric field-dependent.

4. Carrier transport

The photogenerated or injected charge carriers move within the polymer under the influence of electric field. In this process the photoconductive species, for example carbazole groups in PVK, pass electrons to the electrode in the first step and thereby become cation radicals. Cation radicals of PVK are stabilised by the charge (hole) resonance among more than two neighbouring chromophores [37]. The transport of

carriers can now be regarded as a thermally activated hopping process, in which the hole hops from one localised site to another in the general direction of the electric field (Figure 10).

The moving cation radical can accept an electron from the neighbouring neutral carbazole group which in turn becomes a hole. Actually the hole moves within the material while electrons only jump among neighbouring species. In a more chemical terminology, hole transport can therefore be described as a series of redox reactions among equivalent groups.

5. Recombination

Coulombic forces eventually cause recombination of free electrons and holes at recombination sites in the circuit. This process competes with the generation of charge carriers.

6. Trapping

During transit, the carriers do not move with uniform velocity, but reside most of the time in localised states (traps) and only occasionally are released from these traps to move in field direction. The traps can be shallow or deep. These terms are only relative, and refer to the release times. Shallow traps are those from which carriers are released in the time of experiment. The trapping process is responsible for the extremely low charge carrier mobilities in most of the polymers. These mobilities are usually electric field and temperature dependent.

For the characterisation of charge-transport properties two established methods exist: the time of-flight (TOF) technique based on transient photocurrent measurements and the xerographic method based on photoinduced discharge measurements.

QuickTime™ and a
decompressor
are needed to see this picture.

Figure 10. Principles of carrier transport

Poly[N-vinylcarbazole] (PVK)

PVK, a vinyl aromatic polymer prepared by polymerization of N-vinylcarbazole (NVK), is the first and the most widely studied organic polymeric photoconductor.

The polymerisation of NVK is largely controlled by the electronic and steric influence of the carbazole group. Although the electronegative nitrogen atom withdraws electrons from the double bond through an inductive effect, the mesomeric effect of nitrogen which donates its unshared electron pair, offsets the electron withdrawing effect and creates an electron-rich conjugated system. As a result, NVK readily polymerises by cationic initiation and fails to polymerise anionically. Radical polymerization was used in the manufacturing of the material that is marketed by BASF (Luvicanw) and by General Aniline and Film Corporation (Poelectronw).

Apart from the above-mentioned methods of initiation, polymerization of the monomer can be initiated by Ziegler–Natta initiators, by charge transfer and electrochemical processes, as well as by irradiation with γ rays. The polymerization reactions of NVK can be performed in bulk, in solution, in suspension, in solid crystalline state, or as a vapour deposition process.

Due to the bulkiness of the carbazole groups, main chain and side group motions are severely restricted in PVK. The chains are stiff and the polymer has a glass transition temperature of 227 °C which is among the highest known for vinyl polymers. PVK exhibits an excellent thermal stability up to at least 300 °C. Unfortunately this property has never been fully utilized because of the extreme brittleness of the material. Many attempts have been made to improve the mechanical and processing characteristics of PVK by plastification, orientation, blending and copolymerization.

Poly(N-vinylcarbazole) is soluble in common organic solvents like toluene, chloroform and tetrahydrofuran.

A detailed analysis of electronic transitions in the polymer is given by Johnson [38]. Four distinct bands attributed to π – π^* electronic transitions are observed at 345 nm (1L_b), 295 nm (1L_a), 262 nm (1B_a) and 237 nm (1B_b).

Even in dilute solutions fluorescence spectra of PVK are broad and structureless. It is now generally accepted that singlet state emission of this polymer results from the radiative decay of two spectrally distinct excimers [39]. The long wavelength emission

(420 nm) with a lifetime of about 42 ns results from so-called sandwich-like excimer and the high energy emission (λ_{max} at 380 nm) is attributed to another excimer of partially eclipsed configuration. Excimer formation is a loss process from the point of view of photogeneration. Energy migration from a light-excited chromophore to a carrier generation site plays an important role in the charge generation of photoconductivity. Many studies have been carried out in order to clarify the migration process in PVK and related polymers [40]. The trapping of migrating energy at the excimer-forming sites causes a drop in the charge carrier mobility.

Since PVK absorbs only in UV region of spectrum, another component is needed to induce photoconductivity in the visible range, which accomplishes carrier generation either alone or in conjunction with PVK.

2,4,7-Trinitrofluorenone (TNF) is the most widely studied and one of the most effective dopants that renders PVK photosensitivity in the visible range. Although both donor (PVK) and acceptor (TNF) absorb only in the short wavelength region, 450 nm, the charge transfer absorption bands extends up to 700 nm, providing photoresponse throughout the entire visible range [41]. Addition of TNF or some other electron acceptor compounds not only induces photoconductivity in the visible region but also changes the nature of charge carriers. As mentioned above, in pure PVK charge carriers are holes. Upon TNF addition another type of charge carriers, i.e. electrons, appears. When the acceptor concentration increases, the hole mobility decreases whereas electron mobility increases. Doping of PVK with an effective sensitizer can increase its photoconductivity up to the level of the commercial organic photoconductors. Such effective dopants are fullerenes. Fullerenes are responsible for the charge generation in these systems, however initially it was not clear whether the charge-generating process is due to the excitation of fullerene (followed by electron hopping from carbazole to fullerene) or due to the direct excitation of a fullerene/PVK charge transfer complex. More recent data show that the electric field effect on fluorescence quenching and charge generation efficiency correlate well with each other for these systems [42]. These results clearly establish the singlet state of the CT complex as the precursor for charge carriers.

PVK can readily be converted into a p-type semiconductor. Oxidation of polymer films

by chemical [43] or electrochemical [44] methods introduces radical cations and the films become coloured and conductive. Conductivity is a function of degree of oxidation. Electrochemical anodic oxidation converts up to 50% of the carbazolyl groups and the conductivity increases. Other methods of increasing conductivity are molecular doping with iodine [45] or ion implementation [46].

Poly(meth)acrylates containing side-chain carbazole

Polyacrylates and polymethacrylates in which the carbazole groups are separated from the polymer backbone by alkyl spacers of different length have been synthesized by free-radical polymerization of the monomers with AIBN as initiator [32].

Poly(2-(N-carbazolyl)ethylmethacrylate) has been synthesized from the corresponding methacrylate monomer by free-radical polymerization [47]. The polymer has no excimer-forming sites and even its films show a clear monomer fluorescence [48]. A high efficiency of energy migration is characteristic for this polymer. The polymer exhibits charge carrier mobility comparable to that of PVK. A detailed investigation of the photophysical properties of acrylic and methacrylic polymers bearing side chain carbazole and comparison with those of PVK later enabled Ledwith [49] to formulate the rule that carbazole-containing polymers have no excimer-forming sites except when the carbazole units are directly bound to the polymer main chain.

Strohriegl [50] has compared the synthesis of polyacrylates and polymethacrylates with pendant carbazole by two different methods. These methods were free radical polymerization of the corresponding (meth)acrylates and the polymer analogous reaction of N-hydroxylcarbazoles with poly(meth)acryloylchloride. The molecular weights of the polymers obtained by free-radical polymerization with AIBN in toluene solution were rather low and all polymers exhibited a broad molecular weight distribution. The reason is due to low solubility of these polymers in the polymerization medium toluene. In more polar solvents like THF, the molecular weight is limited by chain transfer reactions. High molecular weight poly(meth)acrylates are obtained by analogous reaction of N-hydroxyalkyl-carbazoles with poly(meth)-acryloylchloride. IR and ¹H NMR spectroscopy, as well as elemental analysis show that the reaction yields poly(meth)acrylates with an almost quantitative degree of substitution.

Photorefractive materials

Photorefractive (PR) materials have been extensively studied in the frame of photonic and optoelectronic technologies because they offer the possibility of high optical nonlinearities with low laser power (mW) and therefore they are suitable for applications in the field of dynamic holography, optical signal processing, etc.

PR materials studied up to this date belong essentially to these classes:

- inorganic crystals
- organic materials:
 - polymers and amorphous glasses
 - liquid crystals

The PR effect was first observed in 1966 in a LiNbO₃ crystal, a discovery that launched extensive studies of the effect in inorganics [51]. Until 1990, all PR material have been proposed and demonstrated for PR inorganics, including high-density optical data storage, image processing (correlation, pattern recognition), phase conjugation, optical limiting, simulations of neural networks and associative memories, and programmable optical interconnection [52].

However, the difficult crystal growth and sample preparation required for inorganic PR crystals has limited their use in these applications.

A considerable progress has been made in photorefractive polymers and polymer composites and low molecular mass glasses since the first observation of photorefractivity in organic materials [53].

In contrast with inorganic, organic PR materials and, in particular, polymeric and/or glassy PR materials, offer ease and flexibility of fabrication and control over the properties, which serves as one of the reasons for pursuing the development of organic PR materials.

Organic photorefractive materials are emerging as promising photonic materials for a variety of applications including holographic storage, real time optical processing, imaging, non-destructive testing and phase conjugation [54].

Current status and future prospects of photorefractive polymers are described in various reviews [55].

Inorganic crystals.

Since the early works with LiNbO_3 e LiTaO_3 , PR gratings have been observed in many other inorganic materials, including BaTiO_3 , KNbO_3 , $\text{K}(\text{TaNb})\text{O}_3$, $\text{BaNaNb}_5\text{O}_{15}$, $\text{Bi}_4\text{Ti}_3\text{O}_{12}$, $\text{Bi}_4\text{Ge}_3\text{O}_{12}$, $\text{Sn}_2\text{P}_2\text{S}_6$, $(\text{Zr,Ti})\text{O}_3$ ceramics, etc [51]. Inorganic PR crystals are characterized by electronic band structures which are defined over the entire crystal. The absorption of a photon transfers an electron into the conduction band of the crystal. The excited electron is free to migrate (i.e. diffuse), the charge generation efficiency is generally close to one and it is only slightly field dependent. Due to the electronic band structure, the conductivity of inorganic PR crystals is rather high. On the other hand, traps (represented mainly by ionic impurities) are naturally present at low concentrations in PR crystals, limiting the amplitude of the internal space charge field together with the high dielectric constants which usually accompany high electro-optic coefficients.

The periodic structure of inorganic crystals can be altered by an electric field via the piezoelectric effect. Therefore, depending on the geometry, the presence of an internal space charge field can induce a strain in a PR crystal (due to the piezoelectric effect), and this strain can in turn affect the refractive index of the medium through the photoelastic effect. Thus the PR response of inorganic crystals arises from both the Pockels and the piezoelectric effects, even though the last one usually has only a small part in the process.

Many potentially important applications have been proposed and demonstrated for PR inorganic crystals, including high density optical data storage, image processing (correlation, pattern recognition), phase conjugation, optical limiting, simulations of neural networks and programmable optical interconnection. However, these materials can be used for PR applications only as single crystals, which are quite difficult to grow and expensive, a problem that has been limiting their use.

Photorefractive polymers

In 1990, the first observation of the PR effect in an organic material utilized a carefully grown nonlinear organic crystal 2-(cyclooctylamino)-5-nitropyridine (COANP) doped with 7,7,8-tetracyanoquinodimethane (TCNQ) [52]. The growth of high-quality doped

organic crystals, however, is a very difficult process because most dopants are expelled during the crystal preparation.

Polymeric materials, on the other hand, can be doped with various molecules of quite different sizes with relative ease. Further, polymers may be formed into a variety of thin-film and wave guide configurations as required by the application. The second-order nonlinearity of polymers containing nonlinear chromophores can be produced by poling, whereas in crystals one may only consider the relatively rare subset of crystals with noncentrosymmetric crystal structures.

Photorefractive effect

The photorefractive effect can occur in certain materials which both photoconduct and show a dependence of the optical refractive index upon electric field. The ingredients necessary for producing a PR-material are therefore: a photoionizable charge generator, a transporting medium, trapping sites, and a dependence of the refractive index upon space-charge field.

However, the simple presence of these elements in a material does not guarantee that any diffraction grating produced by optical illumination arises from the photorefractive effect.

When light is incident on a photorefractive material, if the incident light is not uniform in intensity, photogenerated charges will migrate through the transporting component from the illuminated area to the dark area, where these charges get trapped by trapping centers. The resulting charge redistribution creates space charge fields in the material. These fields produce measurable changes in the refractive index through the linear EO effect in non-centrosymmetric materials. The mechanism behind the photorefractive effect is summarized in Figure 11.

The first physical process required for the PR effect is the generation of mobile charge in response to the spatially varying illumination. This may be viewed as the separation of electrons and holes induced by the absorption of the optical radiation, denoted as plus and minus charges in the figure. In organic materials, this effect is likely to be strongly field dependent.

The second element for the PR effect is transport of the generated charges, with one

carrier being more mobile than the other. In Figure 11b, the holes are shown to be more mobile, which is the more common case for organics (if both carriers are equally mobile, the resulting space-charge distribution could have zero internal electric field and hence no PR effect). The physical processes giving rise to charge transport are either diffusion due to density gradients, or drift in an externally applied electric field. Since most polymeric materials with sufficient optical transparency are relatively good insulators, the ability of generated charges to move by diffusion alone is quite limited. Drift is the dominant mechanism for charge transport which stimulates charge to hop from transport molecule to transport molecule.

The third element for the PR effect, especially when long grating lifetimes are desired, is the presence of trapping sites which hold the mobile charge. In real materials, the exact identity of the trapping sites is seldom known in detail. In general terms, a trapping site is a local region of the material where the mobile charge is prevented from participating in transport for some period of time. For example, in a hopping picture, a site with lower total energy for the charge may act as a trap, and the lifetime of the carrier in the trap will be determined by the trap depth compared to thermal energies.

After separation of charge carriers occurs, the resulting space-charge density is shown in Figure 11C. Via Poisson's equation of electrostatics, such a charge distribution produces a sinusoidal space-charge electric field as shown in Figure 11d. Since Poisson's equation relates the spatial gradient of the electric field to the charge distribution, the resulting internal electric field is shifted in space by 90° relative to the interference pattern of the incident light.

Finally, if the optical index of refraction of the material changes in response to an electric field, a spatial modulation of the index of refraction results.

According to the requirements and the mechanism of the photorefractive effect, photorefractive materials must have two main functions, photoconductivity for the establishment of a space charge field and the linear EO effect for the formation of a refractive index grating.

QuickTime™ and a
decompressor
are needed to see this picture.

Figure 11. Schematics of the build-up of photorefractive effect. (a) charge generation; (b) charge transport; (c) charge trapping; (d) space-charge field formation and refractive index modulation.

Photoconductivity in organic materials consists of photocharge generation and charge transporting processes. In amorphous organic photorefractive materials, photocharges can be induced by addition of appropriate sensitizers, such as organic dyes; generated charges can be transported through the hole transporting component, such as carbazole and triphenylamine; the defects in the materials can play a trapping role for these

charges. Second-order NLO chromophores can provide the linear EO effect when the dipole orientation of chromophores is achieved by an applied electric field.

Thus the multifunctionality of organic photorefractive materials can be achieved by two molecular design approaches: the guest–host composite approach and the fully functional polymeric material approach.

Guest-host polymers.

Trapping centres, which represent one of the most important constituents of PR materials, are naturally present in sufficient amounts in polymers, while sensitizer molecules, necessary to create movable charges upon photon absorption, may be introduced by adding appropriate substances to the polymer solution.

The chemical structures of some of the most often used building-block molecules used in order to design PR polymeric materials are shown in Figure 12.

Examples of sensitizers are: 2,4,7-trinitro-9-fluorenone (TNF), C60 and its more soluble derivative PCBM, which are often used in the red region of the spectrum, while, in the near IR, TNFDM is the most common choice. The charge created by photoionization of the sensitizer moves by hopping through charge transport agents (CTA). Large concentrations of CTA of the order of 30 – 40 wt. % are necessary in order to increase the hopping probability. The alternative to CTA is the use of a polymer host where charge transport can occur along the polymer chain itself.

Among photoconducting matrices, PVK, PSX and modified PPV are the most common. Finally, the non-linear element which produces a change in the refractive index in response to the internal space-charge field is provided by doping with NLO chromophores.

In some cases the NLO agent can also provide the necessary photosensitivity, so that doping with an additional sensitizer is not necessary.

The most used chromophores are based on azo-dyes and derivatives of oxopyridone, dicyanostyrene, dicyanomethylenedihydrofuran, pyridone and rigidized polyene. In general, high concentration (25 – 35 wt. %) doping with NLO chromophores is necessary to achieve optimum performance. However, high doping often has the consequence of a reduced stability of the compound.

The first high performance PR polymer was based on PVK:DMNPAA:ECZ:TNF in the ratio 33:50:16:1 wt. % [56]. N-ethylcarbazole (ECZ) is a plasticizer added in order to decrease the T_g and facilitate the reorientation of the DMNPAA chromophores. This compound exhibits Bragg diffraction efficiencies of nearly 100% and net two-beam coupling gain of 207 cm^{-1} at external fields of $90 \text{ V}/\mu\text{m}$ in a $105 \mu\text{m}$ thick sample. The performance of this compound has been approached or equalled later by other compounds based on PVK or PSX polymers [57].

More recently, a compound based on the inert polymer PTCB and DHADC-MNP, as NLO chromophore, showed a quite high gain of 225 cm^{-1} for an applied field of $50 \text{ V}/\mu\text{m}$ in $105 \mu\text{m}$ thick samples [58]. This compound has excellent thermal stability, and the chromophores play the triple function of charge generator, charge transport agent and electro-optic dye.

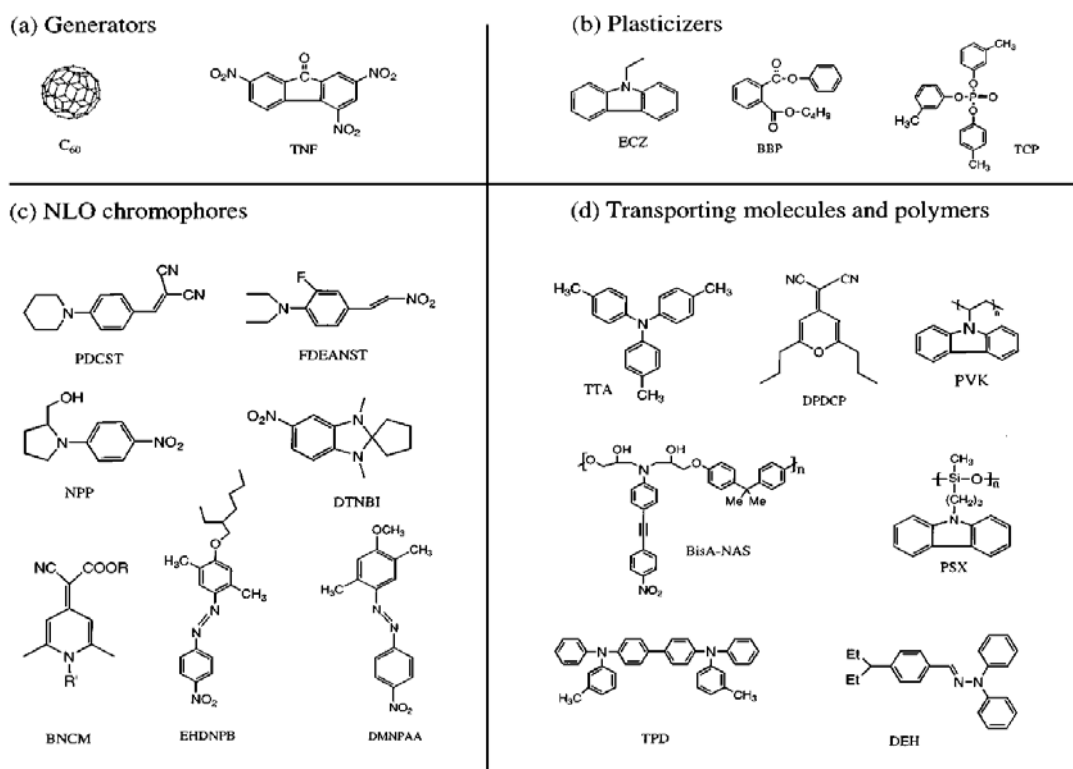


Figure 12. Chemical structures of the most commonly used PR sensitizers, photoconductors, plasticizers, NLO chromophores.

The composite materials approach has the advantage of easy optimization of the multifunctionality by independently varying the nature and concentration of each component.

However, there are inherent problems in phase separation of these doped systems which limit the concentrations of active moieties. In order to overcome this problem, fully functional polymers containing all necessary functional groups either in the polymeric main-chain or in the side-chain have the evident advantage of long-term stability and minimized phase separation. However, the time-consuming chemical synthesis and difficulty in rational design are constant challenges. More recently, amorphous multifunctional and monolithic chromophore approaches to photorefractive materials have also been developed.

Fully functionalized polymers

Fully functionalized PR polymers have attracted attention because they eliminate the problems of phase separation and crystallization and therefore could lead to a better thermal stability and longer life for potential devices. The first fully functionalized PR polymer was reported in 1992 and consisted of a multifunctional polyurethane in which charge generator, charge transport agent, and NLO moieties were incorporated as side chains. This material exhibited a two-beam coupling gain coefficient of only 2.3 cm^{-1} .

Since then, much progress has been made in the development of high-performance fully functionalized PR materials. Among the first polymers to give good efficiency were high T_g prepoled conjugated polymers containing Ru photogenerator complexes, introduced into the polymer backbone [59]. Net gain coefficients of over $\sim 200 \text{ cm}^{-1}$ were obtained but the response time was long (on the order of several hundreds seconds). A very good improvement in response time was obtained in oligothiophenes covalently attached to NLO chromophores (response times of $\sim 40 \text{ ms}$), while polymethacrylates with attached charge transporting carbazole and NLO moieties, sensitized with TNFM, exhibited 100% internal diffraction efficiencies.

Liquid crystals

As already outlined, the most suitable polymers for photorefractivity profit from the strong chromophores reorientational effect that can be observed in compounds with low T_g . Starting from this consideration, the potential for liquid crystals becomes clear. In fact, nematic liquid crystals are ideal for observing the orientational PR effect because of their strong orientational response, and no NLO dopant is required since the liquid crystal itself is the birefringent component. Thus, essentially 100% of the medium contributes to the birefringence rather than a percentage of NLO dopant.

The first investigations of PR effects in doped nematic liquid crystals were performed in 1994 by Rudenko and Sukhov [60]. They used the homeotropically aligned nematic liquid crystal 5CB doped with rhodamine 6G, observed photoconductivity and diffraction efficiency of few % in their holographic experiments.

Since then, the field has witnessed considerable increase in interest and the progress has been rapid. One of the strategies that led to the improvement of the PR performance of liquid crystals was the doping of the material with donor and acceptor molecules, to increase photogeneration efficiency. By using this approach, Wiederrecht et al. [61] were able to demonstrate very high first order diffraction efficiency and gain coefficient in two beam coupling experiments on samples containing perylene and N,N'-di(n-octyl)-1,4,5,8-naphthalenediimide (NI), as electron donors and acceptor, respectively, producing ions and hence photoconductivity by photoinduced electron transfer reactions. An even larger gain coefficient was measured by Khoo et al. [62] in pentylcyanobiphenyl liquid crystal doped with a small amount of C60, showing that doping with fullerenes enhances the PR properties of liquid crystals, as in polymer composites. In addition, it was recently shown that PR sensitivity of LCs can be improved by doping them with carbon nanotubes [63].

To increase the trap density and improve charge carrier mobility, it was proposed to stabilize the LC with low concentrations of a polymer [64, 65]. In this approach, a polymeric monomer is dissolved in an aligned liquid crystal and subsequently photopolymerized with UV radiation in the presence of a photoinitiator. Such materials are referred to as polymer stabilized liquid crystals. Moreover, it was found that PR in LCs can be promoted by surface activation, e.g., by using a photoconductive substrate such as a PR crystal [64] or thin layers of photoconductive polymers on the ITO

surfaces of the LC cell [65]. Other techniques, such as the prealignment of the LC with a magnetic field [66] and the use of various alignment layers [67], also affected PR performance of the LC.

The PR effect was recently observed also in chiral smectic phase, where a faster mechanism of field induced molecular reorientation is involved[68].

Carbazole photorefractive composite materials

Polymers containing the carbazole moiety as charge transporting agent, bifunctional chromophores or multifunctional chromophores have been widely studied in the last years.

Polymers containing side chain azocarbazole functionalities have been prepared by the radical polymerization of the corresponding methacrylate monomers with AIBN as initiator [55, 69]. Films of these polymers were shown to be suitable for photoinducing birefringence reversibly with polarized light, as well as for the inscription of photorefractive diffraction gratings after electric field poling.

In particular, in 1996 Natansohn et al. [70] synthesized poly{(4-nitrophenyl)-3-[N-[2-(methacryloyloxy)ethyl]carbazolyl]}diazene and its photoinduced birefringence, diffraction grating, and photorefractive asymmetric two-beam gain coupling were studied. The monomer was obtained by performing azo coupling in a two-phase water/dichloromethane system in the presence of a phase transfer catalyst. Photoinduced birefringence of up to 0.09 was observed and diffraction efficiencies of up to 25% were obtained. Atomic force microscopy studies revealed that the grating profile exhibited a sinusoidal shape. Asymmetric two-beam coupling is observed, indicating photorefractive properties, but the energy transfer phenomena are more complex, involving also diffraction by the photoinduced gratings. The combination of these three optical properties (photoinduced birefringence, surface gratings, and two-beam couplings) is believed to be unique and may eventually produce an all-optical device built of a single polymer film.

A series of copolymers of carbazole-containing poly(meth)acrylates with electron-withdrawing co-monomers has been recently reported. Thus, 2-(N-carbazolyl) ethyl acrylate has been copolymerized with 2-(2-carboxyl-4,5,7-trinitrofluorenyl)ethyl

acrylate and 2-(3,5-dinitrobenzoyloxy)ethyl methacrylate [71]. Due to the inhibition of radical polymerization by acceptor monomers with nitro groups, molecular weights of the copolymers obtained are usually low. These copolymers form intramolecular charge transfer complexes which are deeply coloured and extend the spectral response of these materials into the visible and near infrared region. Furthermore, problems with the toxicity of acceptor molecules like TNF may be overcome by covalent fixation of acceptor groups to a polymer backbone.

Fully functionalized photorefractive terpolymers were prepared by the terpolymerization of 6-(9-carbazolyl)hexyl methacrylate, NLO-functionalized methacrylate and dodecyl methacrylate [72]. The number average molecular weight (M_n) of these terpolymers ranged from 8000 to 26 000 and their T_g ranged from 47 to 62 °C. It was reported [72] that the terpolymers doped with 1 wt% of (2,4,7-trinitrofluorenylidene)malononitrile showed good photorefractive properties. A net two-beam coupling gain and a diffraction efficiency of 60% were observed at 58 V/mm.

Tamura et al. [73, 74] have synthesized polyacrylates and polymethacrylates having carbazole and tricyanovinylcarbazole side groups. 5-(N-carbazolyl) pentyl methacrylate and acrylate were polymerized using AIBN as initiator. The resulting polymer was reacted with tetracyanoethylene to tetracyanovinylate with ca. 20% of the carbazole units. Photoconductivity, the existence of photocarrier traps, and the electro-optic effect which are required properties for the photorefractive effect have been demonstrated in these polymers without using additional agents such as sensitizers or carrier transport agents. A number of charge transfer copolymers with carbazole groups as electron donors and 2,4,6-trinitrobenzoyloxy or 3,5-dinitrobenzoyloxy groups as electron acceptors have been prepared by Percec et al. [76] who used these materials for fundamental studies on the influence of charge transfer complexation on the mechanical properties of these polymers.

Christiaan Engels et al. [77] have synthesized and characterized a new series of infrared-sensitive photorefractive polymethacrylates containing a Disperse Red type chromophore and carbazole as charge transport agent.

No internal plasticizer was used, but the spacer lengths were varied to reduce the glass transition temperature. A T_g close to room temperature was observed for the

copolymers with hexyl and undecyl spacer lengths. Four-wave mixing and two-beam coupling experiments conducted at 780 nm showed excellent photorefractive properties, with gain coefficients exceeding 150 cm^{-1} and complete internal diffraction at a field of $52 \text{ V } \mu\text{m}^{-1}$. The only drawback here is the slow grating formation of these materials. The improvement of the photorefractive response of these polymers compared to copolymer with internal plasticizer is attributed to the higher polarity and number density of the pendant chromophore.

Characterization of organic photorefractive materials

a. Photoconductivity for the establishment of the space charge field

Photoconductivity in amorphous organic materials consists of photocharge generation and charge transport processes. The charge generation molecules absorbing photons produce electron-hole pairs which, under the influence of a driven electric field, dissociate to produce electrons and holes. These free carriers then migrate through the material via a hopping mechanism by the charge transport components.

Measurement of these properties is an important first step for the characterization of a potential organic photorefractive material. The photocharge generation quantum yield and the photoconductivity can be measured using a simple photocurrent technique.

b. Two-beam coupling (2BC) measurements

In order to unambiguously distinguish between the photorefractive effect and other types of gratings, two-beam coupling measurements must be performed. The phase shift between the refractive index grating and the light interference pattern can be determined by two-beam coupling techniques. This phase shift, or nonlocal nature of the photorefractive effect, gives rise to an asymmetric energy transfer between the two writing beams which does not occur in any of the other refractive index change processes. Therefore, the nonlocal character of the photorefractive effect can be directly confirmed by an observation of the phase shift or the asymmetric energy transfer in two-beam coupling experiments.

The typical geometry of the 2BC experiment is shown in Figure 13a. A PR polymeric sample consists of two conductive but transparent indium tin oxide (ITO)-coated glass slides with a PR polymer film of 30-100 μm thickness in between. Optical beams 1

(“probe” or “signal”) and 2 (“pump”) are incident at angles ϕ_1 and ϕ_2 respectively, and interfere in the PR material, creating a nonlocal diffraction grating. Then, the same beams 1 and 2 partially diffract from the grating they have just created (beams 1 and 2 in the inset of Figure 13a). Because of nonlocality of the grating, one diffracted beam (for example, 1 ϕ) interferes destructively with its companion beam 2, while the other diffracted beam 2 interferes constructively with beam 1. As a result, the beam 1 is amplified (energy gain) while the beam 2 is attenuated (energy loss). It should be emphasized that it is important that the energy transfer persists in *steady-state* because *transient* asymmetric energy exchange is known to occur in materials with local response (photochemistry, absorption and thermal gratings). In inorganic crystals, the direction of energy transfer depends on the sign of the electrooptic coefficient (which is fixed, so that the refractive index change is linear in electric field) and the sign of the charge carrier. In low T_g organic materials, because the materials are poled in situ and the refractive index change is quadratic in local electric field, the energy transfer direction is determined by the direction of majority carrier drift in the electric field and therefore can be reversed by changing the polarity of electric field. As a result of the OE effect, there is another way of reversing the energy transfer, which is to change the polarization of writing beams 1 and 2.

The 2BC experiment involves measurement of the transmitted beam intensities as a function of time, E_0 , K , angles, and so forth.

c. Four-wave mixing measurements

The four-wave mixing experiments reveal a large amount of information about photorefractive materials. Using four-wave mixing techniques, grating formation dynamics can be studied. The diffraction efficiency, a key parameter judging from the performance of the photorefractive effects can also be measured by a four-wave mixing technique (Figure 13b).

QuickTime™ and a
decompressor
are needed to see this picture.

Figure 13. Experimental configuration used in (a) twobeam coupling; (b) four-wave mixing geometry.

References

- [1] H. Rau, Photochemistry and Photophysics, CRC Press, Boca Raton, 1990, Vol. 11, Chapter 4.
- [2] J.F. Rabek, Mechanisms of Photophysical Processes and Photochemical Reactions in Polymers, 1987, 377.
- [3] G. Kumar, D. Neckers, Chem. Rev., 1989,89, 1915.
- [4] S. Kwolek, P.W. Morgan, J.R. Schaefgen, Encyclopedia of Polymer Science and Engineering, 1985, Vol. 9, P 1.
- [5] G.R. Mohlmann, C.P.J.M. Van Der Vorst, Side Chain Liquid Crystal Polymers, Mcardle, C. B., Ed., Plenum and Hall, Glasgon, 1989, Chapter 12.
- [6] [6a] G.S. Attard, J.S. Dave, A. Wallington, C.T. Imrie, F.E. Karasz, Makromol. Chem. 1991,192, 1495. [6b] T. Ikeda, S. Hasegawa, T. Sasaki, T. Miyamoto, M.P Lin, S. Tazuke, Makromol. Chem. 1991,192, 215. [6c] T. Ikeda, S. Horiuchi, D.B Karanjit, S. Kurihara, S. Tazuke, Macromolecules 1990, 23, 36. [6c] A. Angeloni, D. Caretti, M. Laus, E. Chiellini, G. Galli, J. Polym. Sci., Part A, Polym. Chem. 1991, 29, 1865. [6d] S. Ujiie, K. Iimura, Macromolecules 1992,25, 3174. [6e] M. Sisido, R. Kishi, Macromolecules 1991, 24, 4110. [6f] H. Allcock, C. Kim, Macromolecules 1989,22,2596.
- [7] [7a] A.V. Tenkovtsev, O.N Piraner, A.Y. Bilibin, Makromol. Chem. 1991, 192, [7b] K. Iimura, N. Koide, R. Ohta, M. Takeda, Makromol. Chem. 1981,182, 2563.
- [8] V. Shibaev, A. Bobrovsky, N. Boiko, Prog. Polym. Sci., 2003, 28, 729
- [9] D. Eaton, Science 1991, 253, 281
- [10] [10a] S. Stupp, H. Lin, H., Wake, D. Chem. Mater. 1992,4, 947. [10b] H.K. Hall, T. Kuo, T.M Leslie, Macromolecules 1989, 22, [10c] M.L. Schilling, H.E. Katz, Chem. Mater. 1989,1,668. [10d] W. Kohler, D.R. Robello, C.S. Willand, D.J. Williams [10e] J.R. Hill, P. Pantelis, F. Abbasi, P.J. Hodge Appl.Phys. 1988, [10f] C. Ye, Z. Feng, J. Wang, H. Shi, H. Dong, Mol. Cryst. Liq.
- [11] [11a] Z. Sekkat, M. Dumont, Appl. Phys. B. 1992, 54, 486. [11b] H.E. Katz, G.

- Scheller, T.M. Putvinski, M.L. Schilling, W.L. Wilson, C.E.D. Chidsey, *Science* 1991,254, 1485. [11c] K. Kajikawa, T. Anzai, H. Takezoe, A. Fukuda, S. Okada, Matsuda, H. Nakanishi, T. Abe, H. Ito, *Chem. Phys. Lett.* 1992,192, 113.
- [12] D. Williams, *Thin Solid Films* 1992, 216, 117.
- [13] V. Shibaev, A. Bobrovsky, N. Boiko, *Prog. Polym. Sci.* 2003, 28, 729–836
- [14] [14a] T. Todorov, L. Nikolova, N. Tomova, *Appl. Opt.* 1984, 23,4309. [14b] T. Todorov, N. Tomova, L. Nikolova, *Opt. Commun.* 1983, 47, 123.
- [15] A. Natansohn, S. Xie, P. Rochon, *Macromolecules* 1992, 25, 5531.
- [16] A. Natansohn, P. Rochon, J. Gosselin, S. Xie, *Macromolecules* 1992,25, 2268
- [17] J. Griffiths, *Chem. SOC. Reo.*, 1972, 481.
- [18] Z. Sekkat, M. Dumont, *Appl. Phys. B.* 1992, 54, 486
- [19] H. Yamamoto, A. Nishida, *Polym. Internat.* 1991, 24, 145.
- [20] M. Sisido, Y. Ishikawa, M. Harada, K. Itoh, S. Tazuke, *Macromolecules* 1991, 24, 3993.
- [21] M. Muller, R. Zentel, *Makromol. Chem.* 1993, 194, 101.
- [22] M. Muller, R. Zentel, *Macromolecules* 1994, 27, 4404.
- [23] G. Maxein, R. Zentel, *Macromolecules* 1995, 28, 8438.
- [24] L. Nikolova, T. Todorov, M. Ivanov, F. Andruzzi, S. Hvilsted, P.S. Ramanujam, *Opt. Mater.* 1997, 8, 255
- [25] L. Nikolova, L. Nedelchev, T. Todorov, T. Petrova, N. Tomova, V. Dragostinova, P.S Ramanujam, S. Hvilsted, *S. Appl. Phys. Lett.* 2000, 77, 657.
- [26] [26a] L. Angiolini, D. Caretti, L. Giorgini, E. Salatelli E, *J. Polymer Sci., Part A Polym. Chem.*, 1999, 37, 3257. [26b] L. Angiolini, D. Caretti, L. Giorgini, E. Salatelli, *Polymer* 2001, 42, 2005. [26c] L. Angiolini, R. Bozio, L. Giorgini, D. Pedron, G. Turco, A. Daurù, *Chem. Eur. J.*, 2002, 8, 4241. [26d] L. Angiolini, T. Benelli, L. Giorgini, A. Painelli, F. Terenziani, *Chem. Eur. J.* 2005, 11, 6053. [26e] L. Angiolini, T. Benelli, R. Bozio, A. Daurù, L. Giorgini, D. Pedron, E. Salatelli, *Eur. Polym. J.* 2005, 41, 2045. [26f] L. Angiolini, T. Benelli, R. Bozio, A. Daurù, L. Giorgini, D. Pedron, E. Salatelli, *Macromolecules* 2006,39,489.

- [27] C. Barrett, A. Natansohn, P. Rochon, *J. Phys. Chem.*, 1996, 100, 8836.
- [28] C. Barrett, P. Rochon, A. Natansohn, *Chem. Phys.*, 1998, 109, 1505.
- [29] F. Lagugnè Labarhet, T. Buffeteau, C. Sourisseau, *J. Phys. Chem. B*, 1998, 102, 2654.
- [30] A. Natansohn, P. Rochon, *Chem. Rev.* 2002, 102, 4139
- [31] [31a] H. Hoegl, O. Sus, W. Neugebauer, *Ger Offen*, 106, 8115. [31b] H. Hoegl *J. Phys. Chem.* 1965, 69, 755.
- [32] J.V. Grazulevicius, P. Strohriegl, J. Pielichowski, K. Pielichowski, *Prog. Polym. Sci.*, 2003, 28, 1297–1353
- [33] J.H. Burroughes, D. Bradley, A. Brown, R. Marks, K. MacKay, R. Friend, P. Burn, A. Holmes, *Nature* 1990, 347, 539.
- [34] K. Meerholz, L. Volodin, L. Sandalphon, B. Kippelen, N. Peyghambarian, *Nature* 1994, 371, 497.
- [35] [35a] M. Stolka, J. Chilton, *Special Polymers for Electronics and Optoelectronics*, 1995, 284. [35b] P. Borsenberger, D. Weiss, *Organic Photoreceptors for Imaging Xerography*, 1998, 768. [35c] J. Mort, G. Pfister, J. Mort, *Electronic Properties of Polymers*, 1982, 215. [35d] H. Naarmann, P. Strohriegl, *Handbook of Polymer Synthesis, Part B*. 1992, 1353. [35e] P. Strohriegl, J.V. Grazulevicius, *Handbook of Organic and Conductive Molecules and Polymers*, 1997, 553 [35f] J.V. Grazulevicius, P. Strohriegl *Handbook of Advanced Electronic and Photonic Materials and Devices*, 2001, 233.
- [36] S. Nespurek, V. Cimrova, J. Pflieger, I. Kminek, *Polym Adv Technol* 1996, 7(5&6), 459.
- [37] [37a] Y. Tsuji, A. Tsuchida, M. Yamamoto, Y. Nishijima, *Macromolecules* 1988, 21, 665. [37b] A. Tsuchida, A. Nagata, M. Yamamoto, H. Fukui, M. Sawamoto, T. Higashimura, *Macromolecules* 1995, 28, 1285.
- [38] G.E. Johnson, *J. Phys. Chem.* 1974, 78, 1512.
- [39] F. C. De Schryver, J. Vandendriesshe, S. Tapet, K. Demeyer, N. Boens *Macromolecules* 1982, 15, 406.
- [40] [40a] A. Itaya, K. Okamoto, S. Kusabayashi, *Bull. Chem. Soc. Jap.* 1977, 50,

- 22 [40b] W. Klopfer N.Y. Ann Acad. Sci. 1981, 366, 373. [40c] H. Masuhara, N. Tamai, N. Mataga Chem. Phys. Lett. 1982, 91, 209. [40d] S. Ito, K. Yamashita, M. Yamamoto, Y. Nishijima Chem. Phys. Lett. 1985, 117, 171.
- [41] J.M. Pearson, M. Stolka Poly(N-vinylcarbazole), Polymer Monographs, Vol. 61, 1981.
- [42] [42a] Y. Wang, Nature 1992, 356, 585. [42b] Y. Wang, R. West, C.H. Yuan, J. Am. Chem. Soc. 1993, 115, 3844. [42c] Y. Wang, Pure and Appl. Chem. 1996, 68, 1475.
- [43] H. Block, M.A. Cowd, S.M. Walker, Polymer 1977, 18, 781.
- [44] R.G. Compton, F.J. Davies, S.C. Grant, J. Appl. Electrochem. 1986, 16, 239.
- [45] G. Safoula, K. Napo, J.C. Bernede, S. Touhri, K. Alimi, Eur. Polym. J. 2001, 37, 843.
- [46] T. Barbaszewski, M. Wiega, E. Lipinska, F. Starzyk, Phys. Stat. Sol. 1986, 94, 419.
- [47] R. Oshima, M. Biswas, T. Wada, T. Uryu, J. Polym. Sci. Part A, Polym. Chem. 1985, 23, 151.
- [48] M. Keyanpour-Rad, A. Ledwith, A. Hallam, A.M. North, M. Breton, C. Hoyle, J.E. Guillet, Macromolecules 1978, 11, 1114.
- [49] A. Ledwith, N.J. Rawley, S.M. Walker, Polymer 1981, 22, 435.
- [50] P. Stroehriegl, Mol. Cryst. Liq. Cryst. 1990, 1983, 261.
- [51] F. S. Chen, J. ADD-Ph. 1967, 38, 3418.
- [52] A. Ashkin, G.D. Boyd, J.M. Dziedzic, R.G. Smith, A.A. Ballmann, K. Nassau, Appl. Phys. Lett. 1996, 9, 72.
- [53] [53a] K. Sutter, P.J. Gunter, Opt. Soc. Am., Part B 1990, 7, 2274. [53b] S. Ducharme, J.C. Scott, J.R. Twieg, W.E. Moerner, Phys. Rev. Lett. 1991, 66, 1846.
- [54] B. Kippelen, N. Peyghambarian, Crit. Rev. Opt. Sci. Tech. 1997, 68, 343.
- [55] [55a] W. E. Moerner, M. S. Silence, Chem. Rev. 1994, 94, 127-155, [55b] O. Ostroverkhova, W. E. Moerner, Chem. Rev. 2004, 104, 3267-3314 [55c] Y. Zhang, T. Wada, H. Sasabea, J. Mater. Chem., 1998, 8(4), 809–828
- [56] K. Meerholz, B. L. Volodin, Sandalphon, B. Kippelen, N. Peyghambarian,

- Nature 1994, 371, 497
- [57] [57a] O. Zobel, M. Eckl, P. Strohrriegl, D. Haarer, *Adv. Mater.* 1995, 7, 911. [57b] A. M. Cox, R. D. Blackburn, D. P. West, T. A. King, F. A. Wade, D. A. Leigh, *Appl. Phys. Lett.* 1996, 68, 2801. [57c] A. Grunnet-Jepsen, C. L. Thompson, R. J. Twieg, W. E. Moerner, *Appl. Phys. Lett.* 1997, 70, 1515. [57d] F. Wang, Z. Chen, Q. Gong, Y. Chen, H. Chen, *Solid State Commun.* 1998, 106, 299.
- [58] E. Hendrickx, J. Herlocker, J. L. Maldonado, S. R. Marder, B. Kippelen, A. Persoons, N. Peyghambarian, *Appl. Phys. Lett.* 1998, 72, 1679.
- [59] Z. H. Peng, A. R. Gharavi, L. P. Yu, *J. Am. Chem. Soc.* 1997, 119, 4622.
- [60] E. V. Rudenko, A. V. Sukhov, *JETP Lett.* 1994, 59, 142.
- [61] G. P. Wiederrecht, B. A. Yoon, M. R. Wasielewski, *Science* 1995, 270, 1794
- [62] I. C. Khoo, B. D. Guenther, M. V. Wood, P. Chen, M. Y. Shih, *Opt. Lett.* 1997, 22, 1229
- [63] [63a] W. Lee, C. S. Chiu, *Opt. Lett.* 2001, 26, 521. [63b] I. C. Khoo, Y. Ding, Y. Zhang, K. Chen, A. Diaz, *Appl. Phys. Lett.* 2003, 82, 3587.
- [64] N. V. Tabiryan, C. Umeton, *J. Opt. Soc. Am. B.* 1998, 15, 1912.
- [65] [65a] H. Ono, N. Kawatsuki, *Opt. Commun.* 1998, 147, 237 (1998). [66b] M. J. Fuller, C. J. Walsh, Y. Y. Zhao, M. R. Wasielewski, *Chem. Mater.* 2002, 14, 952.
- [66] G. P. Wiederrecht, M. R. Wasielewski, *Appl. Phys. Lett.* 1999, 74, 3459.
- [67] [67a] J. Zhang, V. Ostroverkhov, K. D. Singer, V. Reshetnyak, Y. Reznikov, *Opt. Lett.* 2000, 25, 414. [67b] P. Pagliusi, G. Cipparrone, *J. Appl. Phys.* 2002, 92, 4863. [67c] P. Pagliusi, G. Cipparrone, *Opt. Lett.* 2003, 28, 2369.
- [68] R. Termine, B. C. De Simone, A. Golemme, *Appl. Phys. Lett.* 2001, 78, 688.
- [69] C.J. Hu, R. Oshima, J. Arai, M. Seno, *J. Polym. Sci. Part A, Polym. Chem.* 1988, 26, 2423.
- [70] [70a] M.S. Ho, C. Barrett, J. Paterson, M. Esteghamatian, A. Natansohn, P. Rochon, *Macromolecules* 1996, 29, 4513. [70b] C. Barret, B. Choudhury, A. Natansohn, P. Rocon, *Macromolecules* 1998, 31, 4845. D. Van Steenwinkel, C. Engels, E. Gubbelmans, E. Hendrickx, A. Samyn, A. Persoons,

- Macromolecules 2000, 33, 4074.
- [71] D. Van Steenwinckel, E. Hendrickx, C. Samyn, C. Engels, A.J. Persoons, Mater. Chem. 2000, 10, 2692.
- [72] K. Tamura, Jr H.K. Hall, N. Peyghambarian, Appl. Phys. Lett. 1992, 60, 1803.
- [73] B. Kippelen, K. Tamura, N. Peyghambarian, A.B. Padias, Jr. J.R. Hall, Phys Rev, Part B 1993, 48, 10710.
- [74] J.M. Rodriguez-Parada, V. Percec, Macromolecules 1986, 19, 55.
- [75] C.I. Simionescu, V. Percec, A. Nathanson Polymer 1980, 21, 417.
- [76] C. Engels, D. Van Steenwinckel, E. Hendrickx, M. Schaerlaekens, A. Persoonsb, C. Samyn, J. Mater. Chem. 2002, 12, 951.

Chapter 2: Optically active bisazoaromatic polymers

Introduction

Side chain polymers containing azoaromatic chromophores are widely studied for their potentially unique optical properties [1].

They can be used in advanced micro- and nanotechnologies such as optical data storage [2], nonlinear optical materials [3], holographic memories [4], chiroptical switches [5], surface relief gratings [6], etc.

On the other hand, the induction of helical chirality in polymers has attracted widespread interest for its possible applications in optical devices or data storage also because of its relevance to chiral amplification as it may have occurred at the early stages of life [7].

In the last year [8,9], Angiolini and co-workers have synthesized and investigated methacrylic polymers bearing in the side chain the chiral cyclic (*S*)-3-hydroxypyrrolidine moiety interposed between the main chain and the *trans*-azoaromatic chromophore, substituted or not in the 4' position by an electron-withdrawing group, such as poly[(*S*)-3-methacryloyloxy-1-(4-azobenzene)pyrrolidine] {poly[(*S*)-**MAP**]} [8], poly[(*S*)-3-methacryloyloxy-1-(4'-nitro-4-azobenzene)pyrrolidine] {poly[(*S*)-**MAP-N**]} [8] and poly[(*S*)-3-methacryloyloxy-1-(4'-cyano-4-azobenzene)pyrrolidine] {poly[(*S*)-**MAP-C**]} [9], reported in Figure 1. In these materials, the presence of a rigid chiral moiety of one prevailing absolute configuration favours the establishment of a chiral conformation of one prevailing helical handedness, at least within chain segments of the macromolecules, which can be observed by circular dichroism (CD).

The simultaneous presence of the azoaromatic and chiral functionalities allows the polymers to display both the properties typical of dissymmetric systems (optical activity, exciton splitting of dichroic absorptions), as well as the features typical of photochromic materials (photorefractivity, photoresponsiveness, NLO properties) [10].

Polymers based on bisazobenzene moiety have also attracted an intense attention because of their use in spread photonic applications [11]. It is known in fact, that polymers containing two azo bonds have larger NLO and photoresponsive properties and exhibit enhanced photoinduced anisotropy and thermal stability if compared with similar derivatives bearing in the side chain only one single azoaromatic chromophore [11, 12]. Among the bisazoaromatic materials reported in the literature, the polymeric derivatives deriving from monomer the 2-propenoic acid, 2-methyl-2-[[4-[[4-[(4-cyanophenyl)azo]-2-methylphenyl]azo]phenyl]methylamino]ethyl ester [13], originally designed for optical data storage, show many interesting properties that seem to open a new use of these materials in different applications such as Fabry-Perot modulator and conductive/pyroelectric polymers [14].

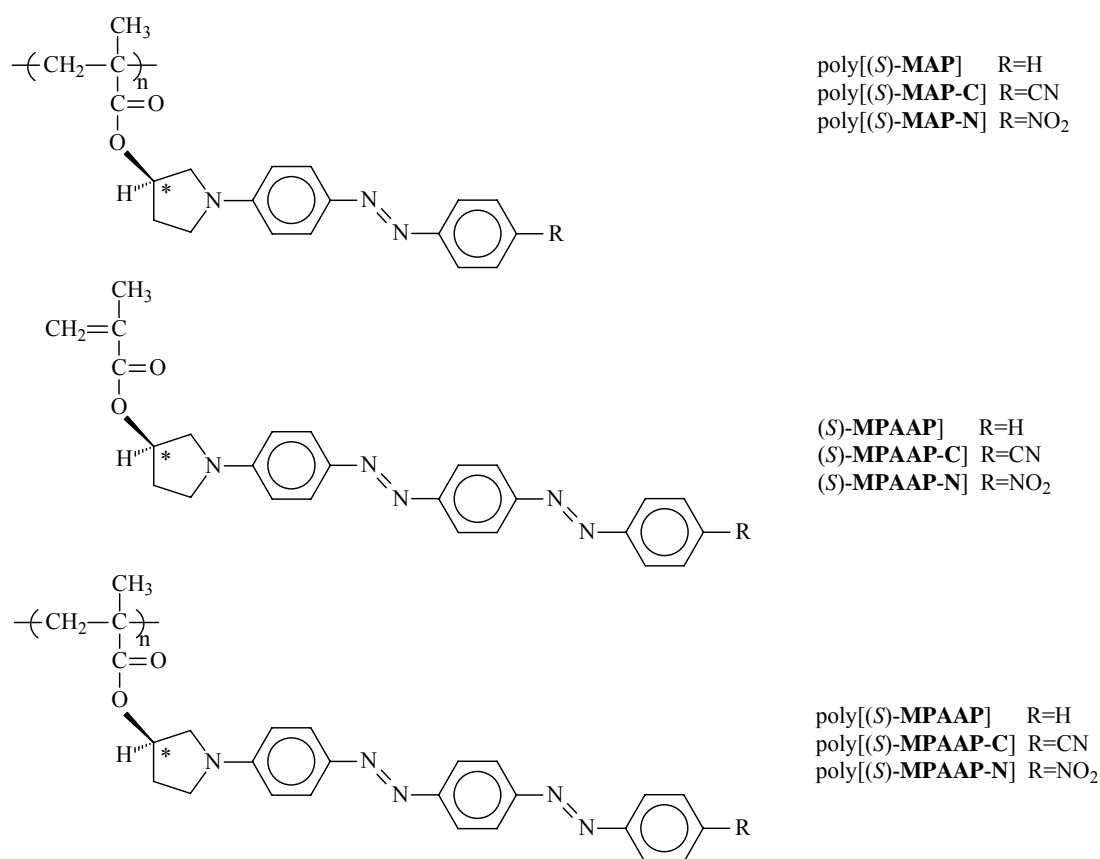


Figure 1. Chemical structures of the investigated polymers and of related homopolymers bearing only one azoaromatic chromophore in the side chain

In this context, it was worth to synthesis and characterize three analogous optically active monomers, (*S*)-3-methacryloyloxy-1-[4'-phenylazo-(4-azobenzene)]-pyrrolidine [(*S*)-**MPAAP**], (*S*)-3-methacryloyloxy-1-[4'-cyanophenylazo-(4-azobenzene)]-pyrrolidine [(*S*)-**MPAAP-C**] and (*S*)-3-methacryloyloxy-1-[4'-nitrophenylazo-(4-azobenzene)]-pyrrolidine [(*S*)-**MPAAP-N**], as well as the corresponding homopolymers obtained by radical polymerization, that contain an additional functionality due to the presence of a chiral group of one single absolute configuration interposed between the chromophore and the main chain. The structures of the new monomers and their related polymeric compounds are shown in Figure 1.

The novel products have been fully characterized and their properties are discussed and compared to those of the above mentioned analogue derivatives bearing only one azoaromatic chromophore in the side chain.

Poly[(*S*)-**MPAAP**] resulted soluble at room temperature in common organic solvent as THF or CHCl₃, instead the limited solubility of the dried poly[(*S*)-**MPAAP-C**] and poly[(*S*)-**MPAAP-N**] restricted their potential uses.

In this context, it was worth the evaluation of the effects induced on the properties of these materials by progressively spacing out the photochromic bisazoaromatic optically active repeating unit along the polymer backbone. This has been achieved through radical copolymerization of the same three optically active monomers (*S*)-**MPAAP**, (*S*)-**MPAAP-C** and (*S*)-**MPAAP-N** with different molar amounts of an inactive *co*-monomer such as methyl methacrylate (**MMA**), in order to obtain the desired corresponding copolymers shown in Figure 2.

The products have been fully characterized in solution and in the solid state as thin films; their thermal behaviours, spectroscopic properties and the photomodulation of their photoinduced birefringence have been discussed in terms of composition in view of their use for optical data storage.

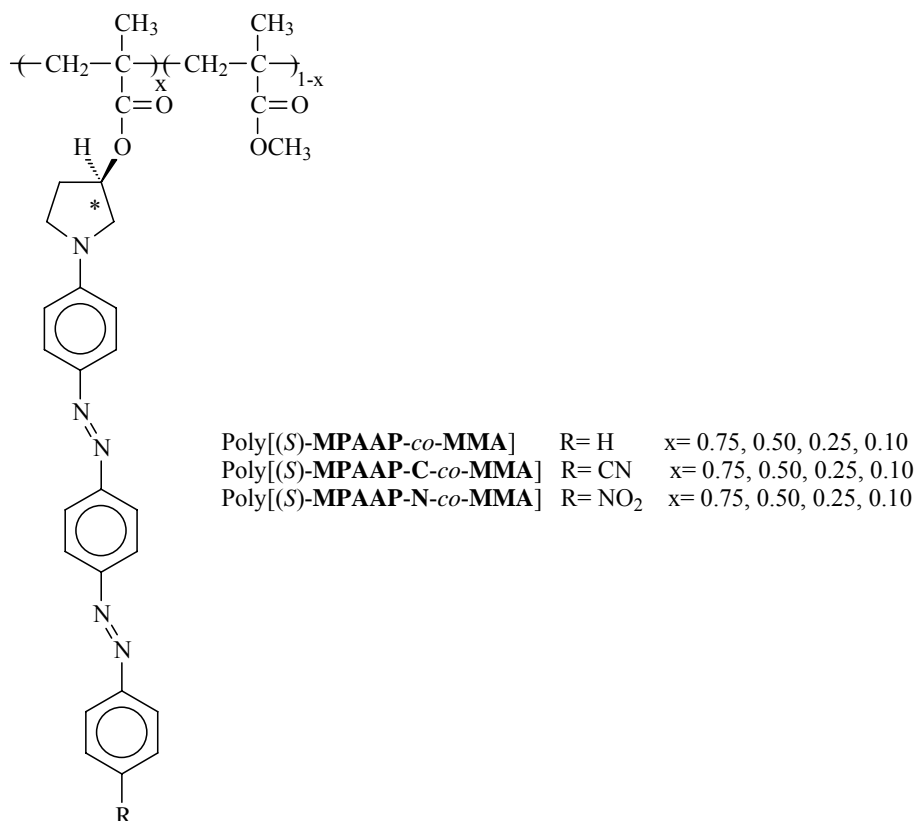


Figure 2. Chemical structures of the copolymers of (*S*)-MPAAP, (*S*)-MPAAP-C and (*S*)-MPAAP-N with MMA.

The photoinduction of birefringence has been assessed on thin films of the investigated copolymers in order to evaluate their behaviour as materials for optical data storage. The results are interpreted in terms of copolymer composition and conformational stiffness of the bisazoaromatic chromophoric *co*-units, which are responsible of a slower optical response rates and poor solubility in comparison to the similar polymers containing only one azo bond. The larger thermal and temporally stable observed properties appear of interest for a potential use of these materials in nanoscale technologies for all-optical data manipulation and in optoelectronics.

Finally, we focused the attention on the effects induced on the thermal and chiroptical behaviours by the insertion of particular achiral comonomers characterized by different side-chain mobility and steric hindrance.

This has been achieved through radical copolymerization of the optically active monomer (*S*)-MPAAP with an inactive *tert*-butyl methacrylate (*tert*-BMA) and triphenylmethyl methacrylate (TrMA) in different molar amounts. The structures of these copolymeric compounds, poly[(*S*)-MPAAP-*co-tert*-BMA]s and poly[(*S*)-MPAAP-*co*-TrMA]s at different percent molar contents of (*S*)-MPAAP *co*-units, are shown in Figure 3.

The amplification of chirality observed, passing from copolymers of [(*S*)-MPAAP] with TrMA to those with *tert*-BMA and MMA, suggests that it is possible to modulate the optical activity of these novel polymers by insertion of different achiral comonomers with different bulky hindrance

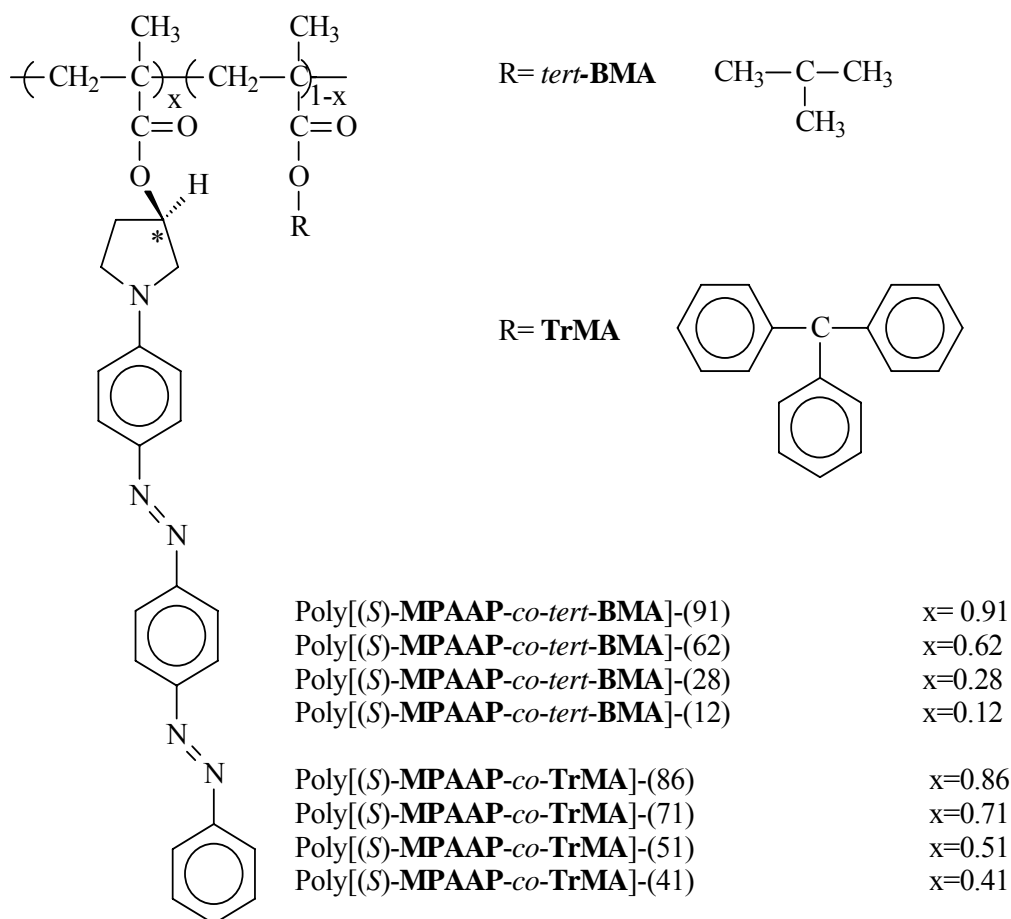


Figure 3. Chemical structures of the investigated copolymers of (*S*)-MPAAP with *tert*-BMA and TrMA.

Optically active methacrylic homopolymers bearing side-chain bisazoaromatic moieties*Synthesis and structural characterization*

The synthesis of the three novel monomers (*S*)-**MPAAP**, (*S*)-**MPAAP-C** and (*S*)-**MPAAP-N** (Scheme 1 and Experimental Part) was carried out starting from (*S*)-**HPP** [8] by coupling with the diazonium salt deriving from *trans*-4-phenylazoaniline, *trans*-4-(4-aminophenylazo)benzotrile and *trans*-4-(4-aminophenylazo)nitrobenzene to give the novel azo derivatives (*S*)-**HPAAP**, (*S*)-**HPAAP-C** and (*S*)-**HPAAP-N**, respectively, which were finally submitted to esterification with methacryloyl chloride.

Table 1. Characterization data of polymeric derivatives

Sample	Yield ^{a)}	\bar{M}_n ^{b)}	\bar{M}_w / \bar{M}_n ^{b)}	T_g ^{c)}	T_d ^{d)}
		g/mol		°C	°C
Poly[(<i>S</i>)- MPAAP]	14	27.300	1.3	191	283
Poly[(<i>S</i>)- MPAAP-C]	46	n. d. ^{e)}	n. d. ^{e)}	165	294
Poly[(<i>S</i>)- MPAAP-N]	16	n. d. ^{e)}	n. d. ^{e)}	176	298

a) Calculated as g of polymer / g of monomer · 100.

b) Determined by SEC in THF at 25°C.

c) Determined by DSC, heating rate of 10°K/min under nitrogen atmosphere.

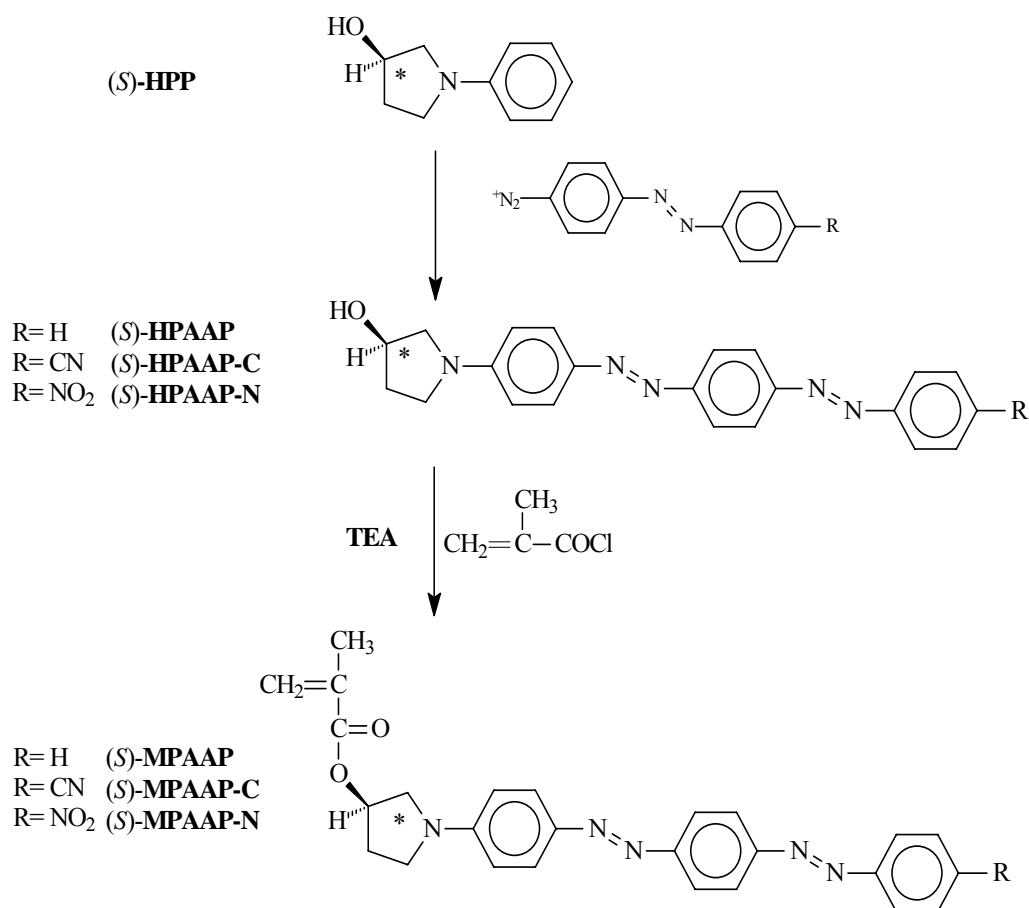
d) Initial decomposition temperature as determined by TGA in air at 20°C/min heating rate.

e) Not determined due to low solubility of the polymers in THF at 25°C.

The structures of the products were confirmed by ¹H-NMR and FT-IR. The optical activity at the sodium D-line of the monomers, as well as of their alcoholic precursors, could not be measured with accuracy because of the strong absorption of the bisazoaromatic chromophore at that wavelength. However, previous data [8,9] concerning the optical purity of the 4'-unsubstituted methacryloyl derivatives bearing in the side-chain one azoaromatic group prepared through a similar synthetic pathway

indicate that an enantiomeric excess of at least 90% was present in those compounds, thus excluding the possibility of racemization at the asymmetric centre in the course of the synthesis. This allows to reasonably attribute an analogous optical purity also to the alcohols and monomers reported here.

Homopolymerization of the monomers was carried out in DMF solution at 65°C under radical conditions by using AIBN as a thermal initiator. The obtained products were repeatedly dissolved in THF or DMF (depending on their solubility), reprecipitated in methanol, and submitted to a final purification from monomeric and oligomeric impurities by exhaustive Soxhlet extraction with methanol followed by acetone. Relevant data for the synthesized macromolecular derivatives are reported in Table 1.



Scheme 1

Poly[(S)-MPAAP] turns out to be soluble at room temperature in THF or CHCl_3 . Instead, the dried samples of poly[(S)-MPAAP-C] and poly[(S)-MPAAP-N] resulted

insoluble at room temperature in common solvents such as CHCl_3 , THF, DMSO, toluene, NMP, nitrobenzene, thus preventing their complete characterization in solution (see experimental part). Similar behaviour was observed in analogous methacrylic copolymers [1g] containing in the side-chain the flexible chromophore 4-[N-ethyl-N-(2-hydroxyethyl)amino]-4'-(4-nitrophenylazo)azobenzene and attributed to the presence of strong dipolar interactions among the bisazoaromatic chromophores in the side chain. However poly[(*S*)-MPAAP-C] resulted sufficiently soluble in $\text{DMF-}d_7$ at 90°C to allow NMR analysis.

The structure of all products was confirmed by FT-IR and, when soluble, by ^1H - and ^{13}C -NMR, confirming the occurrence of polymerization. As shown in Figure 4 for the couple (*S*)-MPAAP-N/poly[(*S*)-MPAAP-N], the spectra display the disappearance of the absorption around $1630\text{--}1636\text{ cm}^{-1}$, related to the stretching vibration of the methacrylic double bond, and the contemporary shift ($10\text{--}20\text{ cm}^{-1}$) of the estereal carbonyl stretching to higher frequencies ($1725\text{--}1732\text{ cm}^{-1}$) with respect to the monomer, due to the reduced electron delocalization determined by the reaction of the methacrylic double bond.

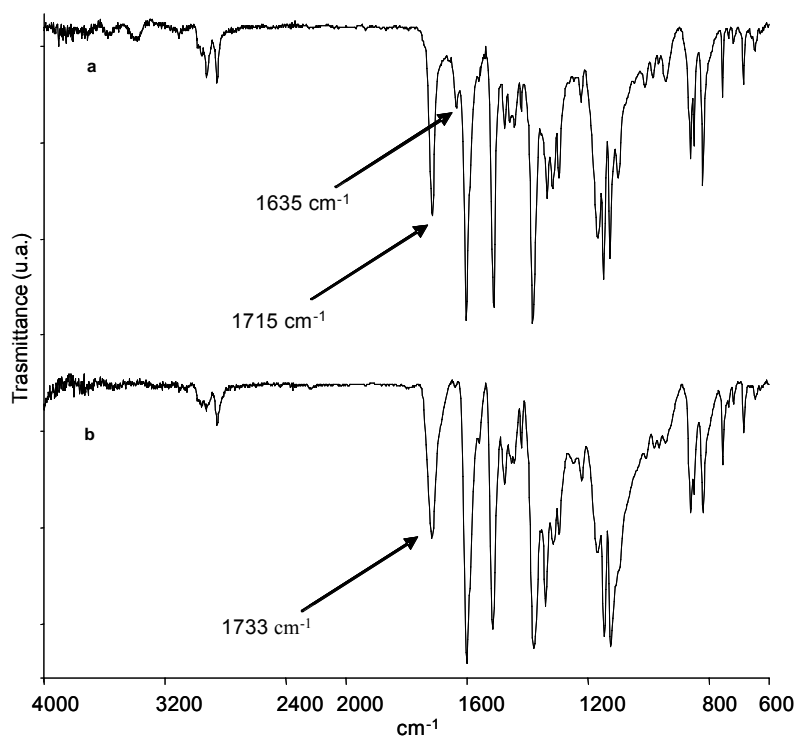


Figure 4. IR spectra of (*S*)-MPAAP-N (a) and poly[(*S*)-MPAAP-N] (b).

Accordingly, in the $^1\text{H-NMR}$ spectra of homopolymeric derivatives, the resonances of the vinylidenic protons of the monomers are absent and the methacrylic methyl resonances are shifted to higher field, as shown for example by the $^1\text{H NMR}$ spectra of (*S*)-**MPAAP-C** and poly[(*S*)-**MPAAP-C**] (Figure 5).

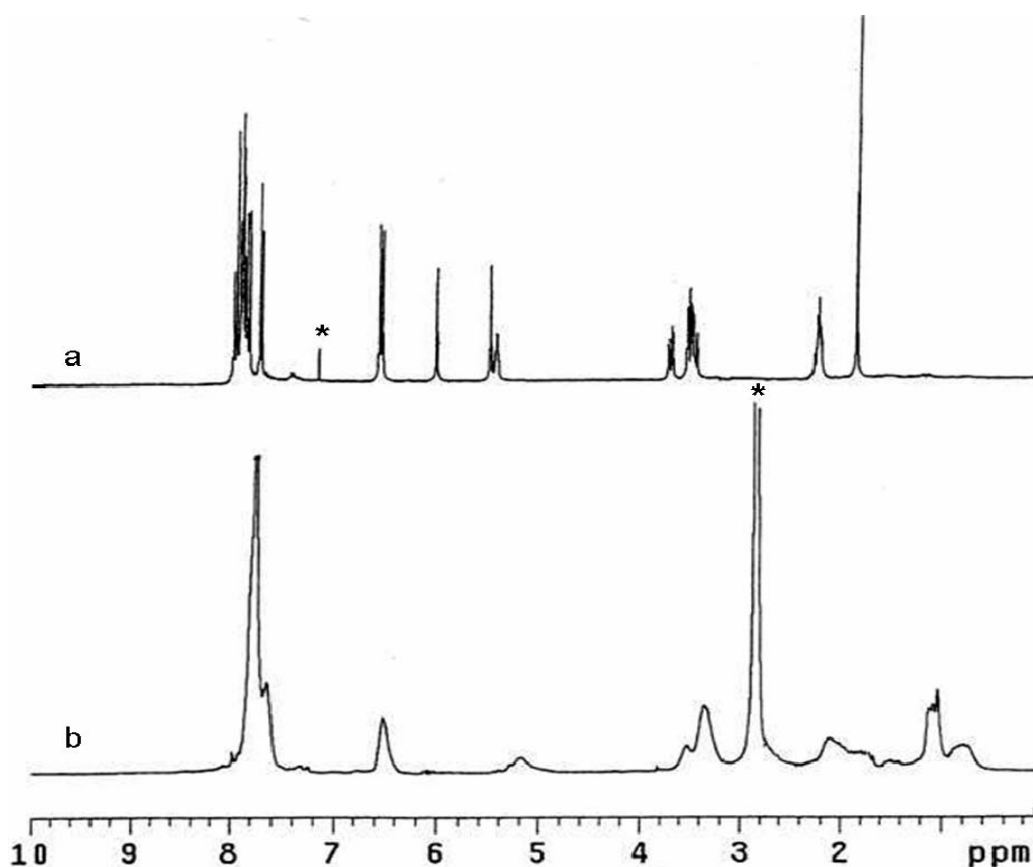


Figure 5. $^1\text{H-NMR}$ spectra of (*S*)-**MPAAP-C** (a) in CDCl_3 and poly[(*S*)-**MPAAP-C**] (b) in $\text{DMF-}d_7$ at $90\text{ }^\circ\text{C}$. Starred signals refer to solvent resonances.

Thermal analysis

The thermal stability of all the polymeric derivatives, which is one of the most important properties for the applicability of these materials in optoelectronics, was determined by thermogravimetric analysis (TGA) and resulted quite similar and very high, with decomposition temperature values (T_d) close to 300°C . This behaviour is due

to the remarkable presence of strong dipolar interactions in the solid state among the bisazoaromatic chromophores located in the side chain.

All the polymeric derivatives exhibit (Table 1) by differential scanning calorimetry (DSC) measurements in the 25-250°C temperature range, only a second order thermal transition attributed to glass transition (T_g). No endothermic melting peaks, attributable to crystalline domains, are evidenced in accordance with the substantially amorphous character of the macromolecules in the solid state.

It is worth observing that poly[(*S*)-**MPAAP**], poly[(*S*)-**MPAAP-C**] and poly[(*S*)-**MPAAP-N**] exhibit a considerably higher T_g value than the related poly[(*S*)-**MAP**], poly[(*S*)-**MAP-C**] and poly[(*S*)-**MAP-N**] (Table1), indicative of larger inter and/or intramolecular polar interactions between the neighbouring side chain aromatic chromophores, due to the increased dipole moment of the bisazoaromatic chromophore, originated by the larger extension of the conjugation with respect to one azoaromatic group.

In Figure 6 it is possible to compare the DSC thermograms of poly[(*S*)-**MAP**] and poly[(*S*)-**MPAAP**].

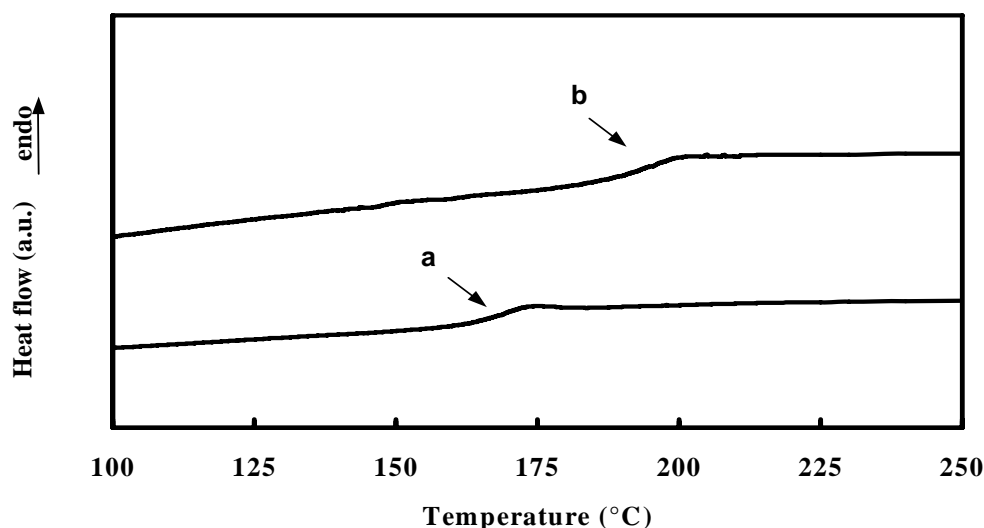


Figure 6: DSC thermograms of poly[(*S*)-**MAP**] (a) and poly[(*S*)-**MPAAP**] (b).

In this context, the quite low T_g values shown by poly[(*S*)-**MPAAP-C**] and poly[(*S*)-**MPAAP-N**] bearing a strong electron acceptor group in the conjugated azoaromatic system that increase the permanent dipole of the chromophore with respect to poly[(*S*)-**MPAAP**] (Table 1), could be due to their lower average molecular weight. In fact, as previously reported [11-14], the thermal properties of this class of polymeric derivatives increase upon increasing their molecular mass and decreasing the polydispersity.

The behavior of the investigated samples is indicative of reduced mobility of the macromolecular chains originated by the presence of both the conformationally rigid pyrrolidine ring interposed between the backbone and the bisazoaromatic chromophore and of strong inter- and/or intramolecular dipolar interactions in the solid state between these latter side chain groups.

Both the good thermal stability and the high value of T_g suggest that these polymeric materials may be promisingly tested for applications in optoelectronics, provided they are suitable modified so as to gain a satisfactory processability.

Absorption spectra

The UV-vis spectrum in CHCl_3 solution of all the monomers and polymers, when soluble, (Table 2 and Figure 7) exhibit two absorption bands, centred in the 450-510 and 280-330 nm spectral regions. The former one, more intense, is attributed to the combined $n-\pi^*$, $\pi-\pi^*$ and internal charge transfer electronic transitions of the bisazoaromatic chromophore; the latter to the $\pi-\pi^*$ electronic transitions of single aromatic rings [15].

As expected, a remarkable bathochromic shift for the first and the second bands, respectively, is observed by comparing poly[(*S*)-**MPAAP**] to poly[(*S*)-**MAP**]. This effect can be attributed to larger conjugation through the bisazoaromatic system upon introduction of an additional azoic bond which delocalizes the π electrons thus reducing the electronic transition energy [11].

Accordingly, a significantly increasing bathochromic effect can be noted for both the bands of polymeric and monomer derivatives on passing from $R = \text{H}$ to CN and NO_2 (Table 2 and Figure 7), as a consequence of the increasing electron-withdrawing capability of the substituent and hence of the conjugation extent in the aromatic

chromophore [16], giving rise to a progressive reduction of the electronic transition energy in the system. It can be therefore deduced that the nitro substituent in 4' position of the bisazoaromatic moiety provides the highest charge delocalization in the investigated systems. Indeed, this group is reported to display a higher acceptor strength than the cyano group in analogous donor-acceptor azoaromatic materials [8,9]. Also, the molar extinction coefficient is likewise increased.

Table 2. UV-vis spectra in CHCl₃ solution at 25°C of monomers and polymeric derivatives

Sample	1 st absorption band		2 nd absorption band	
	$\lambda_{\max}^{\text{a)}$	$\epsilon_{\max} \cdot 10^{-3}^{\text{b)}$	$\lambda_{\max}^{\text{a)}$	$\epsilon_{\max} \cdot 10^{-3}^{\text{b)}$
	nm	Lmol ⁻¹ cm ⁻¹	nm	Lmol ⁻¹ cm ⁻¹
Poly[(<i>S</i>)-MPAAP]	463	33.4	332	17.0
(<i>S</i>)-MPAAP	467	34.5	332	16.7
(<i>S</i>)-MPAAP-C	490	36.7	333	18.8
(<i>S</i>)-MPAAP-N	500	39.1	347	21.0
Poly[(<i>S</i>)-MAP]	408	28.3	258	10.5

a) Wavelength of maximum absorbance.

b) Calculated for one single chromophore.

A significant hypochromism and a blue shift are also observed for the first band when passing from the monomer (*S*)-MPAAP to the corresponding homopolymer poly[(*S*)-MPAAP] (Table 2).

Such a behaviour may be addressed to the occurrence of electrostatic dipolar interactions between neighbouring side-chain aromatic moieties along the backbone [17], as previously observed in several polymeric systems with side-chain azoaromatic chromophores [8,9,10b-10d].

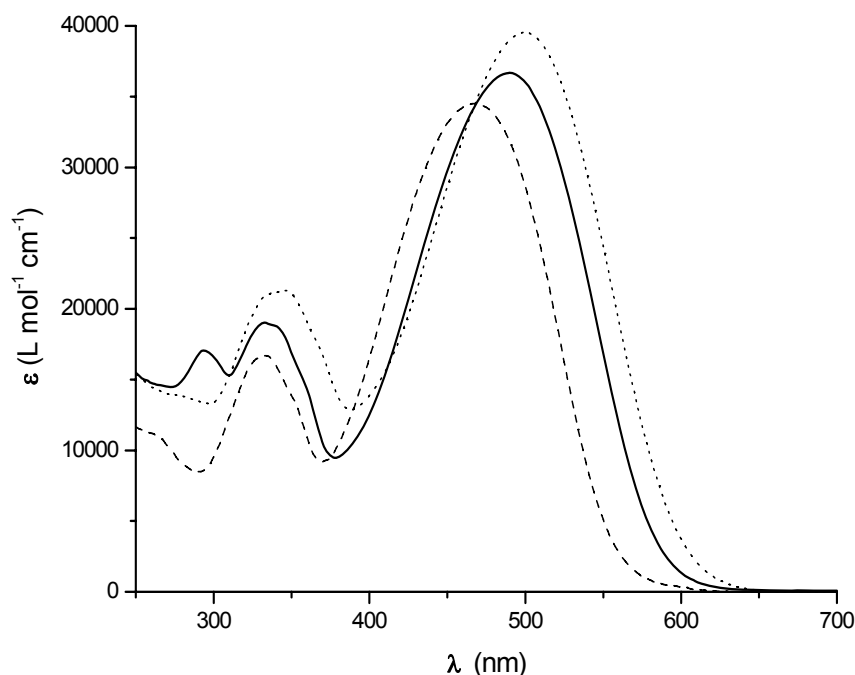


Figure 7. UV-vis spectra in CHCl_3 solution of (*S*)-**MPAAP** (----), (*S*)-**MPAAP-C** (—) and (*S*)-**MPAAP-N** (.....).

Chiroptical properties

The chiroptical properties of poly[(*S*)-**MPAAP**] and of all the monomeric compounds have been investigated by circular dichroism (CD) in the 250-700 nm spectral region in order to assess the conformational features of the macromolecular chains.

The CD spectrum of (*S*)-**MPAAP** in chloroform solution (Figure 8) displays only weak positive and negative dichroic absorptions with maxima centred at 466 and 330 nm (Table 3), strictly related to the 1st and 2nd UV-vis bands, respectively. By contrast, the CD spectrum of poly[(*S*)-**MPAAP**] exhibits two intense dichroic bands of opposite sign and comparable intensity, connected to the electronic transitions of the first UV-vis band, with a cross over point around 454 nm, close to the UV-vis maximum absorption. Such a behaviour is typical of an exciton splitting determined by cooperative interactions between side-chain azoaromatic chromophores disposed in a mutual chiral geometry of one prevailing handedness [8-10].

Table 3. CD spectra in CHCl₃ solution at 25°C of monomers and polymeric derivatives

Sample	1 st absorption band					2 nd absorption band				
	λ_1^{a} nm	$\Delta\varepsilon_1^{\text{b}}$ Lmol ⁻¹ cm ⁻¹	λ_0^{c} nm	λ_2^{a} nm	$\Delta\varepsilon_2^{\text{b}}$ Lmol ⁻¹ cm ⁻¹	λ_3^{a} nm	$\Delta\varepsilon_3^{\text{b}}$ Lmol ⁻¹ cm ⁻¹	λ_0^{c} nm	λ_4^{a} nm	$\Delta\varepsilon_4^{\text{b}}$ Lmol ⁻¹ cm ⁻¹
Poly[(<i>S</i>)- MAP] ^d	445	+7.35	409	387	-6.42	258	-0.32	-	-	-
Poly[(<i>S</i>)- MPAAP]	500	+5.09	450	415	-3.22	350	+0.42	340	318	-0.81
(<i>S</i>)- MPAAP	466	+0.73	-	-	-	330	-0.12	-	-	-
(<i>S</i>)- MPAAP-C	490	+0.66	-	-	-	337	-0.25	-	-	-
(<i>S</i>)- MPAAP-N	503	+0.65	-	-	-	340	-0.40	-	-	-

a) Wavelength (in nanometers) of maximum dichroic absorption.

b) Calculated for one chromophoric repeating unit in polymers.

c) Wavelength of the cross-over of dichroic bands.

d) Ref. [8]

A further exciton coupling of smaller intensity is also present, with a cross over point near to the second UV maximum absorption. Consequently, the much higher optical activity of poly[(*S*)-**MPAAP**] with respect to that one of the corresponding monomer, can be attributed to the presence of dipole-dipole interactions between side-chain neighbouring bisazoaromatic chromophores favouring a conformational arrangement with a prevailing chirality in the macromolecule, at least for chain sections.

Similar results were previously found for the analogous poly[(*S*)-**MAP**], having in the side chain only one azoaromatic moiety [8] (Table 3). A commonly adopted assessment of the strength of dichroic signals is made in terms of chiral anisotropy coefficient, g , defined as the ratio between the CD signal ($\Delta\epsilon$) and the UV-vis absorption coefficient (ϵ) measured for the same sample at the same frequency, usually chosen at the maximum of the CD band [18]. In order to compare the chiroptical properties of poly[(*S*)-**MAP**] and poly[(*S*)-**MPAAP**] and avoid ambiguities and uncertainties due to the choice of a specific frequency, it has been preferred to determine an integrated g -factor, defined as the ratio between the integrated area in absolute value of the CD signal and that of the 1st UV-vis absorption band. With this approach, poly[(*S*)-**MPAAP**] exhibits in chloroform solution a chiral anisotropy degree (0.012×10^{-2}) lower than poly[(*S*)-**MAP**] (0.025×10^{-2}), a result which is presumably due to the intrinsic structural properties of poly[(*S*)-**MAP**], having only one azo bond, sterically less hindered with respect to the bisazoaromatic chromophore, thus favouring a mutual chiral geometry of one prevailing handedness for longer chain sections.

The UV-vis and CD spectra of the native thin film (150 nm thick) of poly[(*S*)-**MPAAP**] are given in Figure 5. The amorphous polymer in the solid state exhibits strong electronic absorptions in the visible and UV region centered at about 453 and 330 nm, respectively, assigned to the same electronic transitions of the bisazoaromatic chromophore previously observed in solution.

The close similarity between the CD spectra of the native polymeric film (expressed as ellipticity) and in solution suggests that macromolecules maintain chiral conformations of one prevailing helical handedness also in the amorphous solid state, at least for chain segments.

The significant intensity of the dichroic bands of poly[(*S*)-MPAAP] makes these bisazoaromatic containing materials potentially available for chiroptical switching applications [8-10].

Studies concerning the photomodulation of their chiroptical properties in the solid state by using one handed circularity polarized irradiation light are currently in progress.

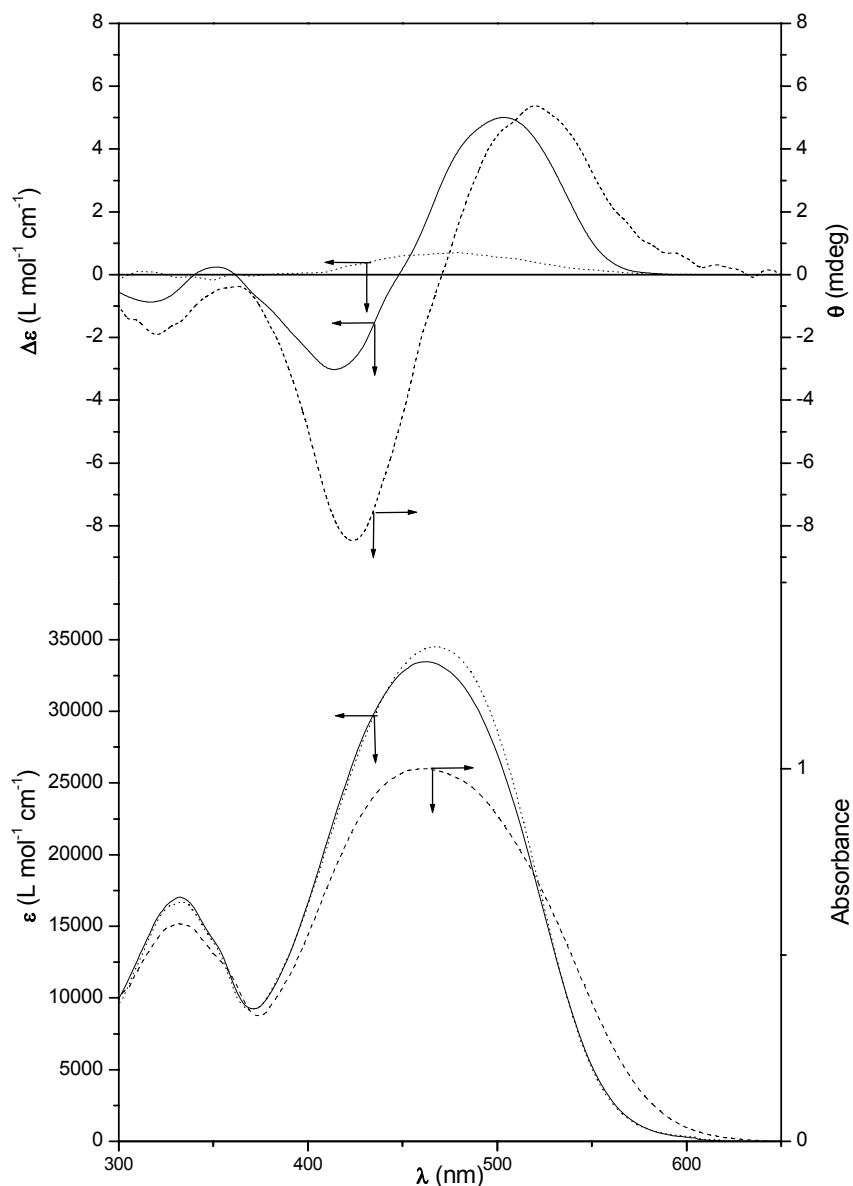


Figure 8. CD spectra (upper) and UV-vis (bottom) absorption spectra of poly[(*S*)-MPAAP] (---) in solid state, poly[(*S*)-MPAAP] (—) and (*S*)-MPAAP (···) in solution.

Optically active methacrylic copolymers bearing side-chain bisazoaromatic moieties

Synthesis and structural characterization of polymeric derivatives

Copolymerization of optically active monomers (*S*)-**MPAAP**, (*S*)-**MPAAP-C** and (*S*)-**MPAAP-N** with methyl-methacrylate (**MMA**), were carried out in DMF solution at 65°C under radical conditions by using AIBN as a thermal initiator. The obtained products (Figure 2) were repeatedly dissolved in THF or DMF (depending on their solubility), reprecipitated in methanol, and submitted to a final purification from monomeric and oligomeric impurities by exhaustive Soxhlet extraction with methanol followed by acetone. Relevant data for the synthesized copolymers are reported in Table 4.

The dried copolymers of (*S*)-**MPAAP-C** and of (*S*)-**MPAAP-N** with **MMA** with a molar chromophore concentration higher than 30% and 15%, respectively, resulted not soluble at room temperature in common solvents such as CHCl₃, THF, DMSO, toluene, NMP, nitrobenzene; thus preventing their complete characterization in solution (see Experimental Part). Similar behaviour was observed in analogous methacrylic copolymers [11] containing in the side-chain the flexible chromophore 4-[N-ethyl-N-(2-hydroxyethyl)amino]-4'-(4-nitrophenylazo)azobenzene and was attributed to the presence of strong dipolar interactions among the bisazoaromatic chromophores in the side chain. However all macromolecular derivatives containing (*S*)-**MPAAP-C** *co*-units resulted sufficiently soluble in DMF-*d*₇ at 90°C to allow NMR analysis.

The occurred polymerizations and the structure of all products were confirmed by FT-IR and, when soluble, by ¹H- and ¹³C-NMR.

The molar final composition of copolymers was assessed by ¹H-NMR (Figure 9) by comparing the integrated signals of aromatic protons in *ortho* to amino group of (*S*)-**MPAAP** *co*-units, located at 6.70-6.30 ppm, to that one related to the methyl ester group of **MMA** *co*-units at 3.50 ppm, after subtraction of the contribution given to the integral by the overlapped resonance of the methylene protons in α position to nitrogen in the pyrrolidine ring of (*S*)-**MPAAP**.

Table 4. Characterization data of polymeric derivatives

Feed in mol (%)		Yield ^a	\bar{M}_n ^b	$\frac{\bar{M}_w}{\bar{M}_n}$	Chromophoric content ^c	T_g ^d
		(%)	(g/mol)		(mol %)	(°C)
(S)-MPAAP	MMA					
75	25	53	24700	1.4	69	170
50	50	35	15200	1.5	34	155
25	75	76	13400	1.8	27	146
10	90	71	12500	2.0	12	138
(S)-MPAAP-C	MMA					
75	25	50	n. d. ^e	n. d. ^e	61	162
50	50	68	21800	1.5	33	160
25	75	76	17600	1.7	26	159
10	90	72	18500	1.5	10	139
(S)-MPAAP-N	MMA					
75	25	34	n. d. ^e	n. d. ^e	n. d. ^f	165
50	50	52	n. d. ^e	n. d. ^e	n. d. ^f	151
25	75	37	n. d. ^e	n. d. ^e	n. d. ^f	154
15	85	41	14900	1.6	10	151
10	90	39	7200	1.6	7	125

a) Calculated as g of polymer / g of monomer · 100.

b) Determined by SEC in THF at 25°C.

c) Determined by ¹H-NMR.

d) Determined by DSC, heating rate of 10°K/min under nitrogen atmosphere.

e) Not determined due to low solubility of the polymers in THF at 25°C.

f) Not determined due to low solubility of the polymers in the solvents for NMR spectroscopy.

To confirm the obtained results, it was carried out an analogous process comparing the signals of (S)-MPAAP and MMA co-units by the ratios of the integrated peak areas in the aromatic and aliphatic regions. Analogous considerations were taken into account in

order to determine the molar compositions of sufficiently soluble copolymers of (*S*)-MPAAP-C (Figure 10) and (*S*)-MPAAP-N with MMA.

Errore.

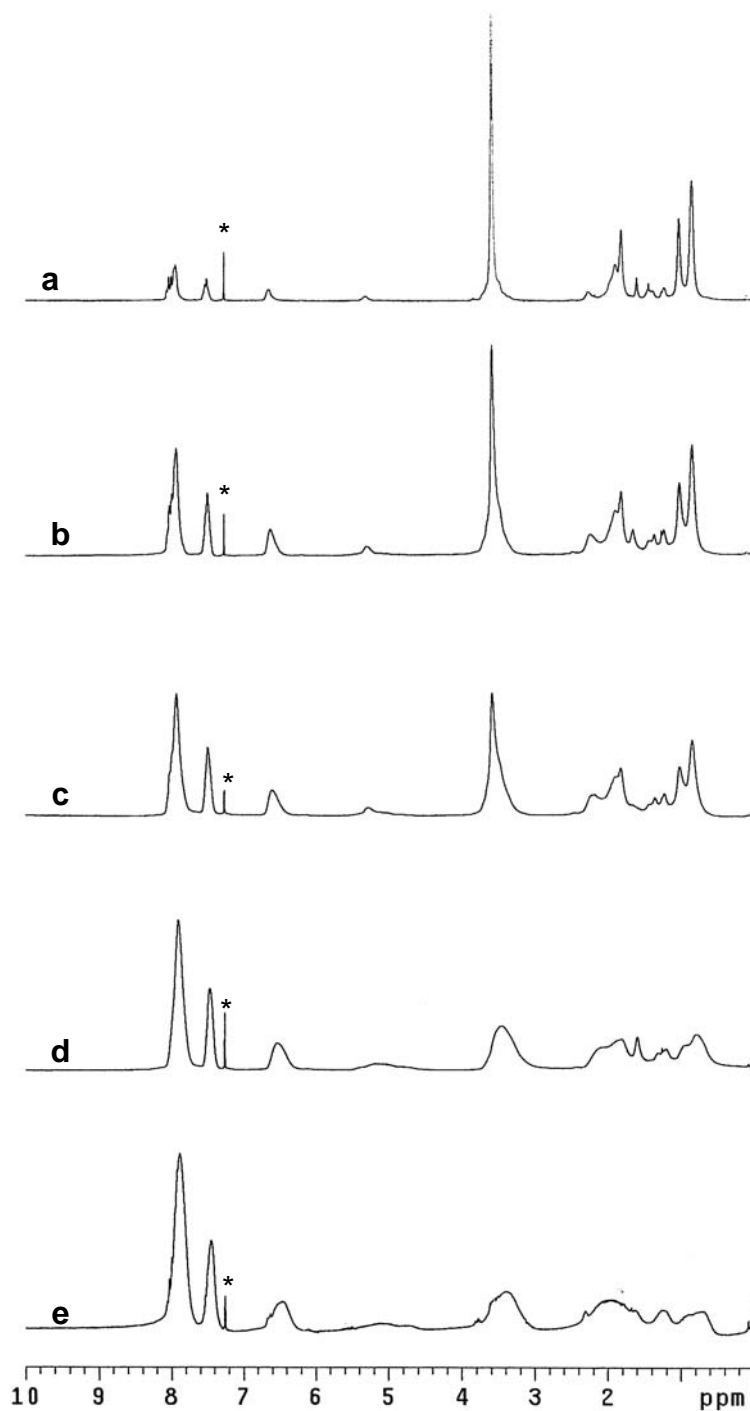


Figure 9. $^1\text{H-NMR}$ spectra of poly[(*S*)-MPAAP-*co*-MMA] (10/90) (a), poly[(*S*)-MPAAP-*co*-MMA] (25/75) (b), poly[(*S*)-MPAAP-*co*-MMA] (50/50) (c), poly[(*S*)-

MPAAP-co-MMA] (75/25) (d) and poly[(*S*)-**MPAAP**] (e) in CDCl₃. Starred signals refer to solvent resonances.

The average results are listed in Table 8 and point out that the molar content of bisazoaromatic *co*-units in the copolymers with **MMA** roughly reflects the feed composition, indicating similar reactivities of the methacrylate monomers and a certain tendency to an alternating distribution of the *co*-units along the polymer chain

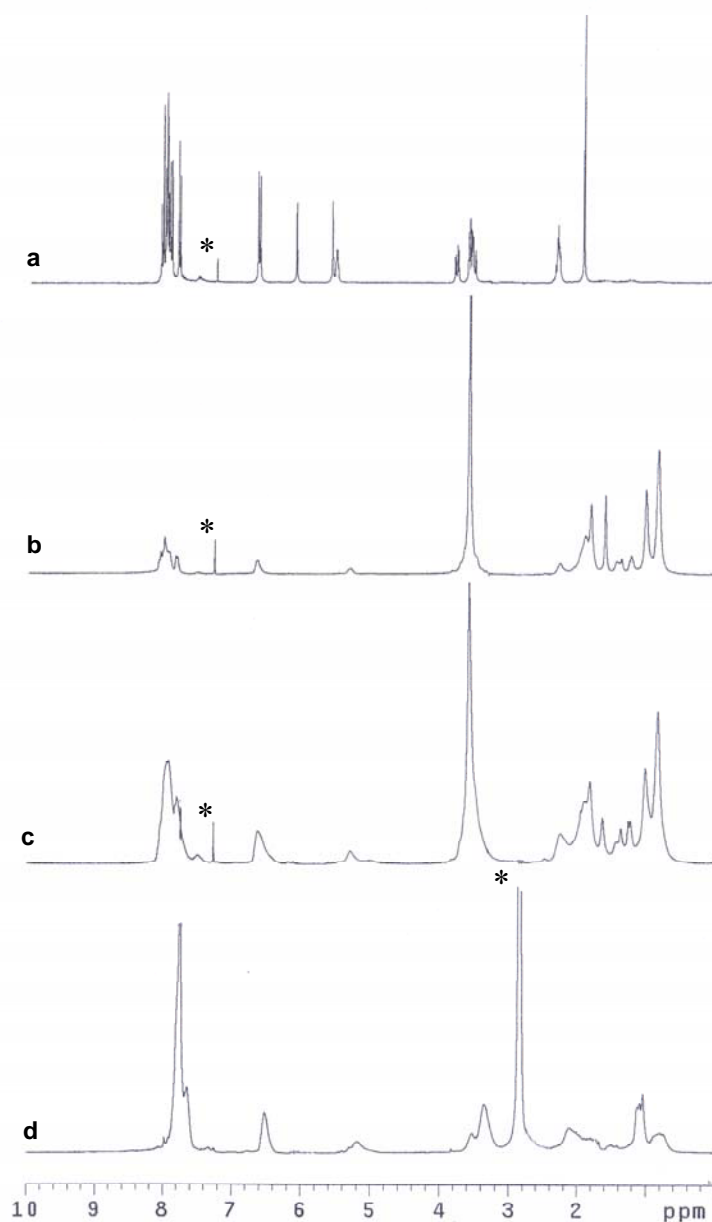


Figure 10. $^1\text{H-NMR}$ spectra of (*S*)-**MPAAP-C** (a), poly[(*S*)-**MPAAP-C-co-MMA**] (25/75) (b), poly[(*S*)-**MPAAP-C-co-MMA**] (50/50) (c) in CDCl_3 and poly[(*S*)-**MPAAP-C**] (d) in $\text{DMF-}d_7$ at 90 °C. Starred signals refer to solvent resonances.

Thermal analysis of polymeric derivatives

The quite high obtained T_g values (Table 4), even for the copolymeric samples poorest in chromophores moieties, (in the range 125-170°C), result very interesting for applications in optoelectronics. For instance Poly(**DRIM**), the methacrylic polymer bearing in the side chain the azo-dye Disperse Red 1, namely 4'-[(2-hydroxyethyl)ethylamino]-4-nitroazobenzene, and deeply investigated as polymeric material for optical storage, exhibits an appreciably lower T_g value (129°C) [1g].

The behavior of the investigated samples is indicative of a reduced mobility of macromolecular chains originated by the presence of strong inter- and/or intramolecular dipolar interactions in the solid state between bisazoaromatic chromophore.

It is evident that, for this type of applications, high values of T_g may guarantee to achieve enhanced temporal stability at room temperature of the photo- or electrically-oriented dipoles in the bulk.

Absorption spectra

All copolymeric compounds, when soluble, exhibited in the UV-vis spectra in CHCl_3 solution (Table 5) two absorption bands, centred in the 450-510 and 280-330 nm spectral regions. The former one, more intense, is attributed to the combined of the $n-\pi^*$, $\pi-\pi^*$ and internal charge transfer electronic transitions of the bisazoaromatic chromophore. The latter to the $\pi-\pi^*$ electronic transitions of single aromatic rings [15].

Poly[(*S*)-**MPAAP-co-MMA**] copolymers display spectroscopic features appearing tendentially more similar to those exhibited by the low molecular weight monomeric compound rather than to those of the homopolymer. Similar behaviour are shown by copolymers containing cyano and nitro 4''-substituent.

The presence of hypochromic effects in polymeric derivatives bearing side chain aromatic chromophores is attributed to the presence of electrostatic dipolar interactions between neighboring aromatic chromophores [17]. Thus, it appears that increasing the

distance between the bisazoaromatic chromophores by insertion, in the macromolecular chain, of non-chromophoric **MMA** *co*-units, the possibility of intramolecular interactions lowers, giving rise to a behaviour more similar to that of the monomer, where the lack of structural restraints originates a random distribution of the chromophores in dilute solution.

Table 5. UV-vis spectra in CHCl₃ solution at 25°C of copolymeric derivates containing **MMA** *co*-units.

Sample	1 st absorption band		2 nd absorption band	
	$\lambda_{\max}^{\text{a)}$	$\epsilon_{\max} \cdot 10^{-3}^{\text{b)}$	$\lambda_{\max}^{\text{a)}$	$\epsilon_{\max} \cdot 10^{-3}^{\text{b)}$
	nm	Lmol ⁻¹ cm ⁻¹	nm	Lmol ⁻¹ cm ⁻¹
Poly[(<i>S</i>)- MPAAP-co-MMA] (75/25)	463	34.3	334	17.0
Poly[(<i>S</i>)- MPAAP-co-MMA] (50/50)	464	34.6	332	15.6
Poly[(<i>S</i>)- MPAAP-co-MMA] (25/75)	465	34.4	332	16.9
Poly[(<i>S</i>)- MPAAP-co-MMA] (10/90)	465	34.4	333	16.8
Poly[(<i>S</i>)- MPAAP-C-co-MMA] (25/75)	488	37.5	334	18,8
Poly[(<i>S</i>)- MPAAP-C-co-MMA] (10/90)	491	38.2	333	19.0
Poly[(<i>S</i>)- MPAAP-N-co-MMA] (15/95)	501	37.8	339	20.8
Poly[(<i>S</i>)- MPAAP-N-co-MMA] (10/90)	500	38.2	344	21.7

a) Wavelength of maximum absorbance.

b) Calculated for one single chromophore.

Chiroptical properties

In the CD spectra of the copolymers of (*S*)-**MPAAP** with **MMA** (Figure 11 and Table 6) the intensities of dichroic absorptions decrease upon decreasing of the content of

bisazoaromatic *co*-units. The copolymer with the lower concentration of chromophore (10%) still shows only one couplet of very low intensity.

Table 6. CD spectra in CHCl₃ solution at 25°C of copolymeric derivatives containing **MMA** co-units

Sample	1 st absorption band					2 nd absorption band				
	$\lambda_1^{a)}$	$\Delta\epsilon_1^{b)}$	$\lambda_0^{c)}$	$\lambda_2^{a)}$	$\Delta\epsilon_2^{b)}$	$\lambda_3^{a)}$	$\Delta\epsilon_3^{b)}$	$\lambda_0^{c)}$	$\lambda_4^{a)}$	$\Delta\epsilon_4^{b)}$
	nm	Lmol ⁻¹ cm ⁻¹	nm	nm	Lmol ⁻¹ cm ⁻¹	nm	Lmol ⁻¹ cm ⁻¹	nm	nm	Lmol ⁻¹ cm ⁻¹
Poly[(S)-MPAAP-co-MMA] (75/25)	498	+4.11	452	418	-2.42	350	+0.31	340	318	-0.70
Poly[(S)-MPAAP-co-MMA] (50/50)	496	+2.22	443	415	-1.20	352	+0.14	342	324	-0.42
Poly[(S)-MPAAP-co-MMA] (25/75)	490	+1.65	443	420	-0.82	315	-0.36	-	-	-
Poly[(S)-MPAAP-co-MMA] (10/90)	475	+1.24	414	399	-0.11	332	-0.08	-	-	-
Poly[(S)-MPAAP-C-co-MMA] (25/75)	512	+1.70	452	416	-0.41	357	+0.25	339	325	-0.30
Poly[(S)-MPAAP-C-co-MMA] (10/90)	500	+1.15	-	-	-	352	+0.25	337	322	-0.22
Poly[(S)-MPAAP-N-co-MMA] (15/95)	501	+0.88	-	-	-	340	-0.42	-	-	-
Poly[(S)-MPAAP-N-co-MMA] (10/90)	500	+0.76	-	-	-	341	-0.35	-	-	-

a) Wavelength (in nanometers) of maximum dichroic absorption.

b) Calculated for one chromophoric repeating unit in polymers.

c) Wavelength of the cross-over of dichroic bands.

Similar results were previously found also for the analogous copolymers [19], having in the side chain only one azoaromatic moiety, and were explained by assuming that the progressive insertion of **MMA** *co*-units in the macromolecules, reduces the cooperative interactions between chiral azoaromatic *co*-units, thus decreasing the conformational order and hence the average length of chain sections with a single prevailing chiral arrangement.

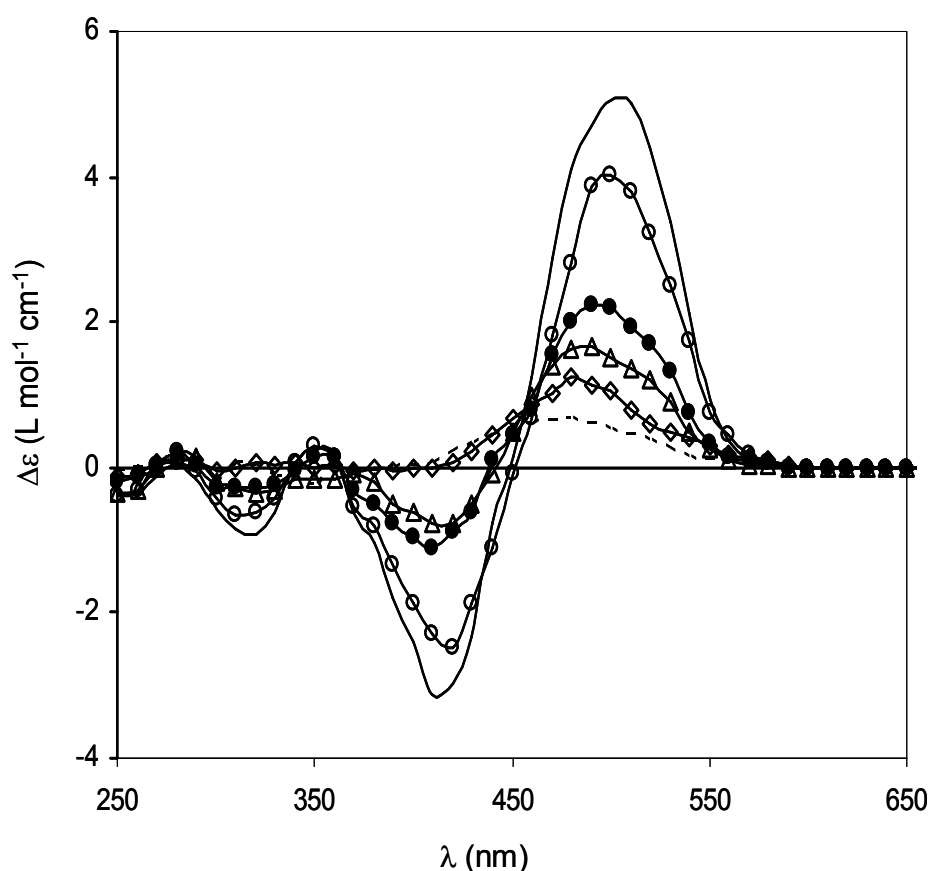


Figure 11. CD spectra in CHCl_3 solution of poly[(*S*)-MPAAP] (—), poly[(*S*)-MPAAP-*co*-MMA] (75/25) (-o-), poly[(*S*)-MPAAP-*co*-MMA] (50/50) (-•-), poly[(*S*)-MPAAP-*co*-MMA] (25/75) (-Δ-), poly[(*S*)-MPAAP-*co*-MMA] (10/90) (-◇-), (*S*)-MPAAP (---).

Accordingly to this view, the CD spectra of copolymers of (*S*)-MPAAP-C and (*S*)-MAAP-N with MMA with a molar chromophore concentration lower than 15%, exhibit only two negative dichroic maximum in correspondence to the UV absorption bands

with a behavior tendentially similar to the related monomers, that exhibit in dilute solution a completely disordered distribution of chromophores with consequent absence of any couplets (Table 6). However, considering the intensity of dichroic absorption in absolute value (Table 6), it appears that even few statistically adjacent chiral units are able to produce a remarkable conformational dissymmetry in the macromolecules. In fact, the copolymers poly[(*S*)-MPAAP-C-co-MMA] at 10% molar content of (*S*)-MPAAP-C and poly[(*S*)-MPAAP-N-co-MMA] at 7% molar content of (*S*)-MPAAP-N show an optical activity appreciably larger than the monomeric compounds. The significant intensity of the dichroic bands of poly[(*S*)-MPAAP] and related copolymers with MMA makes these materials potentially available for chiroptical switching applications [8-10].

The CD spectra of the filmable polymer derivatives, expressed in ellipticity, are quite similar to those shown by the corresponding polymers in solution. (Table7)

Table 7. CD spectra of polymeric derivatives on thin film

Sample	1st absorption band					2nd absorption band				
	λ_1^a	θ_{d1}^b	λ_0^c	λ_2^a	θ_{d2}^b	λ_3^a	θ_{d3}^b	λ_0^c	λ_4^a	θ_{d4}^b
Poly[(<i>S</i>)-MPAAP-co-MMA] (50/50)	516	+0.034	459	423	-0.034	360	+0.002	343	320	-0.007
Poly[(<i>S</i>)-MPAAP-co-MMA] (10/90)	466	+0.003	404	396	-0.001	-	-	-	-	-
Poly[(<i>S</i>)-MPAAP-C-co-MMA] (25/75)	490	+0.033	432	417	-0.008	349	+0.001	325	304	-0.017
Poly[(<i>S</i>)-MPAAP-C-co-MMA] (10/90)	483	+0.004	-	-	-	349	+0.001	331	312	-0.001

a) Wavelength (in nm) of maximum dichroic absorption.

b) Ellipticity (θ_d) normalized for the thickness expressed in mdegree nm⁻¹.

c) Wavelength (in nm) of the cross-over of dichroic bands.

Optical storage experiments on thin film

It is well known that a matching of the absorbance peak with the wavelength of the pumping laser has a positive effect on storage efficiency [1]. For this reason in our

irradiation experiments we have used a laser light operating at 488 nm in resonance with the intense visible electronic transition of the copolymers investigated (Table 5).

To assess the presence of photoinduced linear dichroism and birefringence, films of high optical quality of the polymers have been irradiated with linearly polarized (LP) radiation (writing step) at 488 nm (I about 100 mW/cm^2). After irradiation the polymers show high photoinduced linear birefringence (Figure 12) due to linear ordering of the bisazoaromatic moieties, as evidenced by using a probe radiation at 632.8 nm (I about 1 mW/cm^2), where the samples have negligible absorption.

The photoinduced linear ordering in azobenzene containing materials can be reversibly erased by using circular polarized (CP) or depolarized pump radiation. This is also the case for the investigated polymers, as shown in Figure 12. After irradiation with CP light at 488 nm at room temperature the photoinduced linear birefringence is reduced to a negligible value (erasing step).

Figure 12 suggests that the grow/decay process can be subdivided into a fast and a slow process. The fast process is mainly attributed to the isomerization response of the azo groups, while the slow one is associated with the movement of local polymer segments [6].

The saturated $[\delta n_1]$ and the relaxed linear birefringence $[\delta n_2]$ (Figure 12 and Table 8) increase with the enhancement of the bisazoaromatic content and the permanent dipole of the chromophore in the investigated copolymers.

The relatively high birefringence relaxation of several azopolymers is due to some chromophoric moieties which do not remain oriented on a long term basis, as exhaustively discussed by Natansohn and co-workers [6]. Considering that the macromolecular samples have different azo number density, the most useful comparison among the investigated polymers can be made by calculating birefringence levels per azo unit (δn^*). The average contribution to the orientation per azochromophore is obtained by dividing the maximum birefringence by the azo number density which was calculated from the film density and the azo weight fraction using a described method [6, 11].

Table 8. Characteristics of the photoinduced birefringence

Sample	Chromophoric <i>co</i> -unit content ^a (% mol)	δn_1^b	δn_2^c	S^d	δn^{*e}
Poly[(<i>S</i>)-MAP-C] ^f	100	0.120	0.116	0.93	0.2×10^{-22}
Poly[(<i>S</i>)-MPAAP-C- <i>co</i> -MMA] (10/90)	10	0.110	0.101	0.92	1.5×10^{-22}
Poly[(<i>S</i>)-MPAAP-C- <i>co</i> -MMA] (25/75)	26	0.180	0.165	0.92	1.1×10^{-22}
Poly[(<i>S</i>)-MPAAP- <i>co</i> -MMA] (10/90)	12	0.058	0.045	0.78	1.2×10^{-22}
Poly[(<i>S</i>)-MPAAP- <i>co</i> -MMA] (50/50)	34	0.103	0.082	0.80	1.1×10^{-22}
P3RMM11^g	11.6	0.110	0.100	0.91	1.9×10^{-22}
P3RMM30^g	30.4	0.130	0.120	0.92	1.2×10^{-22}

a) Determined by ¹H-NMR.

b) Saturated photoinduced linear birefringence.

c) Relaxed photoinduced linear birefringence.

d) Relaxation coefficient expressed as the ratio $\delta n_2/\delta n_1$.

e) Photoinduced birefringence per azochromophore. A mass density of 1 g cm^{-3} has been assumed for the polymer films.

f) Ref. [10a].

g) Ref. [11]

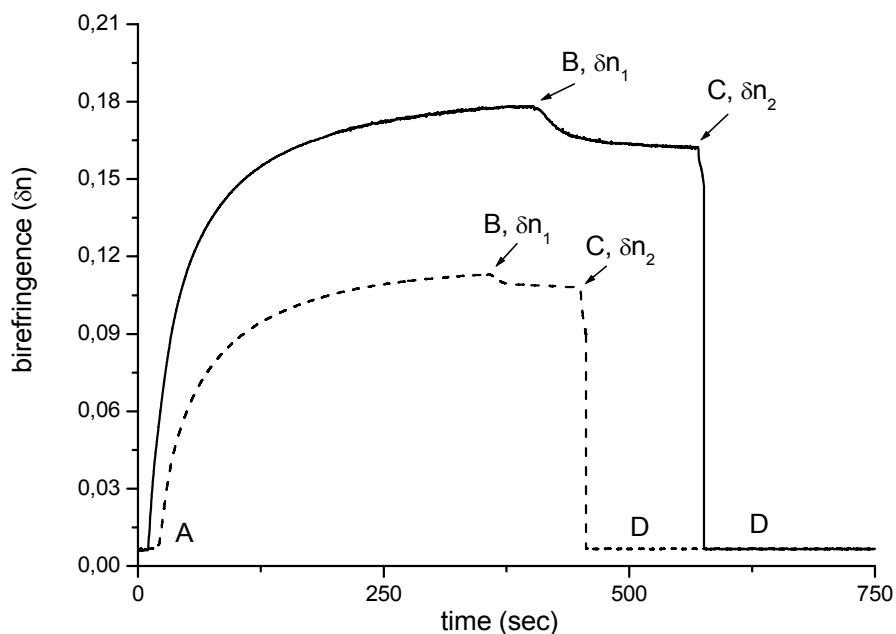


Figure 12. Complete writing-erasing cycle on a 710 nm thick film of poly[(*S*)-MPAAP-C-co-MMA] (25/75) (solid line) and 960 nm thick film of poly[(*S*)-MPAAP-C-co-MMA] (10/90) (dash line) on fused silica. The LP radiation at 488 nm was switched on at point A and switched off at point B. The birefringence signal turns to zero by irradiating with CP light at point C; at point D the erasing CP light was turned off.

As shown in Table 8 the highest birefringence per azo unit is found for Poly[(*S*)-MPAAP-C-co-MMA] (10/90). Such a behaviour can be ascribed to the high bisazoaromatic dilution which reduces the chromophoric dipolar interactions, as demonstrated by the thermal analysis, and allows an improved orientation.

Recently[10a] we have investigated the photoinduced linear optical properties of poly[(*S*)-MAP-C] that, after irradiation with LP light, shows δn_1 of 0.120, which, after removal of the pump, relaxes to a stable value of 0.116, as reported in Table 8. The relaxation is of small extent, with $S=0.93$ (where S is the relaxation coefficient expressed as the ratio $\delta n_2/\delta n_1$), and the induced anisotropy results stable for several months.

In comparison to poly[(*S*)-**MAP-C**], the copolymers containing (*S*)-**MPAAP-C** are characterized by enhanced photoinduced linear birefringence, similar *S* values and higher birefringence per azo unit (Table 8) but displays slower writing/erasing rate.

These behaviours are in agreement with the results reported for analogues methacrylic copolymer **P3RMM11** and **P3RMM30** bearing 11.6 and 30.0 mol%, respectively, of bisazoaromatic dye 4-[N-ethyl-N-(2-hydroxyethyl)amino]-4'-(4-nitrophenylazo)azobenzene (**3RM**) in side chain (Table 8) [11], which depend on photoisomerization quantum yield, on *trans-cis-trans* isomerization rates, on mobility of the polymer segments and on local mobility of the azo moiety. In particular, this last one is controlled by the size of chromophore, by the free volume around the azo moiety, and by the strength of the dipolar interaction between the chromophores [6]. Since the *trans-cis-trans* isomerization cycles require space, enough free volume must be around the azo molecules in order to allow them to align in a certain direction. Being the free volume for photoisomerization larger with increasing sweep volume of the azo residue [11-13] and being the concomitant/concordant isomerizations of the two azo bonds in the same structural units necessary in order to align the side-chain of (*S*)-**MPAAP-C** and of (*S*)-**MPAAP** (as idealized in Figure 13), it appears clear that the kinetics of photorientation of the bisazochromophores are slower than those of the polymer containing (*S*)-**MAP-C**.

The observed photoinduced values for Poly[(*S*)-**MPAAP-C-co-MMA**] (25/75) are larger than those obtained, in the same experimental conditions, for similar achiral systems such as **P3RMM30** [11]. These effects are probably due to their different structures. In fact, the bisazoaromatic moiety in **P3RMM30** is linked to the backbone through a flexible spacer. By contrast, in the investigated chiral copolymers, one of the aromatic rings is conformationally blocked by the pyrrolidine ring, therefore its freedom of rotation around the azo bond is reduced (local mobility) and the T_g values (Table 4) increase which consequently decrease of mobility of the polymer segments. In this way the photoinduced birefringence remains at a higher value and is stable for a longer time than in polymers containing **3RM**.

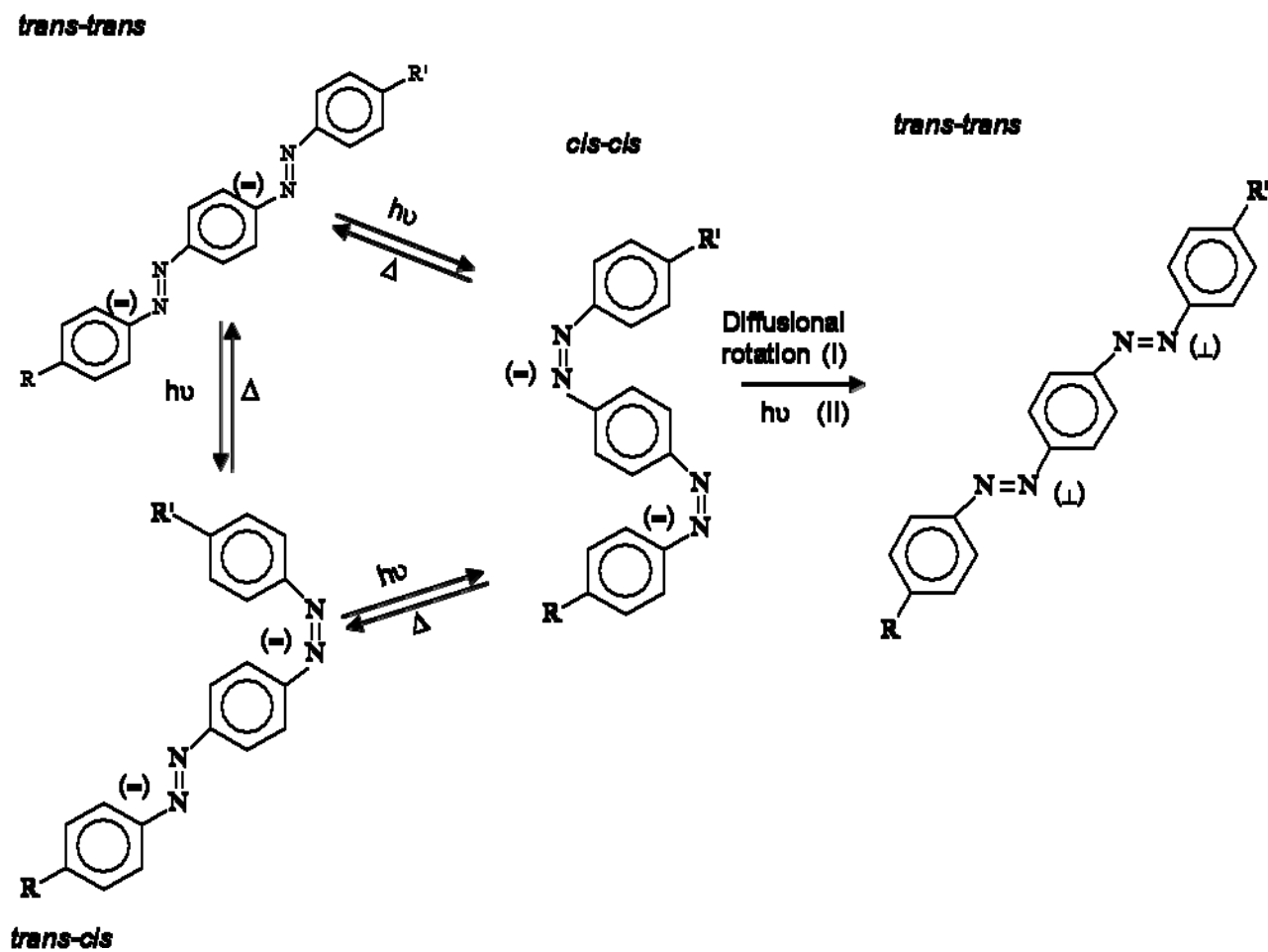


Figure 13. Possible mechanism of isomerization of bisazoaromatic chromophores under laser pumping.

The complete reversibility of the photoinduced linear birefringence of investigated polymeric samples (fatigue resistance properties) as shown for example in Figure 14 after several writing-erasing cycles by photoirradiation alternatively with LP and CP light at 488 nm, seems to be promising for their use in optical storage or more generally in the field of photoresponsive systems. Indeed, after several irradiations steps with LP and CP laser beams alternatively acting on the 870 nm thick film of poly[(*S*)-MPAAP-*co*-MMA] (10/90), the values of maximum photoinduced birefringence (after each irradiation with LP light) and of erased birefringence (after each irradiation with CP light) are quite similar. This indicates that no degradation photoreaction took place upon irradiation with laser light of relatively high intensity (100 mW/cm²). Thus, several cycles could be performed without any significant change in the photoinduced behaviours.

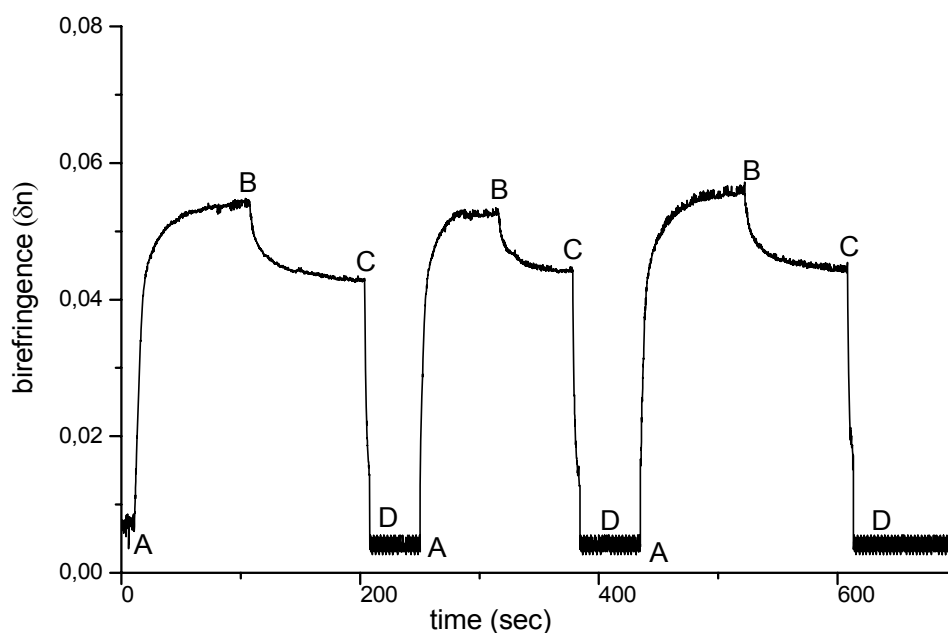


Figure 14. Multiple writing-erasing cycles on a 870 nm thick film of poly[(*S*)-MPAAP-*co*-MMA] (10/90) on fused silica. A, B, C, D as in Figure 12.

Optically active methacrylic copolymers bearing side chain bisazoaromatic moieties: modulation of conformational chirality

The synthesis of two novel series of optically active methacrylic polymers containing a side-chain chiral moiety linked to a photochromic bisazoaromatic chromophore has been carried out by radical copolymerization of the monomer (*S*)-**MPAAP** with *tert*-**BMA** and **TrMA** (Figure 3). The polymeric derivatives have been fully characterized and their spectroscopic and thermal properties compared to those of the monomer, homopolymer and the related copolymers with **MMA** previously investigated (Figure 2).

The optical activity displayed by polymers is discussed in terms of extension of chiral conformation assumed by the macromolecules following the insertion of opportune *co*-monomers which lead to a variation of dipole-dipole interactions between bisazoaromatic chromophores.

Synthesis and characterization of copolymers.

All copolymerization reactions of the optically active monomer (*S*)-**MPAAP** with *tert*-**BMA** and **TrMA** were carried out in glass vials in dry DMF in the presence of AIBN as free radical thermal initiator. Feeds of molar composition as reported in Table 9 (1.0 g of monomers, 2% weight of AIBN in 25 mL of DMF) were introduced into the vials under nitrogen atmosphere, submitted to several freeze-thaw cycles in order to eliminate any trace of dissolved oxygen, and heated at 60°C for 72 hours. The reactions were then stopped by pouring the mixture into a large excess of methanol (200 ml) and the precipitated crude product collected by filtration. The precipitate was repeatedly dissolved in THF (at room temperature) and precipitated again in methanol.

Relevant data for the synthesized copolymers are reported in Table 9.

The conversions were determined gravimetrically and all the products were characterized by FT-IR, ¹H- and ¹³C-NMR.

The molar final composition of copolymers of (*S*)-**MPAAP** with *tert*-**BMA** was assessed by ¹H-NMR (Figure 15) by comparing the integrated signals of aromatic

protons *ortho* to the amino group of (*S*)-**MPAAP** *co*-units, located at 6.70-6.30 ppm, to that one related to the butyl ester group of *tert*-**BMA** *co*-units at 1.60-1.20 ppm, after subtraction of the contribution given to the integral by the overlapped resonances of the main chain protons.

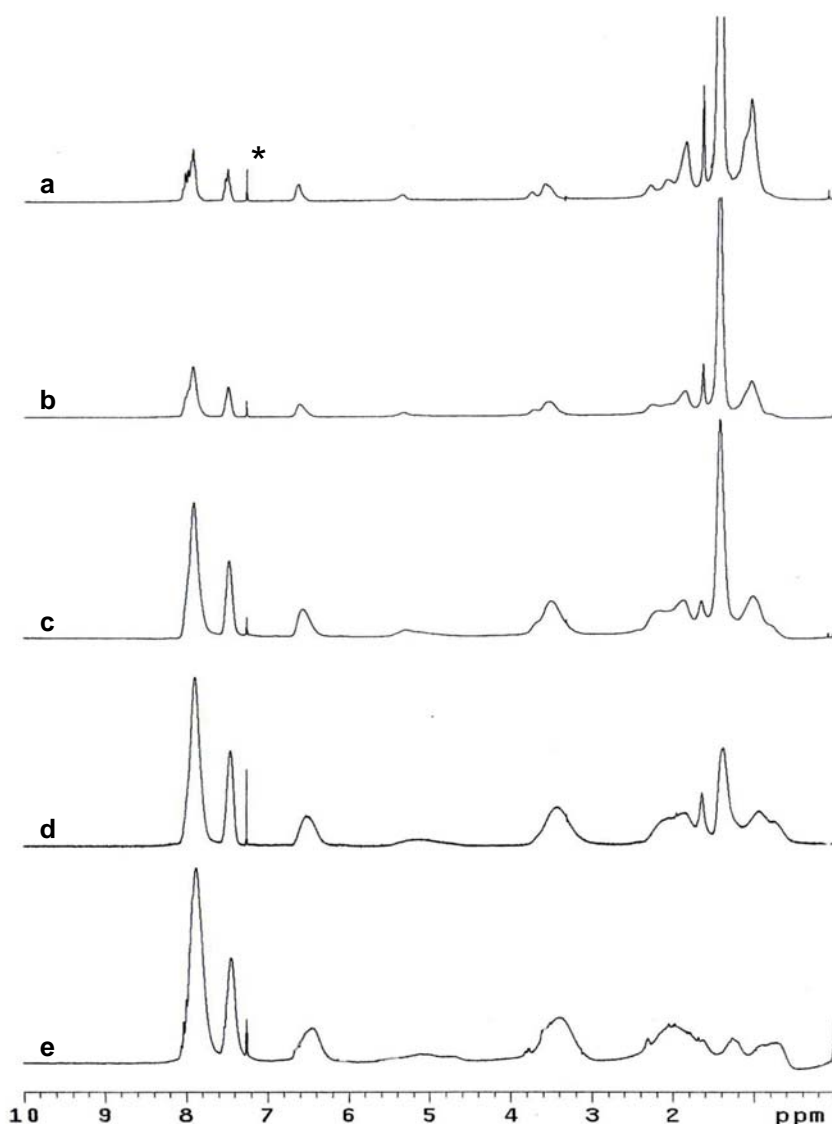


Figure 15. $^1\text{H-NMR}$ spectra in CDCl_3 of poly[(*S*)-**MPAAP-co-tert-BMA**]s at 12% (**a**), 29% (**b**), 62% (**c**), 91% (**d**) molar content of (*S*)-**MPAAP** *co*-units and of poly[(*S*)-**MPAAP**] (**e**). Starred signals refer to solvent resonances.

Table 9. Characterization data of polymeric derivatives

Feed		Yield ^{a)} %	\bar{M}_n ^{b)} g/mol	\bar{M}_w/\bar{M}_n ^{b)}	content (S)-MPAAP % mol ^{c)}	\bar{X}_n ^{d)}	T_g ^{e)} °C	T_d ^{f)} °C
(S)-MPAAP	<i>tert</i> -BMA							
100 ^{g)}	0	14	1.3	62	100	62	191	283
75	25	64	1.7	66	91	66	161	277
50	50	68	1.7	66	62	66	156	275
25	75	69	1.7	84	28	84	148	267
10	90	38	1.5	111	12	111	145	269
(S)-MPAAP	TrMA							
75	25	61	1.8	89	86	89	160	267
50	50	50	1.7	91	71	91	158	257
25	75	31	1.7	74	51	74	151	241
10	90	3	1.4	60	41	60	150	240

a) Calculated as (g polymer/g monomer) · 100.

b) Determined by SEC in THF solution at 25°C.

c) Determined by ¹H-NMR.

d) Average polymerization degree \bar{X}_n calculated according to eq. 1.

e) Glass transition temperature determined by DSC at 10°C/min heating rate under nitrogen flow.

f) Initial decomposition temperature as determined by TGA at 20°C/min heating rate under air flow.

Table 10. Mean sequence lengths (\bar{l}) and molar fraction $X_{(n)}$ (%) of (S)-MPAAP and of achiral *co*-units having sequence length of n units in the investigated copolymers.

(S)-MPAAP ^{a)} (% mol)	$X_{(S)\text{-MPAAP}(n)}$					$X_{\text{achiral comonomer}(n)}$						
	n=1	2	3	4	>4	n=1	2	3	4	>4		
	$\bar{l}_{(S)\text{-MPAAP}}$	$\bar{l}_{\text{tert-BMA}}$										
12.1	1.72	13.70	33.7	28.3	17.8	10.0	10.3	0.5	1.0	1.4	1.7	95.4
28.2	2.87	5.90	12.1	15.8	15.5	13.4	43.2	2.9	4.8	5.9	6.6	79.9
61.8	5.79	2.92	3.0	4.9	6.1	6.8	79.2	11.7	15.4	15.2	13.3	44.2
90.5	13.66	1.73	0.5	1.0	1.4	1.7	95.4	33.6	28.2	17.8	10.0	10.4
	$\bar{l}_{(S)\text{-MPAAP}}$	\bar{l}_{TrMA}										
40.1	1.31	1.75	58.3	27.6	9.8	3.1	1.3	32.8	28.0	18.0	10.2	11.0
51.2	1.71	1.33	34.1	28.4	17.7	9.8	10.0	57.0	27.9	10.3	3.4	1.5
62.3	3.01	1.12	11.1	14.8	14.8	13.2	46.2	80.4	16.6	2.6	0.4	0.1
86.0	6.14	1.05	2.7	4.4	5.6	6.2	81.1	91.6	7.9	0.5	0.0	0.0
	$\bar{l}_{(S)\text{-MPAAP}}$	\bar{l}_{MMA}										
12.1	1.01	7.74	97.8	2.2	0.0	0.0	0.0	1.7	2.9	3.8	4.4	87.2
26.5	1.04	2.88	92.3	7.3	0.4	0.0	0.0	12.0	15.7	15.4	13.4	43.4
34.1	1.17	1.45	72.9	21.3	4.7	0.9	0.2	47.5	29.5	13.8	5.7	3.5
68.8	1.50	1.16	44.7	29.6	14.7	6.5	4.4	74.9	20.1	4.1	0.7	0.1

^{a)} Content in mol % of (S)-MPAAP *co*-units in the copolymers.

The molar final compositions of the copolymers of (S)-MPAAP with TrMa were established by an analogous procedure by comparing the integrated peak areas in both the aromatic and aliphatic regions of (S)-MPAAP and TrMA *co*-units resonances.

As reported in Table 9, the molar content of *co*-units in the copolymers do not reflect the feed composition.

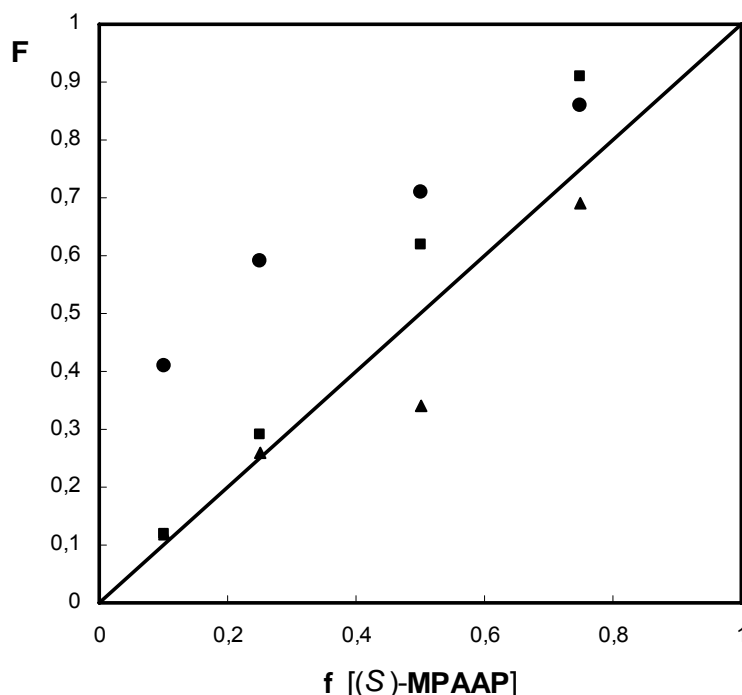


Figure 16. Copolymerization diagrams: molar fraction (F) of (S)-MPAAP *co*-units in poly[(S)-MPAAP-*co*-MMA]s (▲), poly[(S)-MPAAP-*co*-*tert*-BMA]s (■) and poly[(S)-MPAAP-*co*-TrMA]s (●) as a function of molar fraction of (S)-MPAAP in the feed (f).

The copolymerization diagram (Figure 16) clearly indicating an appreciable higher reactivity of (S)-MPAAP with respect to *tert*-BMA and TrMa in all the copolymerization runs. Indeed, an approximate evaluation of the reactivity ratios performed by using the modified Kelen-Tüdös method [20] gives for poly[(S)-MPAAP-*co*-*tert*-BMA]s reactivity ratios $r_{(S)\text{-MPAAP}} = 6.95$ and $r_{\text{tert-BMA}} = 1.32$ with a $r_{(S)\text{-MPAAP}}r_{\text{tert-BMA}}$ product of 9.17 and for poly[(S)-MPAAP-*co*-TrMA]s $r_{(S)\text{-MPAAP}} = 2.93$ and $r_{\text{TrMA}} = 0.08$ with a $r_{(S)\text{-MPAAP}}r_{\text{TrMA}}$ product of 0.23. By contrast, the copolymerization data of (S)-MPAAP with MMA, previously described, give a $r_{(S)\text{-MPAAP}}r_{\text{MMA}}$ product of 0.08 with $r_{(S)\text{-MPAAP}} = 0.13$ and $r_{\text{MMA}} = 0.58$, indicative in this case of a certain tendency to an alternating distribution of the *co*-units along the polymeric chain. This behaviour is clearly due to the larger steric hindrance of *tert*-BMA and TrMA with respect to MMA that favours the possibility of formation of (S)-MPAAP sequences as compared to the related copolymers with MMA.

As a consequence, the mean sequence length of chiral *co*-units ($\bar{l}_{(S)\text{-MPAAP}}$) in the copolymers with **MMA** results shorter than in poly[(*S*)-**MPAAP-co-TrMA**]s and poly[(*S*)-**MPAAP-co-tert-BMA**]s, which are rich of adjacent chiral units having sequence length of $n \geq 3$ units, as shown in Table 10 (where the mean sequence lengths of the *co*-units and the molar fractions of sequences of length n have been calculated utilizing the well known methods reported in the literature [21]).

Thermal analysis of polymeric derivatives

The onset decomposition temperature values (T_d), as determined by thermogravimetric analysis (TGA), are rather high (in the range 240-310 °C) and appear similar for all the copolymeric samples (Table 9). This is indicative of considerable thermal stability of the macromolecular derivatives under the adopted conditions.

The comparison of the T_d values displayed by the copolymers containing **TrMA** and *tert*-**BMA** with those with **MMA** suggests a somewhat lower thermal stability of the former derivatives, which could be attributed to the different chemical nature of the comonomers and/or to a decrease of the dipolar interactions between bisazoaromatic chromophores, although their mean sequence length is higher.

Only second-order transitions originated by glass transitions (T_g), with no melting peaks, are observed in the DSC thermograms of the investigated polymers (Table 9), thus suggesting that the macromolecules are substantially amorphous in the solid state. The T_g values appear quite high, even for the samples poorest in (*S*)-**MPAAP** moieties, laying in the range 140-180°C, thus making possible the application of these copolymeric materials in optoelectronics.

It is worth observing that all the copolymeric derivatives exhibit considerably higher T_g values than the related poly(**MMA**) ($T_g = 105^\circ\text{C}$), [22] poly(*tert*-**BMA**) ($T_g = 107^\circ\text{C}$) [22] and poly(**TrMA**) ($T_g = 133^\circ\text{C}$), [22] thus confirming the presence of strong inter- and/or intramolecular dipolar interactions in the solid state between bisazoaromatic chromophores.

The comparison between the copolymers of *tert*-**BMA** and **TrMA** with those containing **MMA** *co*-units suggests that also a small amount of highly hindering *co*-monomer (*tert*-**BMA** and **TrMA**) appreciably reduces the T_g of the material (Figure 17).

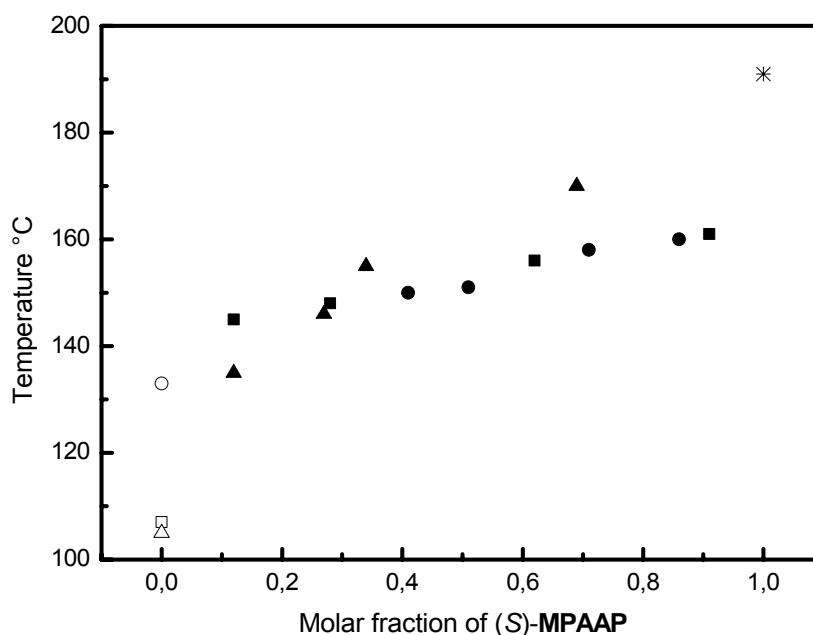


Figure 17. Dependence of the glass transition temperature (T_g) of polymeric derivatives poly[(*S*)-MPAAP-*co*-MMA]s (▲), poly[(*S*)-MPAAP-*co*-*tert*-BMA]s (■) and poly[(*S*)-MPAAP-*co*-TrMA]s (●) in function of the (*S*)-MPAAP content. The values for the homopolymeric derivatives poly(MMA) (Δ), poly(*tert*-BMA) (□), poly(TrMA) (○) and poly[(*S*)-MPAAP] (*) are also reported.

Actually, the derivatives with a molar content of MMA *co*-units as high as 25% display a remarkable enhancement of T_g with respect to the related derivatives containing similar amount of *tert*-BMA and TrMA *co*-units.

This behaviour shows the possibility to modulate the thermal properties of this particular class of polymeric materials containing azoaromatic moieties by copolymerization with suitable amounts of optically inactive *co*-monomers.

In addition, as the decomposition temperatures (T_d) are about 90-180°C higher than the corresponding T_g , a thermal treatment of the material, as required for corona and electric-poling, near the T_g value would not expectedly produce any decomposition. Both the good thermal stability and the high value of T_g suggest therefore that these

polymeric materials may be promisingly used for applications in optoelectronics (optical data storage, chiroptical switches, etc).

Absorption spectra

All copolymeric compounds exhibit (Table 11) analogous absorption spectra of poly[(*S*)-MPAAP] (Table 2).

Table 11. UV-vis spectra in CHCl₃ of the copolymers of (*S*)-MPAAP with *tert*-BMA and TrMA.

Sample	1st band		2nd band	
	$\lambda_{\max}^{\text{a)}$	$\epsilon_{\max} 10^{-3}^{\text{b)}$	$\lambda_{\max}^{\text{a)}$	$\epsilon_{\max} 10^{-3}^{\text{b)}$
	nm	L mol ⁻¹ cm ⁻¹	nm	L mol ⁻¹ cm ⁻¹
Poly[(<i>S</i>)-MPAAP- <i>co-tert</i> -BMA]-(91)	461	33.6	331	16.2
Poly[(<i>S</i>)-MPAAP- <i>co-tert</i> -BMA]-(62)	461	33.1	332	16.5
Poly[(<i>S</i>)-MPAAP- <i>co-tert</i> -BMA]-(28)	465	33.5	331	16.1
Poly[(<i>S</i>)-MPAAP- <i>co-tert</i> -BMA]-(12)	467	35.6	331	16.1
Poly[(<i>S</i>)-MPAAP- <i>co</i> -TrMA]-(86)	465	33.5	333	17.0
Poly[(<i>S</i>)-MPAAP- <i>co</i> -TrMA]-(71)	468	35.0	333	16.8
Poly[(<i>S</i>)-MPAAP- <i>co</i> -TrMA]-(51)	469	35.5	334	16.9
Poly[(<i>S</i>)-MPAAP- <i>co</i> -TrMA]-(41)	470	35.7	333	16.9

^{a)} Wavelength of maximum absorbance.

^{b)} Calculated for one repeating unit in the polymers.

By contrast with the copolymers with MMA (Table5), displaying spectroscopic features more similar to those exhibited by the low molecular weight monomeric compound rather than those of the homopolymer, thus confirming the above mentioned tendency to an alternating distribution of the repeating co-units in these derivatives, the copolymers of (*S*)-MPAAP with *tert*-BMA and TrMA exhibit a behaviour resembling that one of poly[(*S*)-MPAAP]. Indeed, increasing the distance between the bisazoaromatic chromophores, by the progressive insertion in the macromolecular chain of non-Optically active, photoresponsive multifunctional polymeric materials

chromophoric methacrylic *co*-units, allows the possibility of lower dipolar intramolecular interactions. This originates a random distribution in dilute solution of the chromophores, giving rise to a behaviour tendentially more similar to that of the monomer.

As a consequence, the copolymers with higher chromophore content display molar adsorption coefficient values (ϵ_{\max}) similar to poly[(*S*)-**MPAAP**].

In general, it also appears that the electronic transitions of the copolymeric systems in solution are substantially unaffected by the presence in the side chain of different optically inactive *co*-units.

Chiroptical properties

The chiroptical properties of the copolymers of (*S*)-**MPAAP** with *tert*-**BMA** and **TrMA** have been investigated by CD in the spectral region 250-700 nm in order to assess the conformational features of the macromolecular chains (Table 12, Figure 18a/18b) and compared with those of poly[(*S*)-**MPAAP-co-MMA**]s (Table 6) and with related homopolymer poly[(*S*)-**MPAAP**] (Table 3). As previously described, though (*S*)-**MPAAP** does not display any relevant CD band in the 250–700 spectral region, poly[(*S*)-**MPAAP**] shows dichroic absorptions connected to the electronic transitions of the bisazoaromatic chromophore in the *trans* form (Table 3).

The CD spectra of poly[(*S*)-**MPAAP-co-tert-BMA**]s and poly[(*S*)-**MPAAP-co-TrMA**]s are reported in Figure 18a and 18b, respectively. In these cases, the intensities of dichroic absorptions decrease upon decreasing the content of optically active bisazoaromatic (*S*)-**MPAAP** *co*-units (Table 12).

As described for copolymers containing **MMA** (Table 6) this phenomena can be explained by assuming that the progressive insertion of achiral *co*-units in the macromolecules reduces the extent of the cooperative interactions between chiral bisazoaromatic *co*-units, thus decreasing the average length of chain sections with a single prevailing chiral arrangement and hence the conformational order, with respect to poly[(*S*)-**MPAAP**].

Table 12. CD spectra in CHCl₃ of copolymers of (*S*)-**MPAAP** with *tert*-**BMA** and **TrMA**.

Sample	1st band					2nd band				
	$\lambda_1^{\text{a)}$	$\Delta\varepsilon_1$	$\lambda_0^{\text{b)}$	$\lambda_2^{\text{a)}$	$\Delta\varepsilon_2$	$\lambda_3^{\text{a)}$	$\Delta\varepsilon_3$	$\lambda_0^{\text{b)}$	$\lambda_4^{\text{a)}$	$\Delta\varepsilon_4$
	nm	Lmol ⁻¹ cm ⁻¹	nm	nm	Lmol ⁻¹ cm ⁻¹	nm	Lmol ⁻¹ cm ⁻¹	nm	nm	Lmol ⁻¹ cm ⁻¹
Poly[(<i>S</i>)- MPAAP-co-tert-BMA]-(91)	507	+3.73	452	417	-2.18	355	+0.60	339	318	-0.60
Poly[(<i>S</i>)- MPAAP-co-tert-BMA]-(62)	498	+1.62	452	415	-1.46	350	+0.42	334	317	-0.28
Poly[(<i>S</i>)- MPAAP-co-tert-BMA]-(28)	504	+0.98	451	418	-0.90	355	+0.24	335	322	-0.27
Poly[(<i>S</i>)- MPAAP-co-tert-BMA]-(12)	475	+0.79	-	-	-	347	+0.14	326	312	-0.07
Poly[(<i>S</i>)- MPAAP-co-TrMA]-(86)	502	+3.05	452	417	-2.05	351	+0.31	343	317	-0.61
Poly[(<i>S</i>)- MPAAP-co-TrMA]-(71)	503	+2.57	453	418	-1.62	353	+0.23	343	317	-0.61
Poly[(<i>S</i>)- MPAAP-co-TrMA]-(51)	499	+1.58	449	409	-0.96	352	+0.20	343	318	-0.60
Poly[(<i>S</i>)- MPAAP-co-TrMA]-(41)	500	+1.05	446	410	-0.40	355	+0.14	340	320	-0.25

a) Dichroic maximum wavelength.

b) Wavelength at cross over point

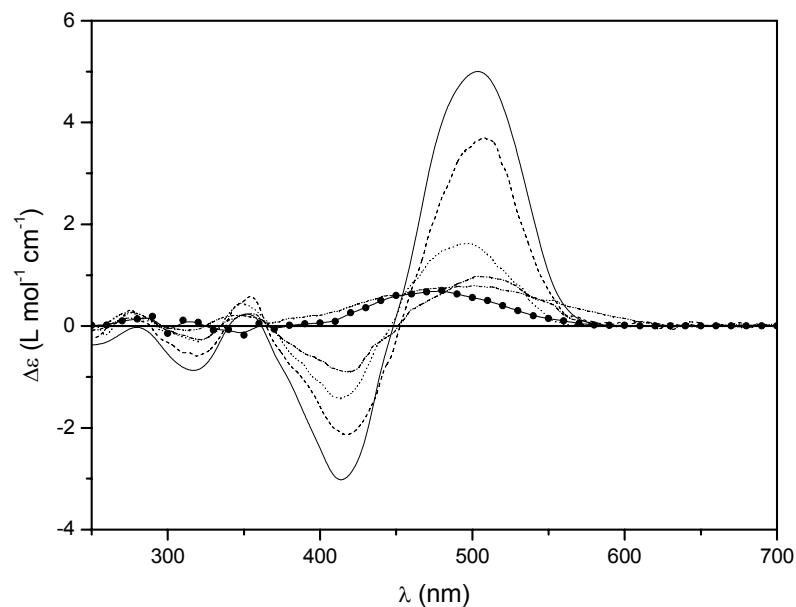


Figure 15a. CD spectra in CDCl_3 of poly[(*S*)-MPAAP-*co-tert*-BMA]s at 12% (-----), 29% (.....), 62% (-----), 91% (.....) molar content of (*S*)-MPAAP *co*-units, poly[(*S*)-MPAAP] (—) and of (*S*)-MPAAP (—●—).

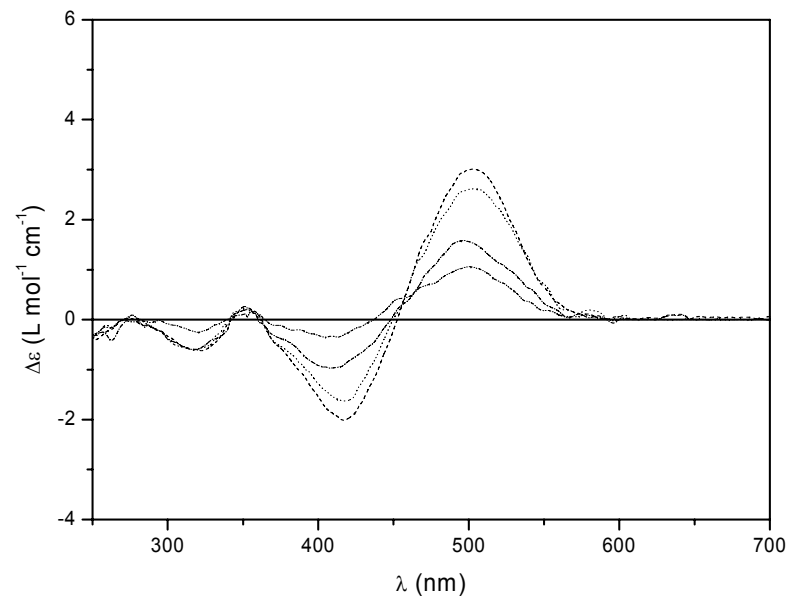


Figure 15b. CD spectra in CDCl_3 of poly[(*S*)-MPAAP-*co-TrMA*]s at 41% (-----), 51% (.....), 71% (-----) and 86% (.....) molar content of (*S*)-MPAAP *co*-units

On the other hand, the chiroptical properties of the investigated copolymers appear influenced by the presence and chemical nature of the achiral *co*-monomer. For example, though the exciton splitting connected to the UV-Vis 1st absorption band is well visible in the CD spectrum of poly[(*S*)-MPAAP-*co*-MMA]-(12) (Figure 11) at a molar content of bisazoaromatic chromophore as low as 12%, poly[(*S*)-MPAAP-*co*-*tert*-BMA]-(12) having the same composition shows only one positive dichroic band, with a behaviour tendentially similar to the monomer, that exhibits in dilute solution a completely disordered distribution of chromophores with consequent absence of any couplet (Table 18).

In order to compare the optical activity and to evaluate the amount of dissymmetric conformations assumed by the macromolecules in chloroform solution, we report in Figure 19 the integrated areas of the dichroic bands connected to the first UV-vis absorption band as a function of the molar content of chiral (*S*)-MPAAP *co*-units of the investigated compounds.

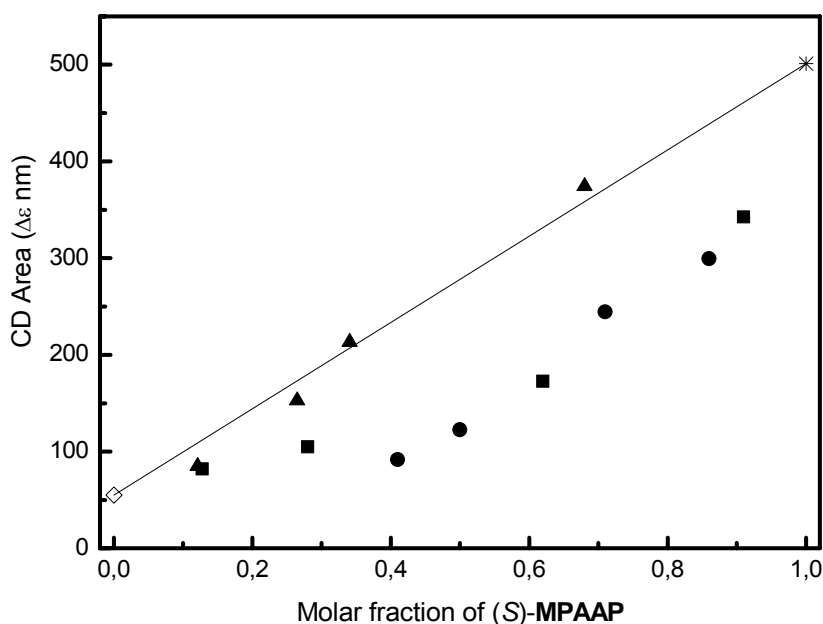


Figure 7. Evolution of the amplitude of the CD exciton couplet of 1st band of poly[(*S*)-MPAAP-*co*-MMA]s (▲), poly[(*S*)-MPAAP-*co*-*tert*-BMA]s (■) and poly[(*S*)-MPAAP-*co*-TrMA]s (●) in function of the (*S*)-MPAAP content. The values for poly[(*S*)-MPAAP] (*) and (*S*)-MPAAP (◇) are also reported.

Significantly different trends are obtained: while the values of CD signals appear to increase linearly with the molar fraction of chiral *co*-units in the copolymers with **MMA**, the experimental CD values of poly[(*S*)-**MPAAP-co-tert-BMA**]s and poly[(*S*)-**MPAAP-co-TrMA**]s result to be substantially lower than those calculated on the basis of a linear dependence on composition (solid line in Figure 19).

The variation of optical activity of the polymeric derivatives with the composition could be ascribed, in principle, also to the main-chain stereoregularity originated by a prevalent microtacticity of the repeating units.

The microtacticity of the investigated copolymers has been evaluated by integration of the ¹³C-NMR signals related to the methacrylic methyl group at about 20 and 18 ppm, belonging to *meso-racemo* (*mr*) heterotactic and *racemo-racemo* (*rr*) syndiotactic triads [23] respectively.

Assuming that the polymerization process follows a Bernoullian statistics, the probabilities of formation of a *meso* dyad *m* (P_m) can be calculated from the integrated signals ratio (*mr/rr*), which corresponds to $2P_m(1-P_m)/(1-P_m)^2$, i.e. to the ratio between the probability of formation of *mr* and *rr* triads [24]. The results (Table 13) confirm that the process follows a Bernoullian statistics, as indicated by the similarity of $P_{m/r}$ with $P_{m/m}$ and of $P_{r/m}$ with $P_{r/r}$, as well as by the sum equal to one of $P_{m/r}$ with $P_{r/r}$ and of $P_{m/m}$ with $P_{r/m}$ [24].

The values for the series of copolymers containing **MMA** and *tert-BMA*, as reported in Table 13, indicate a content of syndiotactic (*rr*) triads around 50-58%, with a probability of formation of *meso* and *racemo* dyads of 0.24-0.32 and 0.68-0.76 respectively, in agreement with literature reports concerning the radical polymerization of **MMA** [24]. The homopolymer poly[(*S*)-**MPAAP**] shows a similar stereoregularity degree (0.31 probability of forming *meso* dyads). Thus, in these polymers the main chain microstructure is essentially atactic, with a predominance of syndiotactic triads suggesting a substantially low stereoregularity of the main-chain.

Table 13. Microtacticity of bisazoaromatic polymeric derivatives as determined by $^{13}\text{C-NMR}^{\text{a}}$

Sample	P_m	P_r	mm (%)	$mr(rm)$ (%)	rr (%)	$P_{m/r}$	$P_{r/m}$	$P_{m/m}$	$P_{r/r}$
Poly[(S)-MPAAP]	0.31	0.69	10	43	47	0.31	0.69	0.31	0.69
Poly[(S)-MPAAP-co-tert-BMA]-(91)	0.28	0.72	8	40	52	0.28	0.72	0.28	0.72
Poly[(S)-MPAAP-co-tert-BMA]-(62)	0.26	0.74	7	39	54	0.26	0.74	0.26	0.74
Poly[(S)-MPAAP-co-tert-BMA]-(28)	0.25	0.75	6	38	56	0.25	0.75	0.25	0.75
Poly[(S)-MPAAP-co-tert-BMA]-(12)	0.28	0.72	8	40	53	0.28	0.72	0.28	0.72
Poly[(S)-MPAAP-co-TrMA]-(86)	0.36	0.64	13	46	41	0.36	0.64	0.36	0.64
Poly[(S)-MPAAP-co-TrMA]-(71)	0.40	0.60	16	48	36	0.40	0.60	0.40	0.60
Poly[(S)-MPAAP-co-TrMA]-(51)	0.43	0.57	18	49	33	0.43	0.58	0.42	0.57
Poly[(S)-MPAAP-co-TrMA]-(41)	0.44	0.56	19	50	31	0.44	0.57	0.43	0.56
Poly[(S)-MPAAP-co-MMA]-(69)	0.32	0.68	10	44	46	0.32	0.68	0.32	0.68
Poly[(S)-MPAAP-co-MMA]-(34)	0.29	0.71	8	41	51	0.29	0.71	0.29	0.71
Poly[(S)-MPAAP-co-MMA]-(27)	0.28	0.72	8	40	52	0.28	0.72	0.28	0.72
Poly[(S)-MPAAP-co-MMA]-(12)	0.24	0.76	6	36	58	0.24	0.76	0.24	0.76

a) P_m and P_r represent the probability of formation of *meso* and *racemo* dyads respectively; mm , $mr(rm)$ and rr are the percent amounts of triads present in the polymers; $P_{m/r}$, $P_{r/m}$, $P_{m/m}$ and $P_{r/r}$ are the calculated probabilities that a given dyad follows a dyad having the same or the opposite relative configuration.

TrMA is known to give partially isotactic polymer by radical polymerization (content of isotactic triad of 64%) [25]. The isotactic specificity in this polymerization has been explained in terms of steric repulsion between the side-chain triphenylmethyl group of an entering monomer and that of the growing chain end which prevents syndiotactic addition, and with the formation of a rigid and stable one-handed helical conformation of the growing polymer chain sustained by the bulky side groups, which improves the isotactic addition of an entering monomer.

In our case, poly[(*S*)-**MPAAP-co-TrMA**]s show a content of isotactic (*mm*) triads ranging from 13% to 19% with the increase of **TrMA** contents, with a probability of formation of *meso* and *racemo* dyads of 0.36-0.44 and 0.56-0.64 respectively (Table 13).

Consequently, it appears that the AIBN-initiated radical copolymerization of **TrMA** with (*S*)-**MPAAP** is poorly stereoselective, with a predominance of heterotactic triads (*mr/rm*), and hence is unable to favour a predominant tacticity of the macromolecules.

Although the investigated copolymers have dissimilar stereoregularities of the main chain, thus however does not give appreciable contributions to the overall optical activity of the macromolecules, which can be only ascribed to the presence in the side chain of conformational dissymmetry originated by the (*S*)-3-hydroxy pyrrolidine bisazoaromatic repeating units at least for chain sections.

On the other hand, considering the mean sequence lengths of the chiral *co*-units ($\bar{l}_{(S)\text{-MPAAP}}$), the molar fractions (%) $X_{(S)\text{-MPAAP}(n)}$ in poly[(*S*)-**MPAAP-co-MMA**]s (reported in Table 10) and the intensity of dichroic absorption in absolute value (Figure 19), it appears that to produce a remarkable conformational dissymmetry in the macromolecules is necessary even few statistically adjacent chiral units or a low fraction of sequences of sufficiently high length. In fact, also the copolymers at lower molar content of (*S*)-**MPAAP** already show an optical activity appreciably larger than the monomeric compound (*S*)-**MPAAP**, although they are constituted by 97,8% of isolated units ($X_{(S)\text{-MPAAP}(1)}$) and only the 2.2% of sequences of 2 repeating units ($X_{(S)\text{-MPAAP}(2)}$).

This is confirmed by recent studies on similar dimeric derivative 2,4-dimethyl-glutaric acid bis-(*S*)-3-[1-(4'-nitro-4-azobenzene)-pyrrolidine ester [10d], corresponding to the

smallest section of photochromic polymers where interchromophore interactions between azobenzene moieties can be present. Its CD spectra, in fact, showed a strong exciton couplet, which suggests that chiral interactions between a couple of chromophores are already important and that the optical activity of these materials should be substantially related to relatively short chain sections with conformational dissymmetry of one prevailing screw sense.

Previously, we have observed that the conformational chirality of these macromolecules strongly depends on their chain length, and increases with the enhancement of the number of adjacent chiral residues of (*S*)-3-hydroxy pyrrolidine in the side chain related to the increase of the average polymerization degree (in the range 2–30).[26]

Nevertheless poly[(*S*)-MPAAP-*co*-TrMA]s and poly[(*S*)-MPAAP-*co*-*tert*-BMA]s, much rich of adjacent chiral units having sequence length of $n \geq 3$ units (Table 10), show optical activity values lower than poly[(*S*)-MPAAP-*co*-MMA]s. Indeed, at the same content of chiral *co*-units, the deviation of the experimental CD values with respect to the linear calculated ones resulted higher on passing from MMA to *tert*-BMA and TrMA (Figure 19).

This behaviour suggests that, at similarity of side-chain chiral residues, main-chain stereoregularity and average sequence length of the chiral *co*-units ($\bar{l}_{(S)\text{-MPAAP}}$), the different extent of optical activity shown by these copolymeric materials has to be only ascribed to the increasing steric hindrance of the side-chain substituents in the achiral *co*-units, which appears to main factor negatively affecting the macromolecular chirality.

Conclusion

Three homopolymeric methacrylates have been obtained by radical polymerization of novel monomers (*S*)-**MAAP**, (*S*)-**MAAP-C** and (*S*)-**MAAP-N**, bearing the optically active (*S*)-3-hydroxy pyrrolidinyl group linked to bisazoaromatic chromophores.

Poly[(*S*)-**MPAAP**] is soluble at room temperature in THF or CHCl₃. By contrast, the dried poly[(*S*)-**MPAAP-C**] and poly[(*S*)-**MPAAP-N**] samples resulted poorly soluble in common organic solvents, thus preventing their complete characterization in solution and as thin films.

The optical activity of poly[(*S*)-**MAAP**], investigated by CD, indicates that the macromolecules assume, both in solution and as solid thin film, highly homogeneous conformations with a prevailing chirality, as demonstrated by the presence of a strong exciton couplets in the CD spectra.

This behaviour can be attributed to the combined presence of the strongly dipolar conjugated bisazoaromatic system with the conformational stiffness of pyrrolidine ring, both of them favouring the instauration of conformational arrangements with a prevailing handedness, at least for chain sections of the macromolecules.

Copolymerization of these three optically active monomers with **MMA** gives polymeric products exhibiting a lower optical activity with respect to the corresponding homopolymers, as a consequence of a reduction of the conformational homogeneity along the macromolecular backbone upon increasing the content of **MMA** *co*-units.

The different amplification of conformational chirality observed passing from the copolymers of (*S*)-**MPAAP** with **TrMA** and *tert*-**BMA** to those with **MMA**, suggests that it is possible to modulate the optical activity of these novel polymers by insertion of different achiral comonomers with different steric hindrance.

Comparison of the T_g values displayed by the copolymers with *tert*-**BMA** and **TrMA** with those containing **MMA** *co*-units suggests that it is possible to modulate the thermal properties of this particular class of polymeric materials containing bisazoaromatic groups by copolymerization with suitable achiral *co*-monomers.

The pronounced red shift of the maximum absorption wavelength on passing from the polymeric derivatives bearing only one azo bond to the bisazoaromatic containing polymers appears of great interest for photoresponsive applications.

Indeed, the properties shown by the polymers investigated suggest that they may be considered as multifunctional derivatives bearing at the same time chemical functionalities potentially useful in photonic devices as well as chiroptical switches.

Photoinduced birefringence experiments show that the synthesized polymers containing two azo bonds present slower optical response rates in comparison to the similar polymers containing only one azo bond. However, large and relatively stable birefringence and all-optical switching effects have been realized in the polymer films having a low content of photochromic *co*-unit (better solubility and processability) which are expected to find applications in photonic devices, such as spatial light modulators, filters, polarizers, optical storage of informations and for optical communication and image processing.

Experimental Section

Chemicals

Trans-4-phenylazoaniline and *trans*-4-(4-aminophenylazo)nitrobenzene (disperse orange) were purchased from Aldrich and crystallized from ethanol/water 1:1 (v:v) before use.

Methacryloyl chloride (Aldrich) was distilled (bp 95°C) under inert atmosphere in the presence of traces of 2,6-di-*tert*-butyl-*p*-cresol as polymerization inhibitor before use.

Chloroform, tetrahydrofuran (THF) and *N,N*-dimethylformamide (DMF) were purified and dried according to the reported procedures [27] and stored under nitrogen over molecular sieves (4 Å).

Methyl methacrylate (**MMA**) (Merck) was purified by distillation under reduced pressure (bp 46°C at 100 mmHg) in the presence of traces of 2,6-di-*tert*-butyl-*p*-cresol as polymerization inhibitor before use.

Triethylamine (Aldrich) was refluxed over dry CaCl₂ for 8 h, then distilled (bp 89°C) under nitrogen atmosphere. 2,2'-Azobisisobutyronitrile (AIBN) (Aldrich) was crystallized from abs. ethanol before use. All other reagents and solvents (Aldrich) were used as received without further purification.

The alcohol (*S*)-3-hydroxy-1-phenyl pyrrolidine [(*S*)-**HPP**] was prepared as previously reported [8].

Trans-4-(4-aminophenylazo)benzotrile was synthesized by a procedure similar to that one described in literature [11, 28].

Measurements

¹H- and ¹³C-NMR spectra were obtained at room temperature, on 5-10% CDCl₃ solutions, unless otherwise stated, using a Varian NMR Gemini 300 spectrometer. Chemical shifts are given in ppm from tetramethylsilane (TMS) as the internal reference. ¹H-NMR spectra were run at 300 MHz by using the following experimental conditions: 24,000 data points, 4.5-kHz spectral width, 2.6-s acquisition time, 128 transients. ¹³C-NMR spectra were recorded at 75.5 MHz, under full proton decoupling,

by using the following experimental conditions: 24,000 data points, 20-kHz spectral width, 0.6-s acquisition time, 64,000 transients.

FT-IR spectra were carried out on a Perkin-Elmer 1750 spectrophotometer, equipped with an Epson Endeavour II data station, on sample prepared as KBr pellets.

UV-Vis absorption spectra were recorded at 25°C in the 650–250 nm spectral region with a Perkin-Elmer Lambda 19 spectrophotometer on CHCl₃, THF or DMA solution by using cell path lengths of 0.1 cm. Concentrations in bisazobenzene chromophore of about $3 \times 10^{-4} \text{ mol}\cdot\text{L}^{-1}$ were used.

Circular dichroism (CD) spectra were carried out at 25°C on a Jasco 810 A dichrograph, using the same path lengths, solutions and concentrations as for UV-Vis measurements. $\Delta\epsilon$ values, expressed as $\text{L}\cdot\text{mol}^{-1}\cdot\text{cm}^{-1}$ were calculated from the following equation: $\Delta\epsilon = [\Theta]/3300$, where the molar ellipticity $[\Theta]$ in $\text{deg}\cdot\text{cm}^2\cdot\text{dmol}^{-1}$ refers to one bisazobenzene chromophore.

Number average molecular weights (\bar{M}_n) of the polymers and their polydispersity indexes (\bar{M}_w/\bar{M}_n) were determined in THF solution by SEC using HPLC Lab Flow 2000 apparatus, equipped with an injector Rheodyne 7725i, a Phenomenex Phenogel 5-micron MXL column and an UV-VIS detector Linear Instruments model UVIS-200, working at 254 nm. Calibration curves were obtained by using monodisperse polystyrene standards in the range 800-35,000.

Melting points (uncorrected) were determined in glass capillaries on a Büchi 510 apparatus at a heating rate of 1°C/min.

The glass transition temperature values (T_g) of polymers were determined by differential scanning calorimetry (DSC) on a TA Instrument DSC 2920 Modulated apparatus adopting a temperature program consisting of three heating and two cooling cycles starting from room temperature (heating/cooling rate 10°C/min under nitrogen atmosphere) under nitrogen atmosphere. Each sample (5-9 mgr) was heated up to below 250°C in order to avoid thermal decomposition.

The initial thermal decomposition temperature (T_d) was determined on the polymeric samples with a Perkin-Elmer TGA-7 thermogravimetric analyzer by heating the samples in air at a rate of 20°K/min.

Amorphous thin films were prepared by spin-coating of a solution of the polymer in tetrahydrofuran onto clean fused silica. The film was then dried by heating above 80°C under vacuum for 12 hours. The film thickness has been measured by a Tencor P-10 profilometer. The native film resulted to be optically isotropic by inspection with a Zeiss Axioscope2 polarising microscope through crossed polarizers fitted with a Linkam THMS 600 hot stage.

The absorption and CD spectra of the film were carried out under the same instrumental conditions as the related solutions.

The photoinduced linear birefringence was measured in situ using a pump and probe set-up by monitoring the transmittance of the samples interposed between two crossed polarizers. The pump radiation at 488 nm was produced by a small frame Ar⁺ laser, Spectra Physics mod. 165, whereas the source for the probe light was a Melles-Griot 10 mW He-Ne laser at 632.8 nm. The degree of linear polarization of the writing pump radiation was enhanced by using a Glan – Taylor prism polarizer, whereas a multiple order $\lambda/4$ quartz waveplate for 488 nm was employed to circularize the pump radiation for the erasing steps.

Monomers

(S)-3-Hydroxy-1-[4'-phenylazo-(4-azobenzene)]-pyrrolidine [(*S*)-**HPAAP**]

Trans-4-phenylazoaniline (4,18 g, 0.018 mol), concentrated hydrochloric acid (10 mL) and distilled water (14 mL) were placed in a 100 ml beaker and cooled down in an ice-water bath at 5 °C. Sodium nitrite (1.25 g) in distilled water (6.8 mL) (kept cool in an ice-water bath) was then added dropwise to the above solution with stirring. The mixture was left in ice bath for 30 minutes. The obtained diazonium salt of *trans*-4-phenylazoaniline was added dropwise to a solution of (*S*)-**HPP** (2.94 g, 0.018 mol) and sodium acetate (14.78 g) in glacial acetic acid (40.00 mL) at 5°C. The resultant deep red coloured solution was stirred vigorously at room temperature for 10h and then neutralized with 30% aq. NaOH. The formed red precipitate was filtered, washed with water, dissolved in dichloromethane, dried on anhydrous Na₂SO₄, and purified by column chromatography (SiO₂, CH₂Cl₂ as eluent). The solvent was evaporated under

reduced pressure and the solid residue was crystallized from CH₂Cl₂ to give 2.75 g of pure (*S*)-**HPAAP** (yield 40.5%, mp=142-144 °C).

¹H-NMR (DMSO-*d*₆): 7.96 (m, 8H, arom. 2'-, 3'-, 2''-CH and arom. *meta* to amino group), 7.54 (m, 3H, arom. 3''- and 4''-CH), 6.64 (dd, 2H, arom. *ortho* to amino group), 4.85 (d, 1H, OH), 4.60 (m, 1H, 3-CH), 3.66-3.36 (m, 4H, 2- and 5-CH₂), 2.13 (m, 2H, 4-CH₂) ppm.

FT-IR (KBr): 3427 (ν_{OH}), 3059 (ν_{CH}, arom.), 2915 and 2847 (ν_{CH}, aliph.), 1600 and 1515 (ν_{C=C}, arom.), 1140 (ν_{C-O}), 856 and 822 (δ_{CH}, 1,4-disubst. arom. rings), 771 and 689 (δ_{CH}, monosubst. arom. ring) cm⁻¹.

UV-VIS in CHCl₃: ε_{max} X 10⁻³ (I_{max}) = 19.9 (332 nm) and 36.0 (474 nm) L mol⁻¹ cm⁻¹.

(S)-3-Hydroxy-1-[4'-cyanophenylazo-(4-azobenzene)]-pyrrolidine [(*S*)-**HPAAP-C**]

The same above described procedure was followed starting from the diazonium salt of *trans*-4-(4-aminophenylazo)benzonitrile. The azo derivative (*S*)-**HPAAP-C** was obtained in 41.2% yield, mp 150-152 °C.

¹H-NMR (CDCl₃/DMSO-*d*₆ 1:1 v/v): 7.90 (m, 4H, arom. *ortho* and *meta* to cyano group), 7.75 (m, 6H, arom. 2'-, 3'-CH and arom. *meta* to amino group), 6.65 (dd, 2H, arom. *ortho* to amino group), 4.80 (d, 1H, OH), 4.60 (m, 1H, 3-CH), 3.70-3.30 (m, 4H, 2- and 5-CH₂), 2.10 (m, 2H, 4-CH₂) ppm.

FT-IR (KBr): 3488 (ν_{OH}), 3078 (ν_{CH}, arom.), 2924 and 2859 (ν_{CH}, aliph.), 2224 (ν_{CN}), 1600 and 1515 (ν_{C=C}, arom.), 1141 (ν_{C-O}), 850 and 824 (δ_{CH}, 1,4-disubst. arom. rings) cm⁻¹.

UV-VIS in CHCl₃: ε_{max} X 10⁻³ (I_{max}) = 20.5 (334 nm) and 37.0 (484 nm) L mol⁻¹ cm⁻¹.

(S)-3-Hydroxy-1-[4'-nitrophenylazo-(4-azobenzene)]-pyrrolidine [(*S*)-**HPAAP-N**]

A similar procedure to that one above described for (*S*)-**HPAAP** was followed starting from the diazonium salt of *trans*-4-(4-aminophenylazo)nitrobenzene. The crude brown precipitate was filtered and washed several times in methanol, dissolved in CH₂Cl₂, dried on anhydrous Na₂SO₄ and directly crystallized in absolute ethanol to give pure (*S*)-**HPAAP-N** (yield 38.0%, mp=172-174 °C).

$^1\text{H-NMR}$ ($\text{DMSO-}d_6$ at 90°C): 8.45 (dd, 2H, arom. *ortho* to nitro group), 8.00 (m, 8H, arom. 2'-, 3'-CH, arom. *meta* to nitro group and *meta* to amino group), 6.70 (dd, 2H, arom. *ortho* to amino group), 4.50 (m, 1H, 3-CH), 3.60-3.20 (m, 5H, 2-, 5- CH_2 and OH), 2.20 (m, 2H, 4- CH_2) ppm.

FT-IR (KBr): 3475 (ν_{OH}), 3032 (ν_{CH} , arom.), 2923 and 2847 (ν_{CH} , aliph.), 1601 and 1514 ($\nu_{\text{C=C}}$, arom.), 1530 ($\nu_{\text{NO}_2\text{as}}$), 1140 ($\nu_{\text{C-O}}$), 857 and 832 (δ_{CH} , 1,4-disubst. arom. rings) cm^{-1} .

UV-VIS in THF: $\epsilon_{\text{max}} \times 10^{-3}$ (I_{max}) = 21.9 (336 nm) and 39.6 (505 nm) $\text{L mol}^{-1} \text{cm}^{-1}$.

(S)-3-Methacryloyloxy-1-[4'-phenylazo-(4-azobenzene)]-pyrrolidine [*(S)*-**MPAAP**]

To an ice-cooled, vigorously stirred solution of *(S)*-**HPAAP** (6.50 g, 16.0 mmol), triethylamine (16.50 ml, 156 mmol), dimethylamino pyridine (0.38 gr, 3.1 mmol), as catalyst, and 2,6-di-*tert*-butyl-4-methyl phenol (0.31 gr) as polymerization inhibitor, in anhydrous THF (500 mL), was added dropwise, under nitrogen atmosphere, methacryloyl chloride (8.30 ml, 80.0 mmol). The mixture was kept ice-cooled for 2 h, then left at room temperature for one night, washed with 0.1 M HCl, 5% Na_2CO_3 and finally with water, in that order, to give crude *(S)*-**MPAAP**.

The final purification was performed by column chromatography (SiO_2 , CH_2Cl_2 as eluent) followed by crystallization from CH_2Cl_2 to give 4.58 g of pure product (65.0% yield, mp $158\text{-}160^\circ\text{C}$).

$^1\text{H-NMR}$ (CDCl_3): 7.98 (m, 8H, arom. 2'-, 3'-, 2''-CH and arom. *meta* to amino group), 7.52 (m, 3H, arom. 3''- and 4''-CH), 6.66 (dd, 2H, arom. *ortho* to amino group), 6.10 and 5.60 (2d, 2H, $\text{CH}_2=$), 5.54 (m, 1H, 3-CH), 3.85-3.56 (m, 4H, 2- and 5- CH_2), 2.30 (m, 2H, 4- CH_2), 1.90 (s, 3H, CH_3) ppm.

FT-IR (KBr): 3105 (ν_{CH} , arom.), 2958 and 2847 (ν_{CH} , aliph.), 1710 ($\nu_{\text{C=O}}$), 1632 ($\nu_{\text{C=C}}$, methacrylic), 1603 and 1515 ($\nu_{\text{C=C}}$, arom.), 1140 ($\nu_{\text{C-O}}$), 858 and 817 (δ_{CH} , 1,4-disubst. arom. rings), 767 and 685 (δ_{CH} , monosubst. arom. ring) cm^{-1} .

(S)-3-Methacryloyloxy-1-[4'-cyanophenylazo-(4-azobenzene)]-pyrrolidine [*(S)*-**MPAAP-C**]

A similar procedure to that one above described for (*S*)-**MPAAP** was followed starting from (*S*)-**HPAAP-C**. The crude acylation product was collected after coagulation into a mixture of water and hexane. The filtrate was dissolved in CHCl₃, dried with anhydrous Na₂SO₄ and crystallized by CHCl₃ (yield 60.1%, mp 167-169 °C).

¹H-NMR (CDCl₃): 8.00 (m, 4H, arom. *ortho* and *meta* to cyano group), 7.80 (m, 6H, arom. 2'-, 3'-CH and arom. *meta* to amino group), 6.65 (dd, 2H, arom. *ortho* to amino group), 6.10 and 5.60 (2d, 2H, CH₂=), 5.50 (m, 1H, 3-CH), 3.85-3.50 (m, 4H, 2- and 5-CH₂), 2.30 (m, 2H, 4-CH₂), 1.90 (s, 3H, CH₃) ppm.

FT-IR (KBr): 3096 (n_{CH}, arom.), 2923 and 2857 (n_{CH}, aliph.), 2221 (ν_{CN}), 1719 (n_{C=O}), 1637 (n_{C=C}, methacrylic), 1601 and 1515 (n_{C=C}, arom.), 855 and 822 (δ_{CH}, 1,4-disubst. arom. rings) cm⁻¹.

(S)-3-Methacryloyloxy-1-[4'-nitrophenylazo-(4-azobenzene)]-pyrrolidine [*(S)*-**MPAAP-N**]

The same above described procedure for (*S*)-**MPAAP** was followed starting from (*S*)-**HPAAP-N** to give pure (*S*)-**MPAAP-N** in 52.3% yield, mp 172-174 °C.

¹H-NMR (CDCl₃/DMSO-*d*₆ 1:1 v/v): 8.40 (dd, 2H, arom. *ortho* to nitro group), 8.05 (m, 8H, arom. 2'-, 3'-CH, arom. *meta* to nitro group and *meta* to amino group), 6.65 (dd, 2H, arom. *ortho* to amino group), 6.10 and 5.60 (2d, 2H, CH₂=), 5.50 (m, 1H, 3-CH), 3.90-3.45 (m, 4H, 2- and 5-CH₂), 2.30 (m, 2H, 4-CH₂), 1.90 (s, 3H, CH₃) ppm.

FT-IR (KBr): 3096 (n_{CH}, arom.), 2924 and 2855 (n_{CH}, aliph.), 1715 (n_{C=O}), 1635 (n_{C=C}, methacrylic), 1603 and 1511 (n_{C=C}, arom.), 1530 (ν_{NO₂as}), 862 and 819 (δ_{CH}, 1,4-disubst. arom. rings) cm⁻¹.

Polymers

The homopolymerizations and copolymerization of the three optically active monomers were carried out in glass vials using AIBN as free radical initiator and dry DMF as solvent. The reaction mixture (1.0 g of monomer, 2% weight of AIBN in 25 mL of DMF) was introduced into the vials under nitrogen atmosphere, submitted to several freeze-thaw cycles and heated at 65 °C for 72 h. The reaction was then stopped by

pouring the mixture into a large excess of methanol (200 ml), and the coagulated polymer filtered off. The solid product was repeatedly redissolved in THF (at room temperature) or DMA (at 90°C) and reprecipitated again in methanol. The last traces of unreacted monomers and oligomeric impurities were eliminated by Soxhlet continuous extraction with methanol followed by acetone. The material was finally dried at 60°C under vacuum for several days to constant weight.

Spectroscopic characterization of relevant synthesized polymers are reported below.

Poly[(S)-MPAAP]

¹H-NMR (CDCl₃): 8.15-7.70 (m, 8H, arom. 2'-, 3'-, 2''-CH and arom. *meta* to amino group), 7.60-7.25 (m, 3H, arom. 3''- and 4''-CH), 6.80-6.20 (m, 2H, arom. *ortho* to amino group), 5.20-4.80 (m, 1H, 3-CH), 3.70-3.00 (m, 4H, 2- and 5-CH₂), 2.40-1.80 (m, 4H, 4-CH₂ and backbone CH₂), 1.40-0.80 (m, 3H, CH₃) ppm.

¹³C-NMR (CDCl₃): 178.4-176.6 (C=O), 154.9, 154.0, 153.4, 150.0, 144.8 (arom. C-N=N-C and C-N-CH₂), 131.7 (arom. 4''-C), 129.7 (arom. 3''-C), 126.3 (arom. 3-C), 124.5 (arom. 2''-C), 123.6 (arom. 2'-C and 3'-C), 112.4 (arom. 2-C), 75.5 (CH-O), 55.1 (main chain CH₂-C), 53.1 (CH-CH₂-N), 46.8 (CH₂-CH₂-N), 45.5 (main chain CH₂-C), 31.4 (CH-CH₂-CH₂), 20.0 and 17.6 (CH₃).

FT-IR (KBr): 3059 (n_{CH}, arom.), 2967 and 2847 (n_{CH}, aliph.), 1724 (n_{C=O}), 1603 and 1515 (n_{C=C}, arom.), 857 and 817 (δ_{CH}, 1,4-disubst. arom. rings), 767 and 685 (δ_{CH}, monosubst. arom. ring) cm⁻¹.

Poly[(S)-MPAAP-C]

¹H-NMR (DMF-*d*₇ at 90°C): 7.95-7.55 (m, 10H, arom. 2'-, 3'-CH, arom. *ortho* and *meta* to cyano group and arom. *meta* to amino group), 6.60-6.40 (m, 2H, arom. *ortho* to amino group), 5.40-5.00 (m, 1H, 3-CH), 3.65-3.20 (m, 4H, 2- and 5-CH₂), 2.35-1.60 (m, 4H, 4-CH₂ and backbone CH₂), 1.55-0.60 (m, 3H, CH₃) ppm.

¹³C-NMR (DMF-*d*₇ at 90°C): 178.5-177.2 (C=O), 155.9 (arom. C-CN), 155.2, 152.9, 150.5, 148.8, 144.8 (arom. C-N=N-C and C-N-CH₂), 133.9 (arom. 3''-C), 126.5 (arom. 3-C), 125.0 (arom. 2''-C), 124.1, 123.8 (arom. 2'-C and 3'-C), 119.2 (CN), 112.4 (arom.

2-C), 75.1 (CH-O), 55.1 (main chain $\underline{\text{C}}\text{H}_2\text{-C}$), 52.5 (CH- $\underline{\text{C}}\text{H}_2\text{-N}$), 46.6 (CH₂- $\underline{\text{C}}\text{H}_2\text{-N}$), 45.5 (main chain CH₂- $\underline{\text{C}}$), 31.4 (CH- $\underline{\text{C}}\text{H}_2\text{-CH}_2$), 19.4 and 17.2 (CH₃).

FT-IR (KBr): 3059 (n_{CH}, arom.), 2963 and 2857 (n_{CH}, aliph.), 2223 (ν_{CN}), 1728 (n_{C=O}), 1602 and 1510 (n_{C=C}, arom.), 854 and 822 (δ_{CH}, 1,4-disubst. arom. rings) cm⁻¹.

Poly[(S)-MPAAP-N]

FT-IR (KBr): 3050 (n_{CH}, arom.), 2949 and 2847 (n_{CH}, aliph.), 1733 (n_{C=O}), 1602 and 1517 (n_{C=C}, arom.), 1531 (ν_{NO₂as}), 859 and 818 (δ_{CH}, 1,4-disubst. arom. rings) cm⁻¹.

Poly[(S)-MPAAP-N-co-MMA] (15)

¹H-NMR (CDCl₃): 8.45-8.20 (m, 2H, arom. *ortho* to nitro group), 8.10-7.80 (m, 8H, arom. 2'-, 3'-CH, arom. *meta* to nitro group and *meta* to amino group), 6.70-6.50 (m, 2H, arom. *ortho* to amino group), 5.40-5.20 (m, 1H, 3-CH), 3.80-3.40 (m, 7H, OCH₃, 2- and 5-CH₂), 2.40-1.60 (m, 6H, 4-CH₂ and backbone CH₂), 1.10-0.70 (m, 6H, backbone CH₃) ppm.

¹³C-NMR (CDCl₃): 178.8-177.6 (C=O), 156.5 (arom. C-NO₂), 153.1, 150.7, 150.0, 149.4, 144.9 (arom. $\underline{\text{C}}\text{-N}=\underline{\text{N}}\text{-C}$ and $\underline{\text{C}}\text{-N-CH}_2$), 126.5 (arom. 3-C), 125.4, 125.2 (arom. 2''-C and 3''-C), 124.2, 123.8 (arom. 2'-C and 3'-C), 112.5 (arom. 2-C), 75.0 (CH-O), 55.1 (main chain $\underline{\text{C}}\text{H}_2\text{-C}$), 53.4 (CH- $\underline{\text{C}}\text{H}_2\text{-N}$), 52.5 (CH₃O), 46.6 (CH₂- $\underline{\text{C}}\text{H}_2\text{-N}$), 45.6-45.2 (main chain CH₂- $\underline{\text{C}}$), 31.2 (CH- $\underline{\text{C}}\text{H}_2\text{-CH}_2$), 19.3 and 17.2 (main chain CH₃).

FT-IR (KBr): 3050 (n_{CH}, arom.), 2949 and 2847 (n_{CH}, aliph.), 1732 (n_{C=O}), 1602 and 1517 (n_{C=C}, arom.), 1530 (ν_{NO₂as}), 859 and 818 (δ_{CH}, 1,4-disubst. arom. rings) cm⁻¹.

Poly[(S)-MPAAP-co-tert-BMA] (62):

¹H-NMR (CDCl₃): 8.15-7.70 (m, 8H, arom. 2'-, 3'-, 2''-CH and arom. *meta* to amino group), 7.60-7.35 (m, 3H, arom. 3''- and 4''-CH), 6.80-6.35 (m, 2H, arom. *ortho* to amino group), 5.30-4.90 (m, 1H, 3-CH), 3.70-3.00 (m, 4H, 2- and 5-CH₂), 2.60-1.60 (m, 4H, 4-CH₂ and backbone CH₂), 1.60-1.20 (m, 9H, C(CH₃)₃ of *tert*-BMA), 1.20-0.80 (m, 6H, backbone CH₃) ppm.

¹³C-NMR (CDCl₃): 178.4-176.6 (C=O), 154.9, 154.0, 153.4, 150.0, 144.8 (arom. $\underline{\text{C}}$ -

N=N-C and C-N-CH₂), 131.7 (arom. 4''-C), 129.8 (arom. 3''-C), 126.3 (arom. 3-C), 124.4 (arom 2''-C), 123.6 (arom. 2'-C and 3'-C), 112.4 (arom. 2-C), 81.7 (C(CH₃)₃ of *tert*-**BMA**), 75.5 (CH-O), 56.1-54.0 (main chain CH₂-C), 53.3 (CH-CH₂-N), 46.5 (CH₂-CH₂-N), 45.6-45.2 (main chain CH₂-C), 31.3 (CH-CH₂-CH₂), 28.5 (C(CH₃)₃ of *tert*-**BMA**), 19.6 and 18.4 (main chain CH₃).

FT-IR (KBr): 3059 (n_{CH}, arom.), 2940 and 2852 (n_{CH}, aliph.), 1724 (n_{C=O}), 1601 and 1514 (n_{C=C}, arom.), 851 and 821 (δ_{CH}, 1,4-disubst. arom. rings), 767 and 688 (δ_{CH}, monosubst. arom. ring) cm⁻¹.

Poly[(S)-MPAAP-co-TrMA] (51):

¹H-NMR (CDCl₃): 8.05-7.60 (m, 8H, arom. 2'-, 3'-, 2''-CH and arom. *meta* to amino group), 7.60-7.40 (m, 3H, arom. 3''- and 4''-CH), 7.40-7.00 (m, 18H arom. **TrMA**), 6.70-6.40 (m, 2H, arom. *ortho* to amino group), 5.30-4.90 (m, 1H, 3-CH), 3.80-3.10 (m, 4H, 2- and 5-CH₂), 2.60-1.80 (m, 6H, 4-CH₂ and backbone CH₂), 1.15-0.80 (m, 6H, backbone CH₃) ppm.

¹³C-NMR (CDCl₃): 178.0-175.5 (C=O), 155.0, 154.0, 153.5, 150.4, 144.8 (arom. C-N=N-C and C-N-CH₂), 143.5 (arom. 1-C of **TrMA**), 131.8 (arom. 4''-C), 129.8 (arom. 3''-C), 129.3 (arom. 3-C of **TrMA**), 128.5 (arom. 2-C and 4-C of **TrMA**), 126.3 (arom. 3-C), 124.5 (arom. 2''-C), 123.7 (arom. 2'-C and 3'-C), 114.6, 112.4 (arom. 2-C), 77.7 (C(Ph)₃ of **TrMA**), 75.1 (CH-O), 56.1-54.0 (main chain CH₂-C), 53.6 (CH-CH₂-N), 46.3 (CH₂-CH₂-N), 45.6-45.2 (main chain CH₂-C), 31.2 (CH-CH₂-CH₂), 20.4 and 18.2 (main chain CH₃).

FT-IR (KBr): 3058 (n_{CH}, arom.), 2942 and 2855 (n_{CH}, aliph.), 1728 (n_{C=O}), 1599 and 1514 (n_{C=C}, arom.), 851 and 819 (δ_{CH}, 1,4-disubst. arom. rings), 765 and 687 (δ_{CH}, monosubst. arom. ring) cm⁻¹.

References

- [1] [1a] Proceedings of the Symposium on Azobenzene-Containing Materials, Boston MA (U.S.A.) 1998, ed. A. Natansohn, *Macromolecular Symposia* 137, 1999. pp.1–165. [1b] A. Natansohn, P. Rochon, M. S. Ho, C. Barrett, *Macromolecules* 1995, 28, 4179. [1c] Y. Wu, Q. Zhang, A. Kanazawa, T. Shiono, T. Ikeda, Y. Nagase, *Macromolecules* 1999, 32, 3951. [1d] C. R. Mendonca, A. Dhanabalan, D. T. Balogh, L. Misoguti, D. S. Dos Santos Jr., M.A. Pereira-da-Silva, J. A. Giacometti, S. C. Zilio, O. N. Jr. Oliveira, *Macromolecules* 1999, 32, 1493. [1e] J. H. Kim, S. Kumar, S. D. Lee, *Phys. Rev. E*, 1998, 57, 5644. [1f] K. Ichimura, *Chem. Rev.*, 2000, 100, 1847. [1g] A. Natansohn, P. Rochon, J. Gosselin, S. Xie, *Macromolecules* 1992, 25, 2268.
- [2] [2a] W. M Gibbons, P. J. Shannon, S. T. Sun, B. J. Swetlin, *Nature* 1991, 351, 49. [2b] N. C. R. Holme, P. S. Ramanujam, S. Hvilsted, *Opt. Lett.* 1996, 21, 902.
- [3] [3a] H. Katz, K. Singer, J. Sohn, C. Dirk, *J. Am. Chem. Soc.* 1987, 109, 6561. [3b] J. A. Delaire, K. Nakatani, *Chem. Rev.* 2000, 100, 1817.
- [4] [4a] T. Todorov, L. Nikolova, N. Tomova, *Appl. Opt.*, 1984, 23, 4588. [4b] L. Andruzzi, A. Altomare, F. Ciardelli, R. Solaro, S. Hvilsted, P. S. Ramanujam, *Macromolecules* 1999, 32, 448. [4c] M. Eich, J. H. Wendorff, B. Reck, H. Ringsdorf, *Macromol. Chem. Rapid Commun.* 1987, 8, 56.
- [5] [5a] G. Iftime, F. L. Labarthe, A. Natansohn, P. Rochon, *J. Am. Chem. Soc.* 2000, 122, 12646. [5b] T. Verbiest, M. Kauranen, A. Persoon, *J. Mat. Chem.* 1999, 9, 2005.
- [6] [6a] Y. Wu, A. Natansohn, P. Rochon, *Macromolecules* 2004, 37, 6090-6095. [6b] A. Natansohn, P. Rochon, *Chem. Rev.* 2002, 102, 4139-4175.
- [7] M. M Green, N. C. Peterson, T. Sato, A. Teramoto, R. Cook, S. Lifson, *Nature* 1995, 268, 1860.
- [8] L. Angiolini, D. Caretti, L. Giorgini, E. Salatelli, *J. Polymer Sci., Part A Polym. Chem.* 1999, 37, 3257.
- [9] L. Angiolini, D. Caretti, L. Giorgini, E. Salatelli, *Polymer* 2001, 42, 4005.

- [10] [10a] L. Angiolini, R. Bozio, A. Daurù, L. Giorgini, D. Pedron, G. Turco, *Chem. Eur. J.* 2002; 8, 4241. [10b] L. Angiolini, T. Benelli, L. Giorgini, A. Painelli, F. Terenziani, *Chem. Eur. J.* 2005, 11, 6053-6353. [10c] L. Angiolini, T. Benelli, R. Bozio, A. Daurù, L. Giorgini, D. Pedron, E. Salatelli, *Eur. Polym. J.* 2005, 41, 2045. [10d] L. Angiolini, T. Benelli, R. Bozio, A. Daurù, L. Giorgini, D. Pedron, E. Salatelli, *Macromolecules* 2006, 39, 489.
- [11] X. Meng, A. Natansohn, P. Rochon, *Polymer* 1997, 38, 2677.
- [12] [12a] J. Wang, L. Z. Zhang, Y. Niu, Z. Liang, Y. Chen, Y. Huang, H. Wang, W. Lin, *Polym Int.* 2003, 52, 1165. [12b] M. Jin, Q. Xing, R. Lu, T. H. Xu, Y. Y Zhao, *J. Polym. Sci., Part A: Polym. Chem.* 2004, 42, 4237.
- [13] [13a] US 2003049549 A1 (2003), Bayern AG, invs.: R. Hagen, T. Bieringer, S. G. Kostromine, H. Berneth. [13b] US 2003113664 A1 (2003), Bayern AG, invs.: R. Hagen, T. Bieringer, S. G. Kostromine, H. Berneth,
- [14] [14a] N. Korneev, O. F. Ramirez, R. P. Bertram, N. Benter, E. Soegel, K. Buse, R. Hagen, S. G. Kostromine, *J. Appl. Phys.* 2002, 92, 1500. [14b] R. P. Bertram, N. Benter, E. Soegel, K. Buse, R. Hagen, S. G. Kostromine, *J. Appl. Phys.* 2003, 94, 6208.
- [15] A. Altomare, F. Ciardelli, M. S. Ghiloni, R. Solaro, N. Tirelli, *Macromol. Chem. Phys.* 1997, 198, 1739
- [16] G. Hallas, *J. Soc. Dyers Color*, 1994, 110, 342.
- [17] [17a] I. Jr. Tinoco, *J. Am. Chem. Soc.* 1960, 82, 4785. [17b] K. Okamoto, A. Itaya, S. Kusabayashi, *Chem. Lett.* 1974, 1167. [17c] F. Ciardelli, M. Aglietto, C. Carlini, E. Chiellini, R. Solaro, *Pure Appl. Chem.* 1982, 54, 521
- [18] [18a] A. Rodger, B. Nord'en, "Circular Dichroism and Linear Dichroism", Oxford University Press, Oxford 1997, chapters 5 and 7. [18b] S. F. Mason, "Molecular Optical Activity and the Chiral Discrimination", Cambridge University Press, Cambridge 1982, chapter 3. [18c] N. Berova, K. Nakanishi, R. W. Woody, "Circular dichroism, principles and applications", Wiley-VCH inc, New York 2000.
- [19] L. Angiolini, D. Caretti, L. Giorgini, E. Salatelli, *Macromol. Chem. Phys.*, 2000, 201, 533

- [20] [20a] T. Kelen, F. Tüdos, *J. Macromol. Sci., Chem.* 1975, 9, 1; [20b] S. P. Rao, S. Ponratman, S. L. Kapur, P. K. Iyer, *J. Polym. Sci., Polym. Lett. Ed.* 1976, 14, 513.
- [21] [21a] F. R. Mayo, C. Walling, *Chem. Rev.*, 1950, 200; [21b] E. Chiellini, R. Solaro, A. Ledwith, G. Galli, *Eur. Polym. J.* 1980, 13, 1654.
- [22] C. Cao, Y. Lin, *J. Chem., Inf. Model.* 2003, 43, 643.
- [23] I. R. Peat, W. F. Reynolds, *Tetrahedron Lett.*, 1972, 1359.
- [24] E. McCord, W. L. Anton, L. Wilczek, S. D. Ittel, S. L. T. J. Nelson, K. D. Raffell, *Macromol. Symp.* 1994, 86, 47.
- [25] H. Yuki, K. Hatada, T. Niinomi, Y. Kikuchi, *Polym. J.* 1970, 1, 36.
- [26] L. Angiolini, T. Benelli, L. Giorgini, E. Salatelli, *Polymer* 2006, 47, 1875.
- [27] D. D. Perrin, W. L. F. Amarego, D. R. Perrin, "Purification of Laboratory Chemicals", Pergamon Press, Oxford 1966.
- [28] DE 2801951 A1 (1973), BASF AG, inv.: G. Lamm.

Chapter 3: Methacrylic polymers bearing side chain carbazole

Introduction

Carbazole has attracted considerable interest as building block in material science for its well known hole-transporting and electroluminescence properties [1].

Since the discovery of the photoconductive character of doped poly(*N*-vinylcarbazole) (PVK), carbazole containing polymers [2-4] have attracted much attention because of their unique features. The use of these materials in advanced micro- and nanotechnologies spreads in many different applications such as photoconductive and photorefractive polymers, electroluminescent devices, programmable optical interconnections, data storage, chemical photoreceptors, NLO, surface relief gratings, blue emitting materials and holographic memory.

On the other hand, an intense attention is currently arisen to investigations dealing with the chiral nanotechnology [5,6] and with the amplification of chirality of polymeric materials in solution as well as in the solid state [7-13].

In this context, stereoregular helical polyacetylenes containing in the side chain the carbazole group functionalized with chiral minidendrons and with chiral menthyl and bornyl groups [14] and optically active vinyl homo- and copolymers with side chain carbazole moieties [16-18] have been reported.

To this regard, we have recently investigated multifunctional optically active photochromic methacrylic polymers bearing two distinct functional groups (i.e. azoaromatic and (*S*)-3-hydroxypyrrolidine and (*S*)-2-hydroxysuccinimide as chiral group of one single configuration) directly linked to the side chain [19].

These materials are characterized by homogeneous conformations with a prevailing chirality, as demonstrated by the presence in their circular dichroism (CD) spectra of intense dichroic bands suitable to reveal the existence of chiral perturbation induced by the chiral moieties onto the electronic transitions of the achiral carbazole chromophore.

To our knowledge, polymers bearing the carbazole group directly linked to the main chain through an optically active group of one absolute configuration have not yet been

reported and could be of potential interest in order to investigate the influence of the macromolecular chirality on the photoconductive and photorefractive properties of this particular class of polymeric materials.

Side chain carbazole linked at the 3-position to the macromolecular main chain can give rise charge carries in the visible region through an induced intramolecular charge transfer complex [20]. In these materials, the macromolecular structure affects the hole transport mechanism because the photoconductivity is related to hole hopping between side chain carbazole units and to the molecular mobility of chromophore, which is usually depressed due to the chemical anchorage to the polymer backbone.

On the other hand, in recent years, a wide range of vinyl monomers and their polymers bearing various photo-active or electro-active chromophores as been extensively studied and applied in the field of advanced composites, optoelectronic materials and devices [21,22].

In this field, polyacrylates and polymethacrylates with pendand 9-phenylcarbazole moieties has been largely studied in order to correlate the architecture of the chromophores to the photochemical and photophysical properties [23].

To improve the conformational order of the macromolecules, we have envisaged the synthesis of polymeric derivatives bearing in the side chain carbazole or phenylcarbazole linked to the (*S*)-2-hydroxy succinimide or the (*S*)-3-hydroxy pyrrolidinyl ring as chiral moieties covalently linked to the main chain through ester bonds.

In addition, the presence of a strong electron-donating or an electron-withdrawing group such as the five membered cyclic pyrrolidinyl moiety or the succinimide residue, respectively, should give the possibility to afford polymeric derivatives characterized by the presence of a strong conjugated donor-acceptor system, potentially suitable to provide photoconductive materials, electroluminescent devices, data storage, chemical photoreceptors, NLO, blue emitting materials and holographic memory.

In this context, the synthesis and characterization of four novel optically active homopolymers (Figure 1), poly[(*S*)-(+)-methacryloyl-2-oxy-N-[3-(9-ethylcarbazole)]-succinimide] {poly[(*S*)-(+)-**MECSI**]}, poly[(*S*)-(-)-methacryloyl-3-oxy-N-[3-(9-ethylcarbazole)]-pyrrolidine] {poly[(*S*)-(-)-**MECP**]}, poly[(*S*)-(+)-methacryloyl-2-oxy-

N-(9-phenylcarbazole)-succinimide] {poly[(S)-(+)-**MCPS**]} and poly[(S)-(+)-methacryloyl-3-oxy-N-(9-phenylcarbazole)-pyrrolidine] {poly[(S)-(+)-**MCPP**]} deriving by radical polymerization of the new corresponding monomers is here reported.

Finally, it was worth the evaluation of the influence of the chirality on the properties of the macromolecules bearing in the side chain the 9-phenylcarbazole. This has been achieved through radical polymerization of an analogous achiral monomer methacryloyl-2-oxyethyl-N-ethyl-N-9-phenylcarbazole-amine [**MCPE**]. The structure of the related achiral polymeric model compound poly[**MCPE**] is reported in figure 1.

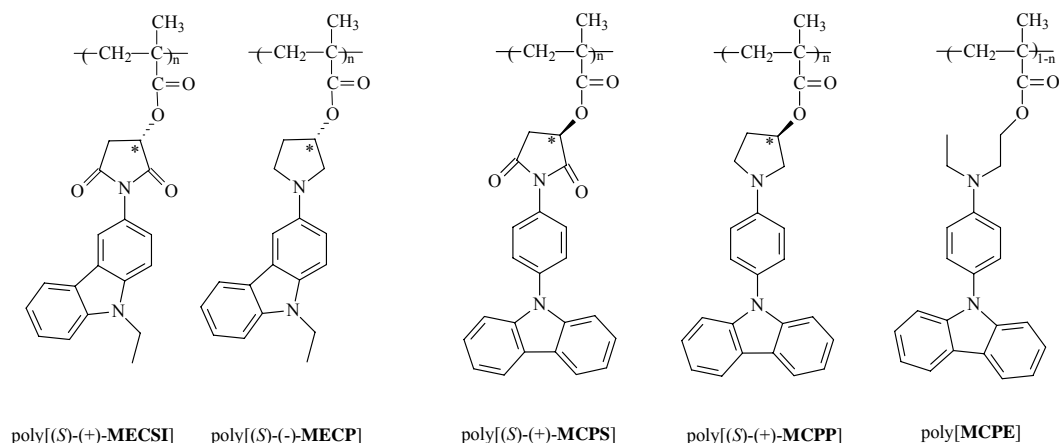


Figure 1: Chemical structures of the investigated polymers

The polymeric derivatives have been fully characterized and their spectroscopic properties compared to those of the corresponding monomers with the aim to evaluate the effect of the macromolecular structure on the physico-chemical properties of these materials.

The optical activity displayed by the polymers is discussed in terms of extent of chiral conformation assumed by the macromolecules as a consequence of their stiffness and the dipole-dipole interactions between the side chain chromophores.

Photoconductivity measurements as a function of applied electric field and irradiation wavelength have been performed on the above polymeric materials to investigate the effect of the presence of different electron-donating or withdrawing moieties linked to the carbazole group.

Methacrylic optically active homopolymers bearing 3 - side chain carbazole moieties

Two novel optically active polymethacrylates bearing in the side chain a cyclic chiral group of one prevailing absolute configuration linked in 3 position to the carbazole chromophore, deriving from the related monomers (*S*)-(-)-methacryloyl-2-oxy-N-[3-(9-ethylcarbazole)]-pyrrolidine [(*S*)-(-)-**MECP**] and (*S*)-(+)-methacryloyl-2-oxy-N-[3-(9-ethylcarbazole)]-succinimide [(*S*)-(+)-**MECSI**], have been prepared and characterized with the aim to obtain materials suitable to photoconductive applications.

Poly[(*S*)-(-)-**MECP**] and poly[(*S*)-(+)-**MECSI**] (figure 1) exhibit remarkable thermal stability, with glass transition temperature around 200°C and decomposition temperatures in the range 330-350°C.

Spectroscopic, thermal and chiroptical characterizations indicate the occurrence of dipolar interactions between the side chain moieties and the presence of an ordered chiral conformation at least for chain segments of the macromolecules. The photoconductive properties are discussed in terms of extent of conjugation in the side chain based on the electron-acceptor or electron-donor properties of the optically active ring linked to the carbazole group.

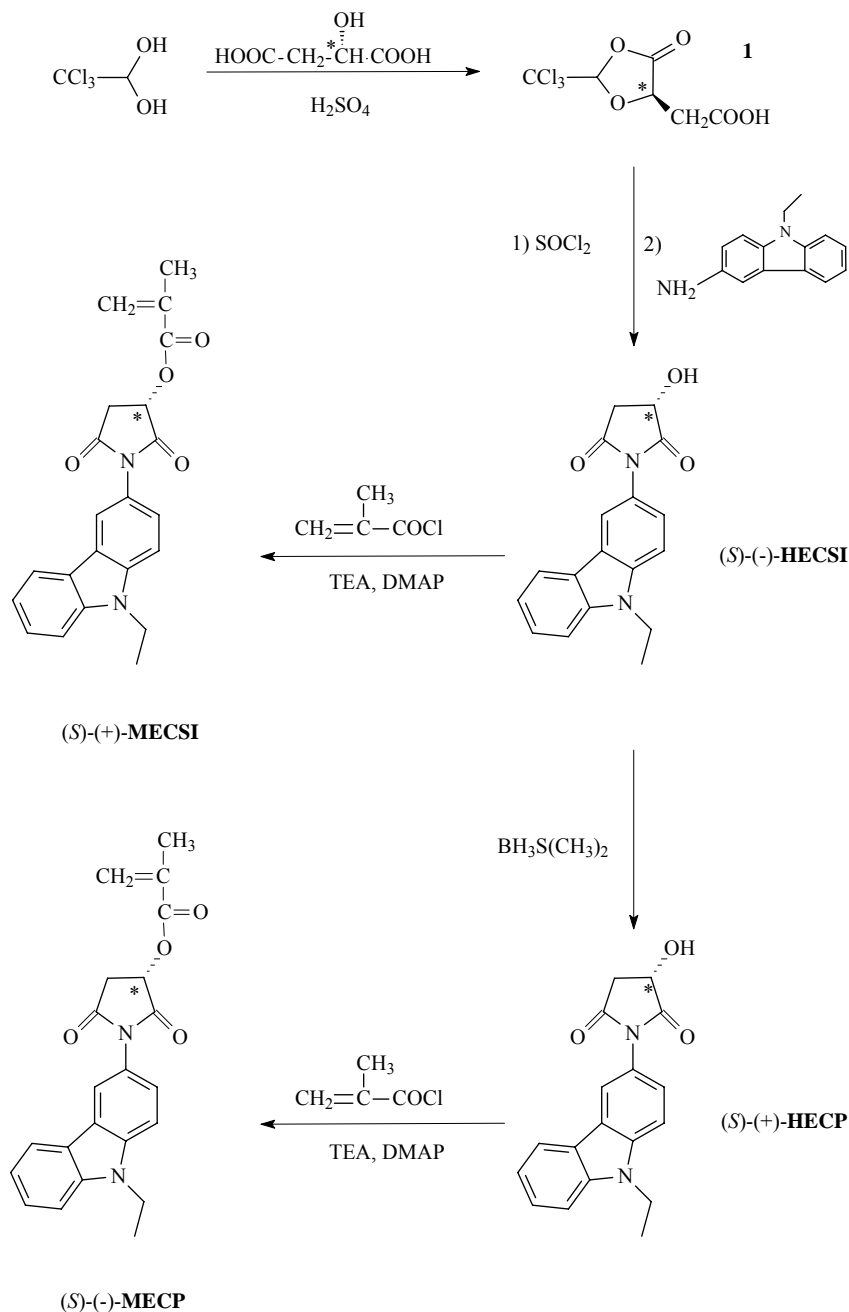
Synthesis and structural characterization of monomers and polymers.

The synthesis of monomers was carried out according to Scheme 1, starting from the chloralide **1**, derived in turn from (*S*)-(-)-malic acid by reaction with chloral hydrate [24], which was submitted to acid chlorination and finally reacted with commercial 3-amino-N-ethyl-carbazole to give the key intermediate alcohol (*S*)-(-)-2-hydroxy-N-[3-(9-ethylcarbazole)]-succinimide [(*S*)-(-)-**HECSI**].

(*S*)-(-)-**HECSI** was then reduced to the desired optically active alcohol (*S*)-(-)-3-hydroxy-N-[3-(9-ethylcarbazole)]-pyrrolidine [(*S*)-(+)-**HECP**] with a similar synthetic procedure used for analogous chiral N-phenylpyrrolidine derivatives [19a, 25].

The new monomers (*S*)-(+)-methacryloyl-2-oxy-N-[3-(9-ethylcarbazole)]-succinimide [(*S*)-(+)-**MECSI**] and (*S*)-(-)-methacryloyl-3-oxy-N-[3-(9-ethylcarbazole)]-pyrrolidine [(*S*)-(-)-**MECP**] were obtained with good yields by esterification of the related alcohols with methacryloyl chloride.

The structures of all the products were confirmed by $^1\text{H-NMR}$ and FT-IR (see Experimental Part).



Scheme 1. Reaction path of the synthesis of monomers (S)-(+)-MECSI and (S)-(-)-MECP

The optical purity of alcohols and monomers reported in the present paper were not measured; however, previous studies on optically active methacryloyl derivatives,

bearing in the side-chain the same chiral groups linked to azoaromatic moieties and prepared through a similar synthetic pathway [19a, 26], indicate that an enantiomeric excess of at least 90% was present in those compounds, thus excluding the possibility of racemization at the asymmetric centre during the synthesis. It is therefore reasonable to assume a similar optical purity for all the low- and high-molecular weight products here investigated.

Polymerization of the monomers, carried out in solution under free radical conditions by using AIBN as a thermal initiator, produced the corresponding polymeric derivatives in acceptable yields after purification, with average molecular weight and polydispersity values, as determined by gel permeation chromatography, in the range expected for this type of process. The polymeric products are completely soluble in common organic solvents such as CHCl_3 and THF, this feature favouring the possibility of their application as thin-films.

Relevant characterization data of the polymeric derivatives are reported in Table 1.

Table 1. Characterization data of polymeric derivatives.

Sample	Yield ^{a)} %	\bar{M}_n ^{b)} g mol ⁻¹	\bar{M}_w/\bar{M}_n ^{b)}	T_g ^{c)} °C	T_d ^{d)} °C
Poly[(S)-(+)- MECSI]	74	12.700	1.7	202	330
Poly[(S)-(-)- MECP]	53	6.650	1.6	210	349

a) Calculated as (g polymer/g monomer)·100;

b) Determined by SEC in THF solution at 25°C;

c) Glass transition temperature determined by DSC at 10°C/min heating rate under nitrogen flow;

d) Initial decomposition temperature as determined by TGA at 20°C/min heating rate under air flow.

The FT-IR spectra of poly[(S)-(+)-**MECSI**] and poly[(S)-(-)-**MECP**] confirmed the occurrence of polymerization involving the methacrylic double bond, with the disappearance of the bands related to the stretching vibration of the methacrylic double bond of the monomers at 1633 and 1628 cm^{-1} , respectively, and the presence of a new absorption band related to the α,β saturated ester group at 1723 and 1725 cm^{-1} ,

respectively, with a shift of 10-20 cm^{-1} to higher frequencies with respect to the stretching carbonyl frequency present in the corresponding monomeric precursors.

The ^1H NMR spectra of polymers, as compared to those of monomers (Figure 2), are in agreement with the proposed structures. In accordance with FT-IR data, the resonances at 5.60 and 6.15 ppm, related to the methacrylic CH_2 protons, are absent in the ^1H -NMR spectra of the polymers, and the methacrylic CH_3 resonance is shifted from 1.95 ppm to higher field. It is also to be noted that the resonances of the polymeric aromatic protons are shifted up field to a variable extent with respect to the monomers, thus indicating the presence of shielding interactions between the side-chain chromophores in solution (see experimental part).

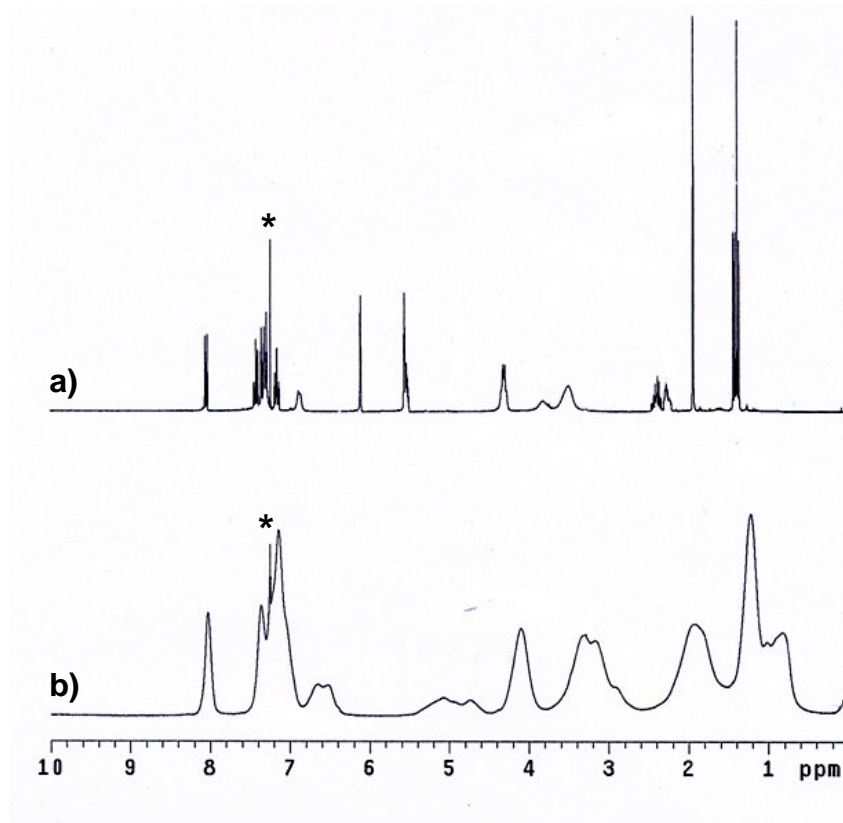


Figure 2. ^1H -NMR spectra in CDCl_3 at 25 $^\circ\text{C}$ of (a) (S) - $(-)$ -**MECP** and (b) poly $[(S)$ - $(-)$ -**MECP**]. Starred signals refer to solvent resonances.

Thermal Analysis

The high glass transition temperatures displayed by poly $[(S)$ - $(+)$ -**MECSI**] and poly $[(S)$ - $(-)$ -**MECP**], as measured by DSC (202 and 210 $^\circ\text{C}$, respectively) should allow a good Optically active, photoresponsive multifunctional polymeric materials

orientational stability of the photoactive chromophores which is of great interest for applications in optoelectronics and photonics (more stable photoinduced birefringence, NLO properties, diffraction gratings, holographic storage, etc.).

The DSC thermograms did not reveal any liquid crystalline behaviour nor melting peaks, thus suggesting that the macromolecules are substantially amorphous in the solid state.

In accordance with a reduced mobility of the macromolecular chains originated by their dipolar structure and conformational stiffness, the T_g values are considerably higher than those of analogous polymers with aliphatic linear spacers between the carbazole chromophore and the methacrylic main chain [27-30].

In particular, poly[(*S*)-(-)-**MECP**] exhibits a higher T_g value than poly[(*S*)-(+)-**MECSI**], indicative of a remarkable presence of strong inter- and/or intramolecular dipolar interactions in the solid state between the side-chain aromatic chromophores which are characterized by high charge delocalization, due to the presence of the electron-rich (*S*)-(+)-3-hydroxy-N-[3-(9-ethylcarbazole)]-pyrrolidine residue.

The thermal stability of poly[(*S*)-(+)-**MECSI**] and poly[(*S*)-(-)-**MECP**], as determined by thermogravimetric analysis (TGA), resulted also very high, with onset decomposition temperature (T_d) of 330 and 349°C, respectively, much higher than those reported for PVK (227°C) [31], deeply investigated as polymeric material for photorefractive applications [1], and for other methacrylic carbazole-containing polymers [28,30]. Again, the higher T_d value for poly[(*S*)-(-)-**MECP**] can be attributed to the increased polar inter- and/or intramolecular interactions between the neighbouring side-chain moieties.

This unexpected high thermal stability and high T_g values suggest that these polymeric materials may be promisingly tested for commercial applications, besides the optical ones, where thermal stability is a fundamental requirement.

Absorption spectra

The UV-vis absorption spectra in chloroform solution of (*S*)-(+)-**MECSI** and poly[(*S*)-(+)-**MECSI**] (Table 2 and Figure 3) exhibit, in the region 250-500 nm, evident absorption bands with maxima centered at about 269, 296, 305 (shoulder), 336 and 349

nm (Table 2) attributed to $\pi\text{-}\pi^*$ electronic transitions of the carbazole chromophore [34]. These bands are related to the three spectral regions, between 350-315 nm ($^1L_b \leftarrow ^1A_1$ electronic transition), 310-280 nm ($^1L_a \leftarrow ^1A_1$ electronic transition) and 280-260 nm ($^1B_2 \leftarrow ^1A_1$ electronic transition) in accordance with Platt notation [34].

By contrast, (*S*)-(-)-**MECP** and poly[(*S*)-(-)-**MECP**] (Table 2 and Figure 3) show four absorption bands: three in the region 250-320 nm with maxima centered at about 267, 296 and 313 (shoulder) nm related to the same $\pi\text{-}\pi^*$ above mentioned electronic transitions of carbazole, and the fourth centered at 392 nm attributed to internal charge transfer of the carbazole chromophore conjugated with the strong electron-donor pyrrolidine ring, which increases the electron density in the carbazole moiety and consequently the permanent dipole moment of the system.

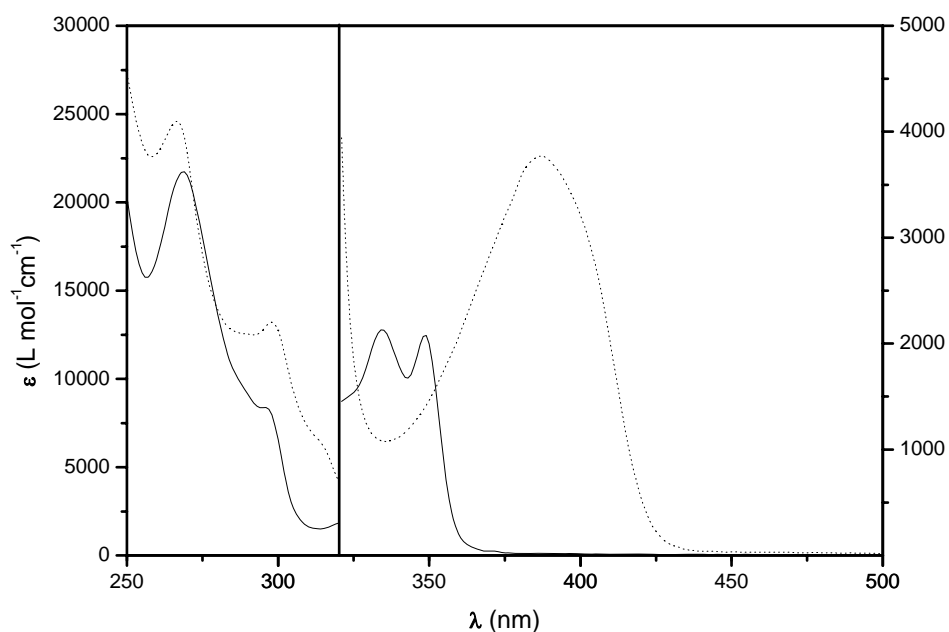


Figure 3. UV-vis spectra in CHCl_3 solution of poly[(*S*)-(+)-**MECSI**] (—) and poly[(*S*)-(-)-**MECP**] (-----).

Table 2. UV-vis spectra in CHCl₃ solution at 25°C of monomers and polymeric derivatives.

Samples	1 st band		2 nd band		3 rd band		4 th band		5 th band	
	$\lambda_{\max}^{\text{a)}$	$\epsilon_{\max}^{\text{b)}$								
	nm	Lmol ⁻¹ cm ⁻¹								
(S)-(+)-MECSI	269	23500	296	9000	305	7500	333	2700	348	2700
Poly[(S)-(+)-MECSI]	269	21700	296	6550	305	6800	336	2100	349	2100
(S)-(-)-MECP	267	28400	298	19200	312	7100	385	4600		
Poly[(S)-(-)-MECP]	267	24600	298	13200	313	5200	392	3700		

- a) Wavelength of maximum absorbance;
b) Calculated for one single chromophore.

While the maxima absorption wavelengths (Table 2) do not substantially change in going from the monomers to the related polymers, a remarkable hypochromic effect is observed when the spectra of (*S*)-(+)-**MECSI** and (*S*)-(–)-**MECP**, where the lack of structural restraints originates a random distribution of the chromophores in dilute solution, are compared with those of the related polymers (Table 2). This behaviour, previously observed in several polymeric systems bearing side-chain aromatic [17, 27, 33] chromophores, is attributed to the presence of electrostatic dipole-dipole interactions between the neighbouring aromatic moieties [34-36]. This particular effect is evident for all the electronic absorption bands and suggests the occurrence of strong interactions between the side-chain carbazole groups, which appear promising for a good photoconductivity even in the absence of dopants.

Chiroptical properties

With the aim to study the dependence of the optical activity on the macromolecular structure of these materials, the specific $\{[\alpha]_D^{25}\}$ and molar $\{[\Phi]_D^{25}\}$ optical rotation in chloroform solution at the sodium D-line of all low and high molecular weight compounds has been determined (Table 3).

Polymers show higher optical rotation values than their corresponding monomers. Indeed, poly[(*S*)-(+)-**MECSI**] displays a $[\Phi]_D^{25}$ which is two order of magnitude higher than that of (*S*)-(+)-**MECSI** and poly[(*S*)-(–)-**MECP**] exhibits optical rotation opposite in sign and ten times larger than that of (*S*)-(–)-**MECP**, thus suggesting that macromolecules are characterized by a higher conformational order with respect to the related monomers. It can also be noticed that the optical rotation of poly[(*S*)-(+)-**MECSI**] is of the same sign but three times larger than that of poly[(*S*)-(–)-**MECP**]. This behaviour could be attributed to the higher rigidity of the cyclic succinimide residue with respect to more conformationally flexible pyrrolidine ring.

Table 3. Specific and molar optical rotation data of the synthesized compounds in CHCl₃ solution at 25°C.

Samples	$[\alpha]_D^{25 \text{ a)}$	$[\Phi]_D^{25 \text{ b)}$
	deg·dm ⁻¹ ·g ⁻¹ ·dL	deg·dm ⁻¹ ·mol ⁻¹ ·dL
(S)-(+)-MECSI	+0.7	+2.63
Poly[(S)-(+)-MECSI]	+177.7	+668.0
(S)-(-)-MECP	-8.1	-28.2
Poly[(S)-(-)-MECP]	+57.6	+200.7

a) Specific optical rotation;

b) Molar optical rotation, calculated as $([\alpha]_D^{25} \cdot M/100)$, where M represents the molecular weight of the monomers or the molecular weight of the repeating unit of the polymers, or in other word the molar optical rotation calculated for carbazole unit.

The observed remarkable contribution to optical activity given by the macromolecular chains could be in principle originated by a prevalent tacticity of the polymeric backbone or, in other words, to stereoregularity of the main chain. To assess this possibility, an evaluation of the microtacticity of the polymeric derivatives has been made based on the ¹³C-NMR signals of the methacrylic methyl group, which displays two resonances located at ≈ 20 and 18 ppm (see experimental part), assigned to *mr* (meso-racemo) and *rr* (racemo-racemo) heterotactic and syndiotactic triads, respectively [37].

Assuming that the polymerization process follows a Bernoullian statistics, the probabilities of formation of a meso dyad m (P_m) can be calculated from the integrated signals ratio (mr/rr), which corresponds to $2P_m(1-P_m)/(1-P_m)^2$, i.e. to the ratio between the probability of formation of *mr* and *rr* triads [37].

P_m values of 0.30 and 0.32, with consequently probabilities P_r values of 0.70 and 0.68, are found for poly[(S)-(+)-MECSI] and poly[(S)-(-)-MECP], respectively. It follows that the percent amounts of *mm*, *mr* (*rm*), and *rr* triads in poly[(S)-(+)-MECSI] are 9, 42 and 49%, respectively. Very closely related values for *mm* (10%), *mr* (43%) and *rr*

(47%) triads have been found also for poly[(*S*)-(-)-**MECP**], thus suggesting a quite similar stereoregularity of the main chain in both the polymers investigated.

It is also confirmed that the addition of (*S*)-(+)-**MECSI** or (*S*)-(-)-**MECP** to the correspondents growing chains is unaffected by the nature of the last repeating unit, and follows a Bernoullian statistics, as indicated by the close similarity of $P_{m/r}$ (0.30 or 0.32, respectively) with $P_{m/m}$ (0.30 or 0.32, respectively) and by the sum of $P_{m/r}$ (0.30 or 0.32, respectively) with $P_{r/m}$ (0.70 or 0.68, respectively) that gives 1.00, where $P_{m/m}$, $P_{r/m}$ and $P_{m/r}$ are the calculated probabilities that a given dyad follows a dyad having the same or the opposite relative configuration.

Thus, the main chain microstructure of the synthesized polymers is essentially heterotactic, with a predominance of syndiotactic triads ($rr = 47\text{-}49\%$) suggesting a substantially low stereoregularity of the main-chain, in agreement with literature reports concerning the radical polymerization of methyl methacrylate [38] of analogous chiral azoaromatic derivatives [19, 25].

As a conclusion, the enhancement of optical activity observed in the investigated polymeric samples is mainly due to conformational effects rather than to a significant stereoregularity degree of the main chain and can be addressed to the remarkable stiffness assumed by the macromolecules in consequence of the presence of the conformationally rigid chiral ring (succinimide and pyrrolidine) pendant to the methacrylic main chain.

The correlation between chiroptical properties and secondary structures of the polymers (conformational features of the macromolecular chains) was probed by CD spectroscopy in the spectral region 250-500 nm and compared to those of the corresponding monomers (Table 4, Figure 4a/4b).

The CD spectrum of (*S*)-(+)-**MECSI** in chloroform solution (Figure 4a) displays, in addition to a significant negative band around 253 nm, five weak positive dichroic absorptions with maxima at 352, 336, 318, 298 and 272 nm (Table 4), strictly related to the UV-Vis electronic transitions of the carbazole chromophore (Table 2).

The CD spectrum of poly[(*S*)-(+)-**MECSI**] (Figure 4a and Table 4) exhibits five relevant positive dichroic bands ($\lambda_{\text{max}} = 351, 336, 316, 297$ and 275 nm) in the spectral region related to the $\pi\text{-}\pi^*$ electronic transition of the carbazole chromophore (Table 2)

and one structured positive dichroic signal of relative intensity in the 270-250 nm spectral region which presents opposite sign with respect to the monomer.

CD spectra of poly[(*S*)-(-)-**MECP**] and (*S*)-(-)-**MECP**] (Figure 5a and Table 4) appear essentially similar to those of the corresponding succinimide containing samples, but the monomer exhibits three low intensity negative dichroic bands at 377, 289 and 257 nm, while the polymer shows only one negative dichroic absorption at 384 nm (Table 4). The imperfect correspondence between the CD and the UV-vis spectrum can be explained by considering that they are originated by a sum of electronic transitions which can be differently influenced by the chirality of the macromolecules.

The intensity of CD signals of polymers is larger than those observed in previously reported optically active vinylic polymers containing carbazole where the chiral residues were not directly linked to the main-chain [15-18]. This behaviour suggests that the insertion of a rigid chiral group interposed between the main chain and the carbazole group favours more the establishment of conformational dissymmetry in the macromolecules, inducing a higher chiral perturbation on the electronic transitions of the carbazole chromophore.

Furthermore, in agreement with polarimetric data (Table 3), the intensity of the CD bands appears much higher in the polymers than in the corresponding monomers. This last occurrence suggests that the presence of the optically active cyclic residue of one prevailing absolute configuration, interposed between the main chain of the polymer and the carbazole chromophore, promotes the adoption of a chiral conformation of one prevailing helical handedness, at least for chain segments of the macromolecules in solution. This conformational effect could be influenced by dipole-dipole interactions between neighbouring carbazole groups. In fact, similar dipolar interactions are much lower or absent in the spectrum of monomers that do not possess any structural restriction and are unable to produce any cooperative interactions between the side-chain carbazole chromophores.

Furthermore, the higher optical activity shown by poly[(*S*)-(+)-**MECSI**] with respect to poly[(*S*)-(-)-**MECP**], can be attributed to different dipole moment of the substituted carbazole chromophores and/or to dissimilar conformational rigidity of the macromolecules due by presence of cyclic succinimide and pyrrolidine residues

Table 4. CD spectra in CHCl₃ solution at 25°C of monomers and polymeric derivatives.

Sample	1 st band		2 nd band		3 rd band		4 th band		5 th band			
	$\lambda_1^{\text{a)}$	$\Delta\varepsilon_1^{\text{b)}$	$\lambda_2^{\text{a)}$	$\Delta\varepsilon_2^{\text{b)}$	$\lambda_3^{\text{a)}$	$\Delta\varepsilon_3^{\text{b)}$	$\lambda_4^{\text{a)}$	$\Delta\varepsilon_4^{\text{b)}$	$\lambda_5^{\text{a)}$	$\Delta\varepsilon_5^{\text{b)}$	$\lambda_6^{\text{a)}$	$\Delta\varepsilon_6^{\text{b)}$
	nm	Lmol ⁻¹ cm ⁻¹										
(S)-(+)-MECSI	253	-2.31	272	+1.10	298	+0.31	318	+0.02	336	+0.16	352	+0.22
Poly[(S)-(+)-MECSI]	-	-	275	+4.24	297	+2.56	316	+0.42	336	+0.54	351	+0.65
(S)-(-)-MECP	259	-0.46	277	+0.14	289	-0.14	313	+0.54	377	-0.09	-	-
Poly[(S)-(-)-MECP]	-	-	271	+1.40	304	+1.25	316	+1.73	384	-0.29	-	-

a) Wavelength of maximum dichroic absorption;

b) Calculated for one repeating unit in the polymer.

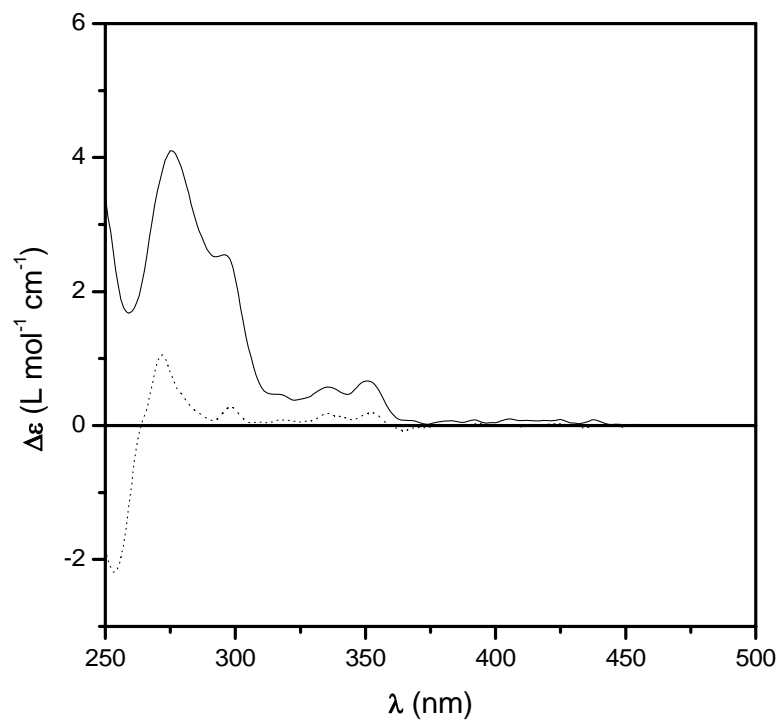


Figure 4a. CD spectra in CHCl_3 solution of (S) - $(+)$ -**MECSI** (---) and poly[(S) - $(+)$ -**MECSI**] (—).

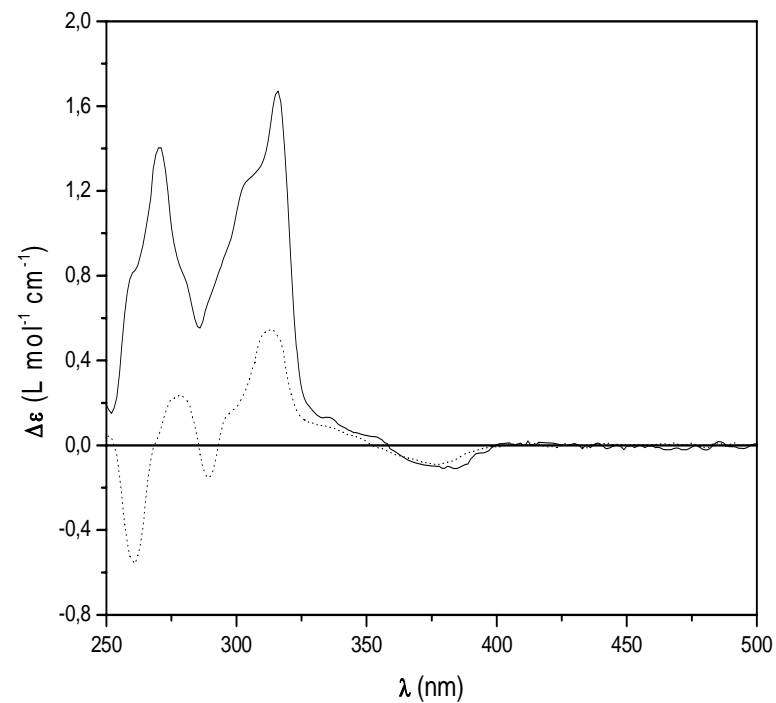


Figure 4b. CD spectra in CHCl_3 solution of (S) - $(-)$ -**MECP** (---) and poly[(S) - $(-)$ -**MECP**] (—).

Photoconductivity

Both the polymeric samples do not require the addition of dopants in order to observe photoconduction. This is not surprising, given the presence of the carbazole moiety, which is well known for its hole conducting properties [1]. In addition, being carbazole directly linked to strong electron-donating or withdrawing groups, the absorption bands are shifted to higher wavelengths and some charge transfer effect can be induced [39], thus increasing the photogeneration efficiency.

As can be noticed in Figure 5, poly[(S)-(-)-MECP] (80 wt % + 20 wt % DPP) shows higher photoconductivity than pure poly[(S)-(+)-MECSI]. This behaviour cannot be ascribed to the presence of plasticizer DPP as demonstrated by similar measurements carried out on a sample of poly[(S)-(+)-MECSI] containing 20 wt % DPP (see inset of Figure 5). Photoconduction measured at different wavelengths follows the trend of the absorption coefficient, increasing with increasing the absorption value.

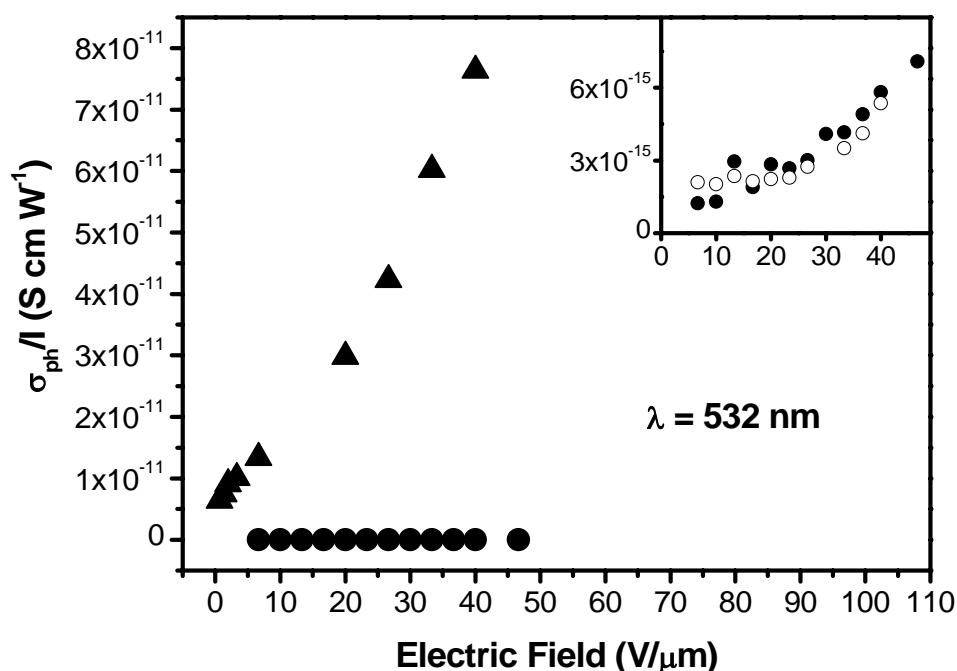


Figure 5. Photoconductivity versus the electric field at 532 nm for poly[(S)-(-)-MECP] : DPP 4:1 (triangle) and poly[(S)-(+)-MECSI] (Circle). Inset: enlargement of poly[(S)-(+)-MECSI] (Circle) and poly[(S)-(+)-MECSI] : DPP 4:1 (open circle) data.

As the absorption coefficients of the two materials at $\lambda = 532$ nm are quite similar, $\alpha = 1267$ cm⁻¹ for poly[(*S*)-(-)-**MECP**] (80 wt % + 20 wt % DPP) and $\alpha = 987$ cm⁻¹ for poly[(*S*)-(+)-**MECSI**], they cannot account for the different observed photoconductivity. The main difference between the two polymers has to be attributed to the presence of a charge-transfer complex between the strong donator pyrrolidine and the carbazole in poly[(*S*)-(-)-**MECP**], as evidenced by the absorption band at 392 nm in the UV-Vis spectrum. Charge transfer can positively affect photoconductivity by two different mechanisms: photogeneration efficiency, due to the stabilization of charged species, and transport parameters, which can be favoured by more efficient holes hopping between more electron-rich carbazole moieties.

Methacrylic optically active homopolymers bearing side-chain 9-phenylcarbazole moieties.

The synthesis of two novel optically active monomers containing 9-phenylcarbazole moieties, such as (*S*)-(+)-methacryloyl-2-oxy-N-(9-phenylcarbazole)-succinimide [(*S*)-(+)-**MCPS**], (*S*)-(-)-methacryloyl-3-oxy-N-(9-phenylcarbazole)-pyrrolidine [(*S*)-(-)-**MCPPI**], is described.

Each monomer has been radically homopolymerized to afford the corresponding optically active polymeric derivative, which have been fully characterized and their spectroscopic and thermal properties compared to those of the achiral model homopolymer poly[methacryloyl-2-oxyethyl-N-ethyl-N-(9-phenylcarbazole)-amine] poly[**MCPE**] (Figure 1).

Synthesis and structural characterization

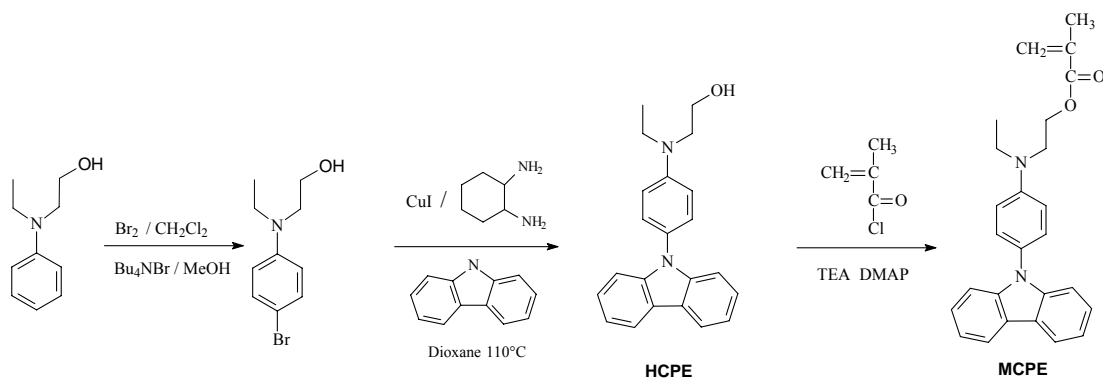
The synthesis of monomers (*S*)-(+)-**MCPS** and (*S*)-(+)-**MCPPI** were carried out according to Scheme 2, starting from the intermediate N-(4-aminophenyl)carbazole, obtained by Ullmann reaction of crude carbazole with 1-bromo-4-nitrobenzene [40].

The intermediate was submitted to reaction with chloralide, derived in turn from (*S*)-(-)-malic acid by reaction with chloral hydrate [24], to give the alcohol (*S*)-(+)-2-hydroxy-N-[4-N-(9-phenylcarbazole)]succinimide [(*S*)-(+)-**HCPS**].

(*S*)-(+)-**HCPS** was then reduced to the desired optically active alcohol (*S*)-(+)-3-hydroxy-N[4-(N-phenylcarbazole)]pyrrolidine (*S*)-(+)-**HCPI** with a similar synthetic procedure used for analogous chiral derivatives [19a, 25].

3-hydroxy-N-ethyl-N-[4-(N-9-phenylcarbazole)]amine [**HCPE**] (Scheme 3) was prepared starting from N-bromo-N-ethyl-N-(2-idrossietil)amine, derived from bromuration of N-ethyl-N-(2-idrossietil)amine [41], which was coupled, under Ullmann condition, with carbazole to afford the desired alcohol [(*S*)-(-)-**HCPI**].

The three monomers (*S*)-(+)-methacryloyl-2-oxy-N-9-phenylcarbazole-succinimide (*S*)-(+)-**MCPS**, (*S*)-(-)-methacryloyl-3-oxy-N-9-phenylcarbazole-pyrrolidine (*S*)-(-)-**MCPPI** and Methacryloyl-2-oxy-N-ethyl-N[4-(N-phenylcarbazole)]amine [**MCPE**]



Scheme 3.

Homopolymerization of the monomers was carried out in glass vials using AIBN as free radical initiator and THF as solvent. The reaction mixture (1.0 g of monomer, 2% weight of AIBN in 10 ml of THF) was introduced into the vial under nitrogen atmosphere, submitted to several freeze-thaw cycles and heated at 60°C for 72 h. The reaction was then stopped by pouring the mixture into a large excess (100 ml) of methanol, and the coagulated polymer filtered off. The solid polymeric product was repeatedly redissolved in THF at room temperature, reprecipitated again with methanol, and finally dried at 60°C under vacuum for several days to constant weight. All products were characterized by FT-IR, ¹H- and ¹³C-NMR. Relevant data for the synthesized homopolymers are reported in Table 5

Table 5. Characterization data of polymeric derivatives.

Sample	Yield ^{a)} %	\bar{M}_n ^{b)} g mol ⁻¹	\bar{M}_w/\bar{M}_n ^{b)}	T_g ^{c)} °C
Poly[(S)-(+)-MCPS]	83	11400	1.9	244
Poly[(S)-(+)-MCPP]	80	7000	1.9	194
Poly[(S)-(+)-MCPE]	80	10100	1.9	129

a) Calculated as (g polymer/g monomer)·100;

b) Determined by SEC in THF solution at 25°C;

c) Glass transition temperature determined by DSC at 10°C/min heating rate under nitrogen flow;

The occurred polymerization was proved by IR spectroscopy by checking the disappearance in the spectra of the absorption at 1630-1635 cm^{-1} , related to the methacrylic double bond, and the contemporary appearance of the band at 1728-1731 cm^{-1} , related to the carbonyl stretching vibration of the α,β saturated methacrylic ester group, shifted to higher frequency by ca. 10 cm^{-1} with respect to the corresponding band of the monomers. Accordingly, in the $^1\text{H-NMR}$ spectra of polymeric derivatives the resonances of the vinylidenic protons of monomeric methacrylate were absent.

Thermal Analysis

Observation of polymeric derivatives with a polarizing microscope did not reveal any liquid crystalline behavior.

Only second-order transitions originated by glass transitions (T_g), with no melting peaks, are observed in the DSC thermograms of the investigated polymers (Table 5), thus suggesting that the macromolecules are substantially amorphous in the solid state.

The T_g values appear quite high can be attributed to the increased polar inter- and/or intramolecular interactions between the neighbouring N-phenylcarbazole side-chain moieties and can be of great interest for applications in optoelectronics (more stable photoinduced birefringence, etc.)

Poly[**MCPE**] exhibit a T_g value (129°C) considerably lower than those shown by poly[(*S*)-(+)-**MCPS**] and poly[(*S*)-(+)-**MCPP**] (224 and 194 °C respectively).

This behavior is indicative of much reduced mobility of the macromolecular chains originated by the presence of the conformational optically active rigid ring interposed between the backbone and the N-phenylcarbazole chromophore thus increasing the stiffness of the macromolecules.

Absorption Spectra.

The UV-vis spectra of the polymers in THF solution exhibit, in accordance with Platt notation [34], distinctive absorption bands related to $^1L_b \leftarrow ^1A_1$, $^1L_a \leftarrow ^1A_1$ and $^1B_2 \leftarrow ^1A_1$ electronic transition of the carbazole chromophore.

Poly[(*S*)-(+)-**MCPP**] (Figure 6 and Table 6) display five absorption bands at 269, 283 (shoulder), 292, 328 e 341 nm related to $\pi-\pi^*$ electronic transition.

By contrast, poly[(*S*)-(+)-**MCPS**] show only four absorption bands at 280 (shoulder), 293, 325 e 339 nm.

The dissimilar nature of the bands can be ascribed to the presence of the succinimide rigid residue that is characterized by a strong electron-withdrawing ability and presents, with respect to the pyrrolidine ring, an inverse permanent dipole moment of the system.

Poly[**MCPE**] shows analogous absorptions bands of Poly[(*S*)-(+)-**MCPP**]. This behaviour can be attributed to the same architectures of the phenylcarbazole moiety and to the similar electron-donating properties of their amminic nitrogen atoms.

An hypochromic effect can be generally observed passing from homopolymer to the corresponding monomers where the lack of structural restraints originates a random distribution in dilute solution of the chromophores.

Such a behavior, frequently noticed in polymeric derivatives bearing side-chain aromatic chromophores, is attributed to the presence of electrostatic dipolar interactions between adjacent chromophores [17, 27, 33].

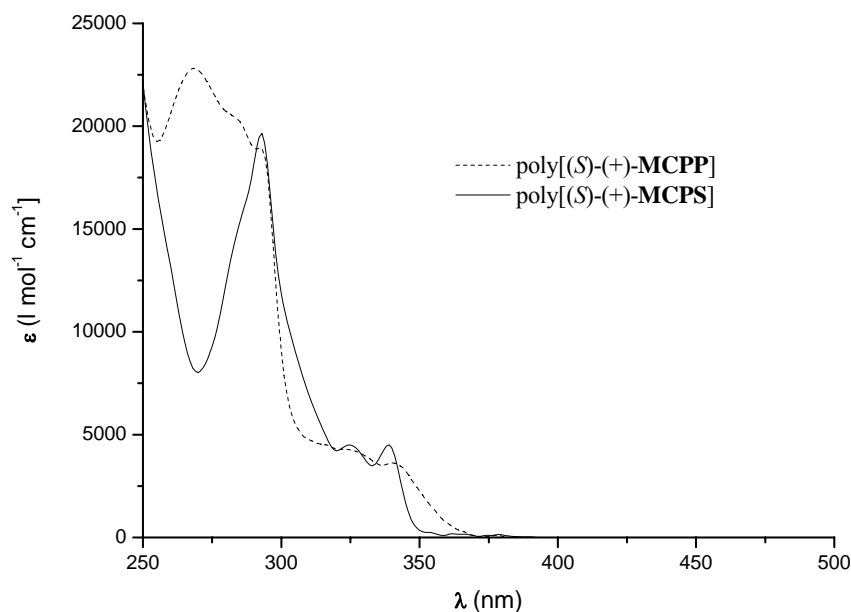


Figure 6. UV-vis spectra in CHCl_3 solution of poly[(*S*)-(+)-**MCPP**] (···) an poly[(*S*)-(+)-**MCPS**] (—)

Table 6. UV-vis spectra in CHCl₃ solution at 25°C of monomers and polymeric derivatives.

Sample	1 st band		2 nd band		3 rd band		4 th band		5 th band	
	$\lambda_{\max}^{\text{a)}}$	$\epsilon_{\max}^{\text{b)}}$								
	nm	Lmol ⁻¹ cm ⁻¹								
(S)-(+)-MCPS	-	-	283	14700	292	18600	325	3000	338	3200
Poly[(S)-(+)-MCPS]	-	-	280	15500	293	19600	325	3500	339	3500
(S)-(+)-MCPP	268	25400	283	21500	292	20000	328	3200	341	3000
Poly(S)-(+)-MCPP]	269	22800	283	20400	293	18900	329	3100	340	2900
MCPE	268	27900	283	24400	292	22150	326	3800	340	3400
Poly[MCPE]	269	22200	283	20100	293	18500	-	-	341	2800

c) Wavelength of maximum absorbance;

d) Calculated for one single chromophore.

Chiroptical properties

The dependence of the optical activity on the macromolecular structure was assessed by measuring the specific $\{[\alpha]_D^{25}\}$ and molar $\{[\Phi]_D^{25}\}$ optical rotation in chloroform solution at the sodium D-line of monomers and homopolymers (Table 7).

Table 7. Specific and molar optical rotation data of the synthesized compounds in CHCl_3 solution at 25°C.

Sample	$[\alpha]_D^{25 \text{ a)}$	$[\Phi]_D^{25 \text{ b)}$
	$\text{deg}\cdot\text{dm}^{-1}\cdot\text{g}^{-1}\cdot\text{dL}$	$\text{deg}\cdot\text{dm}^{-1}\cdot\text{mol}^{-1}\cdot\text{dL}$
(S)-(+)-MCPS	+2.0	+8.5
Poly[(S)-(+)-MCPS]	+6.4	+27.2
(S)-(+)-MCPP	+9.3	+38.2
Poly[(S)-(+)-MCPP]	+9.0	+36.9

a) Specific optical rotation;

b) Molar optical rotation, calculated as $([\alpha]_D^{25}\cdot M/100)$, where M represents the molecular weight of the monomers or the molecular weight of the repeating unit of the polymers, or in other word the molar optical rotation calculated for carbazole unit.

Poly[(S)-(+)-MCPS] shows higher specific and optical rotation values than its corresponding monomer; thus suggesting that the macromolecule is characterized by a higher conformational order with respect to (S)-(+)-MCPS.

Instead, Poly[(S)-(+)-MCPP] and (S)-(+)-MCPP present similar optical activity.

Comparing Poly[(S)-(+)-MCPS] and Poly[(S)-(+)-MCPP] with respect to poly[(S)-(+)-MECSI] and poly[(S)-(-)-MECP], the homopolymers bearing in the side chain derivatives of N-phenylcarbazole display $[\Phi]_D^{25}$ values two order of magnitude lower. This behaviour could be attributed to the structural design of the repeating units of (S)-(+)-MECSI and (S)-(+)-MECP where the chiral succinimide and pyrrolidine residues are directly linked to the carbazole chromophores, without the phenyl groups acting as spacer.

Table 8. CD spectra in CHCl₃ solution at 25°C of monomers and polymeric derivatives.

Sample	1 st band		2 nd band		3 rd band		4 th band		5 th band	
	λ_1^{a}	$\Delta\varepsilon_1^{\text{b}}$	λ_2^{a}	$\Delta\varepsilon_2^{\text{b}}$	λ_3^{a}	$\Delta\varepsilon_3^{\text{b}}$	λ_4^{a}	$\Delta\varepsilon_4^{\text{b}}$	λ_5^{a}	$\Delta\varepsilon_5^{\text{b}}$
	nm	Lmol ⁻¹ cm ⁻¹								
(S)-(+)- MCPS	-	-	283	+0,80	-	-	-	-	340	+0,25
Poli[(S)-(+)- MCPS]	264	+0,64	280	+0,57	308	+2,21	-	-	342	+0,60
(S)-(+)- MCP	269	-0,24	289	+0,56	-	-	328	+0,28	341	+0,13
Poli[(S)-(+)- MCP]	269	-1,66	288	+0,67	-	-	331	+0,40	347	+0,35

a) Wavelength of maximum dichroic absorption;

b) Calculated for one repeating unit in the polymer.

The chiroptical properties of optically active monomers and polymers have been investigated in CHCl_3 solution by CD in the spectral region 250 - 650 nm in order to understand the effect of the conformational features of the macromolecular side chain on the chiroptical properties (Figure 7 and Table 8).

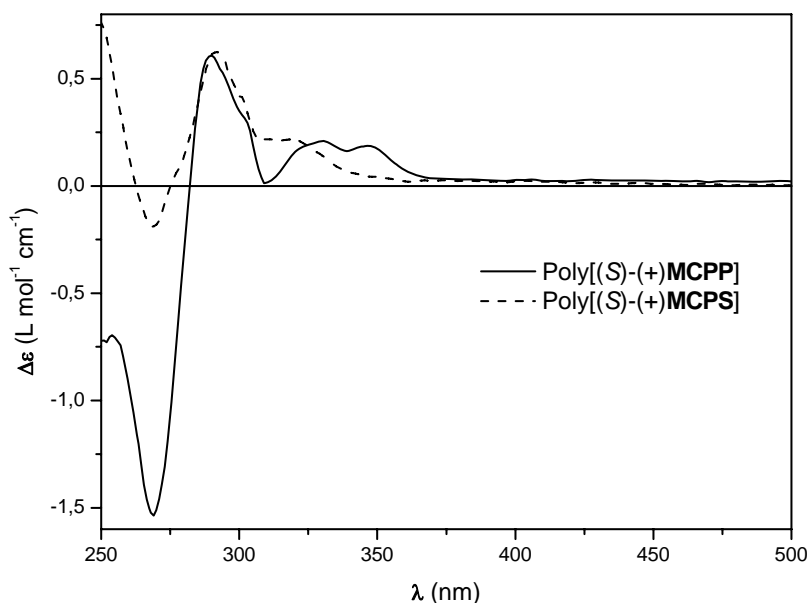


Figure 7. CD spectra in CHCl_3 solution of (S) - $(-)$ -**MCPP** (---) and poly $[(S)$ - $(+)$ -**MCPP**] (—).

The CD spectra Poly $[(S)$ - $(+)$ -**MCPS**] and Poly $[(S)$ - $(+)$ -**MCPP**] are characterized by intense dichroic signals in correspondence to the UV-Vis absorption bands. These signals, which are related to the electronic transitions of the N-phenylcarbazole chromophores, are more intense of those measured in the of the corresponding monomers. The imperfect correspondence between the CD and the UV-vis spectrum can be explained by considering that they are originated by a sum of electronic transitions which can be differently influenced by the chirality of the macromolecules. The CD spectrum of poly $[(S)$ - $(+)$ -**MCPS**] exhibits four relevant positive dichroic bands ($\lambda_{\text{max}} = 342, 308, 280$ and 264 nm) in the spectral region related to the π - π^* electronic transition of the carbazole chromophore (Table 6).

Significantly, the CD spectrum of monomer (*S*)-(+)-**MCPS**, which does not possess any structural restriction, displays weak dichroic signals, related to the UV bands, indicative of the absence of chiral conformations in solution.

CD spectra of poly[(*S*)-(-)-**MCP**] and (*S*)-(-)-**MCP** exhibit four dichroic bands (Figure 7 and Table 8).

Finally it is also noticeable that the increase intensities of the dichroic signals passing from monomers to the related polymers confirm the observation of the establishment of a higher conformational homogeneity of the macromolecules in solution.

This behavior can be ascribed to the cooperative dipole-dipole interactions between neighboring side chain chromophores arranged in a mutual chiral geometry of one prevailing handedness, at least for chain segments of the macromolecules in solution.

Photoconductivity

Poly[(*S*)-(+)-**MCPS**], poly[(*S*)-(+)-**MCP**] and poly[**MCPE**], show higher photoconductivity than poly[(*S*)-(+)-**MECSI**] and Poly[(*S*)-(+)-**MECP**] (Table 9).

Table 9. Photoconductivity of the investigated polymers

Sample	Photoconductivity ^{a)}	Electric Field ^{b)}
Poly[(<i>S</i>)-(+)- MCPS]	$1,5 \cdot 10^{-12}$	50
Poly[(<i>S</i>)-(+)- MCP]	$5,0 \cdot 10^{-12}$	50
Poly[MCPE]	$2,5 \cdot 10^{-11}$	40
Poly[(<i>S</i>)-(+)- MECSI]	$6,0 \cdot 10^{-15}$	40
Poly[(<i>S</i>)-(+)- MECP]	$8,2 \cdot 10^{-11}$	40

a) Expressed in σ/l ($S \cdot cm^{-1} \cdot W$)

b) Expressed in $V/\mu m$

This behaviour could be attributed to the major free grades of movement of the photoconductive carbazole moieties in the N-phenylcarbazole derivatives with respect of the 3-substituted derivatives.

In poly[(*S*)-(+)-**MCPS**], poly[(*S*)-(+)-**MCP**P] and poly[**MCPE**], in fact, the geometrical constraints imposed by chain linking to the chromophore in 9 position seems to favour the adoption of interchromophore geometry permitting a better carrier transport via hopping process between the side chain carbazoles.

Poly[**MCPE**] (Figure 8) shows an higher value of photoconductivity with respect to poly[(*S*)-(+)-**MCPS**], poly[(*S*)-(+)-**MCP**P].

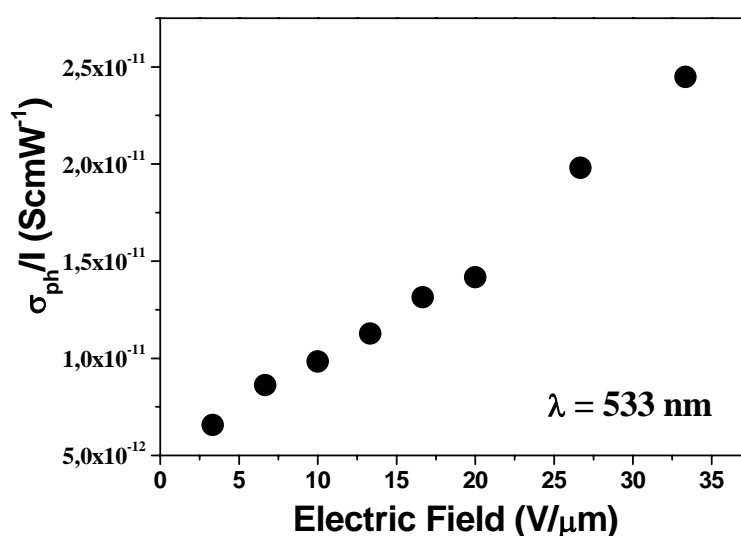


Figure 8. Photoconductivity versus the electric field at 532 nm for poly[**MCPE**]

Also this result can be ascribed to the geometrical architecture of the repeating units. In poly[**MCPE**], the N-phenylcarbazole is linked to the backbone through a flexible spacer; by contrast, in (*S*)-(+)-**MCPS** and (*S*)-(+)-**MCP**P co-units, the chromophores are conformationally hindered by the succinimide and pyrrolidine rings so that its free movements are probably reduced.

These results confirm that the flexibility of the linking group assists the adoption of the parallel overlap of the carbazole chromophores, thus allowing higher values of photoconductivity.

Conclusions

Novel chiral homopolymeric methacrylates poly[(*S*)-(+)-**MECSI**], poly[(*S*)-(–)-**MECP**], poly[(*S*)-(+)-**MCPS**] and poly[(*S*)-(+)-**MCPS**] have been obtained by radical polymerization of the related novel monomers, bearing the optical active residues of the (*S*)-3-hydroxy-pyrrolidine and (*S*)-2-hydroxy-succinimide interposed between the main chain and the carbazole chromophore.

In order to evaluate the influence of the chirality on the properties of the macromolecules bearing in the side chain 9-phenylcarbazole moieties, an analogous achiral polymer poly[(methacryloyl-2-oxyethyl-N-ethyl-N-(9-phenylcarbazole)-amine] poly[**MCPE**] have been synthesised .

Absorption spectra show the presence of dipolar interaction between neighbouring carbazolyl moiety in the side-chain of the polymers.

The relevant induced optical activity shown by homopolymers with respect to monomers indicates that the macromolecules assume, in solution, highly homogeneous conformations with a prevailing chirality, as demonstrated by the presence of relevant absorption bands in the CD spectra and by optical rotation data.

This behaviour can be attributed to the combined effects of the strongly dipolar conjugated carbazole system with the conformational stiffness of optically active rings, favouring the instauration of conformational arrangements with a prevailing handedness, at least for chain sections of the macromolecules. It appears therefore that the conformational rigidity of the optically active group interposed between the main chain and the carbazole moieties plays an important role in determining the extent of conformational order in solution by these macromolecular systems.

The presence of strong dipolar interactions between carbazolyl groups in the solid state also produces relevant thermal properties with high values of T_g and T_d which can be of interest for nanoscale technological applications.

Photoconductivity measurements show that the presence of carbazole makes polymers photoconductive. The strong electron donating character of the pyrrolidine moiety allows the formation in poly[(*S*)-(–)-**MECP**] of a charge-transfer complex, boosting the photoconductive properties with respect to poly[(*S*)-(+)-**MECSI**].

The geometrical constraints imposed by chain linking the carbazole chromophores at the 9-position seem to favour (with respect to attachments at the 3-ring position) the adoption of particular interchromophoric geometries, thus permitting a better carrier transport via hopping process between the side chain carbazoles.

The properties of this new class of optically active carbazole polymers, bearing at the same time different chemical functionalities, may allow a variety of potential applications based on NLO, photorefractivity and all-optical manipulation of information. In particular, the combination of optical storage capabilities based on the modulation of the linear refractive index, photoconductive properties conferred by carbazole moieties, and logical functionality based on chiroptical switching, may lead to the preparation of novel multifunctional materials.

Experimental section

Chemicals

Methacryloyl chloride (Aldrich) was distilled (b.p. = 95°C) under inert atmosphere in the presence of traces of 2,6-di-*tert.* butyl-*p*-cresol as polymerization inhibitor just before use.

The optically active intermediate (*S*)-(+)-5-carboxymethyl-2-trichloromethyl-4-oxo-1,3-dioxolane (malic acid chloralide) (**1**) was prepared starting from (*S*)-(-)-malic acid by reaction with chloral hydrate, according to literature procedures [24].

Toluene, chloroform, dichloromethane and tetrahydrofuran (THF) were purified and dried according to the reported procedures [42] and stored over molecular sieves (4 Å) under nitrogen.

Triethylamine (Aldrich) was refluxed over dry CaCl₂ for 8 h, then distilled (b.p. 89°C) under nitrogen atmosphere. 2,2'-Azobisisobutyronitrile (AIBN) (Aldrich) was crystallized from abs. ethanol before use. All other reagents and solvents (Aldrich) were used as received without further purification.

Measurements

NMR spectra were obtained at room temperature on 5-10% CDCl₃ solutions using a Varian NMR Gemini 300 spectrometer. Chemical shifts are given in ppm from tetramethylsilane (TMS) as the internal reference. ¹H-NMR spectra were run at 300 MHz by using the following experimental conditions: 24 000 data points 4.5-kHz spectral width 2.6-s acquisition time 128 transients. ¹³C NMR spectra were recorded at 75.5 MHz, under full proton decoupling, by using the following experimental conditions: 24000 data points, 20 kHz spectral width, 0.6 s acquisition time, 64000 transients.

FT-IR spectra were carried out on a Perkin-Elmer 1750 spectrophotometer equipped with an Epson Endeavor II data station on sample prepared as KBr pellets.

Number average molecular weight (\bar{M}_n) and polydispersity (\bar{M}_w/\bar{M}_n) were determined in THF solution by SEC using a HPLC Lab Flow 2000 apparatus, equipped with an injector Rheodyne 7725i, a Phenomenex Phenogel 5μ MXL column and a UV-

Vis detector Linear Instruments model UVIS-200, working at 254 nm. Calibration curves were obtained by using several monodisperse polystyrene standards.

UV-vis absorption spectra were recorded at 25°C on a Perkin Elmer Lambda 19 spectrophotometer on CHCl₃ solutions by using cell path lengths of 1 and 0.1 cm for the 500-320 and 320-250 nm spectral regions, respectively. Carbazole chromophore concentrations of about 5·10⁻⁴ mol L⁻¹ were used.

Optical activity measurements were accomplished at 25°C on CHCl₃ solutions with a Perkin Elmer 341 digital polarimeter, equipped with a Toshiba sodium bulb, using a cell path length of 1 dm. Specific and molar rotation values at the sodium D line are expressed as deg·dm⁻¹·g⁻¹·cm³ and deg·dm⁻¹·mol⁻¹·dL, respectively. Molar rotation for polymers refers to the molecular weight of the repeating unit.

Circular dichroism (CD) spectra were carried out at 25°C on CHCl₃ solutions on a Jasco 810 A dichrograph, using the same path lengths and solution concentrations as for the UV-Vis measurements. Δε values, expressed as L·mol⁻¹·cm⁻¹ were calculated from the following expression: Δε = [Θ]/3300, where the molar ellipticity [Θ] in deg·cm²·dmol⁻¹ refers to one carbazole chromophore.

The glass transition temperature (*T_g*) values were determined by differential scanning calorimetry (DSC) on a TA Instrument DSC 2920 Modulated apparatus at a heating rate of 10°C/min under nitrogen atmosphere on samples of 5-9 mg.

The initial thermal decomposition temperature (*T_d*) was determined on the polymeric sample with a Perkin-Elmer TGA-7 thermogravimetric analyzer by heating the samples in air at a rate of 20°C/min.

Samples for photoconductivity measurements were prepared by placing the hot (above *T_g*) polymeric materials, mixed with diphenyl phthalate (DPP) (from Sigma-Aldrich, purified by recrystallization), between two ITO covered glass slides so as to obtain a thickness of 10 μm or 5 μm, as controlled by glass spacers. The real thickness was measured by interferometry [24].

Photoconductivity data were obtained by applying a DC voltage to the sample and measuring the current with a Keithley 6517A Electrometer in the dark and under illumination. The illuminating light was provided by a Newport-Oriel 250W Xenon lamp, coupled with a Newport-Oriel monochromator (mod 74100), with a resulting

light intensity $I \sim 3 \text{ mW/cm}^2$ or, alternatively, by a laser light at 532 nm (from Laser Quantum, mod. Torus), obtaining a light intensity $I \sim 1 \text{ W/cm}^2$.

Synthesis of alcohols and monomers

(S)-(-)-2-Hydroxy-N-[3-(9-ethylcarbazole)]-succinimide [(S)-(-)-HECSI]

The malic acid chloralide **1** (50 mmol) was submitted to chlorination with excess of SOCl_2 (500 mmol) to give the intermediate acid chloride which was directly submitted to the cyclization step. After evaporation under reduced pressure of any unreacted thionyl chloride, dry toluene (200 mL) and 3-amino-N-ethyl-carbazole (50 mmol) were added and heated at reflux under inert atmosphere for 12 h. The solvent was then evaporated under reduced pressure and the crude product purified by column chromatography (SiO_2 , eluent EtOAc/ CH_2Cl_2 1:1 v/v) to give 13.92 g of pure (S)-(-)-HECSI (Yield 91%).

$[\alpha]_D^{25} = -57.0^\circ$ (c=0.995 in CHCl_3).

$^1\text{H-NMR}$ (CDCl_3): 8.06 (d, 1H, arom. 5-H carbazole), 7.95 (s, 1H, arom. 6-H carbazole), 7.50-7.20 (m, 5H, arom. carbazole), 4.80 (m, 1H, 3-CH), 4.40 (q, 2H, N- $\text{CH}_2\text{-CH}_3$ carbazole), 3.90 (m, 1H, OH), 3.30 and 2.95 (2dd, 2H, 4- CH_2), 1.45 (m, 3H, N- $\text{CH}_2\text{-CH}_3$ carbazole) ppm.

FT-IR (KBr): 3428 (ν_{OH}), 3065 (ν_{CH} arom.), 2980 (ν_{CH} aliph.), 1709 ($\nu_{\text{C=O}}$ imide), 1600 ($\nu_{\text{C=C}}$ arom.), 1381 (δ_{CH}), 1194 (ν_{CN}), 772 and 718 (δ_{CH} 1,2,4-trisubst. arom. ring), 746 (δ_{CH} 1,2-disubst. arom. ring) cm^{-1} .

(S)-(+)-3-Hydroxy-N-[3-(9-ethylcarbazole)]-pyrrolidine [(S)-(+)-HECP]

A 2 M solution of borane-dimethyl sulfide complex in THF (30 ml, 0.588 mol) was added dropwise, under inert atmosphere, to a stirred solution of (S)-(-)-HECSI (6 g, 0.196 mol) in dry THF (150 ml) and the mixture kept under reflux for one night. After distillation of the solvent under reduced pressure, 10 g (0.239 mol) of sodium fluoride in dist. water (85 ml) were cautiously added to the solid residue, then the mixture was made acidic (pH 2) with conc. aq. HCl and refluxed 2 h. After treatment with 30% aq.

NaOH (pH 10), the precipitated crude product was filtered, washed with a 1:1 v/v mixture of diethyl ether/THF and finally crystallized from abs. ethanol (yield 82%).

$[\alpha]_D^{25} = +2.0^\circ$ (c=0.198 in CHCl₃).

¹H-NMR (CDCl₃): 8.05 (d, 1H, arom. 5-H carbazole), 7.30 (m, 5H, arom. carbazole), 6.90 (d, 1H, arom. 2-H carbazole), 4.85 (m, 1H, OH), 4.70 (m, 1H, 3-CH), 4.30 (q, 2H, N-CH₂-CH₃ carbazole), 3.60-3.30 (m, 4H, 2- and 5-CH₂), 2.30 (m, 2H, 4-CH₂), 1.40 (t, 3H, N-CH₂-CH₃ carbazole) ppm.

FT-IR (KBr) (cm⁻¹): 3389 (ν_{OH}), 3053 (ν_{CH} arom.), 2980 e 2929 (ν_{CH} aliph.), 1602 (ν_{C=C} arom.), 1328 (δ_{CH}), 794 and 719 (δ_{CH} 1,2,4-trisubst. arom. ring), 741 (δ_{CH} 1,2-disubst. arom. ring) cm⁻¹.

(S)-(+)-Methacryloyl-2-oxy-N-[3-(9-ethylcarbazole)]-succinimide [(S)-(+)-MECSI]

To an ice-cooled, vigorously stirred solution of (S)-(-)-HECSI (3.50 g, 0.113 mol), triethylamine (1.92 ml, 0.135 mol), dimethylamino pyridine (0.135 g) as catalyst, and 2,6-di-*tert*-butyl-4-methyl phenol (0.113 g) as polymerization inhibitor, in anhydrous THF (68 mL), was added dropwise, under nitrogen atmosphere, methacryloyl chloride (1.33 ml, 0.135 mol) in THF (5 ml). The mixture was kept ice-cooled for 2 h, then left at room temperature for one night, concentrated at reduced pressure and the crude product dissolved in chloroform. The chloroformic solution was washed with 0.1 M HCl, 5% Na₂CO₃ and finally with water, in that order.

After drying the organic layer on anhydrous Na₂SO₄ and evaporation of the solvent under reduced pressure, the crude reaction product was purified by column chromatography (SiO₂, CH₂Cl₂/EtOAc 4:1 v/v as eluent) followed by crystallization from abs. ethanol to give 2.05 g of pure product (48.0% yield).

$[\alpha]_D^{25} = +0.7^\circ$ (c=0.980 in CHCl₃).

¹H-NMR (CDCl₃): 8.20 (d, 1H, arom. 5-H carbazole), 7.50 (m, arom. 5H, carbazole), 7.40 (d, 1H, arom. 2-H carbazole), 6.40 and 5.85 (2dd, 2H, CH₂=), 5.80 (m, 1H, 3-CH), 4.50 (q, 2H, N-CH₂-CH₃ carbazole), 3.69 and 3.10 (2dd, 2H, 4-CH₂), 2.08 (s, 3H, CH₃ methacrylic), 1.50 (t, 3H, N-CH₂-CH₃ carbazole) ppm.

¹³C-NMR (CDCl₃): 173.86 (C=O ester), 173.75 (C=O imide), 141.14 (arom. C₁₀ carbazole), 140.32 (arom. C₁₃ carbazole), 136.45 (CH₂=C), 128.62 (CH₂=), 126.98

(arom. C₇ carbazole), 124.36 (arom. C₂ carbazole), 123.99 (arom. C₃ carbazole), 123.23 and 123.02 (arom. C₁₁ and C₁₂ carbazole), 121.48 (arom. C₅ carbazole), 119.97 (arom. C₆ carbazole), 119.63 (arom. C₄ carbazole), 109.62 (arom. C₁ carbazole), 109.41 (arom. C₈ carbazole), 68.77 (3-CH), 38.36 (N-CH₂-CH₃ carbazole), 36.55 (4-CH₂), 18.89 (CH₃ methacrylic), 14.46 (N-CH₂-CH₃ carbazole) ppm.

FT-IR (KBr): 3070 (ν_{CH} arom.), 2969 (ν_{CH} aliph.), 1737 (ν_{C=O} ester), 1697 (ν_{C=O} imide), 1633 (ν_{C=C} methacrylic), 1603 (ν_{C=C} arom.), 1379 (δ_{CH}), 774 and 730 (δ_{CH} 1,2,4-trisubst. arom. ring), 752 (δ_{CH} 1,2-disubst. arom. ring) cm⁻¹.

(S)-(-)-Methacryloyl-3-oxy-N-[3-(9-ethylcarbazole)]-pyrrolidine [(S)-(-)-MECP]

The same procedure adopted for (S)-(+)-MECSI was followed starting from (S)-(+)-HECP (1.5 gr, 0.005 mol), triethylamine (0.91 ml, 0.0064 mol), dimethylamino pyridine (0.06 gr) and 2,6-di-*tert*-butyl-4-methyl phenol (0.05 gr) in THF (150 ml). The acylation reaction was performed by using methacryloyl chloride (0.63 ml, 0.0064 mol). Pure (S)-(-)-MECP was obtained in 56.0% yield (1.05 g) by column chromatography (SiO₂, THF as eluent) followed by crystallization from abs. ethanol.

[α]_D²⁵ = -8.0° (c=1.005 in CHCl₃).

¹H-NMR (CDCl₃): 8.05 (d, 1H, arom. 5-H carbazole), 7.30 (m, 5H, arom. carbazole), 7.20 (d, 1H, arom. 2-H carbazole), 6.10 and 5.80 (2dd, 2H, CH₂=), 5.50 (m, 1H, 3-CH), 4.30 (q, 2H, N-CH₂-CH₃ carbazole), 3.80-3.30 (m, 4H, 2- and 5-CH₂), 2.30 (m, 2H, 4-CH₂), 1.97 (s, 3H, CH₃ methacrylic), 1.40 (t, 3H, N-CH₂-CH₃ carbazole) ppm.

¹³C-NMR (CDCl₃): 167.95 (C=O ester), 142.92 (arom. C₁₀ carbazole), 141.16 (arom. C₁₃ carbazole), 136.96 (CH₂=C), 133.97 (arom. C₃ carbazole), 126.50 (CH₂=), 126.05 (arom. C₇ carbazole), 123.99 and 123.4 (arom. C₁₁ and C₁₂ carbazole), 121.07 (arom. C₅ carbazole), 118.54 (arom. C₆ carbazole), 113.20 (arom. C₂ carbazole), 109.71 (arom. C₁ carbazole), 108.99 (arom. C₈ carbazole), 103.38 (arom. C₄ carbazole), 75.13 (3-CH), 55.87 (5-CH₂), 47.67 (2-CH₂), 38.17 (N-CH₂-CH₃ carbazole), 31.01 (4-CH₂), 18.92 (CH₃ methacrylic), 14.51 (N-CH₂-CH₃ carbazole) ppm.

FT-IR (KBr): 3058 (ν_{CH} arom.), 2972 (ν_{CH} aliph.), 1709 (ν_{C=O} ester), 1628 (ν_{C=C} methacrylic), 1600 (ν_{C=C} arom.), 1326 (δ_{CH}), 787 and 751 (δ_{CH} 1,2,4-trisubst. arom. ring), 720 (δ_{CH} 1,2-disubst. arom. ring) cm⁻¹.

(S)-(+)-2-Hydroxy-N-[4-(N-phenylcarbazole)]succinimide [(S)-(+)-HCPS]

9.7 g (0.0376 mol) of 1-(p-aminophenyl)carbazole and 9.9 g of chloralide (0.0376 mol) were added in dry toluene (136.3 ml) and heated at reflux under inert atmosphere for 12 h. The solvent was then evaporated under reduced pressure and the crude product purified by column chromatography (SiO₂, eluent EtOAc/CH₂Cl₂ 1:1 v/v) to give 5.6 g of pure (S)-(+)-HCPS (Yield 52%).

¹H-NMR (CDCl₃): 8.20-8.10 (d, 2H, arom. 2,7-carbazole), 7.70-7.65 (d, 2H, arom. 4,5-carbazole), 7.60-7.55 (d, 2H, 15,19-phenyl), 7.40 (m, 4H, arom. 1,3,6,8-carbazole), 7.30 (m, 2H, 16,18-phenyl), 4.85 (m, 1H, 3-CH), 3.40 (s, 1H, OH), 3.35 and 2.94 (2dd, 2H, 4.CH₂) ppm.

FT-IR (KBr) (cm⁻¹): 3458 (ν_{OH}), 3050 (ν_{CH} arom.), 2967 (ν_{CH} aliph.), 1706 (ν_{C=O}), 1600 (ν_{C=C} arom.), 1514 (δ_{CH}), 1205 (ν_{C-O}), 850 and 830 (δ_{CH} 1,4- disubst. arom. ring), 744 (δ_{CH} 1,2- disubst. arom. ring).

(S)-(+)-3-Hydroxy-N-[4-(N-phenylcarbazole)]pyrrolidine [(S)-(+)-HCPP]

The same procedure adopted for (S)-(+)-HECP starting from (S)-(+)-HCPS (4 g, 0.00938 mol) to afford, after crystallization in pure hexane, 3.2 g of pure (S)-(+)-HCPP (Yield 82%).

¹H-NMR (CDCl₃) (δ in ppm dal TMS): 8.30-8.20 (d, 2H, arom. 2,7-carbazole), 7.60-7.35 (m, 8H, arom. 1,3,4,5,6,8-carbazole and 15,19-phenyl.), 6.90 (d, 2H, 16,18-phenyl), 4.90 (m, 1H, 3-CH), 3.60-3.50 (m, 4H, 2 and 5- CH₂), 3.40 (s, 1H, OH), 2.40-2.20 (m, 2H, 4.CH₂) ppm.

FT-IR (KBr) (cm⁻¹): 3425 (ν_{OH}), 3050 (ν_{CH} arom.), 2967 (ν_{CH} aliph.), 1605 (ν_{C=C} arom.), 1519 (δ_{CH₂}), 1205(δ_{C-O}), 852 and 815 (δ_{CH} 1,4- disubst. arom. ring), 748 (δ_{CH} 1,2- disubst. arom. ring).

2-Hydroxy-N-ethyl-N-[4-(N-carbazol)]phenyl-amine [HCPE]

A mixture of 7.12 g (0.024 mol) of crude carbazole, 0.55 g of trans-cyclohexanediamine (10 % mol) and 0.46 g of air-stable CuI (10% mol) was prepared in 15 ml of dry dioxane (1 M) at presence of 7 g di K₂CO₃ (2 equiv).

7 g (0.029 mol) of 2-hydroxyethyl-N-ethyl-N-(4-bromophenyl)amine in dry dioxane (10 ml) was then added and the final solution was heated at reflux under inert atmosphere for 24 h.

The cooled mixture was filtered-off and the organic solution was washed with 0.1 M HCl, 5% Na₂CO₃ and finally with water, in that order.

After drying the organic layer on anhydrous Na₂SO₄ and evaporation of the solvent under reduced pressure, the crude reaction product was purified by column chromatography (SiO₂, CH₂Cl₂/EtOAc 1:1 v/v as eluent) followed by crystallization from abs. ethanol to give 3.8 g of pure product (48.0% yield).

¹H-NMR (CDCl₃): 8.20 (d, 2H, arom. 2,7-carbazole), 7.40-7.20 (m, 8H, arom. 1,3,4,5,6,8-carbazole and 15,19-phenyl), 6.90 (d, 2H, 16,18-phenyl), 3.95 (d, 2H, N-CH₂-CH₂), 3.50 (m, 4H, N-CH₂), 1.80 (m, 1H, OH), 1.20 (t, 3H, N-CH₂-CH₃) ppm.

FT-IR (KBr): 3420 (ν_{OH}), 3050 (ν_{CH} arom.), 2967 (ν_{CH} aliph.), 1605 (ν_{C=C} arom.), 1448 (ν_{C-Nas} CH₃), 1360 (ν_{CHs} CH₃), 1231 (ν_{C-O} alcohol), 847 e 816 (δ_{CH} 1,4- disubst. arom. ring), 746 (δ_{CH} 1,2- disubst. arom. ring) cm⁻¹.

(S)-(+)-Methacryloyl-2-oxy-N-(9-phenylcarbazole)-succinimide [(S)-(+)-MCPS]

The same procedure adopted for (S)-(+)-MECSI was followed starting from (S)-(+)-HCPS (2 gr, 0.0047 mol), triethylamine (0.79 ml, 0.0057 mol), dimethylamino pyridine (0.1 gr) and 2,6-di-*tert*-butyl-4-methyl phenol (0.1 gr) in THF (150 ml). The acylation reaction was performed by using methacryloyl chloride (0.79 ml, 0.0057 mol).

Pure (S)-(+)-MCPS was obtained in 70.0% yield (1.70 g) by column chromatography (SiO₂, CH₂Cl₂/EtOAc 1:1 v/v as eluent) followed by crystallization from abs. ethanol.

$[\alpha]_D^{25} = +2.0^\circ$.

¹H-NMR (CDCl₃): 8.20-8.10 (d, 2H, arom. 2,7-carbazole), 7.80-7.70 (d, 2H, arom. 4,5-carbazole), 7.60-7.55 (d, 2H, 15,19-phenyl), 7.40 (m, 4H, arom. 1,3,6,8-carbazole), 7.30 (m, 2H, 16,18-phenyl), 6.35 and 5.75 (2dd, 2H, CH₂ methacrylic), 5.60 (m, 1H, 2-CH), 3.40 and 2.95 (d, 2H, 4-CH₂), 2.00 (s, 3H, CH₃ methacrylic) ppm.

FT-IR (KBr) (cm⁻¹): 3050 (ν_{CH} arom.), 2967 (ν_{CH} aliph.), 1716 (ν_{C=O} ester), 1705 (ν_{C=O} imide) 1633 (ν_{C=C} methacrylic), 1600 (ν_{C=C} arom.), 1512 (δ_{CH2}), 1450 (ν_{C-Nas} CH₃), 1356

($\nu_{\text{CHs}} \text{CH}_3$), 1230($\delta_{\text{C-O}}$), 1161 ($\nu_{\text{C-O}}$), 832 and 810 (δ_{CH} 1,4- disubst. arom. ring), 751 (δ_{CH} 1,2- disubst. arom. ring).

(S)-(+)-Methacryloyl-2-oxy-N-9-phenylcarbazole-pyrrolidine [(S)-(+)-MCPP]

The same procedure adopted for (S)-(+)-MECP was followed starting from (S)-(+)-HCPP (3,5 gr, 0.0107 mol), triethylamine (1.8 ml, 0.0128 mol), dimethylamino pyridine (0.2 gr) and 2,6-di-*tert*-butyl-4-methyl phenol (0.2 gr) in THF (150 ml). The acylation reaction was performed by using methacryloyl chloride (1.24 ml, 0.0128 mol). Pure (S)-(+)-MEPS was obtained in 71.0% yield (2.25 g) by column chromatography (SiO₂, CH₂Cl₂/EtOAc 1:1 v/v as eluent) followed by crystallization from abs. ethanol.

$[\alpha]_D^{25} = +9.3^\circ$

¹H-NMR (CDCl₃): 8.20-8.10 (d, 2H, arom. 2,7-carbazole), 7.40-7.20 (m, 8H, arom. 1,3,4,5,6,8-carbazole and 15,19-phenyl), 6.80 (d, 2H, 16,18-phenyl), 6.15 e 5.60 (2dd, 2H, CH₂ methacrylic), 5.55 (m, 1H, 3-CH), 3.60-3.40 (m, 4H, 2 and 5-CH₂), 2.40-2.30 (m, 2H, 4CH₂), 1.95 (s, 3H, CH₃ methacrylic) ppm.

FT-IR (KBr) (cm⁻¹): 3050 (ν_{CH} arom.), 2967 (ν_{CH} aliph.), 1718 ($\nu_{\text{C=O}}$ ester), 1608 ($\nu_{\text{C=C}}$ arom.), 1519 (δ_{CH_2}), 1450 ($\nu_{\text{CNas}} \text{CH}_3$), 1356 ($\nu_{\text{CHs}} \text{CH}_3$), 1231($\nu_{\text{C-O}}$ alcohol), 1161 ($\nu_{\text{C-O}}$ ester) 850 and 815 (δ_{CH} 1,4- disubst. arom. ring), 748 (δ_{CH} 1,2- disubst. arom. ring).

(S)-(+)-Methacryloyl-2-oxy-N-9-phenylcarbazole-amine [MCPE]

The same procedure adopted for (S)-(+)-MECP was followed starting from (S)-HCPE (3,3 gr, 0.0097 mol), triethylamine (1.63 ml, 0.0128 mol), dimethylamino pyridine (0.2 gr) and 2,6-di-*tert*-butyl-4-methyl phenol (0.2 gr) in THF (100 ml). The acylation reaction was performed by using methacryloyl chloride (1.14 ml, 0.0117 mol).

Pure MCPE was obtained in 55.0% yield (2.1 g) by column chromatography (SiO₂, CH₂Cl₂/EtOAc 1:1 v/v as eluent) followed by crystallization from abs. ethanol.

¹H-NMR (CDCl₃) (δ in ppm dal TMS): 8.20 (d, 2H, arom. 2,7-carbazole), 7.40-7.20 (m, 8H, arom. 1,3,4,5,6,8-carbazole and 15,19-phenyl), 6.90 (d, 2H, 16,18-phenyl), 6.15 and 5.60 (d, 2H, CH₂ methacrylic), 4.50 (d, 2H, N-CH₂-CH₂), 3.70-3.50 (m, 4H, N-CH₂), 2.00 (s, 3H, CH₃ methacrylic), 1.20 (t, 3H, N-CH₂-CH₃).

FT-IR (KBr) (cm^{-1}): 3048 (ν_{CH} arom.), 2978 (ν_{CH} aliph), 1716 ($\nu_{\text{C=O}}$), 1623 ($\nu_{\text{C=C}}$ methacrylic), 1605 ($\nu_{\text{C=C}}$ arom.), 1520 (δ_{CH_2}), 1450 ($\nu_{\text{CNas}} \text{CH}_3$), 1371 ($\nu_{\text{CHs}} \text{CH}_3$), 1169 ($\nu_{\text{C-O}}$ ester), 852 and 814 (δ_{CH} 1,4- disubst. arom. ring), 753 (δ_{CH} 1,4- disubst. arom. ring)

Polymers

The homopolymerization the monomers was carried out in glass vials using AIBN as free radical initiator and dry THF as solvent. The reaction mixture (1.0 g of monomer, 2% weight of AIBN in 25 mL of DMF) was introduced into the vials under nitrogen atmosphere, submitted to several freeze-thaw cycles and heated at 65 °C for 72 h. The reaction was then stopped by pouring the mixture into a large excess of methanol (200 ml), and the coagulated polymer filtered off. The solid product was repeatedly redissolved in THF at room temperature and reprecipitated again in methanol. The last traces of unreacted monomers and oligomeric impurities were eliminated by Soxhlet continuous extraction with methanol followed by acetone. The material was finally dried at 60°C under vacuum for several days to constant weight.

Poly[(S)-(+)-MECSI]

$^1\text{H-NMR}$ (CDCl_3): 8.00-7.60 (m, 1H, arom. 5-H carbazole), 7.50-6.80 (m, 6H, arom. carbazole), 5.80 (m, 1H, 3-CH), 4.00 (q, 2H, N- $\underline{\text{CH}}_2$ - CH_3 carbazole), 3.40-3.10 (m, 2H, 4- CH_2), 2.20-1.05 (m, 8H, N- CH_2 - $\underline{\text{CH}}_3$ carbazole, backbone CH_3 and CH_2) ppm.

$^{13}\text{C-NMR}$ (CDCl_3): 177.32 (C=O ester), 173.51 (C=O imide), 140.75 (arom. C_{10} carbazole), 139.92 (arom. C_{13} carbazole), 126.82 (arom. C_7 carbazole), 124.35 (arom. C_2 carbazole), 123.18 (arom. C_{11} and C_{12} carbazole), 121.45 (arom. C_3 carbazole), 119.97 (arom. C_5 and C_6 carbazole), 114.67 (arom. C_4 carbazole), 109.50 (arom. C_1 carbazole), 109.31 (arom. C_8 carbazole), 68.86 (3-CH), 53.20 ($\underline{\text{C}}\text{H}_2$ -C main chain), 46.12 (CH_2 - $\underline{\text{C}}$ main chain), 38.01 (N- $\underline{\text{C}}\text{H}_2$ - CH_3 carbazole), 36.07 (4- CH_2), 20.60 and 18.89 (CH_3 methacrylic), 14.25 (N- CH_2 - $\underline{\text{C}}\text{H}_3$ carbazole) ppm.

FT-IR (KBr): 3053 (ν_{CH} arom.), 2974 (ν_{CH} aliph.), 1723 ($\nu_{\text{C=O}}$ ester), 1700 ($\nu_{\text{C=O}}$ imide), 1601 ($\nu_{\text{C=C}}$ arom.), 1381 (δ_{CH}), 766 and 727 (δ_{CH} 1,2,4-trisubst. arom. ring), 749 (δ_{CH} 1,2-disubst. arom. ring) cm^{-1} .

Poly[(S)-(-)-MECP]

$^1\text{H-NMR}$ (CDCl_3): 8.05 (m, 1H, arom. 5-H carbazole), 7.50-6.80 (m, 6H, arom. carbazole), 5.20 (m, 1H, 3-CH), 4.30 (m, 2H, N- $\underline{\text{CH}_2}$ - CH_3 carbazole), 3.80-3.50 (m, 4H, 2- and 5- CH_2), 2.10-0.90 (m, 10H, 4- CH_2 , N- CH_2 - $\underline{\text{CH}_3}$ carbazole, backbone CH_3 and CH_2) ppm.

$^{13}\text{C-NMR}$ ($\text{THF-}d_8$): 176.92 (C=O ester), 142.87 (arom. C_{10} carbazole), 141.15 (arom. C_{13} carbazole), 133.92 (arom. C_3 carbazole), 125.66 (arom. C_7 carbazole), 124.50 and 123.73 (arom. C_{11} and C_{12} carbazole), 120.87 (arom. C_5 carbazole), 118.54 (arom. C_6 carbazole), 113.20 (arom. C_2 carbazole), 109.56 (arom. C_1 carbazole), 108.90 (arom. C_8 carbazole), 102.99 (arom. C_4 carbazole), 75.82 (3-CH), 55.10 ($\underline{\text{CH}_2}$ -C main chain), 54.22 (5- CH_2), 47.40 (2- CH_2), 45.86 (CH_2 - $\underline{\text{C}}$ main chain) 37.72 (N- $\underline{\text{CH}_2}$ - CH_3 carbazole), 31.62 (4- CH_2), 19.4 and 17.87 (CH_3 methacrylic), 13.96 (N- CH_2 - $\underline{\text{CH}_3}$ carbazole) ppm.

FT-IR (KBr): 3047 (ν_{CH} arom.), 2969 (ν_{CH} aliph.), 1725 ($\nu_{\text{C=O}}$ ester), 1602 ($\nu_{\text{C=C}}$ arom.), 1334 (δ_{CH}), 788 and 721 (δ_{CH} 1,2,4-trisubst. arom. ring), 744 (δ_{CH} 1,2-disubst. arom. ring) cm^{-1} .

Poly[(S)-(+)-MCPS]

$^1\text{H-NMR}$ (CDCl_3): 8.20-7.80 (d, 2H, arom. 2,7-carbazole), 7.80-6.90 (m, 10H, arom. 1,3,4,5,6-carbazole e 15,16,18,19-phenyl.), 5.60 (m, 1H, 2- CH_2), 3.40-2.95 (m, 2H, 4- CH_2), 2.10-1.00 (m, 3H, CH_3 and CH_2 backbone) ppm.

FT-IR (KBr): 3050 (ν_{CH} arom.), 2967 (ν_{CH} aliph.), 1724 ($\nu_{\text{C=O}}$ ester), 1600 ($\nu_{\text{C=C}}$ arom.), 1512 (δ_{CH_2}), 1365 (ν_{CH_3} CH_3), 1200 ($\nu_{\text{C-O}}$ ester), 850 and 834 (δ_{CH} 1,4-disubst. arom. ring), 748 (δ_{CH} 1,2-disubst. arom. ring) cm^{-1} .

Poly[(S)-(+)-MCPP]

$^1\text{H-NMR}$ (CDCl_3): 8.20-8.00 (d, 2H, arom. 2,7-carbazole), 7.40-7.00 (m, 8H, arom. 1,3,4,5,6,8-carbazole and 15,19-phenyl), 6.80-6.40 (m, 2H, 16,18-phenyl), 5.40-5.00 (m, 1H, 3-CH), 3.70-3.00 (m, 4H, 2 and 5- CH_2), 2.40-0.80 (m, 7H, 4- CH_2 and backbone CH_3 and CH_2) ppm.

FT-IR (KBr): 3050 (ν_{CH} arom.), 2967 (ν_{CH} aliph.), 1737 ($\nu_{\text{C=O}}$ ester) 1608 ($\nu_{\text{C=C}}$ arom.), 1519 (ν_{CH_2}), 1451 (ν_{CNas} CH_3), 1365 (ν_{CHs} CH_3), 1161 ($\nu_{\text{C-O}}$ ester), 851 and 814 (δ_{CH} 1,4-disubst. arom. ring), 746 (δ_{CH} 1,4-disubst. arom. ring) cm^{-1} .

Poly[MCPE]

$^1\text{H-NMR}$ (CDCl_3): 8.20-8.00 (d, 2H, arom. 2,7-carbazole), 7.40-6.40 (m, 18H, arom. 1,3,4,5,6,8-carbazole and 15,19-phenyl), 6.80 (m, 2H, 16,18-phenyl), 3.95 (m, 2H, N- CH_2 - CH_2), 3.70-3.50 (m, 4H, N- CH_2), 2.00 (s, 3H, CH_3 methacrylic), 1.80-0.80 (m, 8H, N- CH_2 - CH_3 and backbone CH_2 and CH_3) ppm.

FT-IR (KBr): 3048 (ν_{CH} arom.), 2978 (ν_{CH} aliph.), 1716 ($\nu_{\text{C=O}}$ ester), 1605 ($\nu_{\text{C=C}}$ arom.), 1520 (ν_{CH_2}), 1450 (ν_{CNas} CH_3), 1371 (ν_{CHs} CH_3), 1169 ($\nu_{\text{C-O}}$ ester.), 852 and 814 (δ_{CH} 1,4-disubst. arom. ring), 753 (δ_{CH} 1,4-disubst. arom. ring) cm^{-1} .

References

- [1] J. V. Grazuleviciusa, P. Strohhrieglb, J. Pielichowski, K. Pielichowski, *Prog. Polym. Sci.* 2003, 28, 1297–1353.
- [2] W. E. Moerner, A. Grunnet-Jepsen, C. L. Thompson, *Annu. Rev. Mater. Sci.* 1997, 27, 583-623.
- [3] P. N. Prasad, M. E. Orczyk, J. Zieba, *J. Phys. Chem.* 1994, 98, 8699.
- [4] K. Meerholz, B. Volodin, B. Sandalphon, N. Kippelen, N. Peyghambarian, *Nature* 1994, 371, 497.
- [5] M. M. Green, R. J. M. Nolte, E. W. Meijer, S. E. Denmark, J. Siegel, *Topics in stereochemistry. Materials-chirality* New York: Wiley-VCH, 2003, 24.
- [6] J. Zhang, M. Albelda, Y. Liu, J.W. Canary, *Chirality* 2005, 17, 404–420.
- [7] T. Kajitani, K. Okoshi, S. Sakurai, J. Kumaki, E. Yashima, *J. Am. Chem. Soc.* 2006, 128, 708-709.
- [8] E. Yashima, K. Maeda, T. Nishimura, *Chem. Eur. J.* 2004, 10, 42-51.
- [9] A. J. Wilson, M. Masuda, R. P. Sijbesma, E. W. Meijer, *Angew. Chem., Int. Ed.* 2005, 44, 2275-2279.
- [10] L. Angiolini, R. Bozio, A. Daurù, L. Giorgini, D. Pedron, G. Turco, *Chem. Eur. J.* 2002, 8, 4241.
- [11] A. Painelli, F. Terenziani, L. Angiolini, T. Benelli, L. Giorgini, *Chem. Eur. J.* 2005, 11, 6053.
- [12] M. M. Green, N. C. Peterson, T. Sato, A. Teramoto, R. Cook, S. Lifson, *Science* 1995, 268, 1860.
- [13] V. Percec, M. Obata, J. G. Rudick, B. B. De, M. Glodde, T. K. Bera, S. N. Magonov, V. S. K. Balagurusamy, P. A. Heiney, *J. Polym. Sci.: Part A: Polym. Chem.*, 2002, 40, 3509–3533.
- [14] J. Qu, R. Kawasaki, M. Shiotsuki, F. Sanda, T. Masuda, *Polymer* 2007, 48, 467-476 .
- [15] E. Chielini, R. Solaro, A. Ledwith, *Makromol. Chem.* 1977, 178, 701.
- [16] E. Chielini, R. Solaro, A. Ledwith, *Makromol. Chem.* 1978, 179,1929.

- [17] E. Chielini, G. Galli, R. Solaro, A. Ledwith, *Macromolecules* 1980, 1913, 1654-1660.
- [18] E. Chielini, G. Galli, R. Solaro, A. Ledwith, *Adv. Polym. Sci.* 1984, 62, 143.
- [19] [19a] L. Angiolini, D. Caretti, L. Giorgini, E. Salatelli, *J. Polymer Sci., Part A Polym. Chem.* 1999, 37, 3257. [19b] L. Angiolini, D. Caretti, L. Giorgini, E. Salatelli, *Polymer* 2001, 42, 4005. [19c] L. Angiolini, T. Benelli, L. Giorgini, A. Painelli, F. Terenziani, *Chem. Eur. J.* 2005, 11, 6053-6353. [10d] L. Angiolini, T. Benelli, R. Bozio, A. Daurù, L. Giorgini, D. Pedron, E. Salatelli, *Eur. Polym. J.* 2005, 41, 2045. [10e] L. Angiolini, T. Benelli, R. Bozio, A. Daurù, L. Giorgini, D. Pedron, E. Salatelli, *Macromolecules* 2006, 39, 489.
- [20] T. Uryu, H. Ohkawa, R. Oshima, *J. Pol. Scie: Part B*, 1998, 26, 1227-1236.
- [21] T. Percec, M. Glodde, TK Bera, Y. Miura, I Shiyonovskaya, KD Singer, *Nature*, 2002, 419, 384-387
- [22] CD. Muller, A. Falcou, N. Reckefuss, M. Rojahn, V. Wiederhirn, P. Rudati, *Nature*, 2003, 421, 829-833
- [23] X. Zhang, L. Zi-Chen, L. Kai-Bo, L. Song, D. Fu-Sheng, L. Fu-Mian, *Prog. Polym. Sci.* 2006, 31, 893-948
- [24] [24a] H. Eggerer, C. Grünwälder, *Liebigs Ann. Chem.* 1964, 677, 200. [24b] H. Shih, G. O. Rankin, *Synthesis* 1989, 11, 866.
- [25] M. A. Shoondorp, A. J. Shouten, J. B. E. Hulshof, E. P. Shuddle, B. L. Feringa. *Recueil* 1994, 113, 250.
- [26] [26a] L. Angiolini, D. Caretti, C. Carlini, L. Giorgini, E. Salatelli, *Enantiomer* 1998, 3, 391. [26b] L. Angiolini, D. Caretti, L. Giorgini, E. Salatelli, *Macromol. Chem. Phys.* 2000, 201, 533.
- [27] L. Angiolini, T. Benelli, L. Giorgini, F. Mauriello, E. Salatelli, *Macromol. Chem. Phys.* 2006, 207, 1805–1813.
- [28] J. E. McGraft, L. Rasmussen, A. R. Shultz, H. K. Shobha, M. Sankarapandian, T. Glass, T. E. Long, A. J. Pasquale, *Polymer*, 2006, 47, 4042-4057
- [29] F. S. Du, Z. C. Li, W. Hong, Q. Y. Gao, F. M. Li, *J. Polym. Sci. Part A: Polym. Chem.* 2000, 38, 679-688.

- [30] C. Barrett, B. Choudhury, A. Natansohn, P. Rochon, *Macromolecules* 1998, 31, 4845.
- [31] J. Pielichowski, *J. Therm. Anal.* 1972, 4, 339-41.
- [32] J. R. Platt, *J. Chem. Phys.* 1949, 7, 484.
- [33] R. N. Majumdar, C. Carlini, *Makromol. Chem.* 1980, 181, 201.
- [34] I. Tinoco Jr., *J. Am. Chem. Soc.* 1960, 82, 4785.
- [35] K. Okamoto, A. Itaya, S. Kusabayashi, *Chem. Lett.* 1974, 1167.
- [36] F. Ciardelli, M. Aglietto, C. Carlini, E. Chiellini, R. Solaro, *Pure Appl. Chem.* 1982, 54, 521.
- [37] I. R. Peat, W. F. Reynolds, *Tetrahedron Lett.* 1972, 13, 1359.
- [38] E. F. McCord, W. L. Anton, L. Wilczek, S. D. Ittel, L. T. J. Nelson, K. D. Raffell, *Macromol. Symp.* 1994, 86, 47.
- [39] X. Zhang, Z.-C. Li, K.-B. Li, S. Lin, F.-S. Du, F.-M. Li, *Prog. Polym. Sci.* 2006, 31, 893-948.
- [40] F. Ullmann, *Ber. Dtsch. Chem. Ges.*, 1903, 36, 2382-2384
- [41] D. Yu, A. Gharavi, L. Yu, *J. Am. Chem. Soc.* 1995, 117, 11680-11686
- [42] D. D. Perrin, W. L. F. Amarego, D. R. Perrin, "Purification of Laboratory Chemicals", Pergamon Press, Oxford, 1966.

Chapter 4: Methacrylic polymers bearing side chain azocarbazole chromophore

Introduction

There is a considerable interest in the synthesis and characterization of polymers containing azoaromatic moieties due to their unique optical properties [1]. These materials can be used in advanced micro- and nanotechnologies such as optical data storage [2], nonlinear optical materials [3], holographic memories [4], chiroptical switches [5], surface relief gratings [6], inscription of channel waveguides [7] etc.

Since the discovery of the photorefractive effect in organic polymers [8], carbazole containing polymers [9] have also attracted much attention because of their photoconductivity.

In this context, multicomponent polymers with structural units containing both photoconductive and electrooptic functionalities in the side-chain can be regarded as potentially suitable materials for photorefractive applications [10]. Indeed, poly(meth)acrylates with the 4-nitrophenyl-3-carbazolyl diazene side group prepared by polymerisation of the corresponding functionalised monomers containing both azo and carbazole groups [11] or by azocoupling post-reaction to carbazole containing polymers [12], proved to show photorefractive and NLO properties as well as photoinduced orientation and formation of surface relief gratings.

On the other hand, an intense interest has currently arisen toward investigations dealing with the amplification of chirality of polymeric materials, in solution as well as in the solid state [13]. To this regard, in previous studies we have reported on optically active photochromic methacrylic polymers bearing in the side chain both a chiral group of one single configuration and the *trans*-azoaromatic moiety with a strongly conjugated electron donor-acceptor system [14] that provides the macromolecules with the further possibility to assume a conformational dissymmetry of one prevailing screw sense which can be revealed by the presence, in the circular dichroism (CD) spectra, of dichroic bands related to the electronic transitions of the chromophore [15]. This functional combination allows the polymers to display both the properties typical of

dissymmetric systems (optical activity, absorption of circularly polarized light in the UV-vis spectral region), as well as the features of photochromic and electrooptic materials [16].

To our knowledge, multifunctional polymers bearing three distinct functional groups (i. e. azoaromatic, carbazole and chiral group of one single configuration) directly linked to the side chain have not yet been reported and could be of potential interest for several advanced application fields, such as optical storage, waveguides, chiroptical switches, chemical photoreceptors, NLO, surface relief gratings, photoconductive materials, etc.

Optically active methacrylic polymer containing side-chain azocarbazole chromophore: poly[(S)-MLECA]

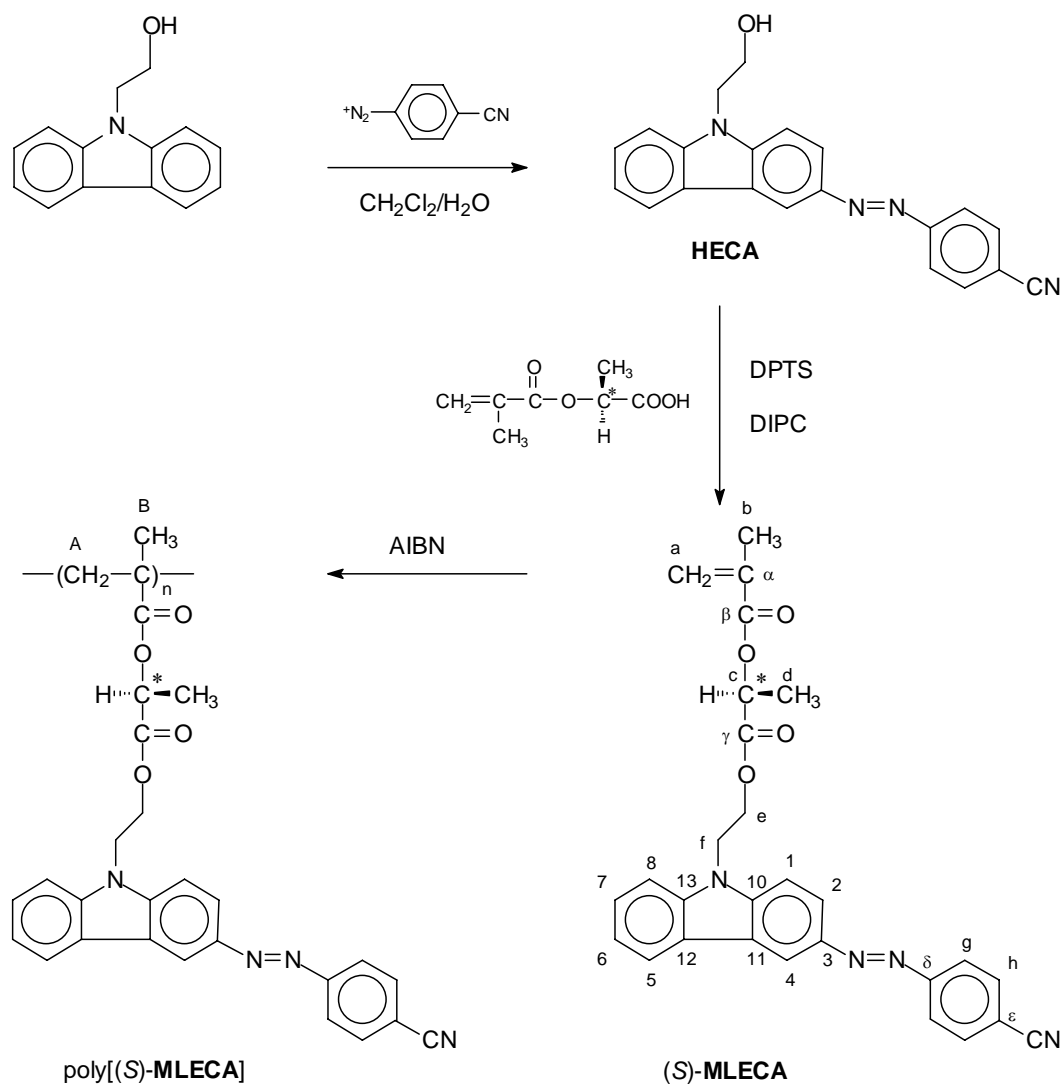
A new optically active photochromic polymethacrylate containing the carbazole moiety, deriving from the chiral monomer (*S*)-(4-cyanophenyl)-[3-[9-[2-(2-methacryloyloxypropanoyloxy) ethyl]carbazolyl]]diazene [(*S*)-**MLECA**] has been prepared and fully characterized with the aim to obtain a multifunctional derivative possessing at the same time chemical moieties suitable to NLO and optical storage, to chiroptical switches, and to photorefractive and photoconductive applications. Spectroscopic, thermal and chiroptical characterizations clearly indicate the occurrence of dipolar interactions between chromophores and the presence of an ordered chiral conformation of one prevailing helical handedness, at least for chain segments of the macromolecules.

Synthesis and structural characterization

(*S*)-**MLECA** was prepared starting from commercial 9-(2-hydroxyethyl)carbazole which was submitted to coupling with 4-cyanobenzenediazonium chloride in biphasic medium (H₂O-CH₂Cl₂) in the presence of sodium dodecyl benzenesulfonate to give (4-cyanophenyl)-[3-[9-(2-hydroxyethyl)carbazolyl]]diazene [**HECA**], by following the same procedure as described for the analogous 4-nitro derivative [11a]. Direct esterification of **HECA** with (*S*)-(-)-methacryloyl-L-lactic acid [17] in the presence of *N,N*-diisopropyl-carbodiimide (**DIPC**) and 4-(diphenylamino)pyridinium 4-toluensulfonate (**DPTS**) as coupling agent and condensation activator, respectively, according to the procedure previously reported for the preparation of high molecular weight polyesters [18], gave finally (*S*)-**MLECA** in the overall yield of 19%.

The monomer was then submitted to radical homopolymerization in THF solution by adopting the usual method employing AIBN (2% w/w of monomer) as thermal initiator (Scheme 1).

Relevant characterization data of poly[(*S*)-**MLECA**] are reported in Table 1.



Scheme 1

The polymeric product, purified by repeated dissolution and reprecipitation in methanol, displayed the expected IR spectrum showing the disappearance of the absorption band at 1636 cm^{-1} , related to the methacrylic double bond, and the contemporary appearance of the band at 1734 cm^{-1} , related to the carbonyl stretching vibration of the α,β saturated methacrylic ester group, shifted to higher frequency by 23 cm^{-1} with respect to the monomeric precursor. Accordingly, in the $^1\text{H-NMR}$ spectrum of the polymeric derivative, shown in Figure 1, the resonances of the vinylidene protons of the monomer were absent. It is also to be noted that the resonances of aromatic protons are shifted up

field to variable extent with respect to the monomer, thus indicating the presence of shielding interactions between the side-chain chromophores in solution.

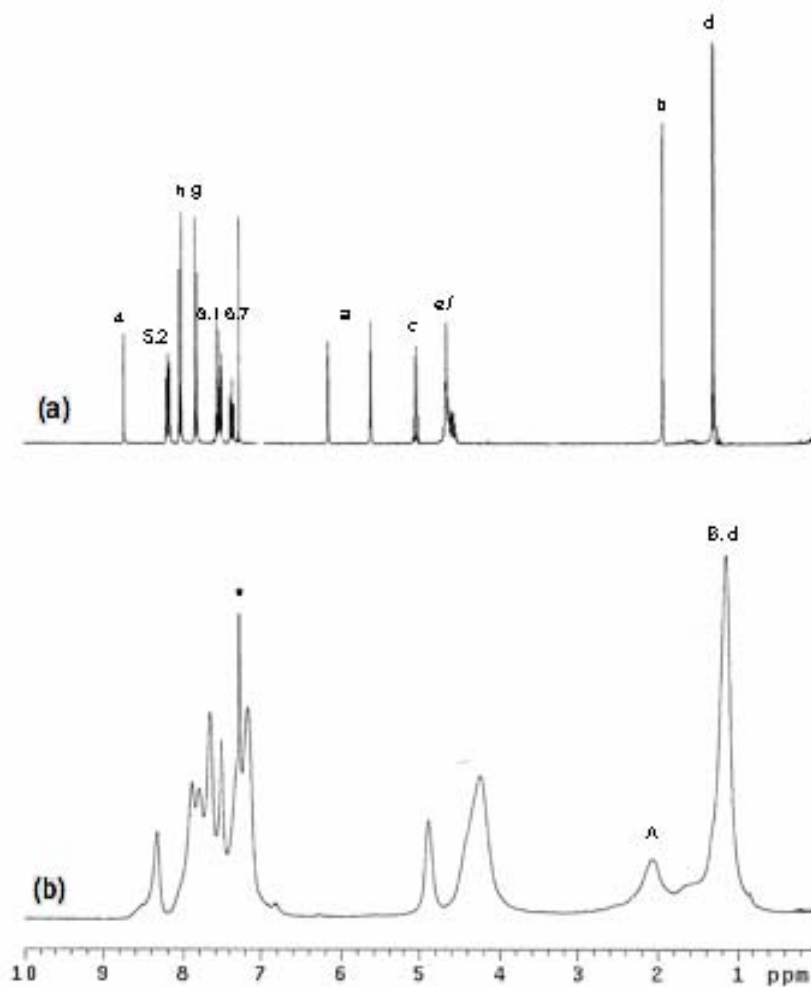


Figure 1. $^1\text{H-NMR}$ spectra of (*S*)-MLECA (a) and poly[(*S*)-MLECA] (b) in CDCl_3 at 25°C . Starred signals refer to solvent resonance. Signals labelled as in Scheme 1.

Poly[(*S*)-MLECA] was obtained in high yield (77% calculated as g of polymer/g of monomer), with a number average molecular weight \bar{M}_n of 13400 gr/mol and polydispersity \bar{M}_w/\bar{M}_n of 1.8. The purified polymeric product was completely soluble in CHCl_3 and THF as well as in strongly polar solvents such as nitrobenzene, 1-methyl-2-pyrrolidinone, dimethylformamide, dimethylacetamide and dimethylsulfoxide, this behaviour favouring the possibility of its application as thin film.

Table 1. Characterization data of Poly[(S)-MLECA]

Sample	Yield ^{a)} %	\bar{M}_n ^{b)} g mol ⁻¹	\bar{M}_w/\bar{M}_n ^{b)}	T_g ^{c)} °C	T_d ^{d)} °C
Poly[(S)-MLECA]	77	6.650	1.8	147	363

a) Calculated as (g polymer/g monomer)·100;

b) Determined by SEC in THF solution at 25°C;

c) Glass transition temperature determined by DSC at 10°C/min heating rate under nitrogen flow;

d) Initial decomposition temperature as determined by TGA at 20°C/min heating rate under air flow.

The microtacticity of poly[(S)-MLECA], evaluated by integration of the ¹³C-NMR signals of the methacrylic methyl group at about 20.22 and 18.50 ppm, assigned to heterotactic *meso-racemo* (*mr*) and syndiotactic *racemo-racemo* (*rr*) triads respectively [19], indicates a content of syndiotactic triads around 52% (with 8 and 40% of isotactic and heterotactic triads, respectively), with a probability of formation of *meso* (P_m) and *racemo* (P_r) dyads of 0.28 and 0.72 respectively, in agreement with literature reports concerning the radical polymerization of methyl methacrylate [20] and of analogous chiral photochromic methacrylic derivatives [14,16]. It is also confirmed that the addition of monomer to the growing chain is unaffected by the nature of the last repeating unit, and follows a Bernoullian statistics, as indicated by the close similarity of $P_{m/r}$ (0.28) with $P_{m/m}$ (0.29) and by the sum of $P_{m/r}$ (0.28) with $P_{r/m}$ (0.72) that gives 1.00, where $P_{m/m}$, $P_{r/m}$ and $P_{m/r}$ are the calculated probabilities that a given dyad follows a dyad having the same or the opposite relative configuration. Thus, the main chain microstructure is essentially atactic, with a predominance of syndiotactic triads ($rr = 52\%$) suggesting a substantially low stereoregularity of the main-chain. As expected, the free radical polymerization of (S)-MLECA is therefore poorly stereoselective and hence is unable to favour a strongly predominant tacticity of the macromolecules.

Thermal Analysis

The thermal stability of poly[(S)-MLECA], as determined by thermogravimetric analysis (TGA), resulted very high, with the onset decomposition temperature (T_d) close

to 363°C, much higher than that reported for poly(**DR1M**) (295°C) [16a], deeply investigated as polymeric material for optoelectronic applications [1a,1b]. This datum is in accordance with the behaviour of other carbazole containing polymers [10a,21] and is indicative of a remarkable presence of strong dipolar interactions in the solid state between the chromophores located in the macromolecular side chains and characterized by high charge delocalization, due to the simultaneous presence of the electron-rich carbazole moiety and the donor-acceptor conjugated azoaromatic system.

Indeed, the polymer glass transition temperature (T_g) is found by DSC at 147°C, that should favour a good orientational temporal stability of the photoactive chromophores of great interest for applications in optoelectronics (more stable photoinduced birefringence, NLO properties, diffraction gratings, holographic storage, etc.). The DSC thermogram did not reveal any liquid crystalline behaviour nor melting peaks, thus suggesting that the macromolecules are substantially amorphous in the solid state. Due to the presence of a much more extended (inter- and/or intra-chain) dipolar interactions between the aromatic systems and the relatively higher average molecular weight, the value of T_g is considerably higher than those (laying in the range 88-99°C) reported by Natansohn [11b] for analogous polymers ($\bar{M}_w = 4450$ and 4200 g/mol, respectively) with aliphatic spacers, similar in length but achiral, between the azocarbazole chromophore and the methacrylic main chain.

Absorption spectra in solution and in thin film

The UV-vis spectra in chloroform solution of (*S*)-**MLECA** and poly[(*S*)-**MLECA**] (Table 2 and Figure 2), exhibit in the region 250-700 nm four evident absorption bands with maxima centered around 410, 331, 318 (shoulder) and 293 nm (Table 2). The first one is attributed to combined electronic transitions such as $n-\pi^*$, $\pi-\pi^*$ and internal charge transfer of the azoaromatic chromophore [22], the others to the sum of several contributions due to the $\pi-\pi^*$ electronic transition of the single 4'-cyano substituted aromatic ring [23] and the $\pi-\pi^*$ electronic transitions of carbazole chromophore [24].

No particular difference between the respective absorption wavelengths is displayed by monomer and polymer. A significant hypochromic effect is however observed when the

spectrum of the monomer, where the lack of structural restraints originates a random distribution of the chromophores in dilute solution, is compared with that of the polymer (Table 1). Such a behaviour, frequently noticed in polymeric derivatives bearing side-chain aromatic chromophores [14, 25], is attributed to the presence of electrostatic dipole-dipole interactions between neighbouring chromophores [26]. In the present case the hypochromic effect is evident in all the electronic bands and suggests the occurrence of strong electronic interactions between side-chain chromophores.

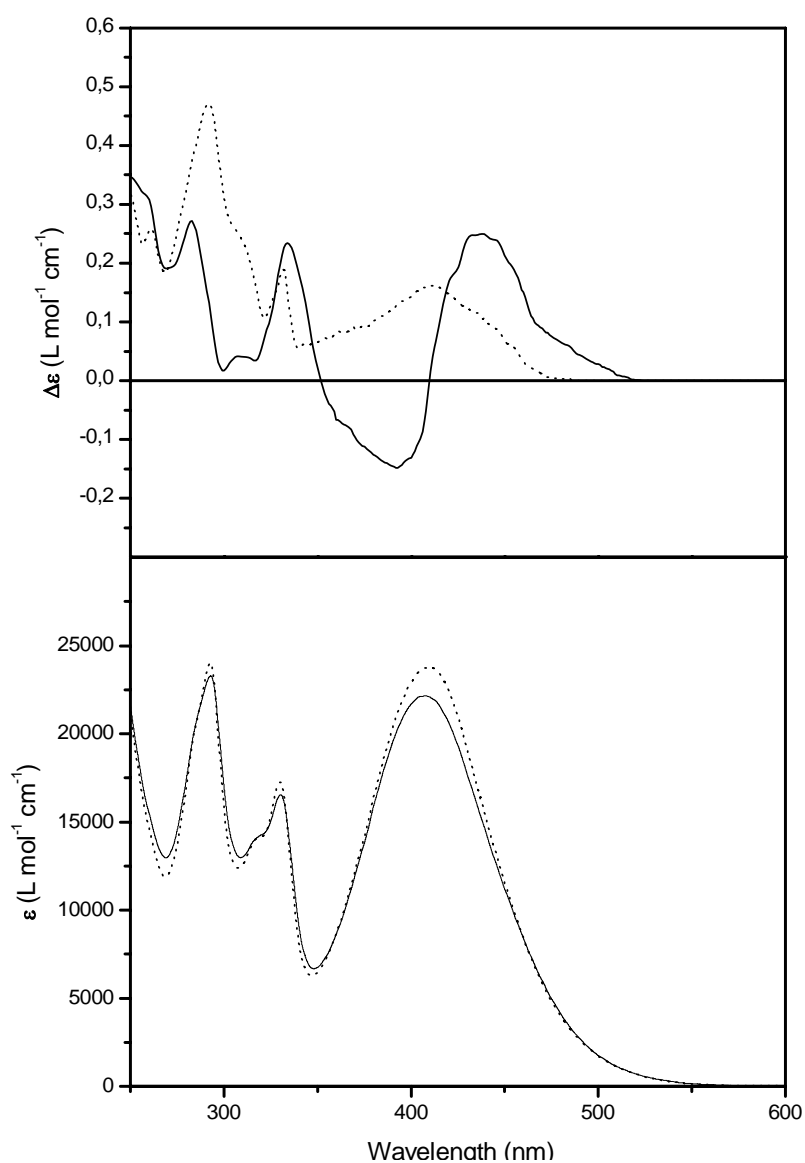


Figure 2. CD (up) and UV-vis (down) spectra of chloroform solution of (*S*)-MLECA (---) and poly[(*S*)-MLECA] (—).

Table 2. UV spectral data in CHCl₃ solution of (*S*)-MLECA and poly[(*S*)-MLECA]^{a)}.

Sample	1 st absorption band		2 nd absorption band		3 rd absorption band		4 th absorption band	
	$\lambda_{\max}^{\text{b)}$	$\epsilon_{\max} \cdot 10^{-3}^{\text{c)}$						
	nm	Lmol ⁻¹ cm ⁻¹						
(<i>S</i>)-MLECA	410	23.8	330	17.3	316sh	14.0	293	24.0
poly[(<i>S</i>)-MLECA]	408	22.2	331	16.5	318sh	14.1	293	23.3

a) At $5 \cdot 10^{-4}$ M chromophore concentration.

b) Wavelength of maximum absorbance.

c) Calculated for one single chromophore.

The electronic spectra of a thin film of poly[(*S*)-MLECA] onto silica fused substrate is shown in Figure 3. The amorphous polymer in the solid state exhibits, in addition to the four absorptions centred around 406, 331, 320 (shoulder) and 294 nm (Figure 3) assigned to the same electronic transitions observed in solution, two strong absorption bands in the region 180-250 nm with maxima centered around 235 and 187 nm (Figure 3). The former is attributed to the π - π^* electronic transitions of carbazole chromophore [24], the latter one to the sum of several contributions due to the carbonyl groups of the L-lactic moieties and the methacrylic residue.

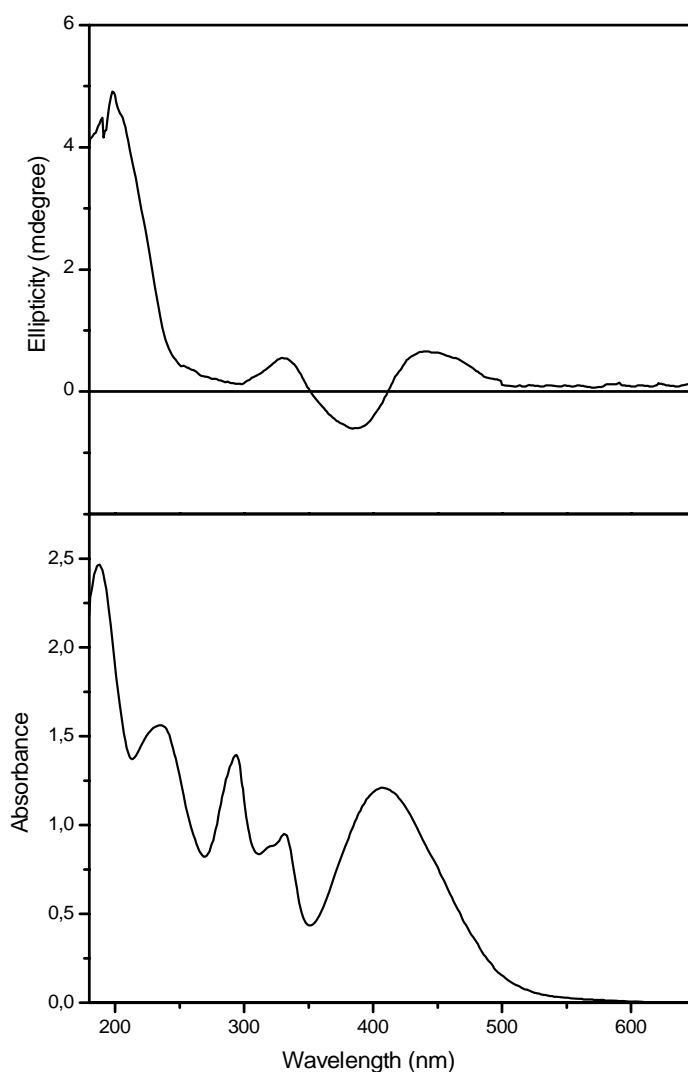


Figure 3. CD (up) and UV-vis (down) spectra of a 210 nm thick film of poly[(*S*)-MLECA] on fused silica as prepared.

In agreement with several reports [27] the observed slight blue-shift of about 4-5 nm of the absorption band of the azoaromatic chromophore displayed by the thin film as compared with the dilute solution, can be attributed to an increase of the intramolecular parallel arrangement of the neighbouring adjacent electric dipoles (H-type aggregation), imposed by the structural constraints of the macromolecules [14,16] and favoured by the predominant presence of racemic dyads located in the main chain (72%), when the solvent is removed and the polymer chains collapse to form the film. This suggests that the absorption features should be mainly originated by intra-chain interactions among chromophores both in solution and in the solid state.

Chiroptical properties in solution and in thin film

The chiroptical properties of poly[(*S*)-MLECA] and (*S*)-MLECA have been investigated by CD in the spectral region 250-700 nm in order to assess the conformational features of the macromolecular chains. The CD spectrum of (*S*)-MLECA in chloroform solution (Figure 2) displays three positive dichroic absorptions with maxima at 410, 331 and 292 nm (Table 3) and a broad band at about 316 nm, strictly related to the UV-vis absorption maxima. By contrast, the CD spectrum of poly[(*S*)-MLECA] (Figure 2 and Table 3) exhibits three relevant positive dichroic bands ($\lambda_{\text{max}} = 333, 315$ and 283 nm) in the spectral region related to the π - π^* electronic transition of the carbazole chromophore [24] and two dichroic signals of opposite sign and comparable intensity, with a crossover point at 409 nm, corresponding to the first absorption maximum in the visible region, related to the electronic transitions of the azoaromatic chromophore (Table 2).

This last occurrence appears typical of exciton splitting determined by cooperative dipole-dipole intra-chain interactions between neighbouring side chain azobenzene chromophores [15] arranged in a mutual chiral geometry of one prevailing handedness [14,16] and suggests that the presence of the optically active L-lactic acid residue of one prevailing absolute configuration, interposed between the main chain of the polymer and the azocarbazole chromophore, favours the adoption of a chiral conformation of one prevailing helical handedness, at least for chain segments of the macromolecules in

solution. Accordingly, similar dipolar interactions are much lower or absent in the spectrum of monomer because of the high dilution.

The CD spectrum of the amorphous thin film (210 nm thick) of poly[(*S*)-MLECA] (Figure 3), expressed in mdegree, is quite similar to that shown by the same polymer in solution (Figure 2), as recently observed in analogue optically active polymeric derivatives bearing the (*S*)-3-hydroxy pyrrolidine residue of one prevailing configuration in the side chain [16]. In addition to the CD bands exhibited in solution, the spectrum displays the presence of a further strong signal located between 210 and 180 nm, related to the electronic transitions centered in the UV-vis spectrum at about 187 nm. Such a behaviour demonstrates the intrinsic chirality of this material that undergoes induced asymmetric perturbation on all its electronic transitions. In particular, the thin film of the polymer exhibits the same CD couplet as in solution, with a crossover point at about 410 nm, associated with dipole-dipole intramolecular interactions of the azoaromatic moieties disposed in a mutual chiral geometry along the backbone.

This finding is in agreement with recent studies on the model dimeric derivative 2,4-dimethyl-glutaric acid bis(*S*)-3-[1-(4'-nitro-4-azobenzene)pyrrolidine ester [16], mimicking the smallest section of polymer where interchromophore interactions can occur. Its CD spectra measured in several solvents show, in the spectral region related to the azoaromatic transitions at longer wavelength, an exciton couplet (of intensity about a third of the signal measured for the corresponding polymer) which suggests that the chiral interactions between a single couple of chromophores in solution are already important and that the optical activity of these materials should be substantially related to relatively short chain sections with a conformational dissymmetry of one prevailing screw sense.

Thus, the close similarity between the CD spectra of the polymer in solution and as thin film suggests that the macromolecules maintain chiral conformations of one prevailing helical handedness also in the solid amorphous state, at least for short chain segments. This may open new possibilities for the use of azocarbazole containing polymers as chiroptical switches, [16] in addition to the usual applications in optics.

Table 3. CD spectral data in CHCl₃ solution of (*S*)-MLECA and poly[(*S*)-MLECA]^{a)}.

Sample	1 st absorption band					2 nd absorption band		3 rd absorption band		4 th absorption band	
	$\lambda_1^{b)}$	$\Delta\varepsilon_1^{c)}$	$\lambda_0^{d)}$	$\lambda_2^{b)}$	$\Delta\varepsilon_2^{c)}$	$\lambda_3^{b)}$	$\Delta\varepsilon_3^{c)}$	$\lambda_4^{b)}$	$\Delta\varepsilon_4^{c)}$	$\lambda_5^{b)}$	$\Delta\varepsilon_5^{c)}$
	nm	Lmol ⁻¹ cm ⁻¹	nm	nm	Lmol ⁻¹ cm ⁻¹	nm	Lmol ⁻¹ cm ⁻¹	nm	Lmol ⁻¹ cm ⁻¹	nm	Lmol ⁻¹ cm ⁻¹
(<i>S</i>)-MLECA	410	+0.16				331	+0.19	nd ^{e)}	nd ^{e)}	292	+0.47
poly[(<i>S</i>)-MLECA]	437	+0.25	409	392	-0.16	333	+0.23	309	+0.04	283	+0.27

a) At 5·10⁻⁴ M chromophore concentration.

b) Wavelength of maximum dichroic absorption.

c) Calculated for one repeating unit in the polymer.

d) Wavelength of the cross-over of dichroic bands.

Optically Induced and Erased Birefringence

In order to assess the photoinduced linear dichroism and birefringence, films of the polymer have been irradiated with linearly polarized (LP) radiation (writing step) at 488 nm ($I \approx 100 \text{ mW cm}^{-2}$). After irradiation, the polymer shows high photoinduced linear birefringence evidenced by using probe radiation at 632.8 nm ($I \approx 1 \text{ mW cm}^{-2}$).

The mechanism of inducing birefringence is based on the selective photochemical excitation of *trans*-azocarbazole groups having a component of their dipole in the same direction of the laser polarization. Every *trans*-azocarbazole group goes through many *trans-cis-trans* photoisomerization cycles, accompanied by changes in orientation. In this mode, the orientation perpendicular to the laser polarization (which is not photochemically activated) will increase its population, creating dichroism and thus birefringence in the material.

Circularly polarized (CP) light activates all azocarbazole groups, thus restoring the initial random orientation. This mechanism is well known in the literature [1,2].

Figure 4 shows the optically induced birefringence curve of poly[(*S*)-MLECA].

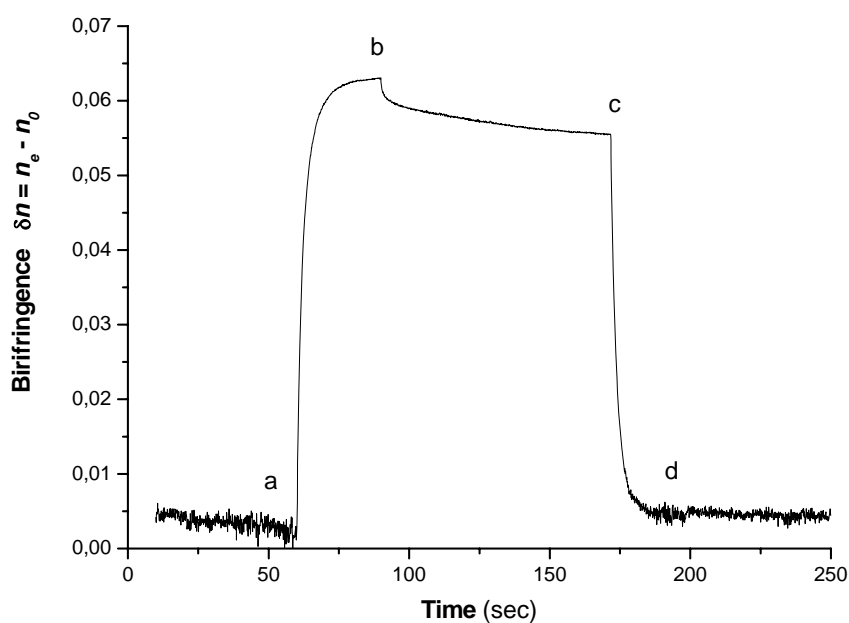


Figure 4. Optically induced birefringence curve registered on a thin film (360 nm) of poly[(*S*)-MLECA].

At point A LP laser beam is engaged and the photoinduced birefringence is rapidly built up to the saturation level. At point B, the writing laser beam is removed and the birefringence begins to drop to a relaxed level where the rate of change of anisotropy is very small. At point C, a CP laser beam is turned on to randomize the orientation of the azo groups; hence, the anisotropy induced by the linearly polarized writing beam is destroyed (D).

The saturation value of the optically induced birefringence is 0.06, which is slightly lower than analogue optically active azopolymer [16a, 16b, 16c]. Although the bulky azocarbazole moiety could in principle increase the conformational rigidity of the macromolecules and magnify the dichroic effect, a lower optically induced birefringence is observed. This observation is reasonable because the polymer has a maximum absorbance at 410 nm while the writing beam is at 488 nm. In order to obtain higher values of photoinduced birefringence it should be sufficient to use a laser beam with a maximum of absorbance closer to 410 nm.

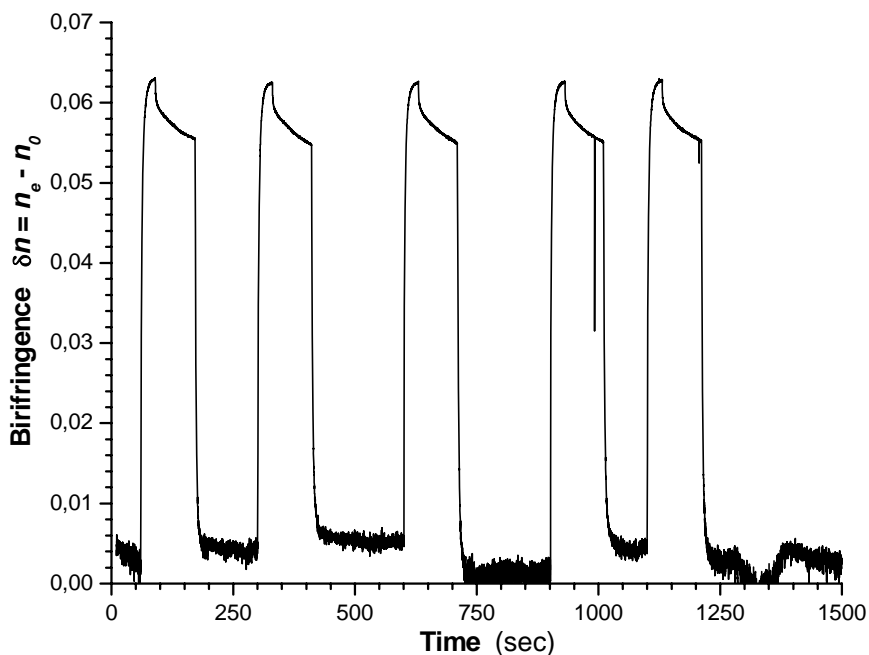


Figure 5. Complete writing-erasing cycles of optically photoinduced birefringence on a thick film (360 nm) of poly[(S)-MLECA].

The lower optically induced birefringence of poly[(*S*)-**MLECA**], with respect to poly[(*S*)-**MAP-C**] [16c], may be also due to the smaller permanent dipole moment of the azocarbazole group.

The complete reversibility of the photoinduced linear birefringence of investigated polymeric samples, which are related to fatigue resistance properties, after several writing-erasing cycles by photoirradiation alternatively with LP and CP light at 488 nm (Figure 5), seems to be promising for use in optical storage or more generally in the field of photoresponsive systems. Indeed, after several irradiations steps with LP and CP laser beams alternatively acting on the 360 nm thick film of poly[(*S*)-**MLECA**], the values of maximum photoinduced birefringence (after each irradiation with LP light) and of erased birefringence (after each irradiation with CP light) are quite similar. This indicates that no degradation photoreaction took place upon irradiation with laser light of relatively high intensity (100 mW/cm²). Thus, several cycles could be performed without any significant change in the photoinduced behaviours.

Photomodulation of chiroptical properties in solid state

Figure 6 shows the CD spectra of a thin solid film of poly[(*S*)-**MLECA**] as grown (full line), after an irradiation cycle with CP-L light (dashed line), and after a subsequent pumping step with CP-R light (dotted line). The pump irradiance was set to 160 mWcm⁻², and during the irradiation cycles we monitored the linear birefringence (negligible in this case).

After irradiation with CP-L light at 488 nm, the CD spectrum of a thin film of poly[(*S*)-**MLECA**] displays two intense dichroic signals of opposite sign, with a crossover point at 470 nm.

The couplet is asymmetric and the crossover point (about 480nm) don't coincide with the maxima of the visible absorption band (410 nm).

The CD spectrum registered after CP-R light, show a net inversion of sign of the dichroic bands. The two spectra actually appear as mirror images of each other. The observed effect is reversible, and the original shape of the CD spectrum can be substantially restored by pumping with CP-L radiation.

Similar results were previously reported for optically active photochromic methacrylic polymers bearing in the side chain a chiral group of one single configuration and an azoaromatic moieties, Poly[(*S*)-MAP-N] and Poly[(*S*)-MAP-C] [16c].

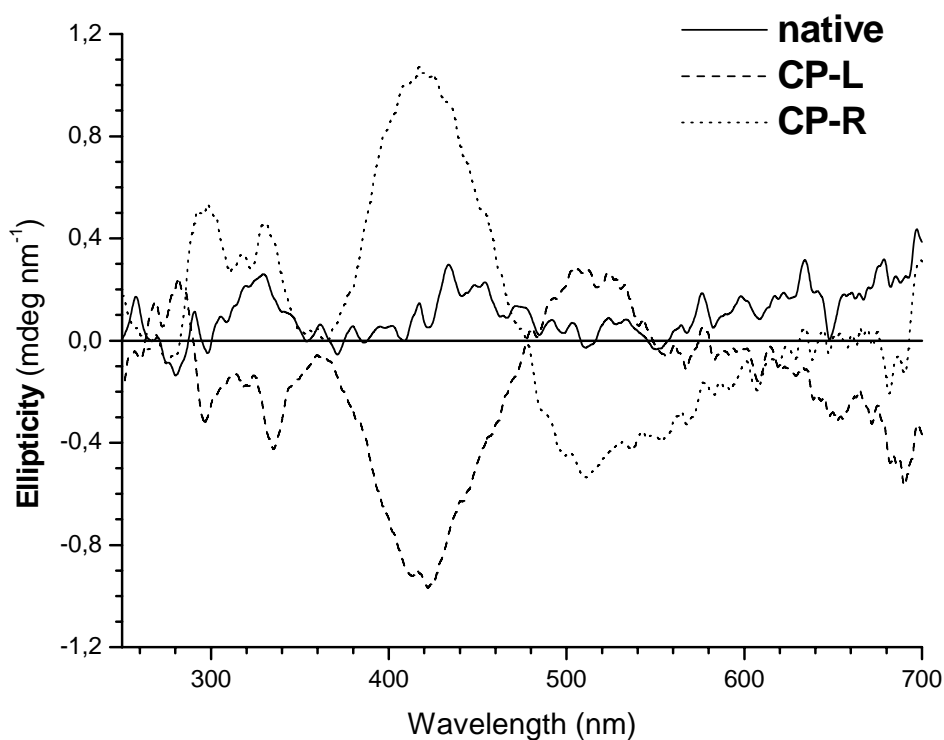


Figure 6. CD spectra of a thin film (150 nm) of poly[(*S*)-MLECA] on silica substrate: native film (full line) and after sequential irradiation with CP-L light (dashed line) and CP-R light (dotted line) at 488 nm ($I=160 \text{ mWcm}^{-2}$).

It is reasonable to assume that the azocarbazole chromophores are organised in a helical geometry of one prevailing handedness in the solid state as well, at least within chain segments. This implies that the polymer chains have a predominant helical structure with a well-defined sense, either left- or right handed.

The effect of CP-L and CP-R radiations on the CD signal can be simply interpreted by assuming its ability to invert the prevailing handedness of the polymer structure, or at least to create a statistical net excess of polymer chain sections with inverted helical sense. The observed phenomena appear to be related to the induction of chirality by CP

light in achiral azobenzene-containing materials reported by Nikolova and co-workers[4a] and Natansohn and co-workers[5], even though the measured ellipticity of our samples, normalised to film thickness, is one order of magnitude lower. In our case, there is an intrinsic chirality of the sample related to the optical activity of the L-Lactic bridge interposed between the azocarbazole-chromophores and the polymer backbone, and it is quite reasonable that in the native films the polymer chains should have a predominant helical conformation. The mechanism of the reversible helical inversion induced by CP radiation is not well understood. In any case, for the investigated polymer, it is not related to a preliminary ordering of the azocarbazole molecules with LP light, as demonstrated in our experiments.

It is known that CP light tends to align the azobenzene side groups along directions close to normal to the film.[1] It is possible that transfer of angular momentum from the CP radiation to the medium, as occurs when a CP photon is absorbed, induces a precession of the chromophores with a sense of rotation congruent with the sense of the CP light. This would mean that CP-L light induces a left-handed organization of the azobenzene molecules, whereas CP-R light induces a right-handed one. It is reasonable to think of the conformational structure of the polymer chains in the native films as being composed of helical sections of opposite handedness where, due to the chiral interaction of the enantiomeric L-lactic moieties, segments of one helicity are thermodynamically favoured with respect to the other, thus conferring a prevailing absolute chirality to the polymer. All the aforementioned CD effects persist for at least one month and are well reproducible.

Photoconductive properties

Measurement of electronic transport properties is an important first step in the characterization of a potential photorefractive polymer [9].

It is not necessary to add dopants in order to observe photoconduction in poly[(S)-MLECA] (Figure 7). This is not surprising, given the presence of the carbazole moieties, which are well known for their hole conducting properties.

The cell was biased with a dc voltage, applying an electric field of up to 60 V/ μm , and was illuminated through the ITO electrode. The photoconductivity was determined by

measuring the photocurrent through the film. A linear dependence of log of normalized photocurrent on the applied field was established. In fact, photoconduction measured at different wavelengths follows the trend of the absorption coefficient, increasing with increasing the absorption value.

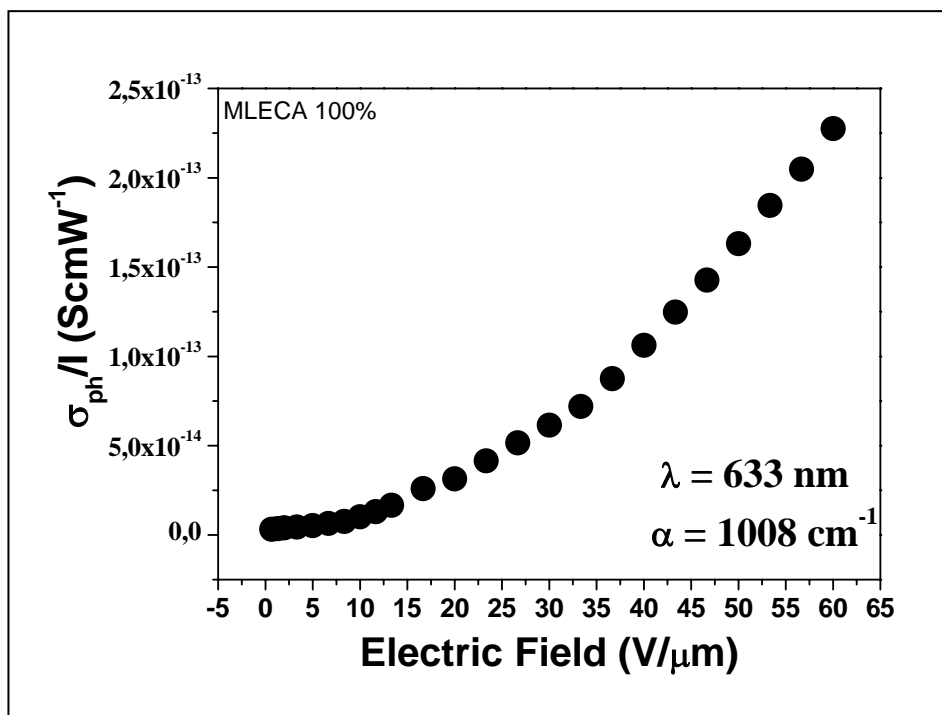


Figure 7. Photoconductivity versus the electric field at 633 nm for poly[(S)-MLECA]

Photorefractive effect

In order to unambiguously distinguish between the photorefractive effect and other types of gratings which may occur in poly[(S)-MLECA], two-beam coupling (2BC) measurement was performed.

As usual with organic materials, a electric field was applied on samples in turn to increase photogeneration efficiency and provide a drift mechanism. In order to have a component of the applied field along the grating wavevector, the sample normal was tilted by 60° with respect to the beam bisector, i.e., $\theta_{\text{ext}} = 60^\circ$.

The PR properties were investigated by monitoring the intensities of two p-polarized coherent He-Ne laser beams superimposed on the sample.

A Typical two beam coupling experiment is shown in Figure 8.

The asymmetric energy transfer is clearly seen by the increase intensity of I_1 and decrease of I_2 , revealing the non-local nature of the grating.

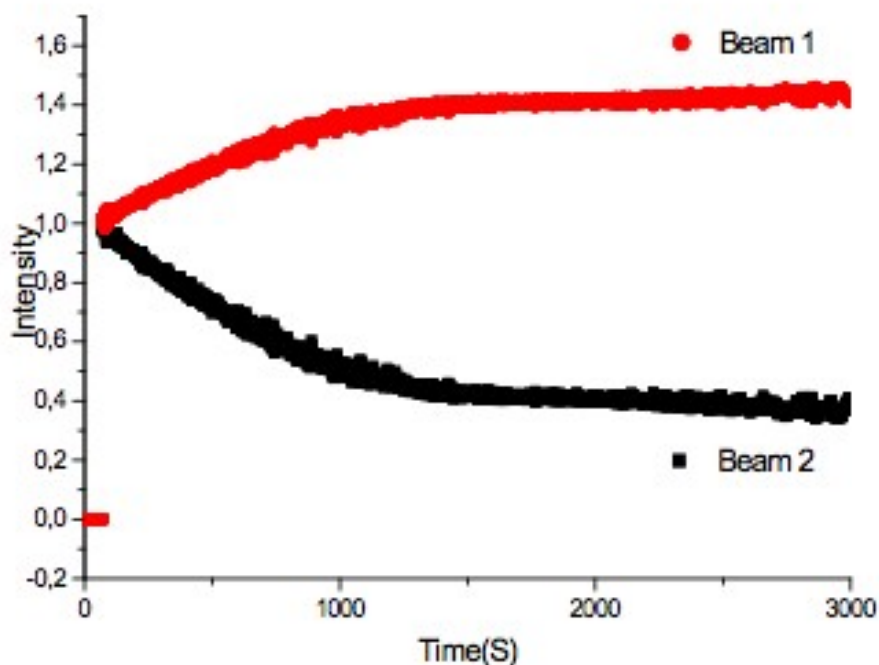


Figure 8. Typical experimental data for two beam coupling experiment. The electric field and the pump beam I_1 are initially on and at $t \gg 1s$ the probe beam I_2 is turned on. The transmitted intensities of both beams are recorded.

In the experiment, the intensity of beam 1 is monitored as beam 2 is switched on at $t = 0$ and switched off at $t = 3000$ s (red circles). In the second experiment, the intensity of beam 2 is monitored as beam 1 is switched on at $t = 0$ and switched off at $t = 3000$ s (black squares). As the grating is written, the intensity of beam 1 increases and the intensity of beam 2 decreases by an approximately equal amount, indicating an index-of-refraction grating which is spatially phase-shifted relative to the light intensity grating. The asymmetric energy transfer is proof of the photorefractive origin of the grating.

Optically Induced Diffraction Grating

Surface relief gratings (SRG) have been inscribed on thick films of poly[(S)-MLECA] using left and right circularly polarized interfering beams at 488 nm (100 mW/cm^2).

The surface gratings produced are permanent as long as the temperature of the sample is kept below its T_g . The surface profiles of the film after the creation of the grating was studied by atomic force microscopy. Some typically results are presented in Figure 9.

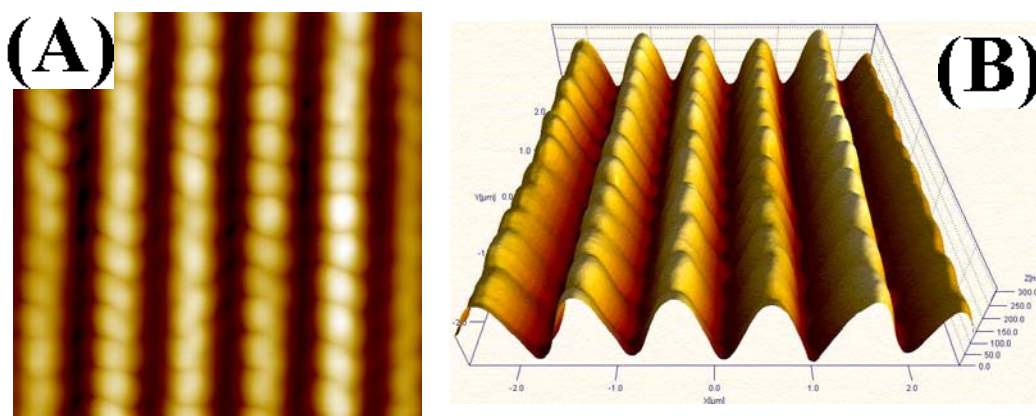


Figure 9 : Bidimensional (A) and tridimensional (B) AFM images $5 \times 5 \mu\text{m}$ of a 400 nm film of poly[(S)-MLECA] after inscription of surface relief grating.

In this case, the SGR profile exhibits a sinusoidal shape, with a grating depth of about 210 nm and grating spacing of about 490 nm.

Apart from the obvious uses of the photoinduced birefringence and surface gratings inscription in optical storage devices, especially holographic storage, applications such as erasable waveguides and optical couplers into films (using the excellent diffraction efficiency) of the SRG can also be envisaged.

Methacrylic polymers bearing side-chain 9-phenylazocarbazole moieties.

The synthesis of a novel optically active monomer containing in side chain a 9-phenylazocarbazole moiety (*S*)-methacryloyl-3-oxy-N-{4-[(4-cyanophenyl)-(3-carbazoil)-diazene]-phenyl}pyrrolidine (*S*)-**MCAPP-C** and its analogous achiral monomer methacryloyl-2-oxyethyl-N-ethyl-N-{4-[(4-cyanophenyl)(3-carbazoil)diazene]}-phenylamine **MCAPE-C**, is described.

Each monomer has been radically homopolymerized and copolymerized to afford the desired polymeric derivatives, which have been fully characterized and their spectroscopic and thermal properties compared.

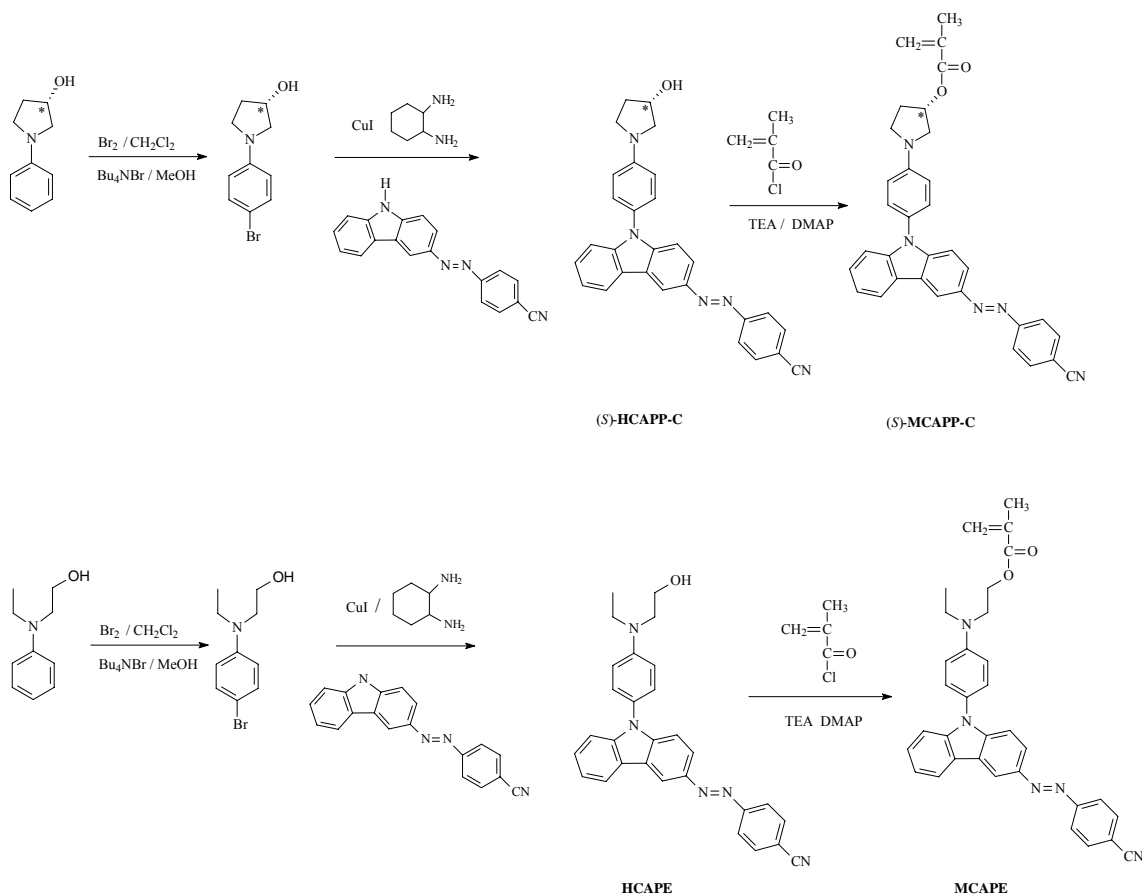
The photoinduction of birefringence has been assessed on films of the investigated macromolecules in order to evaluate their behavior as materials for optical data storage. The results are interpreted in terms of different cooperative behavior and conformational stiffness of (*S*)-**MCAPP-C** and **MCAPE-C** azocarbazole chromophoric co-units

Synthesis and structural characterization

The synthesis of (*S*)-**MCAPP-C** and **MCAPE-C** were carried out according to Scheme 2, starting from (*S*)-(+)-3-hydroxy-N-bromo-pyrrolidine and N-bromo-N-ethyl-N-(2-hydroxyethyl)amine (derived from bromuration of (*S*)-(+)-3-hydroxy-pyrrolidine and N-ethyl-N-(2-hydroxyethyl)amine [28]), which were coupled, under Ullmann's condition [29], with 4-cyanophenylcarbazolyldiazene to afford the desired alcohols (*S*)-**HCAPP-C** and **HCAPE-C**, respectively.

The (*S*)-**MCAPP-C** and **MCAPE-C** were obtained with good yields by esterification of the related alcohols with methacryloyl chloride.

The structures of the novel intermediates and the final products were confirmed by ¹H-NMR and FT-IR.



Scheme 2.

Homo- and copolymerization reactions were carried out in glass vials using AIBN (2 %wt. with respect to the monomers) as thermal initiator and dry DMF as solvent (1 g of monomers in 20 ml of DMF). Feeds of molar composition as reported in Table 4 The monomers were introduced into the vial under nitrogen atmosphere, submitted to several freeze-thaw cycles, and allowed to polymerize at 60°C for 72 h. The polymerization was stopped by pouring the reaction mixture into a large excess of methanol and collected by filtration. The solid polymeric product was repeatedly redissolved in DMF, precipitated again with methanol and submitted to a further purification from monomeric and oligomeric impurities by Soxhlet continuous extraction with methanol. The material was finally dried at 60°C for 4 days under high vacuum.

The radical homo- and copolymerization reaction of (S)-MCAPP-C with MCAPE-C afforded polymeric products with comparable yields and polydispersities (Table 4). All *Optically active, photoresponsive multifunctional polymeric materials*

products were structurally characterized by FT-IR, ^1H and ^{13}C NMR and size exclusion chromatography. Glass transition temperature (T_g) was also determined.

The occurred polymerizations were confirmed by IR spectroscopy, by observing the disappearance in the spectra of the absorption bands of (*S*)-**MCAPP-C** and **MCAPE-C** at 1623-1637 cm^{-1} , related to the methacrylic double bonds, and the contemporary appearance of bands at 1715-1734 cm^{-1} , related to the carbonyl stretching vibration of the α saturated methacrylic ester group, shifted to higher frequency by ca. 10 cm^{-1} with respect to the monomeric precursor.

Accordingly, as shown in Figure 10 for the couple (*S*)-**MCAPP-C**/poly[(*S*)-**MCAPP-C**], in the ^1H NMR spectra of polymeric derivatives, the resonances of the vinylidenic protons of the monomer were absent. The molar composition of copolymers was also determined.

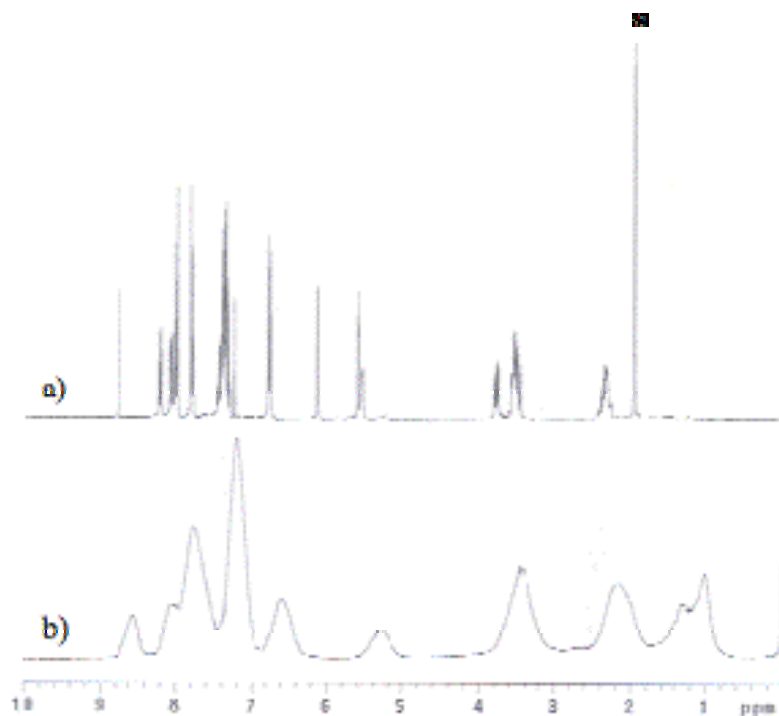


Figure 10. ^1H -NMR spectra of (*S*)-**MCAPP-C** (a) and poly[(*S*)-**MCAPP-C**] (b) in DMF at 25°C. Starred signals refer to solvent resonance.

The narrow value of polydispersity displayed by all samples can be attributed to the exhaustive purification method adopted for the polymeric derivatives.

Table 4. Characterization data of polymeric derivatives.

Sample	Yield ^{a)} %	\bar{M}_n ^{b)} g mol ⁻¹	\bar{M}_w/\bar{M}_n ^{b)}	T_g ^{c)} °C
Poly[(<i>S</i>)- MCAPP-C]	60	6500	1.5	195
Poly[MCAPE-C]	65	10700	1.5	163
Poly[(<i>S</i>)- MCAPP-C -co- MCAPE-C] (48/52)	46	6700	1.6	185

a) Calculated as (g polymer/g monomer)·100;

b) Determined by SEC in THF solution at 25°C;

c) Glass transition temperature determined by DSC at 10°C/min heating rate under nitrogen flow;

The number-average molecular weight progressively increase (Table 4) on passing from poly[(*S*)-**MCAPP-C**] to poly[**MCAPE-C**]. This finding may be attributed, at least partially, to reduced solubility in DMF of the macromolecular derivatives containing higher relative amounts of (*S*)-**MCAPP-C** co-units, which tend to precipitate from the solution during the polymerization process.

Thermal Analysis

Only second-order transitions originated by glass transitions, with no melting peaks, are observed in the DSC thermograms of the investigated polymers (Table 4), thus suggesting that the macromolecules are substantially amorphous in the solid state.

The T_g values appear quite high laying in the range 163-195 °C, that can be of great interest for applications in optoelectronics (more stable photoinduced birefringence, etc.).

In particular, the T_g value of poly[(*S*)-**MCAPP-C**] is considerably higher, of about 32°C, than those measured for poly[**MCAPE-C**].

This behavior is indicative of a reduced mobility of the macromolecular chains containing (*S*)-**MCAPP-C** co-units originated by the presence of the conformational rigid pyrrolidine ring interposed between the backbone and the phenylazocarbazole chromophore.

Indeed, the copolymer poly[(*S*)-**MCAPP-C**-co-**MCAPE-C**] (48/52) shows a T_g value of 185 °C laying between those measured for the corresponding homopolymers.

High values of T_g are required in order to achieve enhanced temporal stability at room temperature of the photo- or electrically oriented dipoles in the bulk.

Absorption spectra

The UV-vis spectra of (*S*)-**MCAPP-C** and poly[(*S*)-**MCAPP-C**] in *N,N*-dimethylacetamide (DMA) solution exhibit in the 250-650 nm spectral region six absorption bands, centered at about 274, 283, 293 (shoulder), 318, 332 e 426 nm (Figure 11 and Table 5).

The band centered about 426 nm can be attributed to combined electronic transitions such as $n-\pi^*$, $\pi-\pi^*$ and internal charge transfer of the azoaromatic chromophore [22], the others to the sum of several contributions due to the $\pi-\pi^*$ electronic transition of the single 4'-cyano substituted aromatic ring [23] and the $\pi-\pi^*$ electronic transitions of carbazole chromophore [24].

No particular difference between the respective maxima absorption wavelengths is displayed by monomers and polymers.

A significant hypochromic effect is however observed when the spectrum of the monomer, where the lack of structural restraints originates a random distribution of the chromophores in dilute solution, is compared with that of the polymer (Table 5).

Such a behavior, frequently noticed in polymeric derivatives bearing side-chain aromatic chromophores [14,25], is attributed to the presence of electrostatic dipolar interactions between adjacent chromophores [26].

The spectroscopic properties in solution of achiral **MCAPE-C**, poly[**MCAPE-C**] and the chiral copolymer poly[(*S*)-**MCAPP-C**-co-**MCAPE-C**] (48/52) are quite similar to those exhibited by the corresponding optically active couple (*S*)-**MCAPP-C**/poly[(*S*)-**MCAPP-C**].

In solution, in first approximation, these spectroscopic data suggests that their electronic transitions are substantially characterized by the analogue nature of the side chain azocarbazole chromophores.

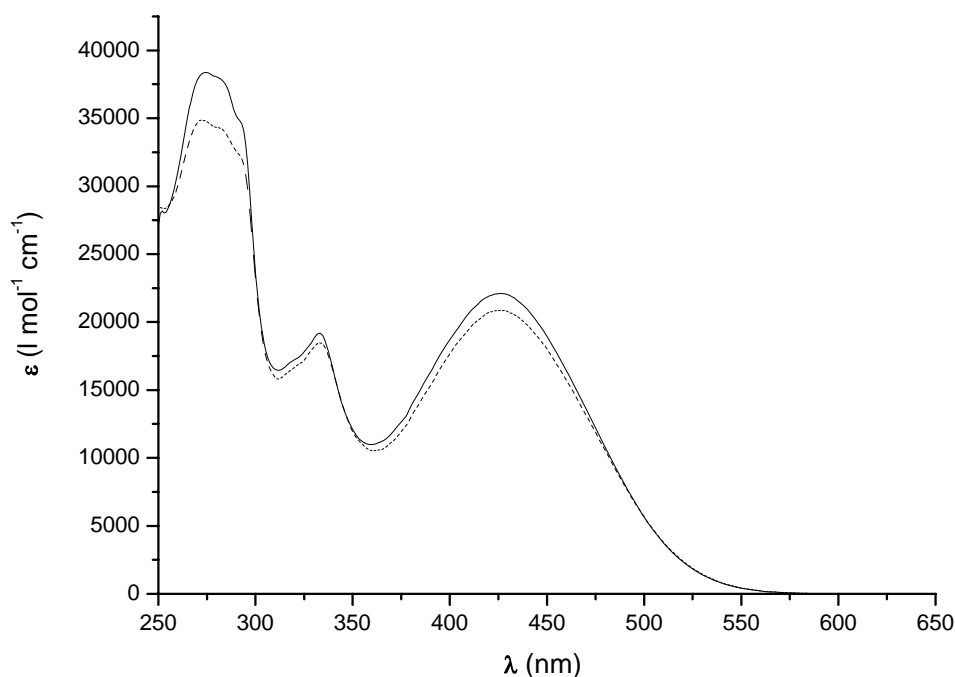


Figure 11. UV-vis spectra in DMF solution of (S)-MPAAP-C (—) and poly[(S)-MPAAP-C] (---)

Chiroptical Properties

The CD spectra of poly[(S)-MCAPP-C] in DMF solution is characterized in the UV-visible region by six dichroic signals at 262, 283, 310, 323, 344 and 452 nm (Table 6 and Figure 12).

In particular, it presents five dichroic bands ($\lambda_{\text{max}} = 262, 283, 310, 323$ and 344 nm) in the spectral region related to the $\pi-\pi^*$ electronic transition of the 9-phenylcarbazole chromophore and one intense positive dichroic signal with maximum centered at 452 nm corresponding to the first absorption band in the visible region, related to the electronic transitions of the azoaromatic chromophore.

Table 5. UV spectral data in DMF solution of the investigate compounds^{a)}.

Sample	1 st absorption band		2 nd absorption band		3 rd absorption band		4 th absorption band		5 th absorption band	
	$\lambda_{\max}^{\text{b)}$	$\epsilon_{\max}^{\text{c)}$								
	nm	Lmol ⁻¹ cm ⁻¹								
(S)-MCAPP-C	273	37500	283	37200	293	34200	333	19000	426	22000
Poly[(S)-MCAPP-C]	272	35000	283	34150	293	31400	334	18500	426	20800
MCAPE-C	272	36200	284	35100	292	33000	332	17400	427	19300
Poly[MCAPE-C]	269	32800	283	32600	292	30700	334	17400	426	19400
Poly[(S)-MCAPP-C-co-MCAPE-C] (48/52)	273	33900	283	32500	292	30000	333	15700	427	16500

a) At $5 \cdot 10^{-4}$ M chromophore concentration.

b) Wavelength of maximum absorbance.

c) Calculated for one single chromophore

Table 6 UV spectral data in DMF solution of (*S*)-**MCAPP-C**, poly[(*S*)-**MCAPP-C**] and poly[(*S*)-**MCAPP-C-co-MCAPE-C**] ^{a)}

Sample	1 st band		2 nd band		3 rd band			4 th band			
	$\lambda_1^{a)}$	$\Delta\epsilon_1^{b)}$	$\lambda_3^{a)}$	$\Delta\epsilon_3^{b)}$	$\lambda_5^{a)}$	$\Delta\epsilon_5^{b)}$	$\lambda_0^{a)}$	$\lambda_6^{a)}$	$\Delta\epsilon_6^{b)}$	$\lambda_7^{a)}$	$\Delta\epsilon_7^{b)}$
(<i>S</i>)- MCAPP-C	265	-0,53	284	+0,31	324	+0,22	-	-	-	425	+0,20
Poly[(<i>S</i>)- MCAPP-C]	262	-1,01	283	+0,39	323	-0,14	332	344	-0,20	452	+0,83
Poly[(<i>S</i>)-(+)- MCAPP-C-co-MCAPE-C] (48/52)	268	-0,22	284	+0,63	335	+0,31	-	-	-	442	+0,44

a) At $5 \cdot 10^{-4}$ M chromophore concentration.

b) Wavelength of maximum dichroic absorption.

c) Calculated for one repeating unit in the polymer.

d) Wavelength of the cross-over of dichroic bands.

By contrast, the CD spectrum of (*S*)-**MCAPP-C** (Figure 12 and Table 6) exhibits only four dichroic signals of lower intensity at 265, 284, 324 and 425 nm.

In correspondence of the UV absorption band at 334 nm (Table 5), the CD spectrum of poly[(*S*)-**MCAPP-C**] presents two signal at 323 and 344 nm of opposite sign and comparable intensity, with a crossover point at 332 nm, which are absent in the spectra in solution of the corresponding monomer (*S*)-**MCAPP-C**, representative of the repeating unit of the polymer.

This behavior is typical of exciton splitting determined by cooperative dipole-dipole interactions between chiral neighboring side chain chromophores [15] arranged in a mutual chiral geometry of one prevailing handedness [14, 16b] and confirms that the presence of the optically active (*S*)-3-hydroxypyrrolidine residue of one prevailing absolute configuration, interposed between the main chain of the polymer and the 9-phenylazocarbazole chromophore, favours the adoption of a chiral conformation of one

prevailing helical handedness, at least for chain segments of the macromolecules in solution.

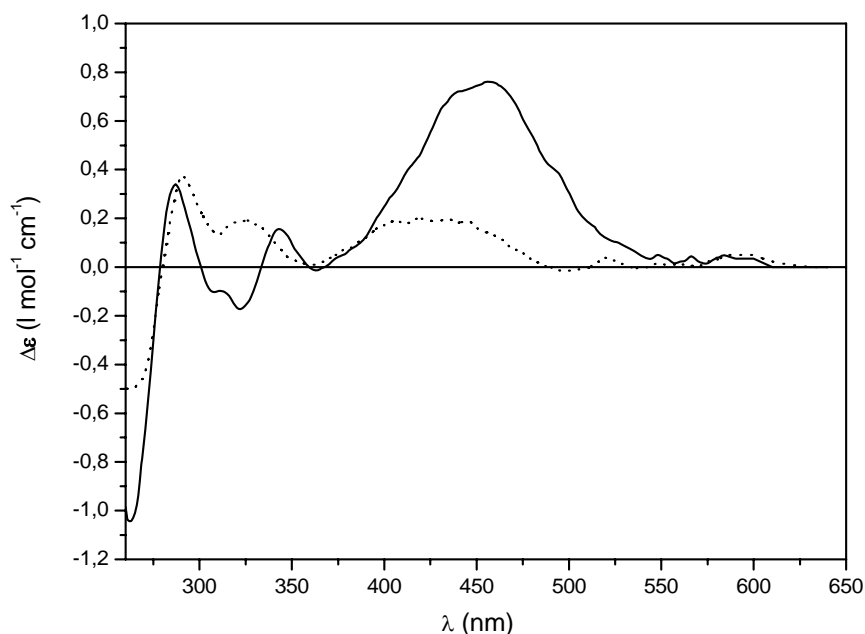


Figure 12. CD spectra in DMF solution of (*S*)-**MPAAP-C** (---) and poly[(*S*)-**MPAAP-C**] (—)

The intensities of dichroic absorptions in DMA solution decrease in the CD spectrum of copolymer poly[(*S*)-**MCAPP-C-co-MCAPE-C**] (48/52), thus confirming that the presence of achiral **MCAPE-C** co-units progressively reduces the extent of the interactions between asymmetrically perturbed chromophoric dipoles ordered according to a chiral arrangement, with respect to the related homopolymer of (*S*)-**MCAPP-C** (Table 6).

In other words, although relevant dipolar interactions between the 9-phenylazocarbazole moieties of (*S*)-**MCAPP-C** and **MCAPE-C** are present, as observed by UV spectroscopy, the chiral co-units of (*S*)-**MCAPP-C** appear substantially unable to maintain the conformational dissymmetry of the optically active homopolymer, when achiral co-units of **MCAPE-C** are also present along the main chain.

This behavior was previously also observed in analogous optically active copolymers of (S)-MAP-N with DR1M [16a].

Studies concerning the photomodulation of their chiroptical properties in the solid state by using one handed circularly or elliptically polarized irradiating light are currently in progress.

Optical Storage Experiments.

It is well-known that a good matching of the absorption wavelength with the wavelength of the pumping laser has a positive effect on storage efficiency.[1]

Being the absorption spectra of the investigated polymers quite similar, a laser light operating at 488 nm, in resonance with their intense electronic transition in the visible (Table 5), has been used in the irradiation experiments in order to gain the same pumping efficiency. To assess the presence of photoinduced linear dichroism and birefringence, films of the polymers have been irradiated with linearly polarized (LP) radiation (writing step) at 488 nm ($I \approx 100 \text{ mW cm}^{-2}$). After irradiation, the samples show high photoinduced linear birefringence due to linear ordering of the azocarbazole moieties, as evidenced by using a probe radiation at 632.8 nm ($I \approx \text{mW cm}^{-2}$). The photoinduced birefringence can be reversibly erased by using circularly polarized (CP) or depolarized pump radiation (erasing step). As example in Figure 13 is shown a complete cycle of irradiation with LP and CP light performed on a thick film of 300 nm of poly[(S)-MCAPP-C-co-MCAPE-C] (48/52).

Table 7: Saturated photoinduced linear birefringence (Δn_1), relaxed photoinduced linear birefringence (Δn_2) and relaxation coefficient of investigated polymers (S).

Sample	Δn_1	Δn_2	$S^a)$
Poly[(S)-MCAPP-C]	0,12	0,11	0,92
Poly[MCAPE-C]	0,12	0,09	0,75
Poly[(S)-MCAPP-C-co-MCAPE-C] (48/52)	0,08	0,06	0,83,

a) expressed as $\Delta n_2/\Delta n_1$

After irradiation with LP light, the saturated photoinduced linear birefringence Δn_1 of poly[(*S*)-MCAPP-C] is 0.12, which, after removal of the pump, relaxes to a stable value Δn_2 of 0.11, as reported in Table 7. The relaxation is of small extent, with a *S* value of 0.92 (where *S* is the relaxation coefficient expressed as the ratio $\Delta n_2/\Delta n_1$), and the induced anisotropy is stable for several months.

These observed values are larger than those obtained, in the same experimental conditions, for poly[MCAPE-C] and poly[(*S*)-MCAPP-C-co-MCAPE-C] (48/52) (Table 7), which show respectively a saturated linear birefringence values of 0.12 and 0.08 under illumination and, after removal of the pump, Δn_2 values of 0.09 and 0.06.

In comparison to poly[MCAPE-C], the chiral homopolymer poly[(*S*)-MCAPP-C] and the copolymer poly[(*S*)-MCAPP-C-co-MCAPE-C] (48/52) are characterized by comparable photoinduced linear birefringence and long-term storage stability but displays higher writing/erasing response and superior stability to repeated cycles of irradiation.

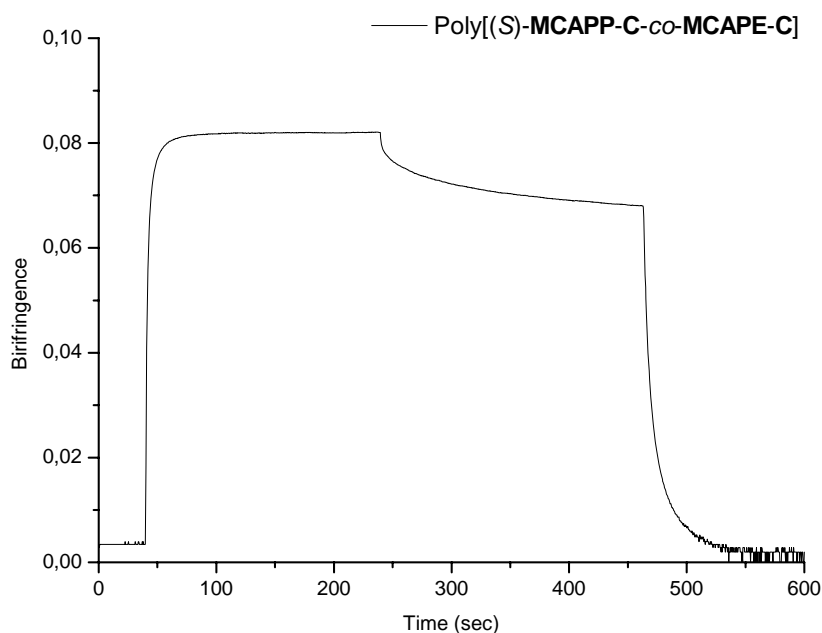


Figure 13. Optically induced birefringence curve registered for poly[(*S*)-MCAPP-C-co-MCAPE-C] (48/52).

This can be attributed to the different chromophoric structure: the azocarbazole moiety in poly[**MCAPE-C**], in fact, is bonded to the backbone through a flexible spacer and may rapidly relax to its original isotropic state; by contrast, in (*S*)-**MCAPP-C** counits, the phenylazocarbazole chromophore is conformationally hindered by the pyrrolidine ring so that its free rotation is probably reduced.

Indeed, the reduced mobility of the macromolecular chains, originated by the presence of the conformationally rigid pyrrolidine ring interposed between the phenylazocarbazole group and the methacrylic main chain, improving the T_g values as discussed above (Table 4).

Conclusions

A new homopolymeric methacrylate has been obtained by radical polymerization of the corresponding monomer (*S*)-**MLECA**, bearing the optical active L-lactic acid residue linked to the chromophore 4-cyanophenyl-3-carbazolyl diazene. This derivative displays pronounced absorption bands (with maximum wavelength around 405-410 nm) of interest for photoresponsive applications utilizing a laser irradiating light of wavelength above 488 nm.

The chiroptical properties of poly[(*S*)-**MLECA**] suggest that the macromolecules assume in solution as well as in thin film homogeneous conformations with a prevailing chirality, as demonstrated by the presence in the CD spectra of an exciton couplet and induced asymmetric perturbation on all the electronic transitions. This behaviour can be attributed to the combined effects of the strongly dipolar conjugated azocarbazole system and the dissymmetry of the L-lactic acid residue, favouring the instauration of chain sections of the macromolecules with a prevailing helical handedness. The presence of strong polar interactions between chromophores in the solid state also produces relevant thermal properties with a high values of T_d and T_g , which can be of interest for nanoscale technological applications.

Photoconductivity and two beam coupling measurements show that the presence of carbazole makes both polymers photoconductive and photorefractive.

Optically active photochromic homopolymer and copolymers deriving from the phenylazocarbazole monomers (*S*)-**MCAPP-C** and **MCAPE-C** have been prepared.

The presence in the macromolecules of the conformationally rigid (*S*)-**MCAPP-C** co-units allows to achieve higher T_g values.

The CD spectra of the investigated optically active homopolymer and copolymers are characterized by dichroic signals related to the electronic transitions of the 9-phenylazocarbazole chromophores. The presence in the spectra of exciton splittings is typical of cooperative interactions between the chromophores disposed in a mutual chiral geometry of one prevailing handedness.

However, the (*S*)-**MCAPP-C** chiral units appear substantially unable to maintain the extent of conformational dissymmetry typical of the homopolymer poly[(*S*)-**MCAPP-**

C], when the flexible achiral counits of **MCAPE-C** are also present along the main chain.

The macromolecules are characterized by enhanced photoinduced linear birefringence. Poly[(*S*)-**MCAPP-C**] and poly[(*S*)-**MCAPP-C-co-MCAPE-C**] (48/52) show higher stability and relaxation with respect to poly[**MCAPE-C**], originated by the presence of the conformationally rigid pyrrolidine ring interposed between the 9-phenylazocarbazole group and the methacrylic main chain, thus allowing the storage of the optical information written over the material.

In conclusion, poly[(*S*)-**MLECA**] and poly[(*S*)-**MCAPP-C**] may therefore be considered as a multifunctional derivatives bearing at the same time chemical functionalities potentially useful for NLO, photorefractive applications and all-optical manipulation of information. In particular, it is possible to envisage applications where the material combines optical storage capabilities, based on the modulation of the linear refractive index, with photoconductivity properties, based on the presence of carbazole moieties, and with photorefractive functionality based on azocarbazole chromophore.

Experimental section

Chemicals

(S)-(-)-Methacryloyl-L-lactic acid was prepared as described [17]. Methacryloyl chloride (Aldrich) was distilled under inert atmosphere in the presence of traces of 2,6-di-*tert*.butyl-*p*-cresol as polymerization inhibitor just before use. (+)-L-Lactic acid (Aldrich), 9-(2-hydroxyethyl)carbazole (Aldrich), 1,3-diisopropylcarbodiimide (**DIPC**, Aldrich) and 4-dimethylaminopyridine (Aldrich) were used as received. 4-Dimethylaminopyridinium 4-toluensulfonate (**DPTS**) was prepared from 4-dimethylaminopyridine and 4-toluensulfonic acid as described [30].

2-bromo-(N-ethyl-amine)ethanol have been obtained as previously reported [28].

Measurements

NMR spectra were obtained at room temperature on 5-10% CDCl₃ solutions using a Varian NMR Gemini 300 spectrometer. Chemical shifts are given in ppm from tetramethylsilane (TMS) as the internal reference. ¹H-NMR spectra were run at 300 MHz by using the following experimental conditions: 24 000 data points 4.5-kHz spectral width 2.6-s acquisition time 128 transients. ¹³C NMR spectra were recorded at 75.5 MHz, under full proton decoupling, by using the following experimental conditions: 24000 data points, 20 kHz spectral width, 0.6 s acquisition time, 64000 transients.

FT-IR spectra were carried out on a Perkin-Elmer 1750 spectrophotometer equipped with an Epon Endeavor II data station on sample prepared as KBr pellets.

Number average molecular weight (\bar{M}_n) and polydispersity (\bar{M}_w/\bar{M}_n) of poly[(S)-**MLECA**] were determined in THF solution by SEC using a HPLC Lab Flow 2000 apparatus, equipped with an injector Rheodyne 7725i, a Phenomenex Phenogel 5 μ MXL column and a UV-Vis detector Linear Instruments model UVIS-200, working at 254 nm. Calibration curves were obtained by using several monodisperse polystyrene standards.

UV absorption spectra were recorded at 25°C on a Perkin Elmer Lambda 19 spectrophotometer on CHCl₃ or DMA solutions by using cell path lengths of 0.1 cm. Azobenzene chromophore concentrations of about 5·10⁻⁴ mol L⁻¹ were used.

CD spectra were recorded at 25°C on a Jasco 810 A dichrograph, using the same path lengths, solutions and concentrations as for UV measurements. Δε values, expressed as L mol⁻¹ cm⁻¹, were calculated by the following equation: Δε = [Θ]/3300, where the molar ellipticity [Θ] in deg cm² dmol⁻¹ refers to one azobenzene chromophore.

The glass transition temperature values were determined by differential scanning calorimetry (DSC) on a TA Instrument DSC 2920 Modulated apparatus at a heating rate of 10°C/min under nitrogen atmosphere on samples of 5-9 mgr.

The initial thermal decomposition temperature (*T_d*) was determined on the polymeric sample with a Perkin-Elmer TGA-7 thermogravimetric analyzer by heating the samples in air at a rate of 20°C/min.

Amorphous thin films were prepared by spin-coating of a solution of the polymer in chloroform for poly[(*S*)-MLECA] (2% w/w) and in DMF for the other polymeric derivatives onto clean fused silica substrates. The films were then dried by heating above 60°C under vacuum for 12 hours. The films thickness, measured by a Tencor P-10 profilometer, was in the range 150-350 nm. Checking of the liquid crystalline behaviour was carried out with a Zeiss Axioscope2 polarising microscope through crossed polarizers fitted with a Linkam THMS 600 hot stage. The absorption and CD spectra of the films were carried out under the same instrumental conditions as the related solutions.

The photoinduced linear birefringence of the polymeric films was measured in situ using a pump and probe set-up by monitoring the transmittance of the samples interposed between two crossed polarisers.

The pump radiation, of λ = 488 nm, was produced by a small frame Ar⁺ laser (Spectra Physics model 165), whereas the source of the probe light at λ = 632.8 nm was a Melles-Griot 1 mW He-Ne laser. A multiple order λ /4 quartz waveplate for 488 nm was used to circularise the pump radiation

Photoconductivity data were obtained by applying a DC voltage to the sample and measuring the current with a Keithley 6517A Electrometer in the dark and under

illumination. The illuminating light was provided by a Newport-Oriel 250W Xenon lamp, coupled with a Newport-Oriel monochromator (mod 74100), with a resulting light intensity $I \sim 3 \text{ mW/cm}^2$ or, alternatively, by a laser light at 532 nm (from Laser Quantum, mod. Torus), obtaining a light intensity $I \sim 1 \text{ W/cm}^2$

The sample cells for two beam coupling experiments were prepared with the external field applied in either the film plane or normal to it.

The laser beam passes through a polarizer and reaches a beam splitter where half of the light is transmitted and half is reflected towards the two mirrors which direct the resulting beams towards the sample. In order to control the polarization and the focusing of the beams, half-wave plates and lenses are placed before the sample

The acquisition is managed by a software that, working as a lock-in amplifier, acquires only the signals at the chopper frequency, thus acquisition of light intensity vs. time can be performed. The voltage applied on the sample may be generated by a power supply (Agilent mod. 33120A for AC voltages or Agilent mod 2342 for DC voltages) and it is then amplified by a Trek mod. 6090 amplifier.

Alcohols and Monomers

(4-Cyanophenyl)-[3-[9-(2-hydroxyethyl)carbazolyl]]diazene [HECA].

4-Cyanoaniline (10 mmol) was dissolved in a solution of concentrated HCl (5 mL) in water (150 mL). The mixture was cooled in an ice bath at temperature below 4°C. Then a solution containing sodium nitrite (11 mmol) in water (5 mL) was added slowly to the 4-cyanoaniline solution. The mixture was stirred in the ice bath for 30 min and sodium dodecyl benzenesulfonate (0.5 g) was added. A solution of 9-(2-hydroxyethyl)carbazole (20 mmol) in CH₂Cl₂ (150 mL) was finally added to the mixture and vigorously stirred one night at room temperature. The brown precipitate was filtered, washed with ethanol (100 ml) and dried under vacuum (68% yield).

¹H-NMR (DMSO-*d*₆): 8.80 (d, 1H, arom carbazole), 8.35 (m, 2H, arom carbazole), 8.05-7.90 (2dd, 4H, arom. 1,4 disubst.), 7.80 (d, 1H, arom carbazole), 7.70 (d, 1H, arom carbazole), 7.30 (d, 1H, arom carbazole), 4.95 (m, 1H, OH), 4.55 (t, 2H, N-CH₂-CH₂-O), 3.82 (m, 2H, N-CH₂-CH₂-O) ppm.

¹³C-NMR (DMSO-*d*₆) (labels as in Scheme 1): 154.46 (C₈), 145.47 (C₃), 143.17 (C₁₀), 141.33 (C₁₃), 133.73 (C_h), 126.56 (C₇), 122.76, 122.65 (C₁₁ and C₁₂), 120.80, 120.00 (C₂, C₄ and C₅), 118.60 (CN), 118.16 (C₆), 115.62 (C_e), 112.02 (C_g), 110.54 (C₁), 110.47 (C₈), 59.50 (C_e), 45.60 (C_f) ppm.

FT-IR: 3338 (ν_{OH}), 3051 (ν_{CH} arom.), 2922 (ν_{CH} aliph.), 2222 (ν_{CN}), 1596 (ν_{C=C} arom.), 1385 (δ CH₃), 852 and 809 (δ_{CH} 1,4-disubst. arom. ring), 770 and 733 (δ_{CH} 1,2,4-trisubst. arom. ring), 746 (δ_{CH} 1,2-disubst. arom. ring) cm⁻¹.

(S)-(4-Cyanophenyl)-[3-[9-[2-(2-methacryloyloxypropanoyloxy)ethyl]carbazolyl]]diazene [(S)-MLECA]

The monomer was obtained by dropping **HECA** (8.3 mmol) at room temperature to a solution of (*S*)-(-)-methacryloyl-L-lactic acid (11.2 mmol) in dry CH₂Cl₂ (20 ml), in the presence of 2,6-di-*tert*-butyl-*p*-cresol (0.06 g) as polymerization inhibitor, under stirring and nitrogen atmosphere. Then, **DPTS** (8.3 mmol) and **DIPC** (2.2 ml, 10.8 mmol) were added under strong stirring. The reaction was left at room temperature for 72 h, the precipitated urea derivative filtered off and the organic solution washed repeatedly with

HCl 1M, Na₂CO₃ 5% and H₂O, in that order. The organic phase was finally dried (Na₂SO₄) and the solvent evaporated under reduced pressure to give the crude product which was submitted to purification by column chromatography (SiO₂, CH₂Cl₂) (28% yield).

¹H-NMR: 8.78 (d, 1H, arom carbazole), 8.20 (m, 2H, arom carbazole), 8.05-7.90 (2dd, 4H, arom. 1,4 disubst.), 7.50 (m, 3H, arom carbazole), 7.25 (d, 1H, arom carbazole), 6.10 and 5.60 (2d, 2H, CH₂=), 5.00 (q, 1H, CH), 4.65 (m, 4H, N-CH₂-CH₂-O), 1.95 (s, 3H, C-CH₃), 1.30 (d, 3H, CH-CH₃) ppm.

¹³C-NMR (labels as in Scheme 1): 171.40 (C_γ), 167.34 (C_β), 155.66 (C_δ), 147.18 (C₃), 143.63 (C₁₀), 141.80 (C₁₃), 136.02 (C_α), 133.90 (C_h), 127.57 (C_a), 127.50 (C₇), 124.35, 124.30 (C₁₁ and C₁₂), 123.76 (C_g), 122.30, 121.64, 121.33 (C₂, C₄ and C₅), 119.46 (CN), 118.23 (C₆), 113.61 (C_e), 109.97 (C₁), 109.80 (C₈), 69.34 (C_e), 63.47 (C_f), 42.57 (C_c), 18.84 (C_b), 17.32 (C_d) ppm.

FT-IR: 3042 (ν_{CH} arom.), 2952 (ν_{CH} aliph.), 2224 (ν_{CN}), 1742 (ν_{C=O} lactic ester), 1711 (ν_{C=O} methacrylic ester), 1625 (ν_{C=C} methacrylic), 1594 (ν_{C=C} arom.), 1385 (δ CH₃), 847 and 819 (δ_{CH} 1,4-disubst. arom. ring), 770 and 733 (δ_{CH} 1,2,4-trisubst. arom. ring), 746 (δ_{CH} 1,2-disubst. arom. ring) cm⁻¹.

(S)-3-Hydroxy-N-{4-[(4-cyanophenyl)-(3-carbazolyl)-diazene]-phenyl}pyrrolidine
[(S)-HCAPP-C]

A mixture of 2.7 g (0.00914 mol) of 4-cyanophenyl-3-carbazolyl-diazene, 0.21 g of trans-cyclohexanediamine (10 % mol) and 0.17 g of air-stable CuI (10% mol) was prepared in 5 ml of dry dioxane (1 M) in presence of 2,65 g di K₂CO₃ (2 equiv).

2,66 g (0.011 mol) of (S)-(-)-3-hydroxyethyl-N-(4-bromophenyl)pyrrolidine in dry dioxane (5 ml) was then added and the final solution was heated at reflux under inert atmosphere for 24 h.

The cooled mixture was filtered-off and the organic solution, concentrated under reduced pressure, was precipitated in MeOH to give 2.5 g of pure product (80.0% yield).

¹H-NMR (CDCl₃): 8.85 (d, 1H, arom. 4-carbazole), 8.35 (d, 1H, arom. 2-carbazole), 8.30 e 8.20 (2dd, 4H, aromatic ring 1,4-disubst.), 7.80-7.40 (m, 2H, 15,19-phenyl and

5H, 1,2,5,6,7,8-carbazole), 6.80 (d, 2H, 16,18-phenyl), 5.05 (d, 1H, OH), 4.60 (s, 1H, 3-CH), 3.60-3.40 (m, 4H, 2- and 5-CH₂), 2.20 (m, 2H, 4-CH₂) ppm.

FT-IR (KBr) (cm⁻¹): 3437 (ν_{OH}), 3050 (ν_{CH} arom.), 2916-2840 (ν_{CH} aliph.), 2217 (ν_{CN}), 1590 (ν_{C=C} arom.), 1350 (ν_{CH₃}), 842 and 812 (δ_{CH} aromatic ring 1,4-disubst.), 769 and 735 (δ_{CH} aromatic ring 1,2,4-trisubst.), 748 (δ_{CH} aromatic ring 1,4-disubst.).

2-Hydroxy-N-ethyl-N-{4-[(4-cyanophenyl)-(3-carbazolyl)-diazene]}phenyl-amine
[HCAPE-C]

The same procedure adopted for [(S)-**HCAPP-C**] starting from 4-cyanophenyl-3-carbazolyl-diazene (4.5 g, 0.015 mol) and 2-hydroxyethyl-N-ethyl-N-(4-bromophenyl)amine (4.42 g, 0.018 mol) to afford 4.81 g of pure **HCAPE-C** (Yield 69%).

¹H-NMR (CDCl₃): 8.80 (s, 1H, arom. 4-carbazole), 8.20 (d, 1H, arom. 2-carbazole), 8.10 (d, 1H, arom. 1-carbazole), 8.00 e 7.80 (2dd, 4H, aromatic ring 1,4-disubst.), 7.50-7.30 (d, 2H, 15,19-phenyl and 4H, 5,6,7,8-carbazole), 6.90 (d, 2H, 16,18-phenyl), 3.90 (d, 2H, N-CH₂-CH₂), 3.60 (m, 4H, N-CH₂), 1.90 (m, 1H, OH), 1.20 (t, 3H, CH₃) ppm.

FT-IR (KBr) (cm⁻¹): 3435 (ν_{OH}), 3050 (ν_{CH} arom.), 2967 (ν_{CH} aliph.), 2222 (ν_{CN}), 1590 (ν_{C=C} arom.), 1350 (ν_{CH₃}), 843 and 812 (δ_{CH} aromatic ring 1,4-disubst.), 766 and 730 (δ_{CH} aromatic ring 1,2,4-trisubst.), 746 (δ_{CH} aromatic ring 1,4-disubst.)

(S)-Methacryloyl-3-oxy-N-{4-[(4-cyanophenyl)-(3-carbazolyl)-diazene]-phenyl}
pyrrolidine [(S)-MCAPP-C]

The same procedure adopted for (S)-**MLECA** was followed starting from (S)-**HCAPP-C** (2 g, 0.00437 mol), triethylamine (0.75 ml, 0.00529 mol), dimethylamino pyridine (0.1 g) and 2,6-di-*tert*-butyl-4-methyl phenol (0.1 g) in THF (50 ml). The acylation reaction was performed by using methacryloyl chloride (0.52 ml, 0.00529 mol).

Pure (S)-**MCAPP-C** was obtained in 68.0% yield (1.60 g) by column chromatography (SiO₂, CH₂Cl₂/EtOAc 1:1 v/v as eluent) followed by crystallization from abs. ethanol.

¹H-NMR (CDCl₃): 8.80 (d, 1H, arom. 4-carbazole), 8.30 (d, 1H, arom. 2-carbazole), 8.25 and 8.20 (2dd, 4H, aromatic ring 1,4-disubst.), 7.80 (m, 2H, 15,19-phenyl and 5H, 1,2,5,6,7,8-carbazole), 6.80 (d, 2H, 16,18-phenyl), 6.20 and 5.40 (2d, 2H, CH₂=), 5.55

(m, 1H, 3-CH), 3.60 (m, 4H, 2- and 5-CH₂), 2.30 (m, 2H, 5-CH₂), 2.00 (s, 3H, C-CH₃) ppm.

FT-IR (KBr) (cm⁻¹): 3050 (ν_{CH} arom.), 2960-2845 (ν_{CH} aliph.), 2228 (ν_{CN}), 1709 (ν_{C=O}), 1637 (ν_{C=C} methacrylic), 1593 (ν_{C=C} arom.), 1460 (ν_{CHas} CH₃), 1350 (ν_{CHs} CH₃), 1150 (ν_{C-O}), 845 and 812 (δ_{CH} arom. ring 1,4-disubst.), 767 and 725 (δ_{CH} arom. ring 1,2,4-trisubst.), 751 (δ_{CH} arom. ring 1,4-disubst.).

Methacryloyl-2-oxyethyl-N-ethyl-N-{4-[(4-cyanophenyl)-(3-carbazoly)-diazene]}phenylamine [MCAPE-C]

The same procedure adopted for (S)-MLECA and (S)-MCAPP-C was followed starting from HCAPE-C (4,8 g, 0.0105 mol), triethylamine (1.78 ml, 0.0127 mol), dimethylamino pyridine (0.25 g) and 2,6-di-*tert*-butyl-4-methyl phenol (0.25 g) in THF (125 ml). The acylation reaction was performed by using methacryloyl chloride (1.23 ml, 0.0127 mol).

Pure MCAPE-C was obtained in 58.0% yield (3.2 g) by column chromatography (SiO₂, CH₂Cl₂/EtOAc 1:1 v/v as eluent) followed by crystallization from abs. ethanol.

¹H-NMR (CDCl₃): 8.80 (d, 1H, arom.4-carbazole), 8.00 and 7.90 (2d, 4H, aromatic ring 1,4-disubst.), 7.80 (d, 2H, 15,19-phenyl), 7.40 (m, 6H, 1,2,5,6,7,8-carbazole), 6.90 (d, 2H, 16,18-phenyl), 6.20 and 5.60 (d, 2H, CH₂=), 4.40 (d, 2H, N-CH₂-CH₂), 3.75-3.60 (m, 4H, N-CH₂), 2.00 (s, 3H, C-CH₃), 1.25 (t, 3H, N-CH₂-CH₃) ppm.

FT-IR (KBr) (cm⁻¹): 3050 (ν_{CH} arom.), 2967 (ν_{CH} aliph.), 2222 (ν_{CN}), 1709 (ν_{C=O}), 1623 (ν_{C=C}), 1595 (ν_{C=C} arom.), 1461 (ν_{CHas} CH₃), 1365 (ν_{CHs} CH₃), 1168 (ν_{C-O} ester), 842 and 811 (δ_{CH} aromatic ring 1,4-disubst.), 766 and 730 (δ_{CH} aromatic ring 1,2,4-trisubst.), 746 (δ_{CH} aromatic ring 1,4-disubst.).

Polymers

The homopolymerization and the copololimerization of the monomers was carried out in glass vials using AIBN as free radical initiator and dry THF or DMF as solvent. The reaction mixture (1.0 g of monomer, 2% weight of AIBN in 25 mL of solvent) was introduced into the vials under nitrogen atmosphere, submitted to several freeze-thaw cycles and heated at 65 °C for 72 h. The reaction was then stopped by pouring the

mixture into a large excess of methanol (200 ml), and the coagulated polymer filtered off. The solid product was repeatedly redissolved in THF or DMF at room temperature and reprecipitated again in methanol. The last traces of unreacted monomers and oligomeric impurities were eliminated by Soxhlet continuous extraction with methanol followed by acetone. The materials were finally dried at 60°C under vacuum for several days to constant weight.

Poly[(S)-(4-cyanophenyl)-[3-[9-[2-(2-methacryloyloxypropanoyloxy)ethyl]carbazolyl]]diazene] {poly[(S)-MLECA]}

The homopolymerization of (S)-MLECA was carried out in glass vials using 2,2'-azobisisobutyronitrile (AIBN) as free radical initiator and THF as solvent. The reaction mixture (0.5 g of monomer, 2% weight of AIBN in 5 ml THF) was introduced into the vial under nitrogen atmosphere, submitted to several freeze-thaw cycles and heated at 70°C for 72 hours. The reaction was then stopped by pouring the mixture into a large excess (100 ml) of methanol, and the coagulated polymer filtered off. The solid product was redissolved in THF, precipitated again with methanol and finally dried under vacuum to constant weight (77% yield).

¹H-NMR: 8.50 (m, 1H, arom carbazole), 8.00-7.00 (m, 11H, arom), 4.90 (m, 1H, CH), 4.30 (m, 4H, N-CH₂-CH₂-O), 2.10-1.20 (m, 5H, CH₂ and CH₃ main chain and 3H, CH-CH₃) ppm.

¹³C-NMR (labels as in Scheme 1): 178.20 (C_β), 170.69 (C_γ), 155.05 (C_δ), 145.77 (C₃), 143.24 (C₁₀), 141.44 (C₁₃), 133.61 (C_h), 127.46 (C₇), 123.98 (C₁₁ and C₁₂), 123.52 (C_g), 122.05, 121.57, 121.29 (C₂, C₄ and C₅), 119.46 (CN), 118.23 (C₆), 113.61 (C_ε), 109.69 (C₁ and C₈), 69.34 (C_e), 63.47 (C_f), 54.29 (C_A), 45.86 (C_α), 42.24 (C_c), 20.22 and 18.50 (C_B), 17.28 (C_d) ppm.

FT-IR: 3047 (ν_{CH} arom.), 2941 (ν_{CH} aliph.), 2224 (ν_{CN}), 1740 (ν_{C=O} lactic ester), 1734 (ν_{C=O} methacrylic ester), 1594 (ν_{C=C} arom.), 1356 (δ CH₃), 844 and 808 (δ_{CH} 1,4-disubst. arom. ring), 762 and 721 (δ_{CH} 1,2,4-trisubst. arom. ring), 746 (δ_{CH} 1,2-disubst. arom. ring) cm⁻¹.

Poly[(S)-Methacryloyl-3-oxy-N-{4-[(4-cyanophenyl)-(3-carbazolyl)-diazene]-phenyl}pyrrolidine] {Poly[(S)-MCAPP-C]}

¹H-NMR (CDCl₃): 8.70-8.40 (m, 1H, arom. 4-carbazole), 8.20-7.60 (m, 6H aromatic ring 1,4-disubst. and 15,19-phenyl), 7.40-7.00 (m, 6H, arom. 1,2,5,6,7,8-carbazole), 6.80-6.60 (m, 2H, 16,18-phenyl), 5.20 (m, 2H, 3-CH), 4.20 (m, 2H, N-CH₂-CH₂), 3.60-3.20 (m, 4H, 2- and 5-CH₂ and 2H, N), 2.20-0.60 (m, 2H, 4-CH₂ and 5H, CH₂ and CH₃ main chain) ppm.

FT-IR (KBr) (cm⁻¹): 3050 (ν_{CH} arom.), 2960-2845 (ν_{CH} aliph.), 2228 (ν_{CN}), 1715 (ν_{C=O}), 1593 (ν_{C=C} arom.), 1460 (ν_{CNas} CH₃) 1350 (ν_{CHs} CH₃), 1150 (ν_{C-O}), 842 and 811 (δ_{CH} aromatic ring 1,4-disubst.), 766 and 730 (δ_{CH} aromatic ring 1,2,4-trisubst.), 746 (δ_{CH} aromatic ring 1,4-disubst.).

Poly[methacryloyl-2-oxyethyl-N-ethyl-N-{4-[(4-cyanophenyl)-(3-carbazolyl)-diazene]}phenylamine] {Poly[MCAPE]}

¹H-NMR (CDCl₃): 8.60 (s, 1H, arom. 4-carbazole), 8.20-7.80 (m, 6H, aromatic ring 1,4-disubst. and 15,19-phenyl), 7.20 (m, 6H, arom. 1,2,5,6,7,8-carbazole), 4.00 (m, 2H, N-CH₂-CH₂-O), 3.50-3.20 (m, 4H, N-CH₂), 1.90-0.60 (m, 5H, CH₃ e CH₂ main chain and 3H, N-CH₂-CH₃) ppm.

FT-IR (KBr) (cm⁻¹): 3050 (ν_{CH} arom.), 2967 (ν_{CH} aliph.), 2222 (ν_{CN}), 1734 (ν_{C=O}), 1595 (ν_{C=C}), 1460 (ν_{CHas} CH₃), 1350 (ν_{CHs} CH₃), 1140 (ν_{C-O}), 842 and 811 (δ_{CH} aromatic ring 1,4-disubst.), 766 and 730 (δ_{CH} aromatic ring 1,2,4-trisubst.), 746 (δ_{CH} aromatic ring 1,4-disubst.).

Poly[(S)-methacryloyl-3-oxy-N-{4-[(4-cyanophenyl)-(3-carbazolyl)-diazene]-phenyl}pyrrolidine-co-methacryloyl-2-oxyethyl-N-ethyl-N-{4-[(4-cyanophenyl)-(3-carbazolyl)-diazene]}phenylamine] {Poly[(S)-MCAPP-C-co-MCAPE-C] (48/52)}

¹H-NMR (CDCl₃): 8.70-8.40 (d, 2H, arom. 4-carbazole), 8.20-7.60 (m, 12H aromatic ring 1,4-disubst. and 15,19-phenyl), 7.40-7.00 (m, 12H, arom. 1,2,5,6,7,8-carbazole), 6.80-6.60 (m, 4H, 16,18-phenyl), 5.20 (m, 2H, 3-CH), 4.2 (m, 2H, N-CH₂-CH₂-O), 3.60-3.20 (m, 4H, 2- and 5-CH₂ and 2H, N-CH₂), 2.20-1.20 (m, 5H, CH₂ and CH₃ main chain and 2H, 4 CH₂ and 3H, N-CH₂-CH₃) .

Charter 4: Methacrylic polymers bearing side chain azocarbazole chromophore

FT-IR (KBr) (cm^{-1}): 3050 (ν_{CH} arom.), 2960-2845 (ν_{CH} aliph.), 2228 (ν_{CN}), 1715 ($\nu_{\text{C=O}}$), 1593 ($\nu_{\text{C=C}}$ aromatic ring linked cyano group), 1460 (ν_{CNas} CH_3) 1350 (ν_{CHs} CH_3), 1150 ($\nu_{\text{C-O}}$), 844 and 814 (δ_{CH} aromatic ring 1,4-disubst.), 766 and 731 (δ_{CH} aromatic ring 1,2,4-trisubst.), 745 (δ_{CH} aromatic ring 1,4-disubst.).

References

- [1] [1a] Proceedings of the Symposium on Azobenzene-Containing Materials, Boston MA (U.S.A.) 1998, ed. A. Natansohn, *Macromolecular Symposia* 137, 1999, pp.1–165; [1b] A. Natansohn, P. Rochon, M.R. Ho, C. Barrett, *Macromolecules* 1995, 28, 4179; [1c] Y. Wu, Q. Zhang, A. Kanazawa, T. Shiono, T. Ikeda, Y. Nagase, *Macromolecules* 1999, 32, 3951; [1d] C. Maertens, P. Dubois, R. Jerome, P.A. Blanche, P.C.J. Lemaire, *Polym. Sci. Part B: Polym. Phys.*, 2000, 38, 205; [1e] C.R. Mendonca, A. Dhanabalan, D.T. Balogh, L. Misoguti, D.S. Dos Santos Jr., M.A. Pereira-da-Silva, J.A. Giacometti, S.C. Zilio, O.N. Oliveira Jr., *Macromolecules* 1999, 32, 1493; [1f] J.H. Kim, S. Kumar, S.D. Lee, *Phys. Rev. E*, 1998, 57, 5644; [1g] K. Ichimura, *Chem. Rev.*, 2000, 100, 1847.
- [2] [2a] W.M Gibbons, P.J. Shannon, S.T. Sun, B.J. Swetlin, *Nature* 1991, 351, 49; [2b] N.C.R. Holme, P.S. Ramanujam, S. Hvilsted, *Opt. Lett.* 1996, 21, 902.
- [3] [3a] H. Katz, K. Singer, J. Sohn, C. Dirk, *J. Am. Chem. Soc.* 1987, 109, 6561; [3b] J. A. Delaire, K. Nakatani, *Chem. Rev.* 2000, 100, 1817
- [4] [4a] T. Todorov, L. Nikolova, N. Tomova, *Appl. Opt.*, 1984, 23, 4588; [4b] L. Andruzzi, A. Altomare, F. Ciardelli, R. Solaro, S. Hvilsted, P.S. Ramanujam, *Macromolecules* 1999, 32, 448.
- [5] [5a] G. Iftime, F.L. Labarthe, A. Natansohn, P. Rochon, *J. Am. Chem. Soc.* 2000, 122, 12646; [5b] T. Verbiest, M. Kauranen, A. Persoon, *J. Mat. Chem.* 1999, 9, 2005.
- [6] [6a] Y. Wu, A. Natansohn, P. Rochon, *Macromolecules* 2004, 37, 6090-6095; [6b] A. Natansohn, P. Rochon, *Chem. Rev.* 2002, 102, 4139-4175.
- [7] [7a] Y. Shi, W. Steier, L. Yu, M. Chen, L. Dalton, *Appl. Phys. Lett.* 1991, 59, 2935; [7b] C. Barrett, A. Natansohn, P. Rochon, C.L. Callender, L. Robitaille, *Proc. SPIE* 1997, 3006, 441.
- [8] S. Ducharme, J.C. Scott, R.J. Twieg, W.E. Moerner, *Phys. Rev. Lett.* 1991, 66, 1846.
- [9] [9a] J.V. Grazulevicius, P. Strohrriegl, J. Pielichowski, K. Pielichowski, *Prog. Polym. Sci.* 2003, 28, 1297-1353; [9b] W.E. Moerner, A. Grunnet-Jepsen, C.L.

- Thompson, *Annu. Rev. Mater. Sci.* 1997, 27, 583-623; [9c] P.N. Prasad, M.E. Orczyk, J. Zieba, *J. Phys. Chem.* 1994, 98, 8699; [9d] K. Meerholz, B. Volodin, B. Sandalphon, N. Kippelen, N. Peyghambarian, *Nature* 1994, 371, 497.
- [10] [10a] A. Altomare, F. Ciardelli, L. Mellini, R. Solaro, *Macromol. Chem. Phys.* 2004, 205, 1611-1619; [10b] C. Engels, D. Van Steenwinckel, E. Hendrickx, M. Schaerlaekens, A. Persoons, C. Samyn, *J. Mater. Chem.* 2002, 12, 951-957; [10c] J. Hwang, J. Sohn, S.Y. Park, *Macromolecules* 2003, 36, 7970; [10d] P. Lundquist, R. Wortmann, C. Geletneky, R. Twieg, M. Jurich, V. Lee, C. Moylan, D. Burland, *Science* 1996, 274, 1182.
- [11] [11a] M. Ho, C. Barrett, J. Paterson, M. Esteghamatian, A. Natansohn, P. Rochon, *Macromolecules* 1996, 29, 4613-4618; [11b] C. Barrett, B. Choudhury, A. Natansohn, P. Rochon, *Macromolecules* 1998, 31, 4845-4851.
- [12] [12] J. Shi, Z. Jiang, S. Cao, *React. Funct. Polym.* 2004, 59, 87-91
- [13] [13a] T. Kajitani, K. Okoshi, S. Sakurai, J. Kumaki, E. Yashima, *J. Am. Chem. Soc.* 2006, 128, 708-709; [13b] E. Yashima, K. Maeda, T. Nishimura, *Chem. Eur. J.* 2004, 10, 42-51; [13c] A.J. Wilson, M. Masuda, R.P. Sijbesma, E.W. Meijer, *Angew. Chem., Int. Ed.* 2005, 44, 2275-2279; [13d] M.M. Green, N.C. Peterson, T. Sato, A. Teramoto, R. Cook, S. Lifson, *Nature*, 1995, 268, 1860.
- [14] [14a] L. Angiolini, D. Caretti, L. Giorgini, E. Salatelli, A. Altomare, C. Carlini, R. Solaro, *Polymer* 1998, 39, 6621; [14b] L. Angiolini, D. Caretti, L. Giorgini, E. Salatelli, *Macromol. Chem. Phys.* 2000, 201, 533; [14c] L. Angiolini, D. Caretti, L. Giorgini, E. Salatelli, *Polymer* 2001, 42, 4005; [14d] L. Angiolini, D. Caretti, L. Giorgini, E. Salatelli, *J. Polymer Sci., Part A Polym. Chem.* 1999, 37, 3257.
- [15] C. Carlini, L. Angiolini, D. Caretti, *Photochromic optically active polymers*, in *Polymeric Materials Encyclopedia*, Salomone, J. C., editor-in-chief; CRC Press: Boca Raton, 1996; Vol. 7, pp. 5116-5123.
- [16] [16a] L. Angiolini, T. Benelli, R. Bozio, A. Daurù, L. Giorgini, D. Pedron, E. Salatelli, *Macromolecules* 2006, 39, 489; [16b] L. Angiolini, T. Benelli, L. Giorgini, A. Painelli, F. Terenziani, *Chem. Eur. J.* 2005, 11, 6053-63; [16c] L. Angiolini, R. Bozio, A. Daurù, L. Giorgini, D. Pedron, G. Turco, *Chem. Eur. J.*

- 2002; 8, 4241; [16d] L. Angiolini, T. Benelli, R. Bozio, A. Daurù, L. Giorgini, D. Pedron, *Synthetic Metals* 2003, 139, 743.
- [17] V.A. Miller, R.R. Brown, Jr. E.B. Gienger, US Pat. 3 067 180 (1962).
- [18] J.S. Moore, S.I. Stupp, *Macromolecules* 1990, 23, 65.
- [19] I.R. Peat, W.F. Reynolds, *Tetrahedron Lett.* 1972, 1359.
- [20] E.F. McCord, W.L. Anton, L. Wilczek, S.D. Ittel, L.T.J. Nelson, K.D. Raffell, *Macromol. Symp.* 1994, 86, 47.
- [21] Z.R. Grabowski, J. Dobkowski, *Pure Appl. Chem.* 1983, 55, 245
- [22] A. Altomare, F. Ciardelli, M.R. Ghiloni, R. Solaro, N. Tirelli, *Macromol. Chem. Phys.* 1997, 198, 1739.
- [23] L. Angiolini, T. Benelli, R. Bozio, A. Daurù, L. Giorgini, D. Pedron, E. Salatelli, *Eur. Polym. J.* 2005, 41, 2045-2054.
- [24] [24a] J. R. Platt, *J. Chem. Phys.* 1949, 7, 484; [24b] G.E. Johnson, *J. Phys. Chem.* 1974, 78, 1512
- [25] [25a] C. Carlini, F. Gurzoni, *Polymer* 1983, 24, 101; [25b] E. Chiellini, R. Solaro, G. Galli, A. Ledwith, *Macromolecules* 1980, 13, 1118.
- [26] [26a] Jr. I. Tinoco, *J. Am. Chem. Soc.* 1960, 82, 4785; [26b] K. Okamoto, A. Itaya, S. Kusabayashi, *Chem. Lett.* 1974, 1167; [26c] F. Ciardelli, M. Aglietto, C. Carlini, E. Chiellini, R. Solaro, *Pure Appl. Chem.* 1982, 54, 521
- [27] [27a] M. Shimomura, T. Kunitake, *J. Am. Chem. Soc.* 1987, 109, 5175; [27b] H. Menzel, B. Weichart, A. Schmidt, S. Paul, W. Knoll, J. Stumpe, T. Fischer, *Langmuir* 1994, 10, 1926; [27c] A. Dhanabalan, D.T. Balogh, Jr. A. Riul, J.A. Giacometti, Jr. O.N. Oliveira, *Thin Solid Films* 1998, 323, 257.
- [28] D. Yu, A. Gharavi, L. Yu, *J. Am. Chem. Soc.*, 117, 11680 (1995)
- [29] Ullmann, F. *Ber. Dtsch. Chem. Ges.*, 36, 2382-2384 (1903)
- [30] D. D. Perrin, W. L. F. Amarego, D. R. Perrin, "Purification of Laboratory Chemicals", Pergamon Press, Oxford, 1966.

**Chapter 5: Optically active copolymers containing in side chain
carbazole and azo chromophores**

Introduction

Polymer based carbazole materials have drawn great attention for their unmatched advantages in preparation of materials, high and controllability of photoconductive performance and devices fabrication flexibility *etc.* [1,4]

In particular, side chain carbazole polymer can give rise charge carries in the visible region through an induced intramolecular charge transfer complex[5]. In these materials, the macromolecular structure affect the hole transport mechanism because the photoconductivity is related to the hole hopping between side chain carbazole units and the molecular mobility of chromophore[5].

In the previous chapters we have discussed the properties of the novel chiral homopolymeric methacrylates poly[(*S*)-(+)-**MECSI**] [6], poly[(*S*)-(-)-**MECP**] [6], poly[(*S*)-(-)-**MEPS**] and poly[(*S*)-(-)-**MEPP**] bearing the optical active residues of the (*S*)-2-hydroxy-succinimide and (*S*)-3-hydroxy-pyrrolidine interposed between the main chain and the carbazole chromophore.

On the other hand, an intense attention is currently arisen to investigations dealing with the side chain polymers containing azoaromatic chromophores for their potentially unique optical properties [7].

They can be used in advanced micro- and nanotechnologies such as optical data storage[8], nonlinear optical materials[9], holographic memories[10], chiroptical switches[11], surface relief gratings[12], etc..

The induction of helical chirality in polymers has attracted widespread interest for its possible applications in optical devices or data storage also because of its relevance to chiral amplification as it may have occurred at the early stages of life [13]

To this regard, in recent studies we have reported on optically active photochromic methacrylic polymers bearing two distinct functional groups (i.e. azoaromatic and a chiral groups of one single configuration) directly linked to the side chain [14].

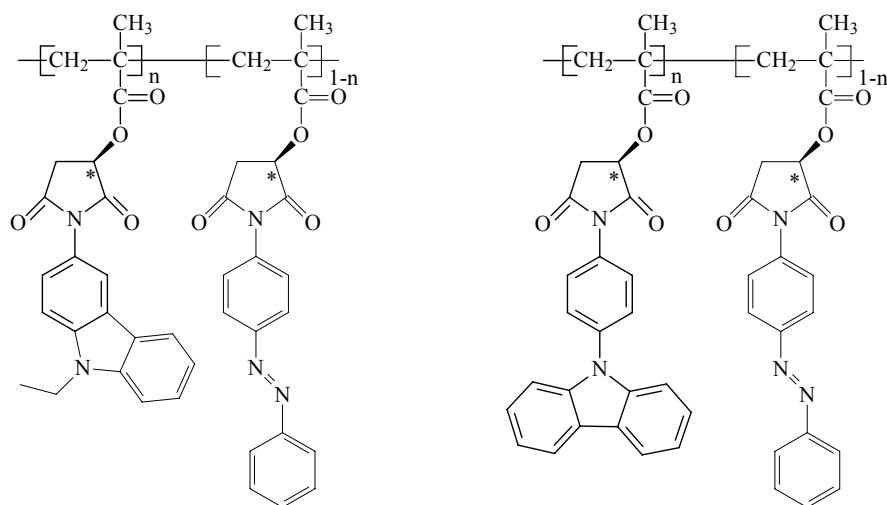
In these materials, the presence of a rigid chiral moiety of one prevailing absolute configuration favours the establishment of a chiral conformation of one prevailing helical handedness, at least within chain segments of the macromolecules, which can be observed by circular dichroism (CD) [15].

The simultaneous presence of the azoaromatic and chiral functionalities allows the polymers to display both the properties typical of dissymmetric systems (optical activity, exciton splitting of dichroic absorptions), as well as the features typical of photochromic materials (photorefractivity, photoresponsiveness, NLO properties) [14].

In this context it was worth to synthesize novel optically active multifunctional methacrylic copolymers containing in side-chains chiral moieties linked to a photochromic azoaromatic and to a photoconductive carbazolic chromophores. This has been carried out by radical copolymerization of the monomer *trans*-(*S*)-(+)-2-methacryloyloxy-N(4-azobenzene)-succinimide (*S*)-(+)-**MOSI** [16] with (*S*)-(+)-methacryloyl-2-oxy-N-[3-(9-ethylcarbazole)]-succinimide (*S*)-(+)-**MECSI** [6] and with (*S*)-(+)-methacryloyl-2-oxy-N-9-phenylcarbazole-succinimide (*S*)-(+)-**MCPS** and by copolymerization of the monomers (*S*)-3-methacryloyloxy-1-(4'-nitro-4-azobenzene)pyrrolidine (*S*)-**MAP-N** [14a, 14b] and (*S*)-3-methacryloyloxy-1-(4'-ciano-4-azobenzene)pyrrolidine (*S*)-**MAP-C** [14b] with (*S*)-(-)-methacryloyl-3-oxy-N-[3-(9-ethylcarbazole)]-pyrrolidine (*S*)-(-)-**MECP** [6] and (*S*)-(-)-methacryloyl-3-oxy-N-9-phenylcarbazole-pyrrolidine (*S*)-(-)-**MCP**P. The structures of the synthesized copolymers are reported in Figure 1.

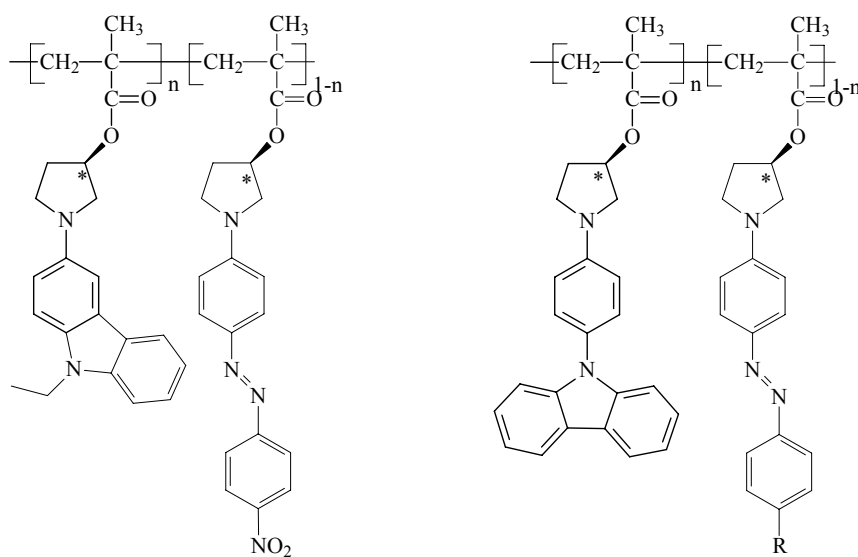
The copolymeric products have been fully characterized and their spectroscopic and thermal properties compared to those of the related optically active monomers and homopolymers.

The properties of this new particular class of optically active azocarbazolic multifunctional polymers, bearing at the same time several chemical functionalities, may allow a variety of potentially commercial applications as such as NLO, photorefractivity and all-optical manipulation of information.



Poly[(S)-(+)-**MECSI**-*co*-(S)-(+)-**MOSI**] (73/23) n=0.73
 Poly[(S)-(+)-**MECSI**-*co*-(S)-(+)-**MOSI**] (51/49) n=0.51
 Poly[(S)-(+)-**MECSI**-*co*-(S)-(+)-**MOSI**] (21/79) n=0.21

Poly[(S)-(+)-**MCPS**-*co*-(S)-(+)-**MOSI**] (55/45) n=0.55



Poly[(S)-(+)-**MECSI**-*co*-**MAP-N**] (50/50) n=0.50

R=CN Poly[(S)-(+)-**MCPP**-*co*-(S)-**MAP-C**] (46/54) n=0.46
 R=NO₂ Poly[(S)-(+)-**MCPP**-*co*-(S)-**MAP-N**] (49/51) n=0.49

Figure 1. Chemical structures of investigated copolymers

***Copolymers containing optically active side chain 3-carbazole and azochromophores:
poly[(S)-(+)-MECSI-co-(S)-(+)-MOSI]s and poly[(S)-(-)-MECP-co-(S)-MAP-N]***

Two novel optically active bi-functionals methacrylic copolymers bearing in the side chain the azoaromatic and 3-carbazole groups linked to the main chain with a chiral group of the 2-hydroxysuccinimide and 3-hydroxypyrrolidine of one prevailing absolute configuration have been prepared and characterized.

All the polymeric derivatives have good thermal stability with glass transition temperature around 200°C and high decomposition temperatures.

Spectroscopic, thermal and chiroptical characterizations indicate the occurrence of dipolar interactions between side chain moieties and the presence of an ordered chiral conformation at least for chain segments of the macromolecules.

Synthesis and structural characterization of copolymers.

Copolymerization of monomers (S)-(+)-**MECSI** and (S)-(-)-**MECP** with [(S)-(+)-**MOSI**] and [(S)-**MAP-N**], respectively, carried out in THF solution under radical conditions by using AIBN as a thermal initiator, produced the desired polymers shown in Figure 1. Relevant data for synthesized copolymers are reported in Table 1 for direct comparison with poly[(S)-(+)-**MECSI**] [6], poly[(S)-(-)-**MECP**] [6], poly[(S)-(+)-**MOSI**] [16] and poly[(S)-**MAP-N**] [14a, 14b] previously investigated.

The occurred polymerization was proved by IR spectroscopy; the copolymers spectra display the disappearance of the absorption around 1630-1636 cm⁻¹, related to the stretching vibration of the methacrylic double bond, and the contemporary shift (10-20 cm⁻¹) of the estereal carbonyl stretching to higher frequencies (1725-1732 cm⁻¹) with respect to the corresponding monomers due to the reduced electron delocalization, determined by the reaction of the methacrylic double bond.

Accordingly, in the ¹H-NMR spectra of polymeric derivatives the resonances of the vinylidenic protons of the monomers are absent and the methacrylic methyl resonances are shifted to higher field. The final molar composition of copolymers was assessed by ¹H-NMR (Figure 2 and Figure 3) by comparing the ratios of the integrated signals of

aromatic protons to that of aliphatic ones. To confirm the obtained results it was followed a quantitative analysis of UV-Vis spectra.

Table 1. Characterization data of copolymeric derivatives.

Feed		Yield ^{a)}	\bar{M}_n ^{b)}	\bar{M}_w/\bar{M}_n ^{b)}	azochromophore content		T_g ^{e)}
% mol					%	g/mol	
(S)-(+)-MECSI	(S)-(+)-MOSI				¹ H-NMR	UV-Vis	
100 ^{e)}	0	74	12700	1.70	100	0	202
75	25	77	10200	2.00	76	69	228
50	50	85	11900	2.00	53	48	228
25	75	80	9400	1.09	24	18	227
0	100 ^{f)}	67	43000	1.4	100	100	294
(S)-(-)-MECP	(S)-MAP-N						
100	0	53	6650	1.60	100	0	210
50	50	65	6700	1.50	50	48	203
0	100 ^{g)}	74	21200	1.3	0	100	208

a) Calculated as (g polymer/g monomer)·1000.

b) Determined by GPC in THF.

c) Determined by ¹H-NMR or UV-Vis.

d) Glass transition temperature determined by DSC at 10°C/min heating rate under nitrogen flow

e) [6].

f) [16]

g) [14a, 14b]

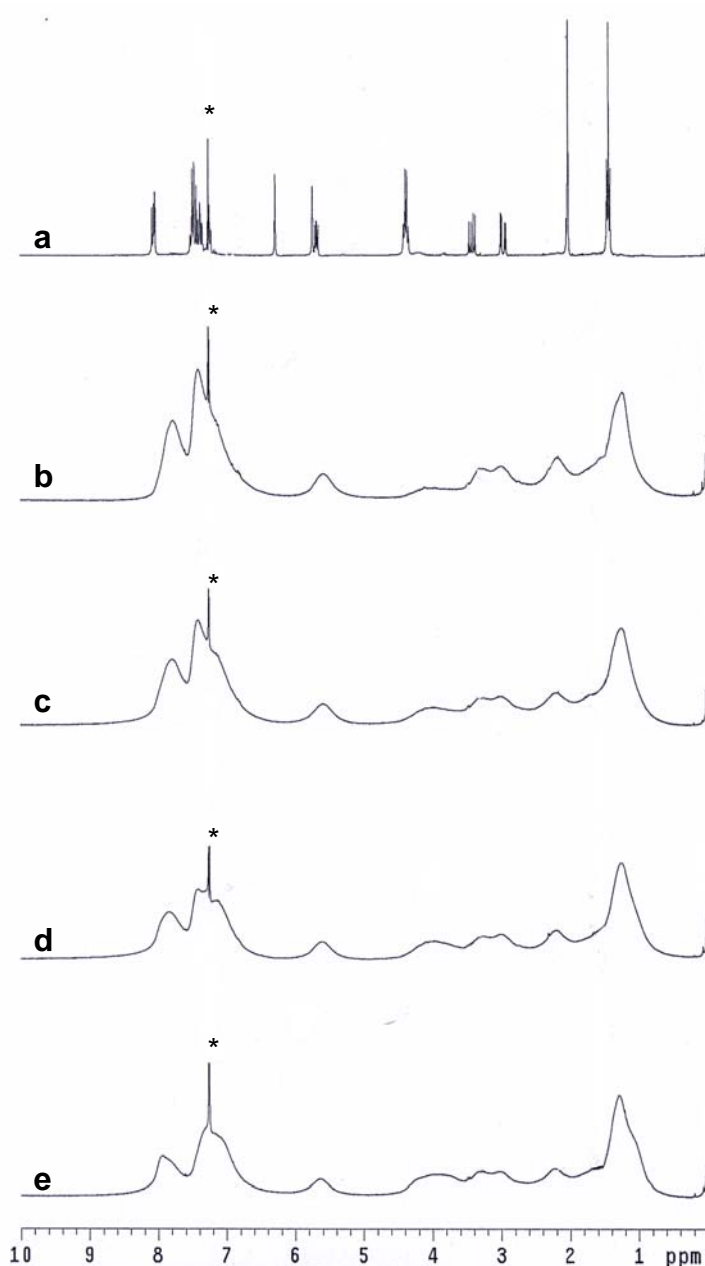


Figure 2. ^1H -NMR spectra in CDCl_3 at 25°C of the monomer (*S*)-(+)-**MECSI** (a), poly[(*S*)-(+)-**MECSI**]-*co*-(*S*)-(+)-**MOSI**] (73/27) (b), poly[(*S*)-(+)-**MECSI**]-*co*-(*S*)-(+)-**MOSI**] (53/47) (c), poly[(*S*)-(+)-**MECSI**]-*co*-(*S*)-(+)-**MOSI**] (25/75) (d) and of poly[(*S*)-(+)-**MECSI**] (e). Starred signals refer to solvent resonances.

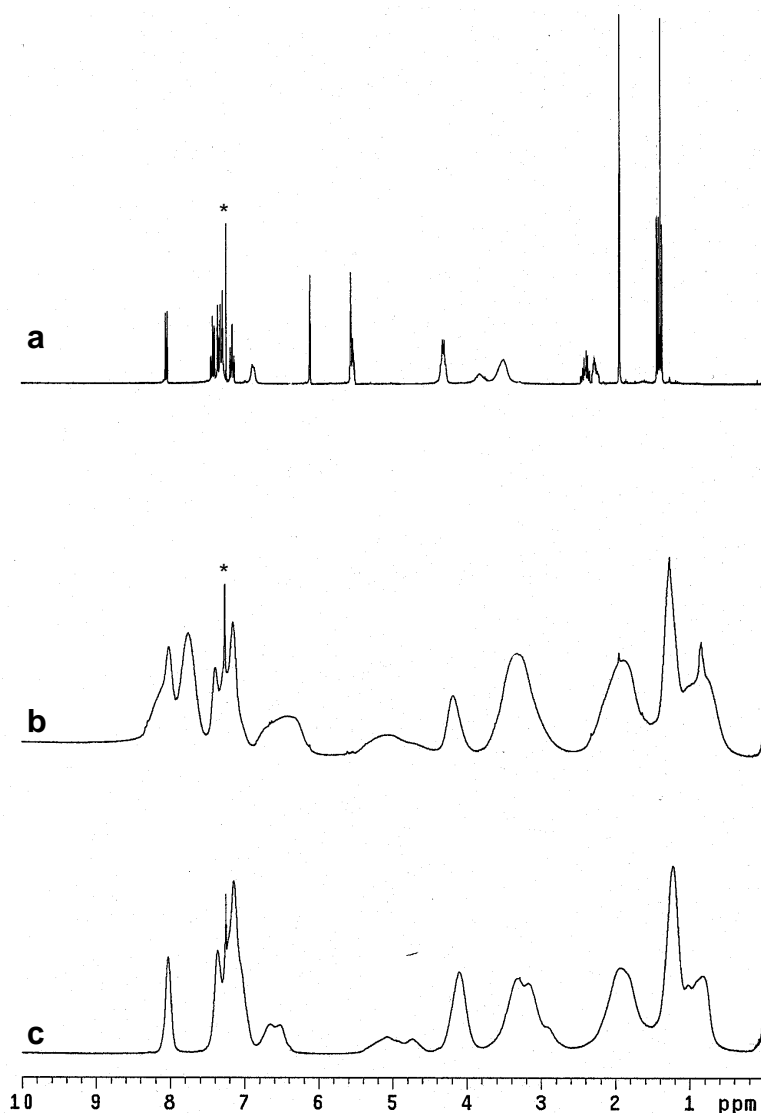


Figure 3. $^1\text{H-NMR}$ spectra in CDCl_3 at 25°C of the monomer $(S)\text{-}(-)\text{-MECP}$ (a), of poly[$(S)\text{-}(-)\text{-MECP-co-(S)-MAP-N}$] (50/50) and of poly[$(S)\text{-}(-)\text{-MECP}$] (c). Starred signals refer to solvent resonances.

Thermal analysis of polymeric derivatives

Observation of a thin film of the copolymers with a polarising microscope did not reveal any liquid crystalline behaviour.

Only second-order transitions originated by glass transitions (T_g), with no melting peaks, are observed in the DSC thermograms of the investigated polymers (Table 1),

thus suggesting that the macromolecules are substantially amorphous in the solid state. The T_g values appear quite high, laying in the range 202-205°C, that can be of interest for applications in optoelectronics.

This high thermal stability can be attributed to the reduced mobility of the macromolecular chains originated by the presence of the conformationally rigid succinimide and pyrrolidine ring interposed between the backbone and the chromophores.

Absorption spectra

As previously described, the UV-Vis absorption spectra in chloroform solution of poly[(S)-(+)-**MECSI**] and poly[(S)-(-)-**MECP**] in the region 250-500 nm, exhibit absorption bands attributed to π - π^* electronic transitions of carbazole chromophore (Table 2) [6]. These bands are related, in accordance with the Platt notation [17], to the three regions of absorbance between 350-315nm ($^1L_b \leftarrow ^1A_1$ electronic transition), 310-280 nm ($^1L_a \leftarrow ^1A_1$ electronic transition) and 280-260nm ($^1B_2 \leftarrow ^1A_1$ electronic transition).

Poly[(S)-(+)-**MOSI**] [16] exhibits two bands related to the n- π^* and π - π^* electronic transitions of the azobenzene chromophore around 447 and 320 nm, respectively (Table 2). Poly[(S)-**MAP-N**] shows, in the 250-650 nm spectral region (Table 2), two absorption bands, centered at about 470 and 290 nm, and related, the former, to combined n- π^* , π - π^* , and internal charge-transfer electronic transitions of the conjugated azoaromatic chromophore and the latter to the π - π^* electronic transition of the aromatic ring.

As expected, the UV-Vis absorption bands of the copolymers investigated display λ_{max} values similar to those of the corresponding monomers and related homopolymers (Table 2).

In particular, a qualitative analysis of the absorption bands centred at 269 e 322 nm, respectly distinctive of (S)-(+)-**MECSI** e (S)-(+)-**MOSI** co-units, shows how their relative intensity change passing from poly[(S)-(+)-**MECSI-co-(S)-(+)-**MOSI****] (73/27) to poly[(S)-(+)-**MECSI-co-(S)-(+)-**MOSI****] (25/75). (Figure 4)

It is worth to observe that it is not possible a quantitative investigation of the copolymers in the spectral area from 250 to 380 nm, associated to the sum of many different electronic transitions, with different extinction coefficients, of the two comonomers.

In order to calculate the molar amounts of (*S*)-(+)-**MOSI** and (*S*)-**MAP-N** co-units in the copolymers, the macromolecular derivatives have been exclusively investigated at the absorption bands centered at 446 and 472 nm, respectively, where the absorbance is due only to their azoaromatic chromophores.

In this way and assuming that the extinction molar coefficients are identical to the one measured for the related homopolymers, it was calculated the concentration of azoaromatic co-unit.

The molar composition calculated for poly[(*S*)-(+)-**MECSI-co-(S)-(+)-**MOSI****]s and poly[(*S*)-(-)-**MECP-co-(S)-**MAP-N****] (50/50), reported in Table 1, are in accordance with those assessed with ¹H-NMR analysis.

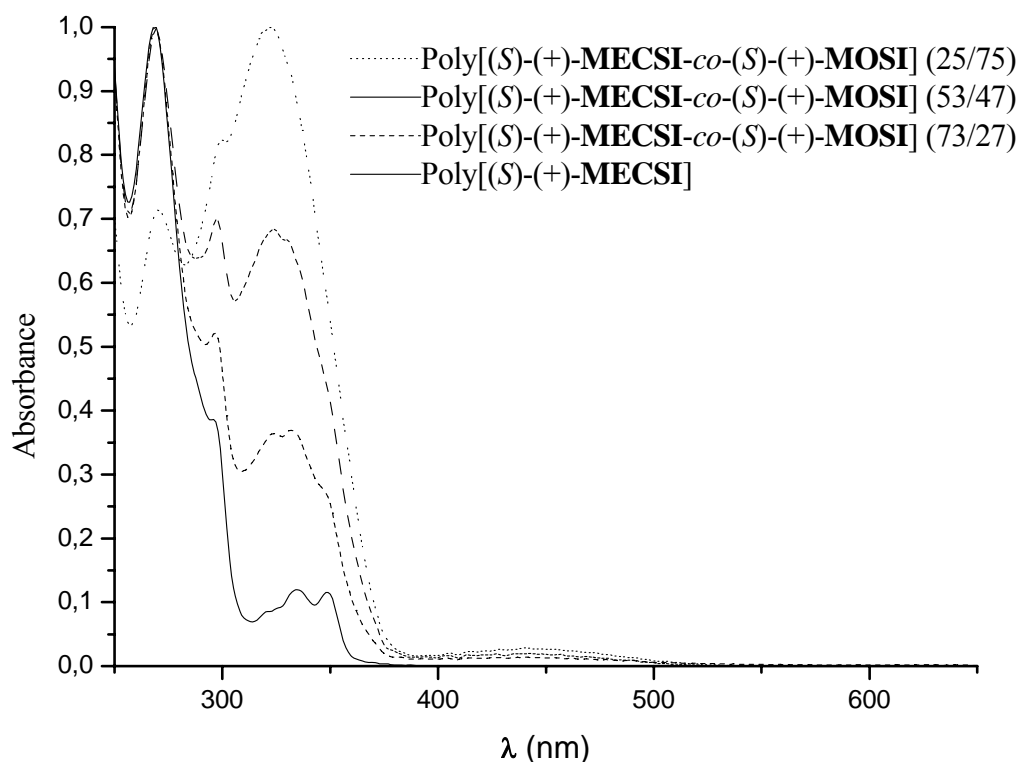


Figure 4. UV-Vis spectra in CHCl₃ solution of investigated copolymers poly[(*S*)-(+)-**MECSI-co-(S)-(+)-**MOSI****]s normalized for their maximum absorbance.

Table 2: UV-vis spectra in CHCl₃ solution at 25°C of copolymeric derivates of monomers and the corresponding homopolymers

Sample	1 st band		2 nd band		3 rd band		4 th band		5 th band	
	$\lambda_{\max}^{\text{a)}$	$\epsilon_{\max}^{\text{b)}$								
	m	Lmol ⁻¹ cm ⁻¹	nm	Lmol ⁻¹ cm ⁻¹						
Poly[(<i>S</i>)-(+)- MECSI] ^{c)}	269	21700	296	6550	305	6800	336	2100	349	2100
Poly[(<i>S</i>)-(+)- MECSI-co-(S)-(+)-MOSI] (73/27)	269	nd	296	nd	335	nd	350	nd	447	nd
Poly[(<i>S</i>)-(+)- MECSI-co-(S)-(+)-MOSI] (53/47)	269	nd	296	nd	333	nd	350	nd	447	nd
Poly[(<i>S</i>)-(+)- MECSI-co-(S)-(+)-MOSI] (25/75)	269	nd	296	nd	336	nd	350	nd	447	nd
Poly[(<i>S</i>)-(+)- MOSI] ^{d)}	-	-	-	-	320	23000	-	-	447	600
Poly[(<i>S</i>)-(-)- MECP] ^{e)}	267	24600	298	13200	313	5200	392	3700	267	24600
Poly[(<i>S</i>)-(-)- MECP-co-(S)-MAP-N] (50/50)	267	nd	297	nd	338	nd	-	-	472	nd
Poly[(<i>S</i>)- MAP-N] ^{e)}	-	-	287	11100	-	-	-	-	472	28000

a) Wavelength of maximum absorbance.

b) Calculated for one single chromophore.

c) Ref. [6]

d) Ref. [16]

e) Ref. [14a, 14b]

Chiroptical properties

With the aim to study the dependence of the optical activity on the macromolecular structure of poly[(*S*)-(+)-**MECSI-co-(S)-(+)-**MOSI**]s, the specific $\{[\alpha]_D^{25}\}$ and molar $\{[\Phi]_D^{25}\}$ optical rotation in chloroform solution at the sodium D-line of all low and high molecular weight compounds have been determined (Table 3).**

Table 3. Specific and molar optical rotation data of the synthesized compounds in CHCl₃ solution at 25°C

Sample	$[\alpha]_D^{25}$ ^a	$[\Phi]_D^{25}$ ^b
(<i>S</i>)-(+)- MECSI ^c	+0.7	+2.63
Poly[(<i>S</i>)-(+)- MECSI] ^c	+177.7	+668.0
Poly[(<i>S</i>)-(+)- MECSI-co-(S)-(+)-MOSI] (73/27)	+158.2	+589.9
Poly[(<i>S</i>)-(+)- MECSI-co-(S)-(+)-MOSI] (53/47)	+166.7	+616.6
Poly[(<i>S</i>)-(+)- MECSI-co-(S)-(+)-MOSI] (25/75)	+183.0	+669.9
(<i>S</i>)-(+)- MOSI ^d	+18.6	+67.6
Poly[(<i>S</i>)-(+)- MOSI] ^d	+202	+734.0

a) Specific optical rotation.

b) Molar optical rotation, calculated as $([\alpha]_D^{25} \cdot M/100)$, where M represents the molecular weight of the monomers or the molecular weight of the repeating unit of the polymers, or in other word the molar optical rotation calculated for carbazole unit.

c) Ref. [6]

d) Ref. [16]

The optical activities of poly[(*S*)-(+)-**MECSI-co-(S)-(+)-**MOSI**]s copolymers, as measured CHCl₃ solution at the sodium D line (Table 3 and Figure 5), appear much higher than those given by the corresponding monomers.**

These findings suggest that a remarkable contribution to optical activity by the macromolecular chains is present which could be attributed to conformational and/or configurational effects originated by a prevalent tacticity of the polymer backbone.

It is also worth observing that copolymers shown values of molar optical rotation slightly lowers to those calculate for poly[(*S*)-(+)-**MECSI**] and poly[(*S*)-(+)-**MOSI**].

This suggesting that the co-monomers behave in a cooperative way both because linked to the main chain with the same 2-hydroxysuccinimide group both because the dipolar interaction between the two chromophore (carbazole and azobenzene) can supportive favour a chiral supramolecular conformation.

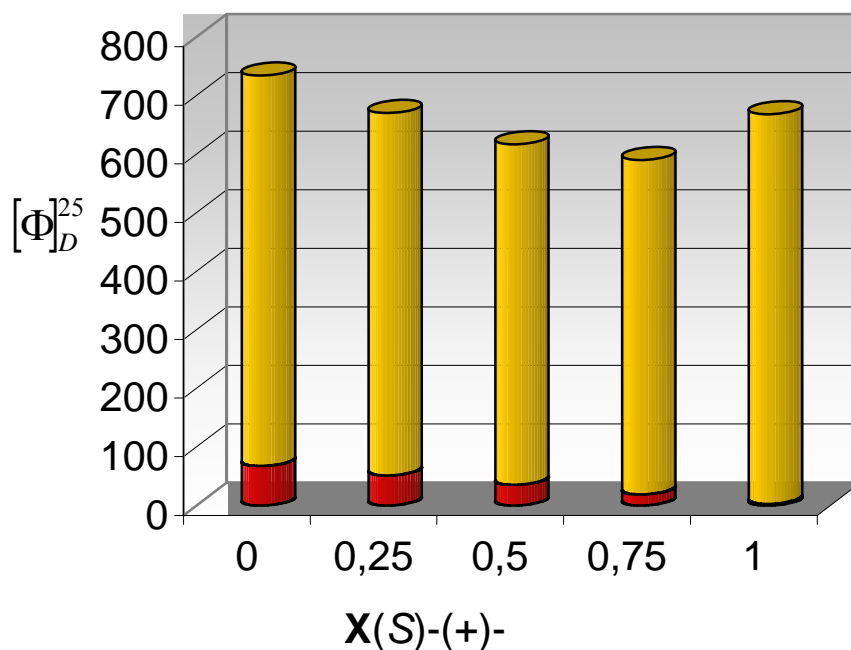


Figure 5. Molar optical rotation of poly[(S)-(+)-**MECSI**], poly[(S)-(+)-**MOSI**] and copolymers poly[(S)-(+)-**MECSI-co-(S)-(+)-MOSI**]s as a function of molar fraction of [(S)-(+)-**MECSI**] co-unit.

The chiroptical properties of all copolymeric compounds have been investigated by CD spectroscopy in the 250-700 nm spectral region in order to assess the conformational features of the macromolecular chains (Table 4 and Figure 5).

As expected, the dichroic bands observed in the CD spectra of poly[(S)-(+)-**MECSI-co-(S)-(+)-MOSI**]s strictly depend on the co-units molar composition.

Poly[(S)-(+)-**MECSI-co-(S)-(+)-MOSI**] (73/27) shows a behaviour quite similar to poly[(S)-(+)-**MECSI**] (Table 4 and Figure 5) [6] but still showing dichroic bands centered at 320 e 450 nm related to the electronic transition of azoaromatic chromophore.

Table 4. CD spectra in CHCl₃ solution at 25°C of monomers and polymeric derivatives

Sample	1st band		2nd band		3rd band		4th band		5th band		6th band										
	$\lambda_1^{a)}$	$\Delta\varepsilon_1^{b)}$	$\lambda_0^{a)}$	$\lambda_2^{a)}$	$\Delta\varepsilon_2^{b)}$	$\lambda_3^{a)}$	$\Delta\varepsilon_3^{b)}$	$\lambda_4^{a)}$	$\Delta\varepsilon_4^{b)}$	$\lambda_5^{a)}$	$\Delta\varepsilon_5^{b)}$	$\lambda_0^{a)}$	$\lambda_6^{a)}$	$\Delta\varepsilon_6^{b)}$	$\lambda_7^{a)}$	$\Delta\varepsilon_7^{b)}$	$\lambda_8^{a)}$	$\Delta\varepsilon_8^{b)}$	$\lambda_0^{a)}$	$\lambda_9^{a)}$	$\Delta\varepsilon_9^{b)}$
Poli[(S)-(-)-MECSI] ^{c)}	-	-	269	275	+4.24	297	+2.56	-	-	336	+0.54	-	-	-	351	+0.65	-	-	-	-	-
Poly[(S)-(+)-MECSI-co -(S)-(+)-MOSI] (73/27)	277	+3.98	-	-	-	298	+3.09	-	-	335	+2.01	-	-	-	447	-0.21	-	-	-	-	-
Poly[(S)-(+)-MECSI-co -(S)-(+)-MOSI] (53/47)	277	+2.55	-	-	-	299	+2.00	-	-	337	+3.56	-	-	-	442	-0.61	-	-	-	-	-
Poly[(S)-(+)-MECSI-co -(S)-(+)-MOSI] (25/75)	276	+0.63	-	-	-	295	-0.34	-	-	302	-0.20	309	339	+5.56	441	-0.21	-	-	-	-	-
Poly[(S)-(+)-MOSI] ^{d)}	-	-	-	-	-	-	-	-	-	300	-2.73	-	340	+7.57	-	-	425	-0.05	-	490	+0.06
Poly[(S)-(-)-MECP] ^{c)}	-	-	-	271	+1.40	304	+1.25	316	+1.73	-	-	-	-	-	-	-	384	-0.29	-	-	-
Poly[(S)-(-)-MECP-co -(S)-MAP-N](50/50)	267	+0.73	-	-	-	303	+0.99	316	+1.85	-	-	-	-	-	-	-	425	-0.68	444	501	+3.45
Poly[(S)-MAP-N] ^{d)}	-	-	-	-	-	285	-0.37	-	-	-	-	-	-	-	-	-	428	-6.04	-	515	+8.49

a) Wavelength of maximum dichroic absorption, expressed in nm

b) Calculated for one repeating unit in the polymer, expressed in l mol⁻¹cm⁻¹

c) Ref. [6]

e) Ref. [16]

d) Ref. [14a, 14b]

By contrast, the CD spectrum of poly[(*S*)-(+)-**MECSI**-*co*-(*S*)-(+)-**MOSI**] (25/75) exhibits two dichroic bands of opposite sign of different intensity connected to the electronic transitions of the first UV-Vis band of the azoaromatic moieties, with a cross over point around 309 nm, close to the related UV-vis maximum absorption (Table 2). Such a behaviour is more similar to poly[(*S*)-(+)-**MOSI**] and is typical of an exciton splitting determined by cooperative interactions between side-chain azoaromatic chromophores disposed in a mutual chiral geometry of one prevailing handedness [16].

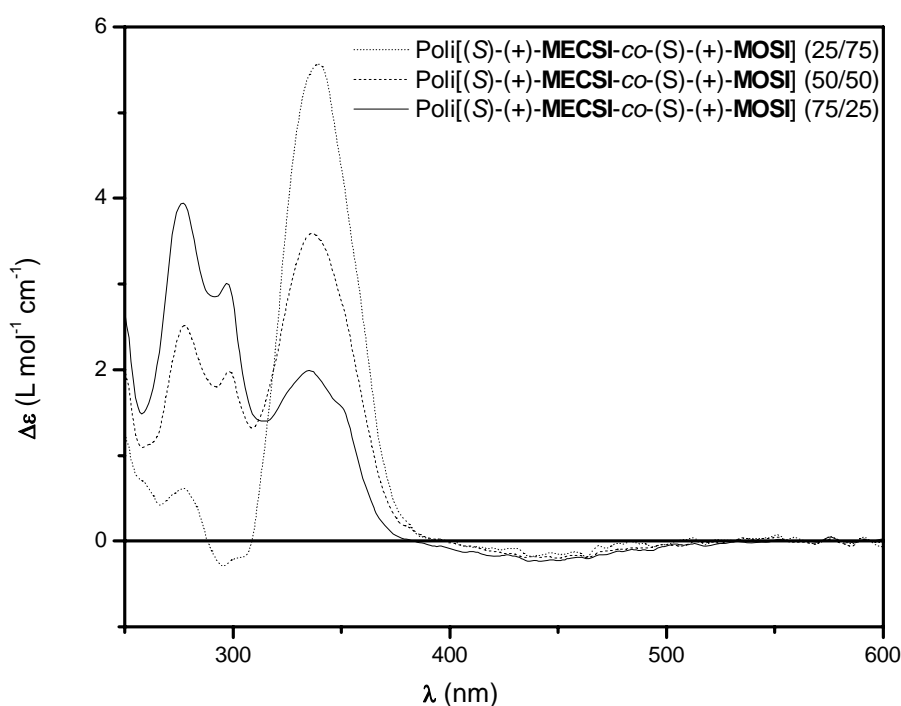


Figure 6. CD spectra in CHCl_3 solution of poly[(*S*)-(+)-**MECSI**-*co*-(*S*)-(+)-**MOSI**]s

The intensities of dichroic bands registered for the copolymeric compounds are more intensive than the related monomers (*S*)-(+)-**MECSI** and (*S*)-(+)-**MOSI**, in accordance with the optical activity data. (Table 3)

The interpretation of these data suggests that the insertion of different percentage of co-units of (*S*)-(+)-**MECSI** and of (*S*)-(+)-**MOSI** don't affects the cooperative dipolar interaction between the chiral co-units in the copolymers with the consequence that the

macromolecules maintain a chiral conformation similar to the those observed for the corresponding homopolymers.

The CD spectra of poly[(*S*)-**MAP-N**] (Table 4) [14a, 14b], both in DMA solution and as thin film, are characterized in the visible region by two intense dichroic signals of opposite sign and similar intensity with a crossover point roughly corresponding to the absorption maximum at 477 nm. These signals, which are related to the electronic transitions shown in the absorption spectra by the azobenzene chromophores, are absent in the spectra in solution of the corresponding monomer, (*S*)-**MAP-N**, representative of the repeating unit of the polymer [14a, 14b].

This behavior observed is typical of exciton splitting determined by cooperative dipole-dipole interactions between neighboring side chain azobenzene chromophores arranged in a mutual chiral geometry of one prevailing handedness [14-16].

The CD spectra of poly[(*S*)-(-)-**MECP**], as described in Chapter 3, exhibit four dichroic bands more intense than those measured for (*S*)-(-)-**MECP** confirming the establishment of a higher conformational homogeneity by the macromolecules in solution

As expected, the CD spectrum of poly[(*S*)-(-)-**MECP-co-(S)-MAP-N**] (50/50) display a behaviour similar to those described for the corresponding homopolymers (Table 4 and Figure 7). Infact, poly[(*S*)-(-)-**MECP-co-(S)-MAP-N**] (50/50) shows two dichroic signals of opposite sign and lower intensity with respect to poly[(*S*)-**MAP-N**], with a crossover point around 442 nm.

The remarkable optical activity and the intensity of dichroic band of all macromolecular compounds suggest that the amplification of chirality observed passing from monomers to copolymers is probably due to conformational effects. Thus confirming that the presence of a rigid chiral moiety of one prevailing absolute configuration, interposed between the main chain of the polymer and the azoaromatic chromophore, favors the adoption of a chiral conformation of one prevailing helical handedness, at least for chain segments of the macromolecules in solution and is persistent also in the solid state.

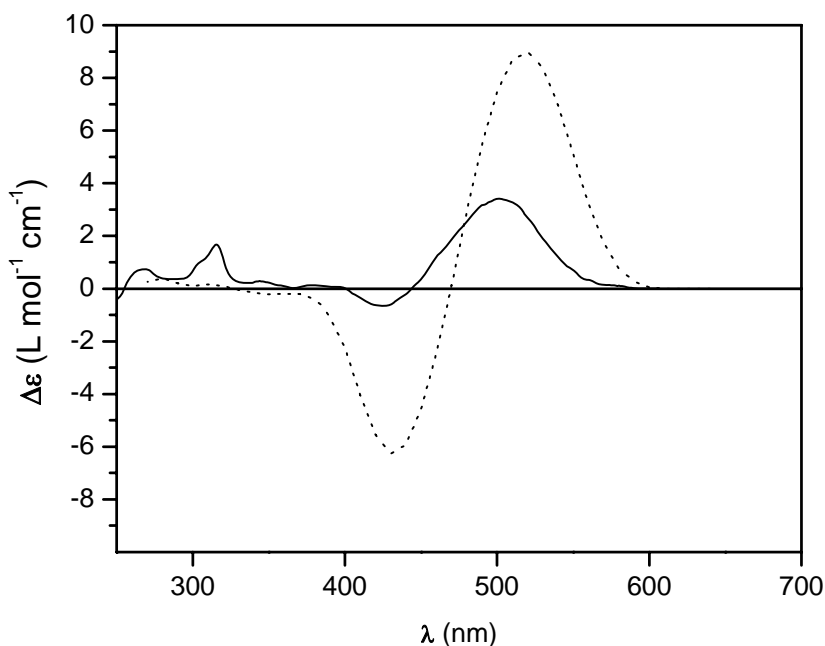


Figure 7. CD spectra in DMF solution of poly[(*S*)-(-)-**MECP-co-(S)-MAP-N**] (50/50) (—) and poly[(*S*)-**MAP-N**] (---).

Photomodulation of chiroptical properties in thin solid film.

The CD spectra of amorphous thin films of poly[(*S*)-(-)-**MECP-co-(S)-MAP-N**] (50/50) (130 nm thick, dashed line), as represented in Figure 8 and expressed in terms of ellipticity normalized for thickness, are quite similar to those shown by the same polymer in solution.

In accordance with the absorption spectra, a blue shift of the CD bands is observed on passing from the solution to the solid state. The close similarity between the CD spectra of the native polymer films and this of the copolymer in solution suggests that the macromolecules maintain chiral conformations of one prevailing helical handedness also in the solid amorphous state, at least for chain segments.

Furthermore Figure 8 shows the CD spectra of a film of poly[(*S*)-(-)-**MECP-co-(S)-MAP-N**] (50/50) as grown (full line), after an irradiation cycle with CP-L light (dashed line), and after a subsequent pumping step with CP-R light (dotted line). The pump

irradiance was set to 160 mWcm^{-2} , and during the irradiation cycles we monitored the linear birefringence (negligible in this case).

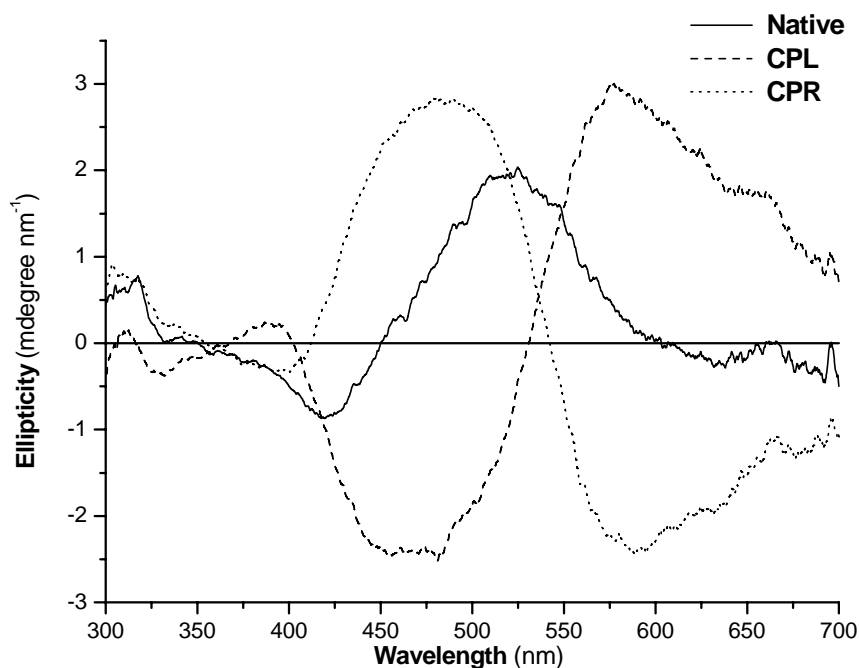


Figure 8. CD spectra of a thin film (150 nm) of poly[(*S*)-(-)-**MECP-co-(*S*)-MAP-N**] (50/50) on glass, recorded from the native film (full line) and after sequential irradiation with CP-L light (dashed line) and CP-R light (dotted line) at 488 nm ($I=160 \text{ mWcm}^{-2}$).

Irradiating with CP-L light at 488 nm the CD spectrum of a thin film of poly[(*S*)-(-)-**MECP-co-(*S*)-MAP-N**] (50/50) displays two intense dichroic signals of opposite sign, with the crossover point at 477 nm.

The couplets is asymmetric and the crossover point around 525nm and don't coincide with the maxima of the visible absorption band (450 nm).

The CD spectrum registered with CP-R shown a net inversion of signs of the dichroic bands. The two photoinduced spectra actually appear as mirror images of each other. The observed effect is reversible, and the original shape of the CD spectrum can be substantially restored by pumping with CP-L radiation.

Similar results were previously reported for optically active photochromic methacrylic polymers bearing in the side chain both a chiral group of one single configuration [14b].

It is reasonable to assume that the azobenzene chromophores are organised in a helical geometry of one prevailing handedness in the solid state as well, at least within chain segments. This implies that the polymer chains have a predominant helical structure with a well-defined sense, either left- or right handed.

However, the CD data alone do not allow us to establish the absolute sense of the helix, that is, whether it is left or right. The effect of CP-L and CP-R radiations on the CD signal can be simply interpreted by assuming its ability to invert the prevailing handedness of the polymer structure, or at least to create a statistical net excess of polymer chain sections with inverted helical sense. The mechanism of the reversible helical inversion induced by CP radiation is not well understood. In any case, for the investigated polymers, it is not related to a preliminary ordering of the azobenzene molecules with LP light, as demonstrated in our experiments.

Optically Induced and Erased Birefringence.

In order to assess the photoinduced linear dichroism and birefringence, films of the polymers have been irradiated with linearly polarized (LP) radiation (writing step) at 488 nm ($I \approx 100 \text{ mW cm}^{-2}$). After irradiation the polymers show high photoinduced linear birefringence evidenced by using probe radiation at 632.8 nm ($I \approx 1 \text{ mW cm}^{-2}$).

After irradiation with LP light, poly[(*S*)-**MAP-N**] shows a saturated photoinduced linear birefringence Δn_1 of 0.218, which, after removal of the pump, relaxes to a stable value Δn_2 of 0.211 [14b, 14d].

Poly[(*S*)-(-)-**MECP-co-(S)-MAP-N**] (50/50) display intermediate properties. The copolymer, in fact, displays a rapid increase of Δn_1 , with writing rate constants similar to poly[(*S*)-**MAP-N**], and then a slow growth to the saturation level of 0.08 (Figure 9). When the pumping light is turned off, a relaxation to the stable value of Δn_2 0.07 occurs, with a birefringence relaxation coefficient of 0.87, higher than that of poly[(*S*)-**MAP-N**].

The induced anisotropy is observed to stay stable for several months and can be reversibly erased by using CP pump radiation at 488 nm at room temperature.

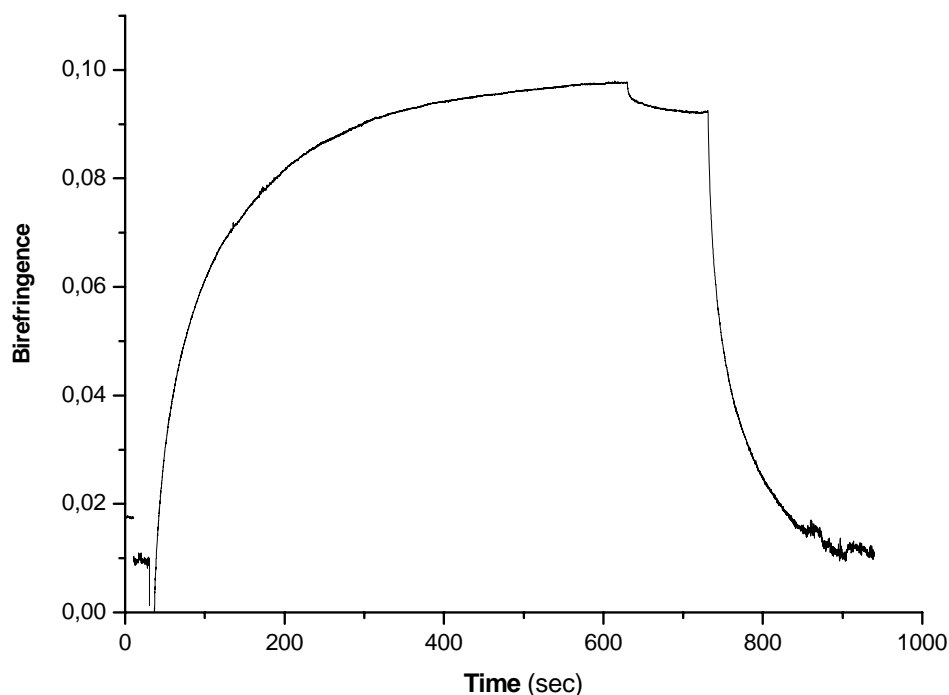


Figure 9. Optically induced birefringence curve registered for [(*S*)-(-)-**MECP-co-(S)-MAP-N**] (50/50).

Poly[(*S*)-(-)-**MECP-co-(S)-MAP-N**] (50/50) appears completely amorphous both before and after the irradiation steps, as checked by polarizing microscopy, and the driving force for the observed cooperative effect may be due to the dissimilar electrostatic dipolar interactions between adjacent (*S*)-**MAP-N** chromophores (as evidenced by the absorption and CD spectra) or to steric factors (free volume necessary for the motion of azo groups), or to a combination of both.

The complete reversibility of the photoinduced linear birefringence of the investigated copolymers, which is related to fatigue resistance properties, as shown in Figure 10, seems to be promising for use in optical storage or more generally in the field of photoresponsive systems. Indeed, after several irradiations steps with LP and CP laser beams alternatively acting on the film, the values of maximum photoinduced birefringence and erased birefringence are quite similar. This indicates that no degradation photoreactions or relevant mass motions take place on irradiation by laser

light of relatively high intensity (100 mW/cm^2). Thus, several cycles could be performed without any significant change in the photoinduced behavior.

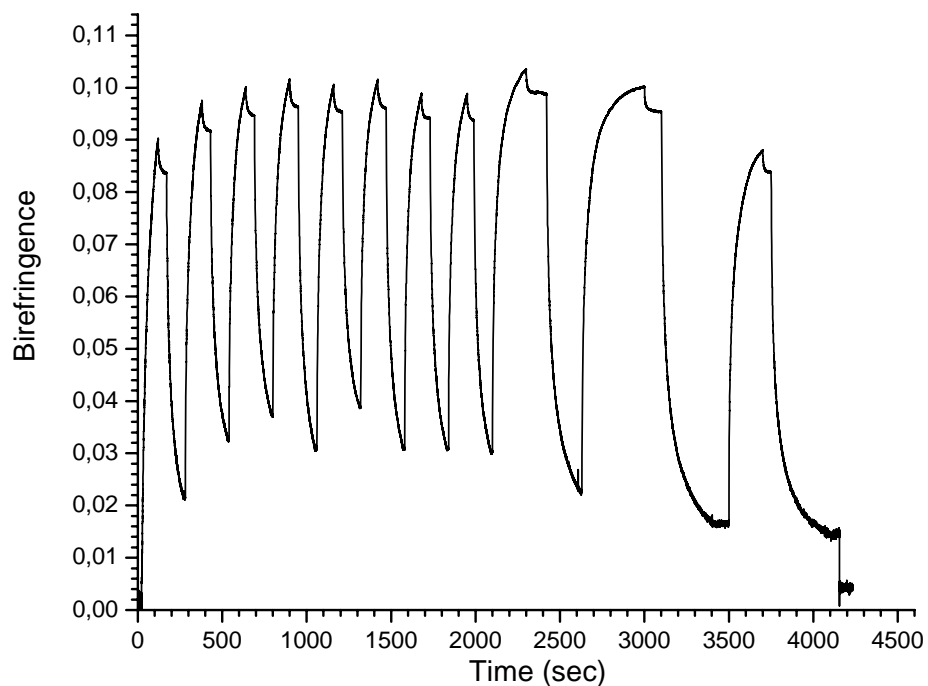


Figure 10. Complete writing-erasing cycles of optically photoinduced birefringence on a thick film of Poly[(*S*)-(-)-MECP-co-(*S*)-MAP-N] (50/50)

Copolymers containing optically active side chain 9-phenylcarbazole and azochromophores: poly[(S)-(+)-MCPS-co-(S)-(+)-MOSI], poly[(S)-(-)-MCP-PP-co-(S)-MAP-N] and poly[(S)-(-)-MCP-PP-co-(S)-MAP-C]

The synthesis and the structural characterization of new bi-functionals optically active co-polymers poly[(S)-(+)-MCPS-co-(S)-(+)-MOSI] and poly[(S)-(-)-MCP-PP-co-(S)-MAP-N] and poly[(S)-(-)-MCP-PP-co-(S)-MAP-C] have been synthesized with the aim to obtain multifunctional material which can be considered at the same time as a photonic material for NLO and optical storage, for chiroptical switches, and for photorefractive and photoconductive applications.

The optical active co-monomers (S)-(+)-MOSI, (S)-MAP-N and (S)-MAP-C were used as the electro-optic side-chain and the 9-phenylcarbazole derivatives (S)-(+)-MCPS and (S)-(-)-MCP-PP as the holes transport side-chain co-monomers.

Spectroscopic and thermal characterizations clearly indicate the occurrence of dipolar interactions between chromophores and the presence of an ordered chiral conformation of one prevailing helical handedness, at least for chain segments of the macromolecules.

Synthesis and structural characterization of copolymers.

Copolymerization of optically monomers (S)-(+)-MECPS and (S)-(-)-MCP-PP with (S)-(+)-MOSI and (S)-MAP-N and [(S)-MAP-N], respectively, were carried out in THF solution under radical conditions by using AIBN as a thermal initiator.

The obtained products were repeatedly dissolved in THF, reprecipitated in methanol, and submitted to a final purification from monomeric and oligomeric impurities by exhaustive Soxhlet extraction with methanol followed by acetone. Relevant data for the synthesized copolymers are reported in Table 5.

The occurred polymerizations and the structures of all products were confirmed by FT-IR and by ¹H- and ¹³C-NMR.

The IR spectra of the copolymeric derivatives display the disappearance of the absorption related to the stretching vibration of the methacrylic double bond and the contemporary shift (10-20 cm⁻¹) of the estereal carbonyl stretching to higher frequencies

with respect to the monomers, due to the reduced electron delocalization determined by the reaction of the methacrylic double bond.

The molar final composition of copolymers was assessed by $^1\text{H-NMR}$ by comparing the integrated signals of aromatic protons in *ortho* to amino group of azochromophoric *co*-units, located at 6.70-6.30 ppm, to those related to the aromatic protons of the 9-phenylcarbazole *co*-units.

Table 5. Characterization data of polymeric derivatives X_n

<i>Sample</i>	<i>Yield</i> ^{a)}	\bar{M}_n	\bar{M}_w/\bar{M}_n ^{b)}	T_g
		^{b)}		^{e)}
	%	g/mol		°C
poly[(<i>S</i>)-(+)- MCPS - <i>co</i> -(<i>S</i>)-(+)- MOSI] (45/55)	80	9.9	1.6	192
poly[(<i>S</i>)-(-)- MCP - <i>co</i> -(<i>S</i>)- MAP-N] (51/49)	50	7.5	1.5	181
poly[(<i>S</i>)-(-)- MCP - <i>co</i> -(<i>S</i>)- MAP-C] (54/46)	70	8.5	1.5	183

^{a)} Calculated as (g polymer/g monomer)·1000.

^{b)} Calculated according to eq. 1).

^{c)} Determined by $^1\text{H-NMR}$ or UV-Vis.

^{d)} Glass transition temperature determined by DSC at 10°C/min heating rate under nitrogen flow

Thermal analysis

The glass transition temperatures for the investigated copolymers are shown in Table 5. All the polymeric derivatives exhibit by differential scanning calorimetry (DSC) measurements only a second order thermal transition attributed to glass transition (T_g) in the range of 180-195°C (Table 5). No endothermic melting peaks, attributable to crystalline domains, are evidenced in accordance with the substantially amorphous character of the macromolecules in the solid state.

The behavior of the investigated samples is indicative of reduced mobility of the macromolecular chains originated by the presence of both the conformationally rigid pyrrolidine ring interposed between the backbone and the azoaromatic and 9-phenylcarbazole chromophores and of strong inter- and/or intramolecular dipolar interactions in the solid state between these latter side chain groups.

The high value of T_g suggest that these copolymeric materials may be promisingly tested for applications in optoelectronics, provided they are suitable modified so as to gain a satisfactory processability.

Absorption spectra

The UV-vis spectrum in THF solution of all the monomers and copolymers are reported in Table 6.

The absorption bands observed in the copolymers strictly depend on the UV-Vis properties of the single co-units: as shown for example in Figure 11 for poly[(*S*)-(+)-**MCPP-co-(*S*)-MAP-C**] (*S*)-(+)-**MCPP** and (*S*)-**MAP-C**.

The azoaromatic co-units exhibit, in the spectral range of 250-600 nm, two absorption bands: the former one, more intense, attributed to the combined $n-\pi^*$, $\pi-\pi^*$ and internal charge transfer electronic transitions of the azoaromatic chromophore; the latter to the $\pi-\pi^*$ electronic transitions of single aromatic rings. [14,16]

The phenylcarbazole co-units are characterized by distinctive absorption bands related to ${}^1L_b \leftarrow {}^1A_1$, ${}^1L_a \leftarrow {}^1A_1$ and ${}^1B_2 \leftarrow {}^1A_1$ electronic transition of the carbazole chromophore [17].

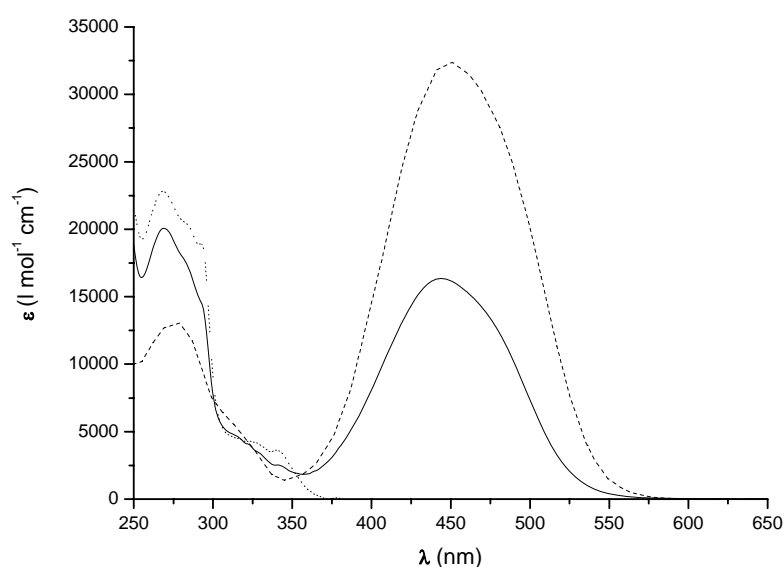


Figure 11: UV-Vis spectra in THF in solution of poly[(*S*)-(+)-**MCPP-co-(*S*)-MAP-C**] (—) (*S*)-(+)-**MCPP** (···) and (*S*)-**MAP-C** (- - -)

Table 6. UV-Vis spectra in THF solution of the investigated copolymers.

Sample	1st band		2nd band		3rd band		4th band		5th band		6th band	
	$\lambda_{\max}^{\text{a)}$	$\epsilon_{\max}^{\text{b)}$										
	nm	Lmol ¹ cm ⁻¹										
Poly[(<i>S</i>)-(+)- MCPS - co-(<i>S</i>)-(+)- MOSI]	-	-	-	-	293	17000	325	13700	-	-	442	4400
Poly[(<i>S</i>)-(+)- MCP - co-(<i>S</i>)- MAP-C]	269	20500	282	18000	293	14600	331	3400	341	2500	445	16700
Poly[(<i>S</i>)-(+)- MCP - co-(<i>S</i>)- MAP-N]	269	17400	283	16100	292	14400	330	3000	-	-	468	14700

a) Wavelength of maximum absorbance.

b) Calculated for one single chromophore.

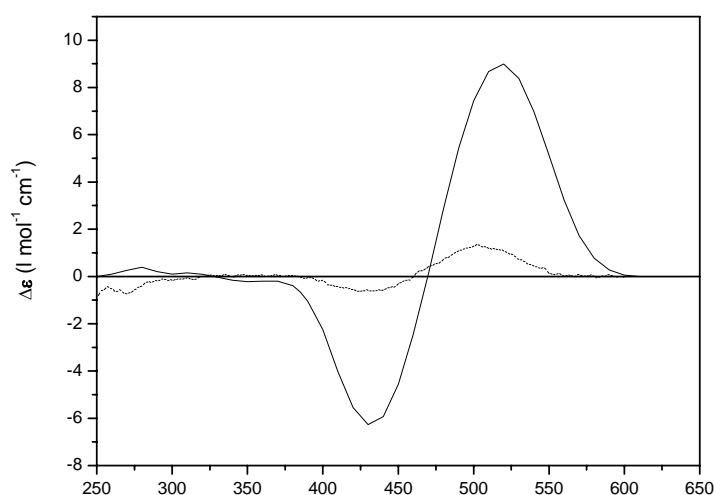
Thus, the UV-Vis spectrum of poly[(*S*)-(+)-**MCPS**-co-(*S*)-(+)-**MOSI**], poly[(*S*)-(+)-**MCPP**-co-(*S*)-**MAP-C**] and poly[(*S*)-(+)-**MCPP**-co-(*S*)-**MAP-N**] display behaviours similar to those described of the corresponding monomers (Table 6).

A small hypochromism and blue shift is observed when passing from the monomers to the related copolymer (Table 7).

Such a behaviour may be addressed to the occurrence of electrostatic dipolar interactions between neighbouring side-chain aromatic moieties along the backbone [15], as previously observed in several polymeric systems with side-chain azoaromatic chromophores [14,16].

Chiroptical properties in solution

CD spectra in THF solution (Table 8) poly[(*S*)-(+)-**MCPS**-co-(*S*)-(+)-**MOSI**], poly[(*S*)-(-)-**MCPP**-co-(*S*)-**MAP-N**] (Figure 12) and poly[(*S*)-(-)-**MCPP**-co-(*S*)-**MAP-C**] exhibit, in addition to weak bands around 269 and 280 nm related to the π - π^* electronic transition of phenylcarbazole chromophore, two dichroic signals of opposite sign and similar intensity, connected to the electronic transitions of the UV-Vis first band of (*S*)-(+)-**MOSI**, (*S*)-**MAP-N** and (*S*)-**MAP-C** with crossover points around 305, 428 and 460 nm, respectively, close to the corresponding UV-Vis maximum absorptions.



Errore.

Figure 12. CD spectra in DMF solution of poly[(*S*)-(-)-**MCPP**-co-(*S*)-**MAP-N**] (50/50) (---) and poly[(*S*)-**MAP-N**] (—)

Table 7. CD spectra in THF solution of investigated copolymers.

Sample	1st band		2nd band		3rd band				4th band		
	$\lambda_1^a)$	$\Delta\epsilon_1^b)$	$\lambda_3^a)$	$\Delta\epsilon_3^b)$	$\lambda_5^a)$	$\Delta\epsilon_5^b)$	$\lambda_0^c)$	$\lambda_6^a)$	$\Delta\epsilon_6^b)$	$\lambda_8^a)$	$\Delta\epsilon_8^b)$
	nm	l mol ⁻¹ cm ⁻¹	nm	l mol ⁻¹ cm ⁻¹	nm	l mol ⁻¹ cm ⁻¹	nm	nm	l mol ⁻¹ cm ⁻¹	nm	l mol ⁻¹ cm ⁻¹
Poli[(S)-(+)-MCPS-co-(+)-MOSI]	-	-	-	-	297	-0,96	305	342	+3,03	442	-0,24
Poli[(S)-(+)-MCP-PP-co-MAP-C]	270	+0,69	286	0,17	410	-0,33	428	480	+2,06		
Poli[(S)-(+)-MCP-PP-co-MAP-N]	269	-0,71	336	+0,21-	430	-0,60	460	503	+1,36		

a) Wavelength of maximum absorbance.

b) Calculated for one single chromophore

c) Wavelength of crossover point

These excitonic couplet are not present in the CD spectra of the monomers which, in solution, do not possess any structural restriction, display only weak dichroic signals related to UV-Vis bands indicative of the absence of chiral conformations in solution.

Such a behavior is typical of an exciton splitting determined by cooperative interactions between side-chain azobenzene chromophores disposed in a mutual chiral geometry of one prevailing handedness.

These results suggest that all the copolymeric derivatives assume in THF solution conformational arrangements with a prevailing chirality, at least for chain sections and that the conformational rigidity of the optically active group interposed between the main chain and the aromatic chromophores plays an important role in determining the extent of conformational order in solution by these macromolecular systems. This favors the assumption by the azoaromatic and 9-phenylcarbazole chromophores of regular orientations, despite the repulsion induced by the local electric fields when permanent dipoles are present.

Optically Induced Birefringence

Films of the copolymers have been irradiated with linearly polarized (LP) radiation (writing step) at 488 nm ($I \approx 100 \text{ mW cm}^{-2}$). After irradiation the polymers show high photoinduced linear birefringence evidenced by using probe radiation at 632.8 nm ($I \approx 1 \text{ mW cm}^{-2}$) where the polymers have negligible absorption.

Figure 13 present the writing-erasing curve for poly[(*S*)-(-)-MCP-*co*-(*S*)-MAP-C] showing the typical change of photoinduced birefringence signals of the polymers when the pumping LP light is on or off.

It is clear that there is a rapid increase at the beginning of pumping by the 488 nm laser beam then a slow growth to the saturation level. When the pumping light is turned off a slight relaxation to stable values occurs as some chromophoric moieties do not remain oriented on a long-term basis.

The photoinduced linear ordering, as shown in Figure 13, can be reversibly erased by using CP or depolarized pump radiation. After irradiation with CP light at room temperature the photoinduced linear birefringence is reduced to a negligible value (erasing step).

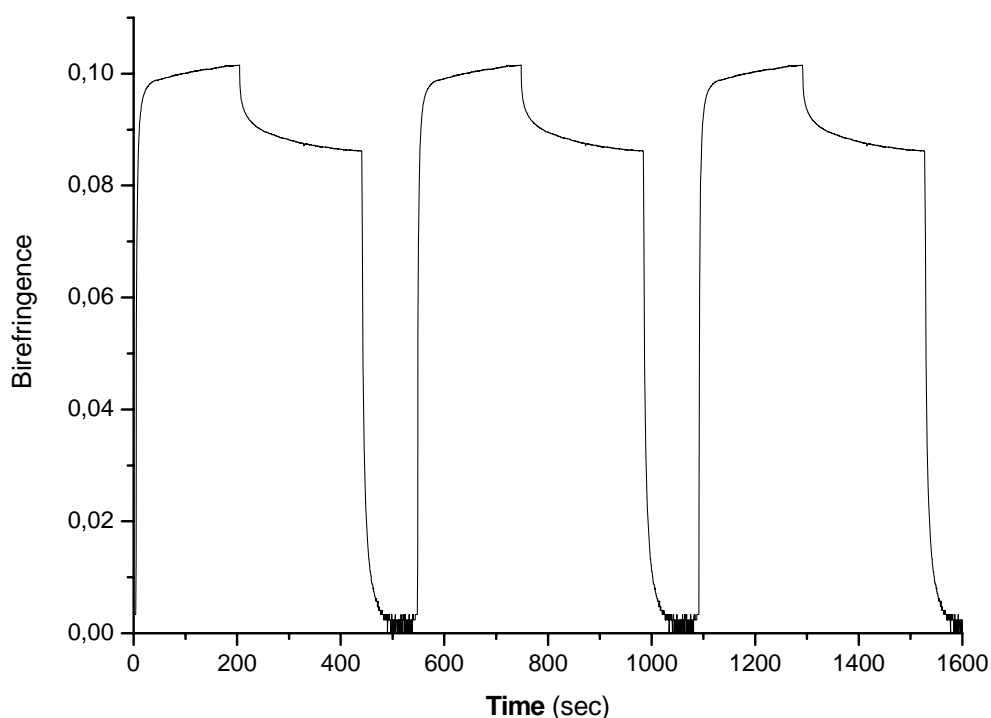


Figure 13. Complete writing-erasing cycles of optically photoinduced birefringence on a thick film of poly[(*S*)-(-)-MCP-PP-co-(*S*)-MAP-C].

As shown in Figure 13 for poly[(*S*)-(+)-MCP-PP-co-(*S*)-MAP-C], the complete reversibility of the photoinduced linear birefringence of investigated copolymeric samples, which are related to fatigue resistance properties, after several writing-erasing cycles by photoirradiation alternatively with LP and CP light at 488 nm, seems to be promising for use in optical storage or more generally in the field of photoresponsive systems. Indeed, after several irradiations steps with LP and CP laser beams alternatively acting on the 200 nm thick film of poly[(*S*)-(-)-MCP-PP-co-(*S*)-MAP-C], the values of maximum photoinduced birefringence (after each irradiation with LP light) and of erased birefringence (after each irradiation with CP light) are quite similar. This indicates that no degradation photoreaction took place upon irradiation with laser light of relatively high intensity (100 mW/cm^2). Thus, several cycles could be performed without any significant change in the photoinduced behaviours.

Optically Induced Diffraction Grating

Surface relief gratings (SRG) have been inscribed on thin films of poly[(*S*)-(-)-**M CPP**-co-(*S*)-**MAP-C**] and poly[(*S*)-(-)-**M CPP**-co-(*S*)-**MAP-N**] in using left and right circularly polarized interfering beams at 514 nm (100 mW/cm²).

The gratings were optically inscribed onto the films using a setup illustrated in Figure 14.

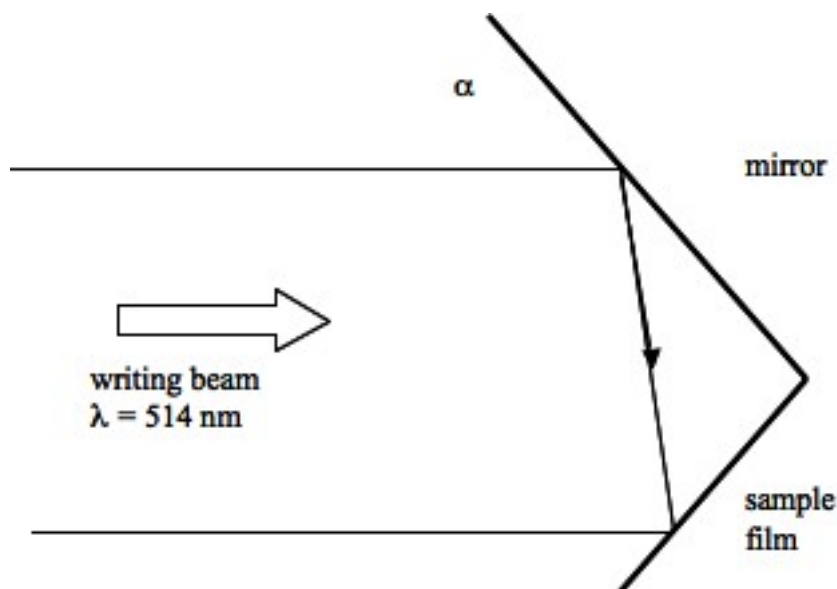


Figure 12. Setup for optically inscribing surface relief gratings.

The writing beam was formed by expanding and collimating a 5 mW circularly polarized argon laser beam at 514 nm to a diameter of 3 mm giving a power density of 70 mW/cm². These power levels were not high enough to produce permanent surface damage as would be caused in the case of ablation. This beam was incident onto the sample holder which consisted of a sample stage set at right angles to a front surface mirror. The portion of the beam which strikes the mirror is reflected back into the sample to interact with the direct beam and form an interference pattern on and throughout the sample. The wavelength of the laser as well as the angle of incidence α of the writing beam to the sample holder can be adjusted to change the spacing of the interference pattern. The light in the interference pattern is absorbed by the polymer film and the formation of a grating has been observed.

The grating spacing is easily controlled by selecting the incidence angle α .

The time evolution of the optically induced grating is monitored using a He-Ne probe beam at 633 nm. This beam is used because it is not absorbed by the film and can be left on without disturbing the results. The probe beam is nearly parallel to the writing beam and the films are sufficiently thin so that the Bragg condition on the angle of incidence is not a critical parameter in these measurements.

Atomic force microscope AFM was used to examine the surface of the polymer films where gratings with spacing ranging from 360 to 1000 nm had been inscribed. The gratings show a typical sinusoidal profile as shown in Figure 15.

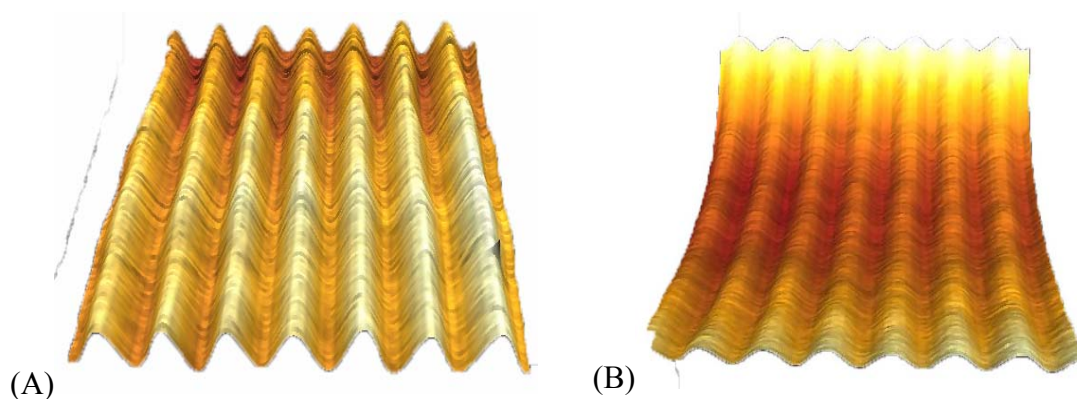


Figure 15. Tridimensional AFM image 5x5 μm of a 400 nm film of (A) poly[(S)-(+)-**M CPP**-co-(S)-**MAP-C**] and (B) poly[(S)-(+)-**M CPP**-co-(S)-**MAP-N**]

The gratings can also be erased by heating the polymer above its glass transition temperature and/or another grating can be inscribed.

Conclusion

Optically active multifunctional polymeric derivatives deriving from the radical copolymerization of azoaromatic monomers, such as (*S*)-(+)-**MOSI**, (*S*)-**MAP-N** and (*S*)-**MAP-C**, with carbazole monomers, such as (*S*)-(+)-**MECSI**, (*S*)-(-)-**MECP**, (*S*)-(-)-**MEPS** and (*S*)-(-)-**MEPP**, have been prepared and fully characterized.

The remarkable optical activity and the intensity of dichroic bands of all copolymeric compounds suggest that the amplification of chirality observed passing from monomers to polymers is probably due to a conformational effect. This behaviour suggests that the main effect on the macromolecular conformation is due to the chiral groups of the (*S*)-2-hydroxysuccinimide and of the (*S*)-3-hydroxypyrrolidine linked between the main chain and the carbazole and azobenzene chromophore that can provide to the macromolecules to assume a conformational dissymmetry of one prevailing screw sense.

The presence in the side-chain of conformationally rigid chiral residues of the (*S*)-2-hydroxysuccinimide and of the (*S*)-3-hydroxypyrrolidine allows to achieve high *T_g* values which can be of interest for applications in optoelectronics.

The macromolecular derivatives are characterized by enhanced photoinduced linear birefringence with high stability and relaxation values with respect to analogue copolymer systems present in literature, thus allowing the storage of the optical information written over the material.

The photomodulation of the chiroptical properties of thin polymeric film seems to offer the possibility of producing reversible chiroptical switching between two enantiomeric chiral arrangements of the macromolecular materials.

Surface relief gratings (SRG) have been inscribed on thick films of the copolymers using left and right circularly polarized interfering beams at 488 nm (100 mW/cm²).

The surface gratings produced are permanent as long as the temperature of the sample is kept below its *T_g*.

Due to many properties shown, it is possible to consider these multifunctional copolymeric derivatives of potential interest for several advanced applications, such as optical storage, waveguides, chiroptical switches, chemical photoreceptors, NLO, surface relief gratings, photoconductive materials, etc.

Experimental section

Chemicals

Monomers (*S*)-(+)-**MECSI**, (*S*)-(+)-**MECP**, (*S*)-**MCPS**, (*S*)-**MCP**, (*S*)-(+)-**MOSI**, (*S*)-**MAP-N** and (*S*)-**MAP-C** were synthesized as previously reported [6,15].

Tetrahydrofuran (THF) was purified and dried according to the reported procedures[18] and stored over molecular sieves (4 Å) under nitrogen.

2,2'-Azobisisobutyronitrile (AIBN) (Aldrich) was crystallized from abs. ethanol before use. All other reagents and solvents (Aldrich) were used as received without further purification.

General procedure of the radical copolymerization

The copolymerizations were carried out in glass vials using AIBN as free radical initiator and THF as solvent. The reaction mixture (1.0 gr of monomers, 2% weight of AIBN in 20 ml THF) was introduced into the vial under nitrogen atmosphere, submitted to several freeze-thaw cycles and heated at 60°C for 72 h. The reaction was then stopped by pouring the mixture into a large excess (100 ml) of methanol, and the coagulated polymer filtered off. The solid polymeric product was repeatedly dissolved in THF at room temperature and precipitated several times in methanol. The macromolecular material was finally dried at 60°C under vacuum for several days to constant weight. All products were characterized by FT-IR and by ¹H- and ¹³C-NMR. Relevant data for the synthesized copolymers are reported in Table 1.

Poly[(*S*)-(+)-MECSI-co-(*S*)-(+)-MOSI] (73/27)

¹H-NMR (CDCl₃) (δ in ppm dal TMS): 8.00-6.80 (m, 16H, aromatic), 5.80 (m, 1H, CH-CH₂), 4.00 (m, 2H, N-CH₂-CH₃), 3.40-3.10 (m, 2H, CH-CH₂), 2.20-1.05 (m, 5H, CH₃ e CH₂ main chain and 3H, N-CH₂-CH₃).

FT-IR (KBr) (cm⁻¹): 3047 (ν_{CH} aromatic), 2974 (ν_{CH} aliphatic), 1723 (ν_{C=O} ester aliphatic and ν_{C=O} imidic), 1600(ν_{C=C} aromatic), 1379 (δ_{CH₃}), 840 (δ_{CH} aromatic ring 1,4-bissubstituted), 766 e 724 (δ_{CH} aromatic ring 1,2,4-trisubstituted), 746 (δ_{CH} aromatic ring 1,2-bissubstituted), 700 e 690 (δ_{CH} aromatic ring monosubstituted)

Poly[(*S*)-(+)-**MECSI**-*co*-(*S*)-(+)-**MOSI**] (51/49)

¹H-NMR(CDCl₃) (δ in ppm dal TMS): 8.00-6.80 (m, 16H, aromatic), 5.80 (m, 1H, CH-CH₂), 4.00 (m, 2H, N-CH₂-CH₃), 3.40-3.10 (m, 2H, CH-CH₂), 2.20-1.05 (m, 5H, CH₃ e CH₂ main chain e 3H, N-CH₂-CH₃).

FT-IR (KBr) (cm⁻¹): 3053 (ν_{CH} aromatic), 2974 (ν_{CH} aliphatic), 1723 (ν_{C=O} ester aliphatic e ν_{C=O} immidici), 1600(ν_{C=C} aromatic), 1379 (δ_{CH₃}), 841 (δ_{CH} aromatic ring 1,4-disubstituted), 766 e 727 (δ_{CH} aromatic ring 1,2,4-trisubstituted), 749 (δ_{CH} aromatic ring 1,2-bissubstituted), 700 e 688 (δ_{CH} aromatic ring monosubstituted)

Poly[(*S*)-(+)-**MECSI**-*co*-(*S*)-(+)-**MOSI**] (21/79)

¹H-NMR (CDCl₃) (δ in ppm dal TMS): 8.00-6.80 (m, 16H, aromatic), 5.80 (m, 1H, CH-CH₂), 4.00 (m, 2H, N-CH₂-CH₃), 3.40-3.10 (m, 2H, CH-CH₂), 2.20-1.05 (m, 5H, CH₃ e CH₂ main chain e 3H, N-CH₂-CH₃).

FT-IR (KBr) (cm⁻¹): 3053 (ν_{CH} aromatic), 2980 (ν_{CH} aliphatic), 1723 (ν_{C=O} ester aliphatic e ν_{C=O} immidici), 1600(ν_{C=C} aromatic), 1381 (δ_{CH₃}), 839 (δ_{CH} aromatic ring 1,4-disubstituted), 769 e 724 (δ_{CH} aromatic ring 1,2,4-trisubstituted), 746 (δ_{CH} aromatic ring 1,2-bissubstituted), 700 e 688 (δ_{CH} aromatic ring monosubstituted)

Poly[(*S*)-(-)-**MECP**-*co*-(*S*)-**MAP-N**] (50/50):

¹H-NMR (CDCl₃): 8.05-6.80 (m, 15H, 8H azo-arom. e 7H carbazole), 5.20 (m, 1H, CH-CH₂), 4.30 (m, 2H, N-CH₂-CH₃), 3.80-3.50 (m, 4H, -CH₂-N pyrrolidine), 2.10-0.90 (m, 2H, CH₂-CH pyrrolidine, 5H, CH₃ e CH₂ main chain e 3H N-CH₂-CH₃ carbazole) ppm.

FT-IR (KBr) (cm⁻¹): 3047 (ν_{CH} arom.), 2969(ν_{CH} aliph.), 1725 (ν_{C=O} aliph. ester), 1602 e 1516 (ν_{C=C} arom.), 1334 (δ_{NO₂}), 855 e 822 (δ_{CH} arom. rings, 4-disubst.), 788-744 (δ_{CH} arom. ring 1,2,4-trisubst.), 714 (δ_{CH} arom. ring 1,2-disubst.)

Poly[(*S*)-(+)-**MCPS**-*co*-(*S*)-(+)-**MOSI**] (55/45)

¹H-NMR (CDCl₃): 8.00-7.00 (m, 20H, arom.), 5.70 (m, 2H, c-H-succinimide), 3.40-2.90 (2dd, 4H, d-H-succinimide), 2.10-1.00 (m, 3H, CH₃ e 2H, CH₂ main chain) ppm.

FT-IR (KBr) (cm^{-1}): 3050 (ν_{CH} arom.), 2967 (ν_{CH} aliph.), 1724 ($\nu_{\text{C=O}}$ ester), 1600 ($\nu_{\text{C=C}}$ arom.), 1512 (δ_{CH_2}), 1365 (ν_{CH_3} CH₃), 1200 ($\nu_{\text{C-O}}$ ester), , 851 e 830 (δ_{CH} arom. ring 1,4-disubst.), 747 (δ_{CH} arom. ring 1,2-disubst.).

Poly[(*S*)-(+)-**MCPP**-*co*-(*S*)-**MAP-N**] (49/51)

¹H-NMR (CDCl₃): 8.30-8.20 (d, 2H, arom. 2,7-carbazole), 7.80-7.00 (m, 14H, arom. 1,3,4,5,6,8-carbazole, 15,19-phenyl, e 6H arom. (*S*)-**MAP-N**), 6.80-6.30 (m, 4H, 16,18-phenyl and 2H ortho (*S*)-**MAP-N**), 5.40-5.20 (m, 2H, d-CH-pyrrolidine), 3.60-3.40 (m, 8H, c,f-CH₂ pyrrolidine), 2.40-1.00 (m, 4H, CH₂-pyrrolidine and 5H - CH₃ and CH₂ - main chain) ppm.

FT-IR (KBr) (cm^{-1}): 3046 (ν_{CH} arom.), 2970 (ν_{CH} aliph.), 1727 ($\nu_{\text{C=O}}$ ester) 1608 ($\nu_{\text{C=C}}$ arom.), 1517 (ν_{CH_2}), 1448 (ν_{CNas} CH₃), 1375 (ν_{CH_3} CH₃), 1161 ($\nu_{\text{C-O}}$ ester), 851 e 814 (δ_{CH} arom. ring 1,4-disubst.), 746 (δ_{CH} arom. ring 1,2-disubst.).

Poly[(*S*)-(+)-**MCPP**-*co*-(*S*)-**MAP-C**] (46/54)

¹H-NMR (CDCl₃): 8.30-8.20 (d, 2H, arom.2,7-H-carbazole), 7.80-7.00 (m, 14H, arom.1,3,4,5,6,8-H-carbazole, 15,19-H-arom and arom. (*S*)-**MAP-C**), 6.80-6.40 (m, 4H, 16,18-H-arom.), 5.40-5.20 (m, 2H, chiral CH), 3.60-3.40 (m, 8H, CH₂), 2.40-2.00 (m, 4H, CH₂), 1.60 (s, 6H, CH₃ main chain) ppm,.

FT-IR (KBr) (cm^{-1}): 3050 (ν_{CH} arom.), 2967 (ν_{CH} aliph.), 1737 ($\nu_{\text{C=O}}$ ester) 1608 ($\nu_{\text{C=C}}$ arom.), 1519 (ν_{CH_2}), 1451 (ν_{CNas} CH₃), 1365 (ν_{CH_3} CH₃), 1161 ($\nu_{\text{C-O}}$ ester), 851 e 814 (δ_{CH} arom. ring 1,4-disubst.), 746 (δ_{CH} arom. ring 1,2-disubst.).

Measurements

NMR spectra were obtained at room temperature on 5-10% CDCl₃ solutions using a Varian NMR Gemini 300 spectrometer. Chemical shifts are given in ppm from tetramethylsilane (TMS) as the internal reference. ¹H-NMR spectra were run at 300 MHz by using the following experimental conditions: 24 000 data points 4.5-kHz spectral width 2.6-s acquisition time 128 transients. ¹³C NMR spectra were recorded at 75.5 MHz, under full proton decoupling, by using the following experimental

conditions: 24000 data points, 20 kHz spectral width, 0.6 s acquisition time, 64000 transients.

FT-IR spectra were carried out on a Perkin-Elmer 1750 spectrophotometer equipped with an Epson Endeavor II data station on sample prepared as KBr pellets.

Number average molecular weight (\bar{M}_n) and polydispersity (\bar{M}_w/\bar{M}_n) were determined in THF solution by SEC using a HPLC Lab Flow 2000 apparatus, equipped with an injector Rheodyne 7725i, a Phenomenex Phenogel 5 μ MXL column and a UV-Vis detector Linear Instruments model UVIS-200, working at 254 nm. Calibration curves were obtained by using several monodisperse polystyrene standards.

UV-vis absorption spectra were recorded at 25°C on a Perkin Elmer Lambda 19 spectrophotometer on CHCl₃ solutions by using cell path lengths of 1 and 0.1 cm for the 500-320 and 320-250 nm spectral regions, respectively. Carbazole chromophore concentrations of about 5·10⁻⁴ mol L⁻¹ were used.

Optical activity measurements were accomplished at 25°C on CHCl₃ solutions with a Perkin Elmer 341 digital polarimeter, equipped with a Toshiba sodium bulb, using a cell path length of 1 dm. Specific and molar rotation values at the sodium D line are expressed as deg·dm⁻¹·g⁻¹·cm³ and deg·dm⁻¹·mol⁻¹·dL, respectively. Molar rotation for polymers refers to the molecular weight of the repeating unit.

Circular dichroism (CD) spectra were carried out at 25°C on CHCl₃ solutions on a Jasco 810 A dichrograph, using the same path lengths and solution concentrations as for the UV-Vis measurements. $\Delta\epsilon$ values, expressed as L·mol⁻¹·cm⁻¹ were calculated from the following expression: $\Delta\epsilon = [\Theta]/3300$, where the molar ellipticity $[\Theta]$ in deg·cm²·dmol⁻¹ refers to one carbazole chromophore.

The glass transition temperature values were determined by differential scanning calorimetry (DSC) on a TA Instrument DSC 2920 Modulated apparatus at a heating rate of 10°C/min under nitrogen atmosphere on samples of 5-9 mgr.

The initial thermal decomposition temperature (T_d) was determined on the polymeric sample with a Perkin-Elmer TGA-7 thermogravimetric analyzer by heating the samples in air at a rate of 20°C/min.

Absorption spectra of the films were carried out under the same instrumental conditions as the related solutions. The photoinduced linear birefringence was measured in situ

using a pump and probe setup by monitoring the transmittance of the samples interposed between two crossed polarizers. The pump radiation at 488 nm was produced by a small frame Ar⁺ laser, Spectra Physics model 165, whereas the source for the probe light was a Melles-Griot 10 mW He-Ne laser at 632.8 nm. The degree of linear polarization of the writing pump radiation was enhanced by using a Glan-Taylor prism polarizer, whereas a multiple order *i*/4 quartz waveplate for 488 nm was employed to circularize the pump radiation for the erasing steps.

Refenceres

- [1] J.V. Grazuleviciusa, P. Strohrrieglb, J. Pielichowskic, K. Pielichowski, *Prog. Polym. Sci.* 28 (2003) 1297–1353
- [2] W.E. Moerner, A. Grunnet-Jepsen, C.L. Thompson, *Annu. Rev. Mater. Sci.* 1997, 27, 583-623;
- [3] P.N. Prasad, M.E. Orczyk, J. Zieba, *J. Phys. Chem.* 1994, 98, 8699;
- [4] K. Meerholz, B. Volodin, B. Sandalphon, N. Kippelen, N. Peyghambarian, *Nature* 1994, 371, 497
- [5] T. Uryu, H. Ohkawa, R. Oshima, *J. Pol. Scie: Part B: Poly Phy Vol 26*, 1227-1236 (1988).
- [6] L. Angiolini, L. Giorgini, A. Golemme, F. Mauriello, R. Termine, *Macromol Chem Phys*, in press 2008.
- [7] [7a] *Proceedings of the Symposium on Azobenzene-Containing Materials*, Boston MA (U.S.A.) 1998, ed. A. Natansohn, *Macromolecular Symposia* 137, 1999. pp.1–165. [7b] A. Natansohn, P. Rochon, M. S. Ho, C. Barrett, *Macromolecules* 1995, 28, 4179. [7c] Y. Wu, Q. Zhang, A. Kanazawa, T. Shiono, T. Ikeda, Y. Nagase, *Macromolecules* 1999, 32, 3951. [7d] C. R. Mendonca, A. Dhanabalan, D. T. Balogh, L. Misoguti, D. S. Dos Santos Jr., M.A. Pereira-da-Silva, J. A. Giacometti, S. C. Zilio, O. N. Jr. Oliveira, *Macromolecules* 1999, 32, 1493. [7e] J. H. Kim, S. Kumar, S. D. Lee, *Phys. Rev. E*, 1998, 57, 5644. [6f] K. Ichimura, *Chem. Rev.*, 2000, 100, 1847. [7g] A. Natansohn, P. Rochon, J. Gosselin, S. Xie, *Macromolecules* 1992, 25, 2268.
- [8] W. M Gibbons, P. J. Shannon, S. T. Sun, B. J. Swetlin, *Nature* 1991, 351, 49. [8b] N. C. R. Holme, P. S. Ramanujam, S. Hvilsted, *Opt. Lett.* 1996, 21, 902.
- [9] H. Katz, K. Singer, J. Sohn, C. Dirk, *J. Am. Chem. Soc.* 1987, 109, 6561. [9b] J. A. Delaire, K. Nakatani, *Chem. Rev.* 2000, 100, 1817.
- [10] T. Todorov, L. Nikolova, N. Tomova, *Appl. Opt.*, 1984, 23, 4588. [10b] L. Andruzzi, A. Altomare, F. Ciardelli, R. Solaro, S. Hvilsted, P. S. Ramanujam, *Macromolecules* 1999, 32, 448. [10c] M. Eich, J. H. Wendorff, B. Reck, H. Ringsdorf, *Macromol. Chem. Rapid Commun.* 1987, 8, 56.

- [11] G. Iftime, F. L. Labarthe, A. Natansohn, P. Rochon, *J. Am. Chem. Soc.* 2000, 122, 12646. [11b] T. Verbiest, M. Kauranen, A. Persoon, *J. Mat. Chem.* 1999, 9, 2005.
- [12] Y. Wu, A. Natansohn, P. Rochon, *Macromolecules* 2004, 37, 6090-6095. [12b] A. Natansohn, P. Rochon, *Chem. Rev.* 2002, 102, 4139-4175.
- [13] M. M Green, N. C. Peterson, T. Sato, A. Teramoto, R. Cook, S. Lifson, *Nature* 1995, 268, 1860.
- [14] [14a] L. Angiolini; L. Giorgini, E. Salatelli, *e-Polym.* 2003, no. 037. [14b] L. Angiolini, R. Bozio, A. Daurù, L. Giorgini, D. Pedron, G. Turco, *Chem. Eur. J.* 2002; 8, 4241. [14b] L. Angiolini, T. Benelli, L. Giorgini, A. Painelli, F. Terenziani, *Chem. Eur. J.* 2005, 11, 6053-6353. [14c] L. Angiolini, T. Benelli, R. Bozio, A. Daurù, L. Giorgini, D. Pedron, E. Salatelli, *Eur. Polym. J.* 2005, 41, 2045. [14d] L. Angiolini, T. Benelli, R. Bozio, A. Daurù, L. Giorgini, D. Pedron, E. Salatelli, *Macromolecules* 2006, 39, 489.
- [15] C. Carlini, L. Angiolini, D. Caretti, *Photochromic optically active polymers*, in *Polymeric Materials Enciclopedia*, , Salomone, J. C., editor-in-chief; CRC Press: Boca Raton, 1996; Vol. 7, pp. 5116-5123.
- [16] L. Angiolini, D. Caretti, L. Giorgini, E. Salatelli, *Macromol. Chem. Phys.* 2000, 201, 533.
- [17] J.R. Platt, *J Chem. Phys.* 17, 484 (1949)
- [18] D. D. Perrin, W. L. F. Amarego, D. R. Perrin, "Purification of Laboratory Chemicals", Pergamon Press, Oxford 1966

Acknowledgements

I would like to express my gratitude to the many people who made this thesis possible. Dott. Loris Giorgini for his provided guidance, profound skill and wisdom throughout the course of this research.

I would also like to thank Prof. Luigi Angiolini and all his research collaborators for their knowledge and expertise.

This work would not have been achievable without the assistance and the help of Libero and Gianluca.

I would like to express my gratitude to Prof. Paul Rochon and Prof. Nunzi for having given me the opportunity to work together.

A special thanks goes to all my friends whose generosity and insight has been so helpful.

I would like to thank my parents for their unconditional support and love. In so many ways, this endeavor could not have happened without their help over the years.

Finally, I would like to thank Adriana. Without her love, patience and encouragements, I couldn't have been able to do this work.

Cisco

*If the milk turn out to be sour,
I ain't the kinda pussy to drink it*

Lock & Stock and Two Smoking Barrels (1998), Guy Ritchie

